1968

Hydrocracking of Normal Hexane and Cyclohexane Over Zeolite Catalysts.

William Julian Hatcher Jr
Louisiana State University and Agricultural & Mechanical College

68-10,742

HATCHER, Jr., William Julian, 1935-

HYDROCRACKING OF NORMAL HEXANE AND CYCLOHEXANE OVER ZEOLITE CATALYSTS.

Louisiana State University and Agricultural and Mechanical College, Ph.D., 1968
Engineering, chemical

University Microfilms, Inc., Ann Arbor, Michigan

HYDROCRACKING OF NORMAL HEXANE AND CYCLOHEXANE OVER ZEOLITE CATALYSTS

A Dissertation

Submitted to the Graduate Faculty of the
Louisiana State University and
Agricultural and Mechanical College
in partial fulfillment of the
requirements for the degree of
Doctor of Philosophy

in

The Department of Chemical Engineering

by
William Julian Hatcher, Jr.
B. of Chem. Engr., Georgia Institute of Technology, 1957
M. S. in Chem. Engr., Louisiana State University, 1964
January, 1968

ACKNOWLEDGEMENTS

Particular acknowledgement is given to Dr. Alexis Voorhies, Jr., whose advice and ideas helped immeasurably. His help is greatly appreciated.

Special acknowledgement is made to the members of Esso Research and Engineering Company as this organization sponsored the research project. Sincere acknowledgement is expressed to the research staff at the Esso Research Laboratories in Baton Rouge, Louisiana for furnishing the necessary equipment, catalysts, and invaluable consultation.

The author wishes to express his indebtedness to the Petroleum Processing Laboratory of the Chemical Engineering Department for the use of their facilities.

Special gratitude is expressed to Mrs. Marie Jines for her diligence in typing this manuscript.

TABLE OF CONTENTS

LIST OF TABLES

LIST OF FIGURES

ABSTRACT

The hydrocracking reaction, scission of carbon-to-carbon bond plus hydrogenation, was investigated, using n-hexane and cyclohexane as reactants. Two crystalline aluminosilicate catalysts were studied. These zeolite catalysts were the hydrogen, or acid, form of synthetic faujasite and mordenite. Both of the catalysts had been impregnated with palladium. Typical hydrocracking conditions were 550-800°F, 765 psia, 10 moles of hydrogen per mole of hydrocarbon reactant, and a liquid hourly space velocity of 2 volumes per hour of hydrocarbon per volume of catalyst.

The mordenite catalyst was found to be more active than the faujasite catalyst for hydrocracking; however, both catalysts had extremely high hydrocracking activity. The reactivity of cyclohexane was higher than n-hexane with the faujasite catalyst; the reverse was the case with the mordenite catalyst. The results of hydrocracking a n-hexane-cyclohexane mixture over the faujasite were predicted successfully from the results of pure compound studies. This implied that the adsorption of n-hexane and cyclohexane were about equal on the faujasite. Although cyclohexane was less reactive than n-hexane over the mordenite catalyst, the cyclohexane was preferentially converted from a mixture of n-hexane and cyclohexane. This implies that cyclohexane is more adsorbed than n-hexane on the mordenite.

The integral reactor data were correlated with a simplified model which assumed the reaction mechanism could be described as an irreversible reaction between the hydrocarbon and hydrogen. This model was first order with respect to the hydrocarbon. The effect of increasing the hydrogen partial pressure was found to be compatible with a "dual site" catalytic mechanism.

Complete data from over 120 experimental runs are presented.

CHAPTER I

INTRODUCTION

The increasing demand for high quality gasoline, accompanied by a decreasing demand for middle distillates, has played a major role in the recent developments in hydrocracking processes. Modern hydrocracking has emerged as a key tool for refiners to use in balancing refinery production and market demands. The first modern-day commercial unit was put into operation in 1961, and six years later there were more than fifty units in operation or under construction. Feed stocks have expanded to range from naphtha to residua, including refractory materials not easily converted by other processes. Products currently range from liquefied petroleum gas to heating oil.

Hydrocracking was originally developed and applied commercially in Germany in 1927. The original purpose was for converting coal and tars into high quality liquid fuels. In this country, this early version of hydrocracking proved useful in the production of high quality diesel fuel and lubricating oils from petroleum feed stocks. During World War II hydrocracking made an important contribution in supplying aviation fuel requirements. However, this process proved to be economically unattractive due to the high pressure equipment and hydrogen manufacturing equipment required.

Perhaps the most significant factor in the recent rejuvenation of hydrocracking has been the development of new catalysts. These catalysts have excellent activity and activity maintenance at operating conditions far less severe than in the old process. The availability of cheap hydrogen by-product from other processes also contributed to the recent hydrocracking growth.

The original catalyst for hydrocracking was tungsten disulfide. This catalyst soon was replaced by tungsten disulfide on a clay support. The modern catalysts are dual function catalysts having a balance of both cracking and hydrogenating activity. The cracking activity is typically supplied by an acidic support such as silica-alumina, and the hydrogenating activity by a dispersed metal or metals such as tungsten and nickel.

In the nineteen sixties, zeolites became important catalysts for several types of conversion processes. These crystalline aluminosilicates also have been used for ion-exchange in water softening and in selective adsorption applications. Synthetic zeolites have been found to have extremely high crystalline regularity. The fact that zeolites have pore diameters of the same order of magnitude as individual molecules adds to their interesting catalytic characteristics.

This dissertation represents a very small fraction of the extensive research currently being carried out on zeolite catalysts. This particular study is an investigation of two synthetic zeolites, mordenite and faujasite, with respect to how they hydrocrack n-hexane and

cyclohexane. The purpose of the work presented in this dissertation is (1) to evaluate the hydrocracking activity and selectivity of the selected catalysts and (2) to develop a mathematical model for the hydrocracking of n-hexane and cyclohexane using mechanisms from the literature as a guide.

CHAPTER II

LITERATURE REVIEW

A. Crystalline Zeolites

1. Introduction

The unique properties of zeolites have attracted increasing attention from the chemical process industry and scientific circles in the past few years. Zeolites, crystalline aluminosilicate minerals, were discovered and named by Baron Cronstedt in 1756. These minerals were recognized for their ability to exchange their metal cations by treatment with aqueous solutions of various salts. Amorphous, gel, aluminosilicates having this cation exchange ability also were called "zeolites".

Early work on the sorptive properties of zeolites was summarized by McBain[40] who proposed the name, "molecular sieve". No other solids have been found to be so specific and quantitative in separating mixtures on the basis of the size and shape of the constituent molecules, and the name, "molecular sieve," is particularly apt. Water softening, selective adsorption, and catalysis are among the major uses of zeolites. Many of the unique properties of zeolites depend on their structure, and investigations stimulated by these properties have revealed much about their remarkable molecular architecture. Excellent

reviews of research on zeolites have been published by Barrer[5], Breck[15], and Nikolina et al.[48]

2. Physical Properties of Crystalline Zeolites

a. General

There are over thirty different crystalline zeolites occuring in nature. Several of these have been synthesized in the laboratory. Some synthetic variants of the natural zeolites have been made in which properties, such as chemical composition and sorptive properties, may differ from the naturally occuring counterparts.

All zeolites, natural and synthetic, may be represented by the empirical formula[15]

$$Me_{x/n}\left[(AlO_2) \times (SiO_2)_y\right] \cdot M\,H_2O.$$

The "Me" represents a metal cation of valence "n", and "M" represents the molecules of water. The number of water molecules associated with one unit cell can vary over a range of at least 15 to 264.[15] The Si/Al ratio or y/x ratio of the empirical formula ranges from unity for zeolite type A to a value of five for mordenite.

A pyramid, or tetrahedron, is the basic building block common to all zeolite crystal structures. This tetrahedron has an oxygen atom at each of the four corners and a silicon atom in the center. An aluminum atom can be substituted for the silicon atom. Silicon, however, has four electrons to share with the oxygen atoms, whereas aluminum has only three. Therefore, aluminum needs a monovalent cation in

order to make up for this deficiency. Alternately, the aluminum can share a divalent cation. Figure I (page 7) shows tetrahedra with silicon-oxygen, aluminum-sodium-oxygen, and aluminum-calcium-oxygen. Each of the four oxygens of a tetrahedron has a free valence bond, and the tetrahedra can be connected by these free bonds.

These tetrahedra can be joined together to form many different zeolite crystal structures. The crystal structures can be classified in three general groups: (1) chainlike or fibrous crystals, (2) layer structures, and (3) semi-rigid three dimensional structures.[44] Mordenite is a member of the first group, and faujasite is a member of the third group.

b. Faujasite

Faujasite, an important zeolite, is found in nature and can be synthesized. Synthetic zeolite type Y is a well-known member of the faujasite family. A typical empirical formula for type Y is:

$$Na_{56}\left[(AlO_2)_{56}(SiO_2)_{136}\right] \cdot 264\,H_2O.$$

Type X has a similar crystal structure to type Y; however, in type X the Si/Al ratio is lower. A typical formula for type X is:

$$Na_{86}\left[(AlO_2)_{86}(SiO_2)_{106}\right] \cdot 264\,H_2O.$$

Both natural and synthetic faujasite have a void volume of 0.35 cc/gm based on the amount of water contained per gram of dehydrated catalyst.

The structure of faujasite is a truncated octahedra as shown in Figure 2 (page 8). Each vertex represents a silicon or aluminum atom

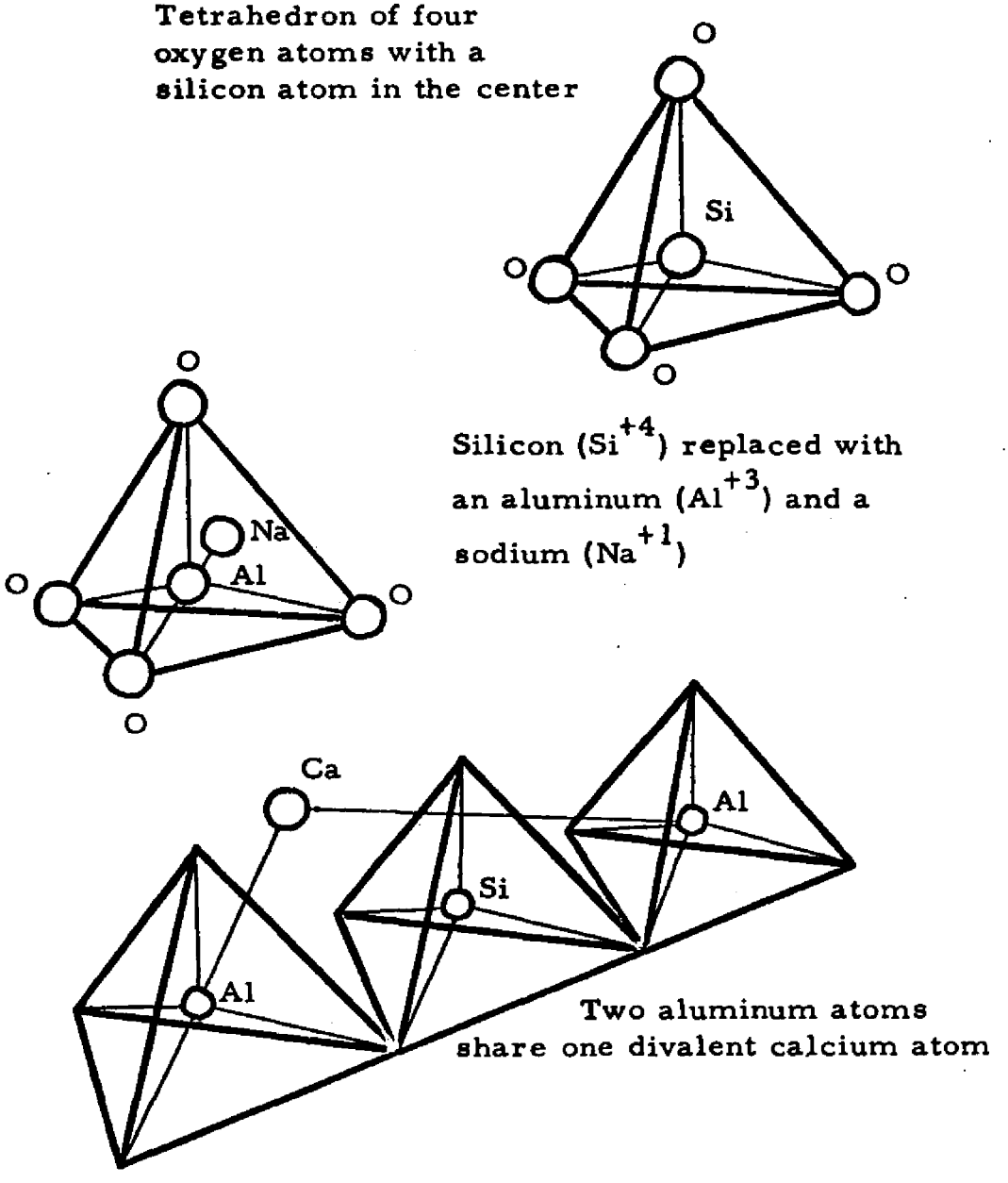

Figure 1 . Basic Framework of Zeolite Crystals.

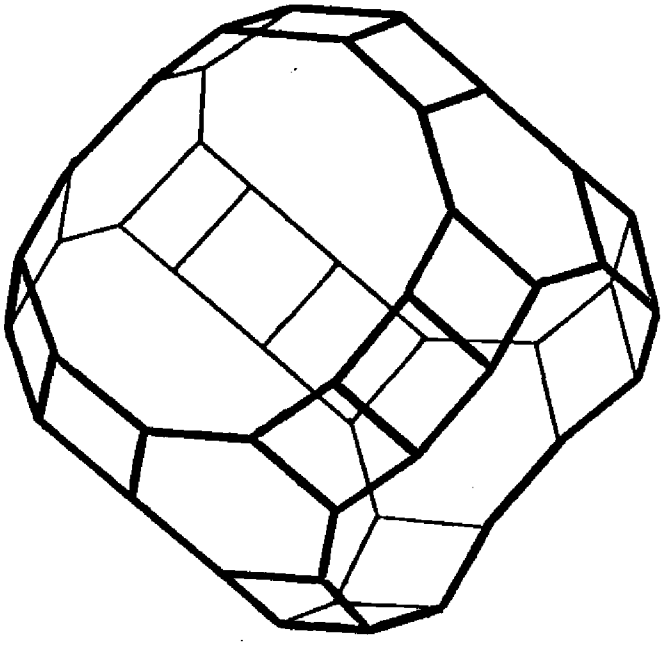

Figure 2 . Structure of Type X or Y Zeolite.

of the basic tetrahedron, and each "edge" represents a linking or "bridging" oxygen atom. Access to the inner cavity or "cage-like" network is by four 12-sided windows each having a diameter of about 9 angstroms. The inner cavity has a diameter of about 11 angstroms.

c. Mordenite

Mordenite, a member of the chainlike crystal group, is found in nature and can be synthesized. Recent patents to Norton Company[74,75] and to Air Liquide[77] concern the synthesis of mordenite. Barrer[3, 4, 6, 7, 8] has carried out several investigations of the sorptive properties and the synthesis of mordenite.

The formula for mordenite is:

$$Na_8\left[(AlO_2)_8\,(SiO_2)_{40}\right] \cdot 24\,H_2O.$$

The void volume is 0.14 cc/gm, considerably less than that of faujasite.

The mordenite structure can be compared to a bundle of parallel tubes. A cross-sectional view of the mordenite crystal structure appears in Figure 3 (page 10). The silicon and aluminum atoms are at the points of intersection, and the oxygen atoms are represented by the lines. This cross-section is repeated at regular intervals, forming parallel elliptical tubes. These tubes with a major diameter of about 7 angstroms and a minor diameter of about 6 angstroms extend through the entire crystal. The parallel tubes are connected by small elliptical openings with major and minor diameters of about 5 and 4 angstroms respectively.

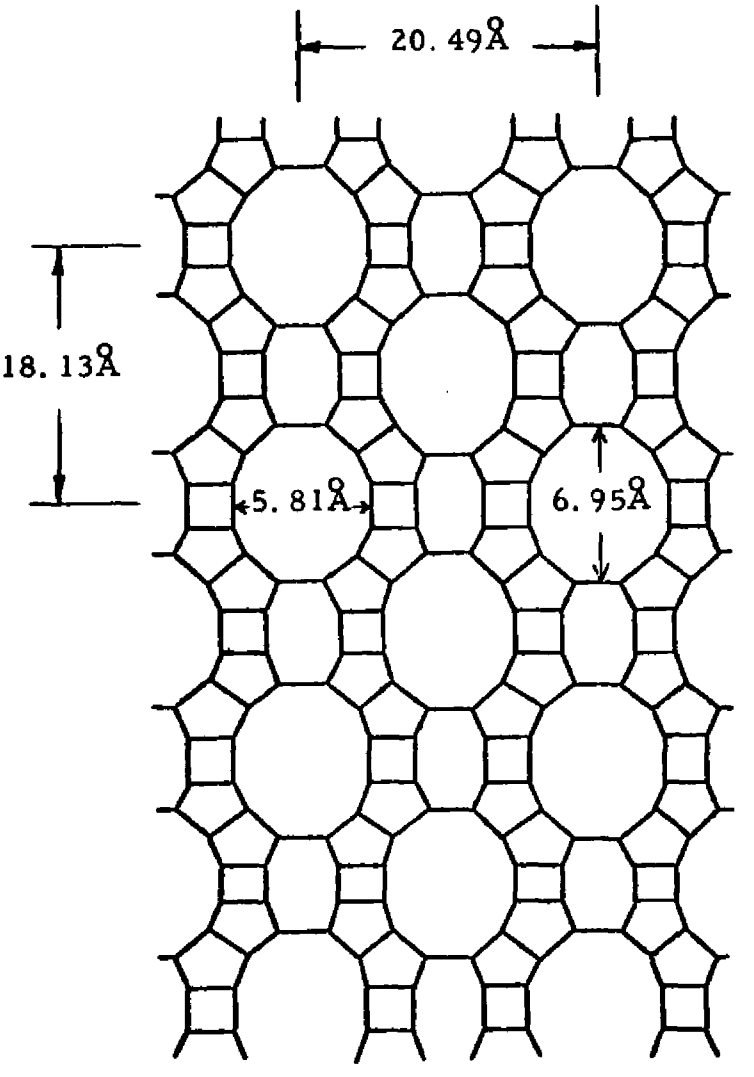

Figure 3. Cross-Sectional View of Mordenite[20].

3. Catalytic Properties of Crystalline Zeolites

a. General

The first patent for a zeolite catalyst was issued in 1917[82]. This patent concerned a palladium-exchanged chabasite for hydrogenation reactions. The first of the contemporary patents appeared in 1960. Since that time patent offices in the United States and other countries have been flooded with applications concerning zeolite catalysts. The current commercial use of zeolite catalysts is considerable, and it is being expanded rapidly.

The unique crystal structure of zeolites offers chemical researchers the possibility of "selective catalysis". That is, a zeolite can be selected such that the pores can admit the desired reactant and exclude larger compounds. An example of this was reported by Weisz and co-workers[68]. A sodium type 5A zeolite was used in the dehydration of butanol to form butenes. Normal butanol could enter the 5A pore and was converted easily to butene; however, isobutanol was too bulky to enter the 5A pore and remained unchanged.

Many zeolite catalysts can be modified by exchanging the sodium in the aluminum tetrahedron for other cations. For example, ammonium ions may be substituted for the sodium. Then the ammonia can be driven off by heating. Exactly what is left after the ammonia is driven off is subject to question. It has been referred to as the hydrogen

form of zeolite, the decationized form, and the acid form. Hydrogen-zeolites have been found to be extremely active catalysts by numerous investigators.

Other cations also are exchanged for the sodium in zeolites. A calcium exchanged type X catalyst was reported to be very active for isomerizing heptanes and larger paraffins[97]. Calcium and sodium type X were reported active for catalytic cracking[25]. Rare earth exchanged zeolites have been found to be active catalysts for the alkylation of aromatics[62,63], catalytic reforming[76, 80, 81], catalytic cracking[61], and hydrocracking[99].

Catalytic cracking is a very important process catalyzed by zeolites. The majority of the petroleum refiners now are using zeolite based catalysts. Many zeolites have been investigated for catalytic cracking including type 5A[68], type X[25, 61], natural and synthetic faujasite[52, 43, 69], mordenite[1, 34, 35, 43, 69], type ZK5[43], gmelinite[43], chabazite[43], stilbite[43], and offretite[43].

Another important reaction using zeolite catalysts is isomerization. Most of the reported investigations of isomerization concerned the hydrogen form of zeolite. Some of the zeolites were impregnated with a hydrogenation-dehydrogenation metal, such as platinum or palladium, while others were not impregnated. The literature includes the isomerization of alkylaromatics[14, 72] and paraffins[9, 16, 24, 42, 54, 98].

Hydrocracking is another refining process that appears to be a potential for zeolite catalysts. Most of the reported zeolite catalysts for hydrocracking were the hydrogen form of zeolites impregnated with a hydrogenation-dehydrogenation metal. Synthetic faujasite, type Y, appears to be the most commonly reported catalyst. Mordenite[10, 38] and type X[18] also have been tested.

Platinum impregnated zeolites have been described by several investigators for catalytic reforming.[42, 76, 79, 80, 81, 83, 85] The alkylation reaction of olefins and aromatics is catalyzed by zeolites.[42, 62, 63, 89] Norton[49] investigated several zeolites, including types A and X, for the polymerization of propylene. Zeolites impregnated with molybdenum trioxide[42] and cobalt[87] catalyze hydrodesulfurization reactions. Other reactions reported to be catalyzed by zeolites include the disproportionation of alkylaromatics[78], methanol synthesis[84], hydrogenation of aromatics[42], the Fischer Tropsch type of hydrogenation reaction[71, 86], condensation reactions of carbonyl compounds[64], methanation[44], and the dehydrogenation of ethylbenzene[44].

b. Faujasite

Faujasites, including type Y, are the most widely used zeolite catalysts.[44] The large windows into the crystal "cage" are sufficient in size to admit most hydrocarbon molecules, so faujasites are not of the molecular shape-selective variety. Nevertheless, faujasites are extremely active catalysts for many reactions.

The faujasite catalyst can be modified in several ways to facilitate the desired reaction. The sodium form of faujasite (Na-faujasite) can be ion exchanged to replace the sodium ions with other metal cations. As mentioned previously, a very active catalyst is synthesized by exchanging the sodium for ammonium ions and then driving off the ammonia. The resulting hydrogen form of faujasite (H-faujasite) is very active for catalytic cracking[43, 44, 69], isomerization [14, 44, 54], alkylation[44, 63], and several other reactions. The H-faujasite provides acidic active sites required for the catalytic activity in these reactions. Exchanging the sodium ions for multivalent cations also results in highly active catalysts.[44]

Another method of modifying faujasites is to impregnate various metals on the zeolite surface. For example, H-faujasite is impregnated with palladium for isomerization reactions. The palladium provides the dehydrogenation-hydrogenation activity and the H-faujasite the acidic activity required in dual function catalysts.

c. Mordenite

Mordenite has smaller pores than faujasite (7 versus 9 Angstroms). Also the active sites in the crystal structure of mordenite are much less accessible. The mordenite "tube-bundle" extends completely through the 1 to 5 micron particles of synthetic mordenite. This means that a single tube has a length to diameter ratio greater than 1000.

Despite the disadvantages of its structural characteristics, H-mordenite has been found to be more active than H-faujasite for the

catalytic cracking of n-hexane[43, 69], the isomerization of n-pentane[16], and the isomerization of n-hexane[9]. Keough and Sand[35] first recognized the catalytic properties of mordenite in 1961. Keough[34] later reported the high activity of H-mordenite and Ba-mordenite in the catalytic cracking of cumene, cetane, and decane. In this study Keough concluded that mordenite had an effective pore diameter of 9 Angstroms.

Beecher[9] demonstrated that H-mordenite, unlike H-faujasite, did not require impregnation with a dehydrogenation-hydrogenation metal for the isomerization of n-pentane and n-hexane. Bryant[16] found that palladium impregnated H-mordenite was more active than the zinc or magnesium forms of mordenite impregnated with palladium.

The hydrogen form of mordenite from natural mordenite was found to be active for the isomerization of n-butane and cyclohexane. Adams and co-workers[1] found H-mordenite to be very active for catalytic cracking of gas oil, but that the mordenite deactivated rapidly. Also a recent patent[73] describes a hydrocracking process using a mordenite catalyst.

B. Hydrocracking

1. Introduction

In petroleum refining there are two types of hydrogenation. Examples of one type, simple hydrogenation, are the saturation of olefins and the conversion of aromatics to naphthenes. The second type is

destructive hydrogenation or hydrocracking. Hydrocracking has been described as catalytic cracking with hydrogenation superimposed.

Commercial hydrocracking has developed rapidly in the last few years. The first modern-day commercial unit was put in operation in 1961[59]. Since that time hydrocracking has become a key tool in balancing refinery production and market demands. In 1967 there were more than fifty units in operation or under construction.[58] Feed stocks range from naphtha to residua, including refractory materials not easily converted by other processes and materials too contaminated to be catalytically cracked. Products currently range from liquefied petroleum gas to heating oil.

2. Early Hydrocracking

In 1927 the original hydrocracking process was developed in Germany by the I. G. Farbenindustrie for converting lignite or brown coal into gasoline. This process is one of the oldest catalytic processes in petroleum refining. In this country it was applied from 1931 to 1944[46]. This early version of hydrocracking proved valuable in the production of high quality diesel fuel and lubricating oils from petroleum feed stocks. During World War II, the process was used to produce high octane aviation gasoline. However, this early process was economically unattractive and was abandoned in favor of the now well-known catalytic cracking process, which also converts high boiling feed stocks to lower boiling products. The major disadvantages in

hydrocracking were that high pressure equipment was required and that hydrogen consumed in the process had to be manufactured.

The early hydrocracking process employed a fixed-bed, non-regenerative catalyst system. Since the chemical reaction is exothermic, make-up hydrogen was added at several points down the catalyst bed to serve as a cooling medium and to supply some of the hydrogen required for the hydrocracking reaction. Reactor pressures of 200 atmospheres or greater were required to inhibit coking reactions that would destroy catalyst activity. Reactor temperatures were in the range of 600 to 1000°F. Hydrogen for the process was made in auxiliary equipment by the methane-steam reaction.

The original catalyst for hydrocracking was tungsten disulfide. Catalysts such as tungsten disulfide and molybdenum disulfide were found to be highly active for hydrocracking and were promoted rather than poisoned by sulfur containing hydrocarbon compounds. These catalysts gave high gasoline yields, but the gasolines were low in octane number.

The next catalyst development was supporting the tungsten disulfide on a natural clay. Montmorillonite clay treated with hydrofluoric acid is an example of the support. About 10% WS_2 was placed on the support. The supported catalyst had about the same volumetric activity as the unsupported catalyst, but gasoline octane numbers from the supported catalyst were much higher. These high octane numbers

were due to the high content of branched paraffins and aromatics in the product.

3. Modern Hydrocracking

The domestic refiner's interest in hydrocracking has been renewed due to the increasing demand for high quality gasoline and a decreasing demand for middle distillates. However, the most significant factor in the recent growth of hydrocracking has been the development of improved catalysts. The new catalysts are capable of maintaining activity at operating conditions far less severe than the catalyst of the original hydrocracking process. Another factor in the resurgence of hydrocracking has been the availability of cheaper hydrogen. Hydrogen is a by-product from the catalytic reforming process and also can be manufactured by an improved methane-steam process.

Most of the modern hydrocracking processes are fixed bed, similar to the early version, but operating at about half of the total pressure of the early process. One exception is the ebullating bed process offered for licensing by Hydrocarbon Research Corporation and Cities Service Research and Development.[58] In this process, high linear gas velocities are used to expand the catalyst bed. The catalyst bed has enough fluidity to permit semi-continuous replacement. Staging of the catalyst bed permits selective withdrawal of contaminated catalyst from the bottom of the bed. Other fixed bed processes are offered for liscensing by the Institut Francais du Petrole and Badische Aniline-und-Soda-Fabrik, Houdry and Gulf Research, Chevron Research

and Universal Oil Products, and Union Oil and Esso Research and Engineering.[26, 41, 58]

Modern hydrocracking processes use dual function catalysts having both cracking and hydrogenating activity. The cracking activity is supplied by an acidic support such as silica-alumina or silica-magnesia. Zeolites also have been described as supports for hydrocracking catalysts. The hydrogenating activity is supplied by certain metals or metal sulfides. These metals are mostly from groups VI B and VIII of the periodic table. The dual function catalysts are characterized by their extreme versatility with regard to both feed stocks that can be used and products that can be made.

The most important application of hydrocracking, especially in this country, has been the conversion of gas oils into high quality gasoline. Another application outside of the United States has been the conversion of high boiling distillates or residua to middle distillates. Other uses of the hydrocracking process include jet fuel production from gas oils, residuum hydroprocessing, and liquefied petroleum gas (LPG) production from low octane naphtha.

4. Hydrocracking of Naphtha

Liquid petroleum gas (LPG) is used extensively as a fuel in many parts of the world. Generally, these areas do not have readily available petroleum and natural gas. The LPG must be transported to these areas, and usually the cost of shipping is high due to the required pressure vessels and refrigeration equipment. In some cases, it is

more economical to ship a petroleum liquid, such as naphtha, and convert the liquid to LPG at the point of use. Hydrocracking has been shown capable of producing high yields of LPG plus high octane pentanes and hexanes from a low octane naphtha.[29, 53, 58] Four commercial plants using the Isomax process, licensed by Chevron Research and Universal Oil Products, are currently in this service.[58] One of these plants is in Hawaii, and three are in Japan.

5. Hydrocracking Mechanism Studies

a. General

The functions of a hydrocracking catalyst consist of isomerization, cracking, and hydrogenation. Present catalysts for hydrocracking are dual function catalysts containing hydrogenation and acidic sites. Hydroisomerization and other catalytic reforming reactions also require dual function catalysts.[67] The interrelationships between the hydrogenation-dehydrogenation sites and the acidic sites are complex and are the subject of much debate.

A simplified mechansim for hydrocracking can be based on the rather extensive literature of hydroisomerization and catalytic cracking with a few modifications. As in hydroisomerization,[45] one of the roles of the metallic component is to convert paraffins and naphthenes to olefin intermediates. Hydrocracking can occur even when the hydrogenation component and the acidic component are separated by macroscopic distances.[67] Carbonium ions are formed and can be assumed to follow the mechanism for catalytic cracking.[65] The highly reactive

acidic sites then cause rearrangement and dissociation of the carbonium ion with the release of an olefin.

The reactions occurring on the acidic sites of a dual function catalyst have been found to be rate-limiting in general. For example, in hydroisomerization, isomerization of carbonium ions by skeletal rearrangement has been reasoned to be the slow step.[36] Following the same reasoning, steps leading to scission of the carbon to carbon bond have been suggested as the slow step in hydrocracking.[11] Yet no simple relationship exists between hydrocracking activity and the number of acidic sites.[38]

If acidity is the most important correlating variable, acidity measurements on unaged catalysts must include many acidic sites that are active only very briefly and have no relation to the "lined-out" catalyst activity. Therefore it has been postulated that only the acidic sites close to metal sites are kept free from coke and active.[11] Then the equilibrium catalyst activity should be related to the number of acidic sites that can be kept free from coke by the metal crystallites.

An interesting feature of hydrocracking is that lower molecular weight hydrocarbons produced during the reaction are not in thermodynamic equilibrium. Thus, it is possible to obtain butane and pentane fractions containing several times the proportion of branched isomers that equilibrium would predict. Flinn and co-workers adequately explained the high branched isomer fractions by a rapid isomerization

reaction, then cracking, with little readsorption of the cracked products.[23] They illustrated this theory by hydrocracking n-hexadecane, n-octane, decalin (decahydronaphthalene), tetralin (tetrahydronaphthalene), and n-butylbenzene over a sulfided nickel on silica-alumina catalyst.

b. Hydrocracking Paraffins and Olefins

Coonradt and Garwood[19] proposed a more complicated mechanism for hydrocracking paraffins. This mechanism involves the formation of an olefin at the metal (dehydrogenation) site, the formation of a carbonium ion at the acidic site, and then either isomerization of the carbonium ion by skeletal rearrangement or hydrocracking of the carbonium ion to a smaller ion plus an olefin. The smaller carbonium ion could then isomerize and be converted to an olefin and then a paraffin, or it could hydrocrack. The olefin produced by the original hydrocracking reaction could either be hydrogenated to a paraffin at the metal site or converted to another carbonium ion at the acidic site. This new ion would be available for further reaction. It was suggested that the relative hydrogenation, isomerization, and cracking activities and the relative adsorption of the intermediates control the types of products produced from hydrocracking. The types of products can be changed drastically by altering the relationships of the hydrogenation and acidic functions.

Myers and Munns[47] reported that platinum on silica-alumina catalysts were more active than platinum on alumina catalysts for

hydrocracking pentanes, hexanes, and heptanes. They found that nickel on SiO_2 or SiO_2-Al_2O_3 produced very high methane concentrations in the hydrocracked product. In hydrocracking pentanes and hexanes they found that the relative frequency of carbon-to-carbon bond cleavage was about the same for all carbon positions in the molecule with platinum catalysts. The center bonds were broken preferentially in heptane hydrocracking with platinum on SiO_2-Al_2O_3, producing propane and butanes. Later Weisz[67] attributed indiscriminate bond cleavage to reaction at the metal sites alone and termed this "hydrogenolysis" as opposed to a dual function "hydrocracking" which preferentially produces fragments of three or four carbon atoms.

Archibald and co-workers[2] investigated hydrocracking of C_4 to C_{16} paraffins and olefins with tungsten disulfide on HF treated "Filtrol" clay and tungsten disulfide on silica-alumina. They reported that the mechanism for hydrocracking paraffins was similar to catalytic cracking and that the following rules apply for hydrocracking:

1. The normal paraffin reacts to form a secondary carbonium ion at any secondary carbon atom in the molecule.
2. Cracking occurs at a carbon-carbon bond in a position once removed from (beta position) the carbonium ion carbon atom and yields an olefin and a smaller secondary or tertiary carbonium ion.

3. When more than one beta bond is available, these alternate bonds crack with equal probability provided that the resulting olefin is C_3 or larger and the accompanying carbonium ion is C_4 or larger.
4. Carbonium ions from the inital step crack further until reduced in size to C_7 or smaller fragments.
5. One half of the olefins are assumed to form secondary or tertiary carbonium ions and crack further until reduced to C_6 or smaller.

Hartwig[28] investigated the isomerization and hydrocracking of n-hexane over palladium on metal oxide supports. His data indicated an apparent activation energy of about 60 kcal/gmole for hydrocracking n-hexane. Guenther[27] investigated hydrocracking of higher molecular weight paraffins over a tungsten disulfide catalyst. He reported that his data fit a first order reaction rate model and that the activation energy was about 64 kcal/gmole. Pollitzer and co-workers[53] reported that in hydrocracking n-heptane with the commercial Isomax catalyst over 85 mole % of the cracked product was propane and butanes, indicating the carbonium ion mechanism. There was not enough C_1 and C_2 to account for the C_5 and C_6 products. This indicates the formation of an intermediate by a combination of two fragments and subsequent hydrocracking of this intermediate.

Henke and co-workers[29] also found in hydrocracking n-hexane that the molar ratios of C_5/C_1 and C_4/C_2 of the product were greater than unity and that propane was the predominant product. They suggested that a C_3 carbonium ion reacting with a C_6 olefin to form a C_9 carbonium ion, which subsequently is hydrocracked, would explain these molar ratios. They also found that n-pentane and isopentane hydrocracked at the same rate.

Hutchins[31] investigated the hydrocracking of pentane over a platinum on alumina catalyst. He found that:

1. Isopentane hydrocracks faster than n-pentane.
2. The hydrocracking rate is maximized at 100-250 psia.
3. The hydrocracking rate decreases as hydrogen partial pressure increases.
4. The hydrocracking rate varies with pentane partial pressure raised to a power greater than one.
5. The hydrocracking rate is very temperature sensitive, increasing about ten-fold from 700° to $800^{\circ}F$.
6. The hydrocracking of pentanes data fit a model which assumes the controlling step to be a collision of a gas-phase pentane molecule with an olefin adsorbed adjacent to two vacant sites.

Sinfelt and Rohrer[60] found that some isoparaffins hydrocrack more readily than n-paraffins over a platinum on alumina catalyst. For example, 2, 2, 4 trimethylpentane hydrocracked six times faster than n-octane. Zhang[70] found that high hydrogen partial pressures were beneficial to hydrocracking C_{16}-C_{20} normal paraffins over nickel sulfide on silica-alumina, but adverse over tungsten sulfide-nickel sulfide on alumina. Langlois and co-workers[37] found that sulfiding a nickel on silica-alumina catalyst produced the following in hydrocracking n-decane:

1. The overall rate of reaction increased greatly over that of the unsulfided catalyst.
2. The predominant reaction changed from isomerization to cracking.
3. Hydrocracked products were C_3-C_7 isoparaffins instead of normal paraffins.
4. The product from isomerization is more highly branched.

Their explanation of this difference in catalyst performance was that some of the nickel formed salts with the silica-alumina and thus neutralized some of the acidic sites. Upon sulfiding, the H_2S combined with the nickel from the nickel silica-alumina salts and regenerated the original strong acidic sites of the silica-alumina.

c. Hydrocracking of Naphthenes

The generally accepted mechanism for naphthene hydrocracking is similar to that of paraffins. First, a cyclic olefin is formed. Then the olefin is converted to a carbonium ion. The carbonium ion can be isomerized or cracked. Egan and co-workers[21] found in hydrocracking C_9-C_{12} alkylcyclohexanes over a nickel sulfide-on silica-alumina catalyst that the branched chains were selectively "pared". The principal hydrocracked product was isobutane. The cycloalkane ring was unexpectedly stable. Egan and co-workers suggested that the carbon-to-carbon bonds in the ring might crack about as readily as the side chains, but that in cracking the ring, the probability of recyclization is particularly high. This is because the alkene double bond is held in the immediate vicinity of the reactive cationic center by the carbon chain. Therefore, the net loss of ring structures would be small, and the essentially irreversible side chain cleavage would predominate.

Kaliberdo and Kalechits[33] investigated cyclohexane hydrocracking over a tungsten disulfide on clay catalyst. They proposed a mechanism which involved isomerization to methylcyclopentane followed by selective ring opening to 2-methylpentane.

Iijima and co-workers[32] found that hydrocracking cyclohexane over a platinum on alumina catalyst was a first order reaction with an activation energy of 30-35 kcal/gmole. Chang and Kalechits[17] also found that cyclohexane hydrocracking with a platinum catalyst was first order.

d. Hydrocracking with Zeolite Catalysts

Clement and co-workers[18] investigated the reactions of cyclohexane and benzene over several forms of type X synthetic zeolite. These included Na-X, Ca-X, Mg-X, Ce-X. It was concluded that the more acidic catalyst was more reactive for hydrocracking and that hydrocracking followed a carbonium ion mechanism. Propane and butanes were the major components of the hydrocracked product.

Beecher and co-workers[10] studied the hydrocracking of decane and decahydronaphthalene (decalin) over two types of synthetic mordenite catalysts. One catalyst was palladium on H-mordenite, and the other was palladium on alumina deficient H-mordenite. Some of the alumina had been acid extracted from the mordenite crystal structure in the second catalyst. The apparent activation energy for decane hydrocracking was 33 kcal/gmole for the Pd-H-mordenite catalyst and 44 kcal/gmole for the Pd-alumina deficient-H-mordenite. These catalysts may have some diffusional limitations as evidenced by the 33-44 kcal/gmole activation energies. Data from a tungsten disulfide catalyst indicated an activation energy of 64 kcal/gmole.[27] Beecher et al. found that decalin hydrocracking had an apparent activation energy of 25 kcal/gmole with both catalysts. They also found that decalin had a lower reaction rate than decane when hydrocracked in pure compound studies, but that decalin was preferentially converted in a decane-decalin mixture.

Osipov and Khavkin[50] investigated hydrocracking over a nickel impregnated zeolite catalyst. Their data indicated a first order reaction.

C. Products From Hexane Hydrocracking

1. Hexane Isomers

The catalysts used in this research have been found to be excellent isomerization catalysts.[9, 16, 54] Therefore, all five hexane isomers were expected to be in the product from experimental runs on n-hexane hydrocracking. These paraffins are n-hexane (n-C_6), 3-methylpentane (3-MP), 2-methylpentane (2-MP), 2, 3-dimethylbutane (2, 3-DMB), and 2, 2-dimethylbutane (2, 2-DMB). Several investigators have studied the equilibrium concentrations of the hexane isomers.[13, 22, 54, 55, 56, 57] These studies are illustrated in Figures 4-8 (pages 30-34). Beecher[9] used the data from Ridgway and Schoen[55] as the standard in his study of hexane isomerization over a mordenite catalyst, and these data also will be used as the standard in this study.

2. Hydrocracked Products

The hydrocracked products from hexane hydrocracking should be mostly paraffins with a molecular weight lower than hexane. These products would include methane, ethane, propane, n-butane, isobutane, n-pentane, and isopentane. Neopentane (2, 2 dimethylpropane) is not naturally occurring and is not expected in the hydrocracked products. Equilibrium concentrations calculated from free energy data[56] indicate

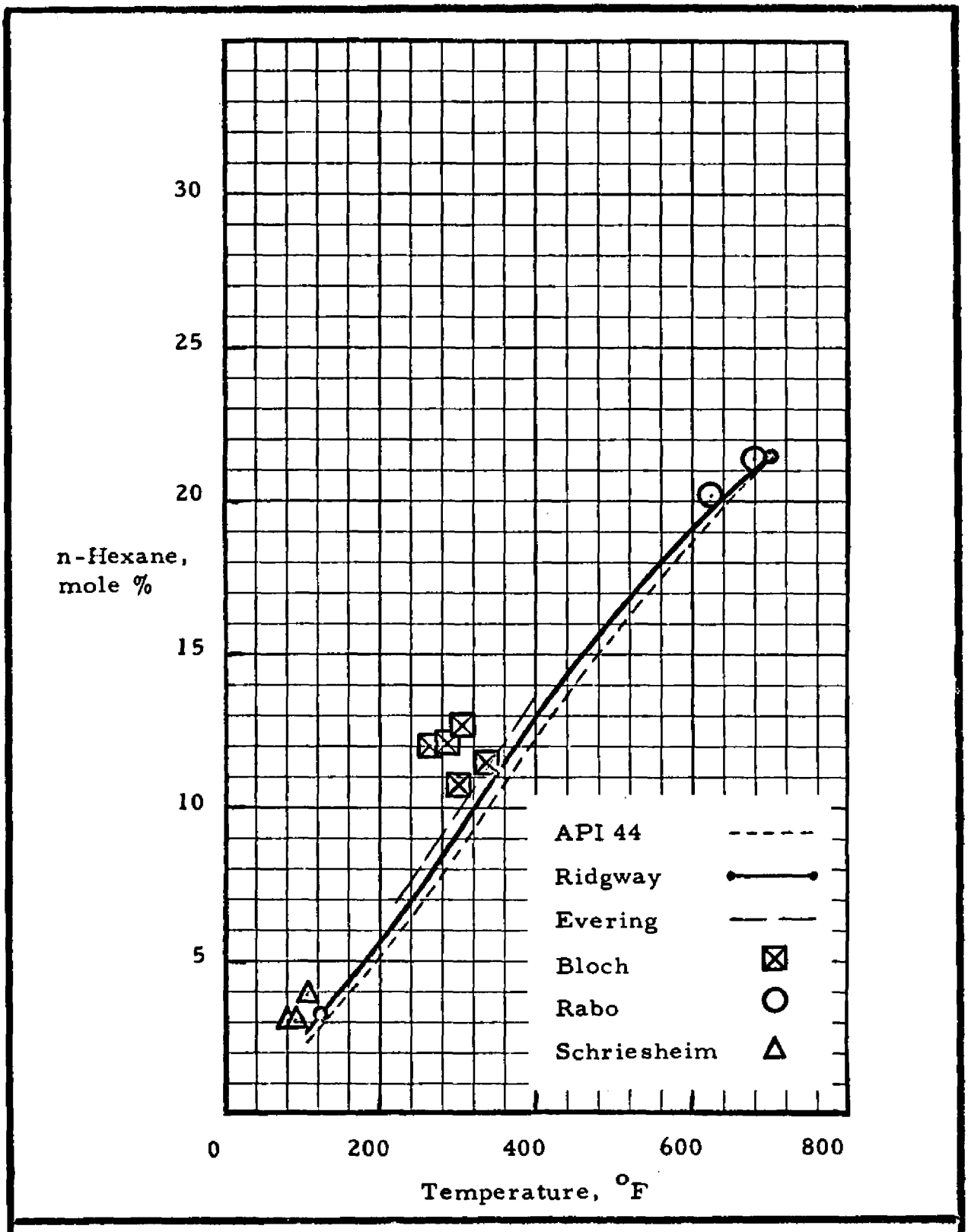

Figure 4. Vapor Phase Hexane Isomer Equilibrium For n-Hexane.

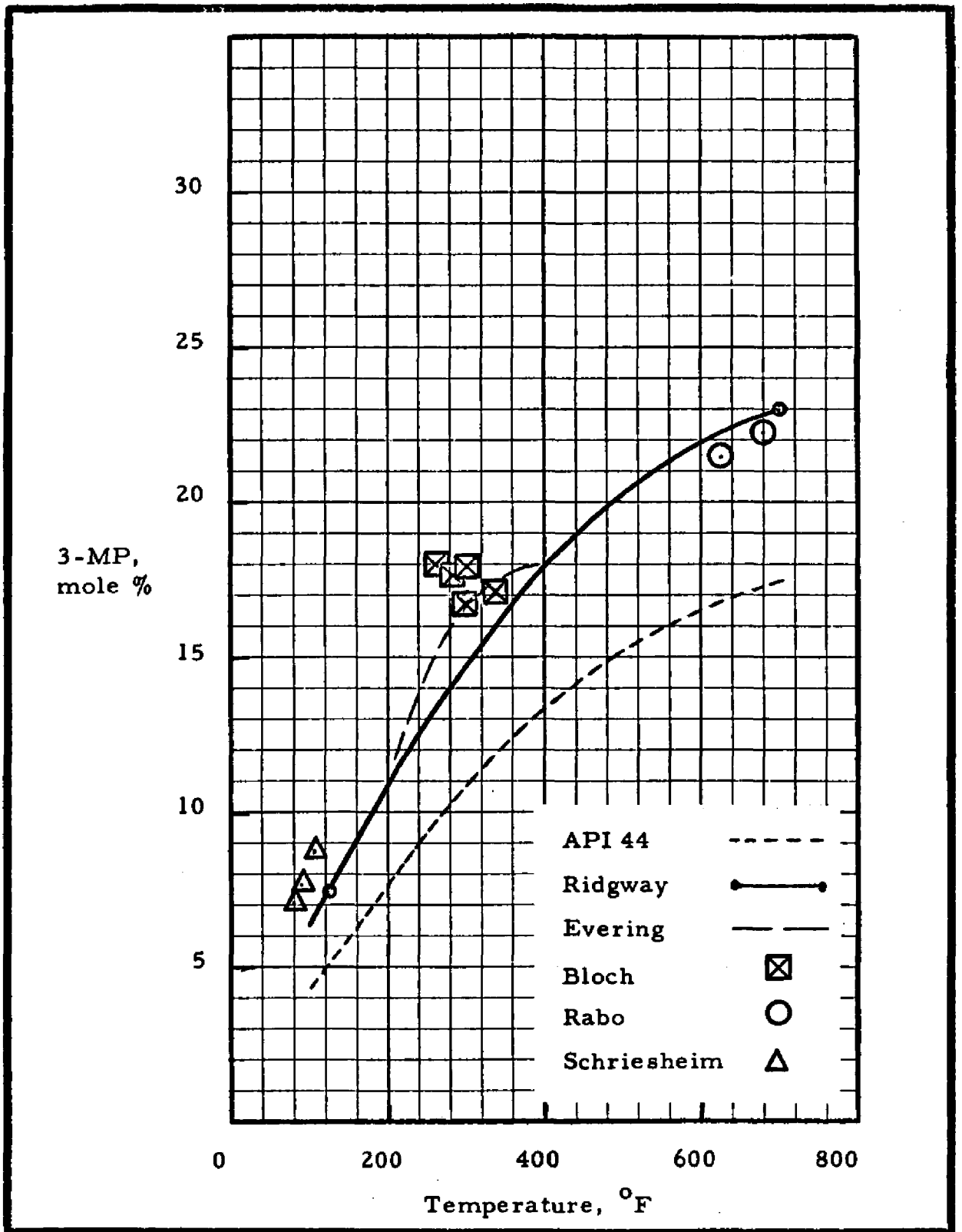

Figure 5 . Vapor Phase Hexane Isomer Equilibrium For 3-MP.

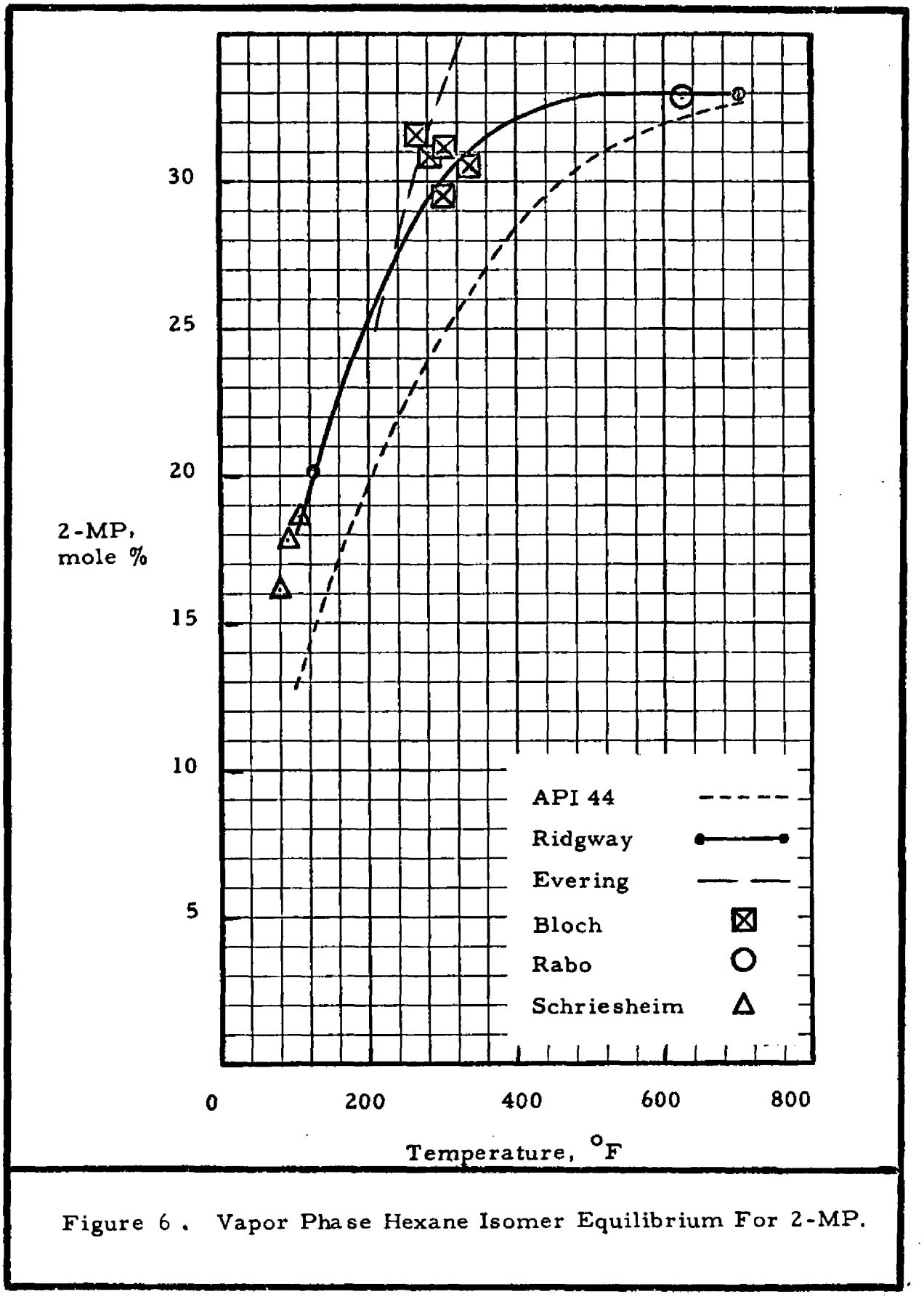

Figure 6. Vapor Phase Hexane Isomer Equilibrium For 2-MP.

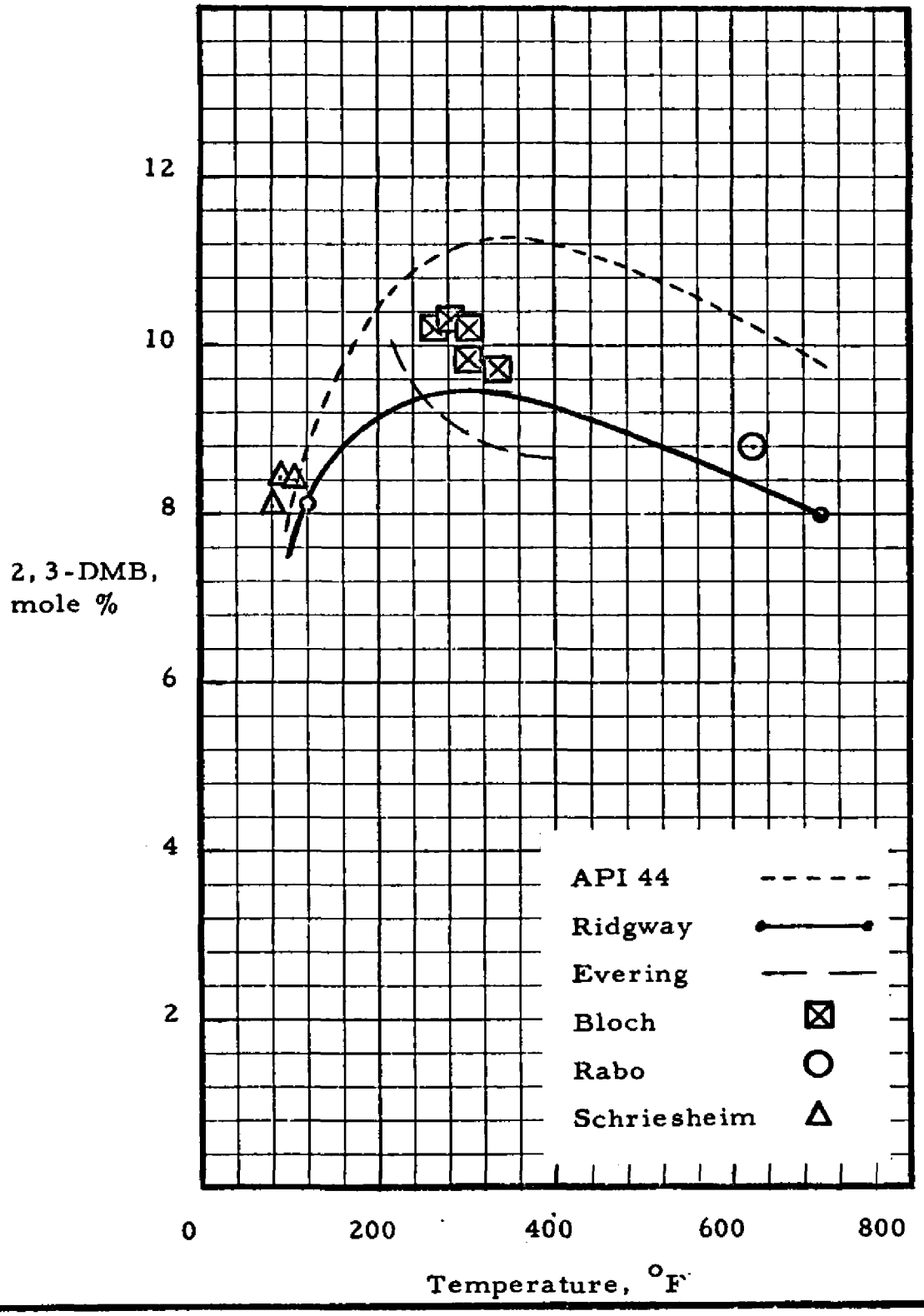

Figure 7. Vapor Phase Hexane Isomer Equilibrium For 2, 3-DMB.

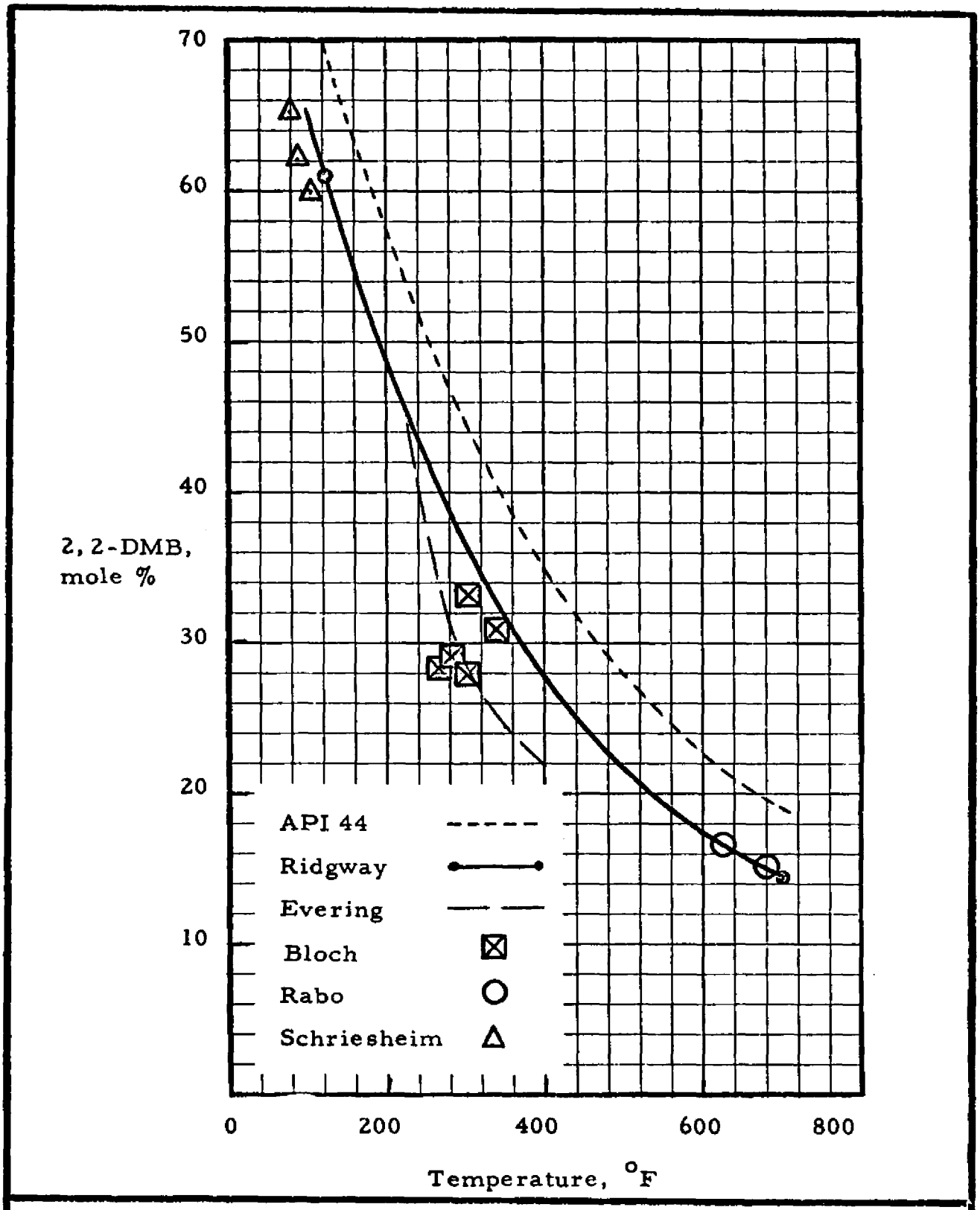

Figure 8 . Vapor Phase Hexane Isomer Equilibrium For 2, 2-DMB.

that essentially complete conversion of hexane to lighter paraffins is thermodynamically possible. Thermodynamic equilibrium calculations also show that low molecular weight olefins might be formed in very small concentrations (<0. 1 %).

3. Benzene

Calculations of the equilibrium concentrations of benzene formed by dehydrocyclization of n-hexane show that very little benzene would be thermodynamically feasible at the operating conditions used in this study.

D. Products From Cyclohexane Hydrocracking

1. Isomerization

Isomerization of the cyclohexane to methylcyclopentane can be expected in this research. The equilibrium concentrations of cyclohexane and methylcyclopentane calculated from free energy data are presented in Figure 9 (page 36).

2. Hydrocracked Products

As in n-hexane hydrocracking, lower molecular weight paraffins are produced in cyclohexane hydrocracking. Also ring opening of the cyclohexane and methylcyclopentane can produce hexane isomers.

3. Benzene

The production of several percent benzene would be thermodynamically feasible at the operating conditions used in this study of

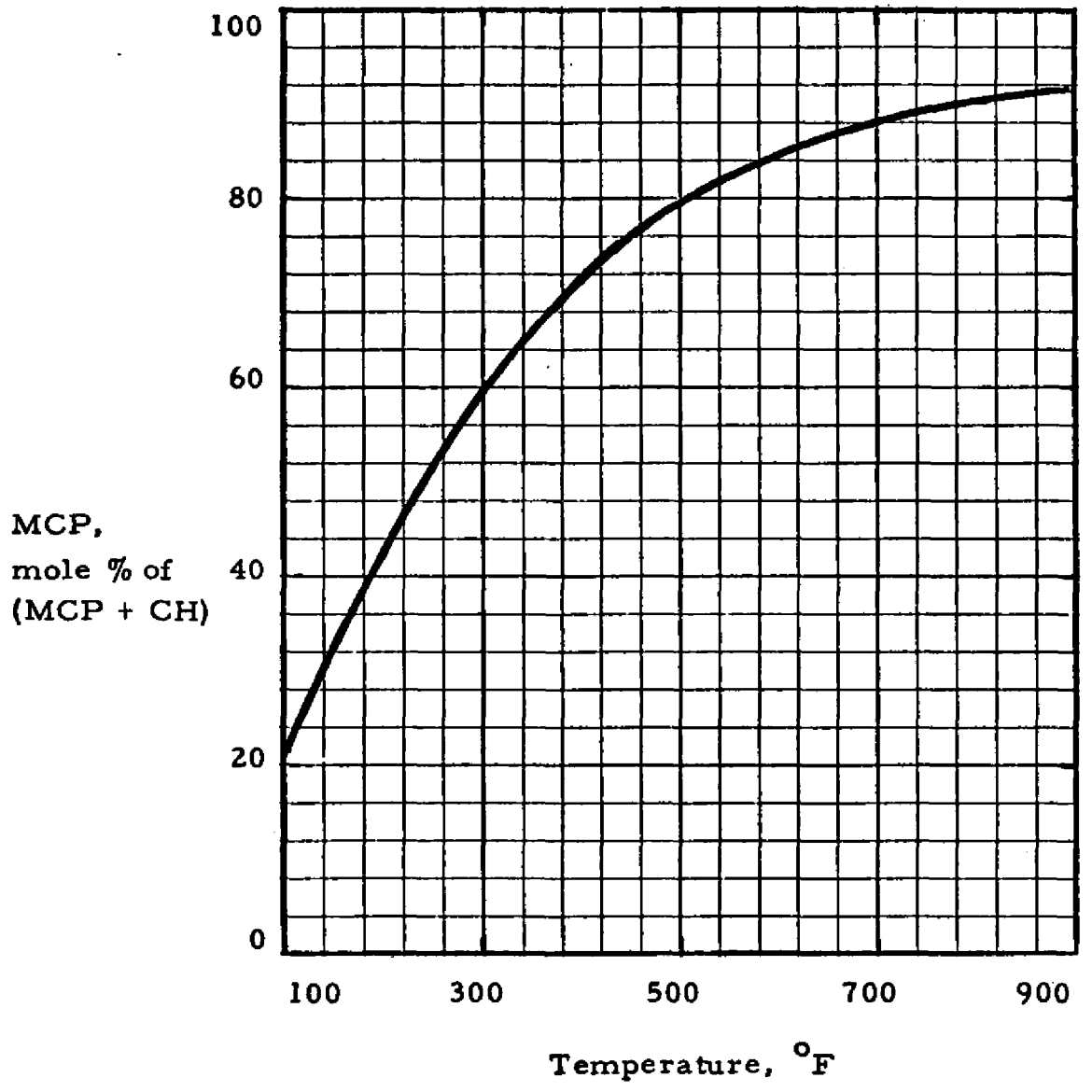

Figure 9. Vapor Phase Methylcyclopentane - Cyclohexane Equilibrium

cyclohexane hydrocracking. However, no appreciable benzene concentrations were found.

E. Conclusions from the Literature Survey

Several conclusions pertinent to this work can be drawn from the literature review. First, several zeolite catalysts are very active for isomerization of paraffins. Pd-H-mordenite has been shown to be more active than Pd-H-faujasite in the isomerization of n-pentane and n-hexane. Both mordenite and faujasite are active for hydrocracking practical feed stocks as evidenced in the patent literature.[73, 88, 90-96, 102, 103]

The reactions at the acidic site of dual function catalysts appears to be the controlling step in both hydrocracking and hydroisomerization. In hydrocracking, the actual scission reaction on the acidic site is the rate-controlling step. The hydrocracking reaction is first order with respect to the hydrocarbon for several reactants. Activation energies for hydrocracking n-hexane and cyclohexane over noble metal on alumina catalysts have been found to be about 60 and 30-35 kcal/gmole respectively. In hydrocracking decane over Pd-H-mordenite the activation energy was lower than that found for other catalysts. This indicates possible diffusional limitations in the mordenite pores for decane.

CHAPTER III

EXPERIMENTAL EQUIPMENT AND PROCEDURE

A. General

The equipment used in this study was originally obtained from Esso Research Laboratories for a research project sponsored by Esso Research and Engineering Company. Bryant, the original member of the research project, carried out the plans and design of this equipment. Modifications to the system were carried out by the author. The equipment is located in the Petroleum Processing Laboratory of the Chemical Engineering Department at Louisiana State University.

B. Equipment

1. Reactor System

a. Flow Plan

A simplified flow plan of the liquid feed system, gas feed system, reactor system, and the product recovery equipment appears in Figure 10 (page 39). The reactor system including the product recovery equipment was located inside a walk-in hood, the liquid feed system was located beside the hood, and the gas feed system was located partly outside the building and partly in the hood.

b. Reactor

A sketch of the reactor is shown in Figure 11 (page 40). The reactor itself was made of 1/2" schedule 80 Inconel pipe and held up to

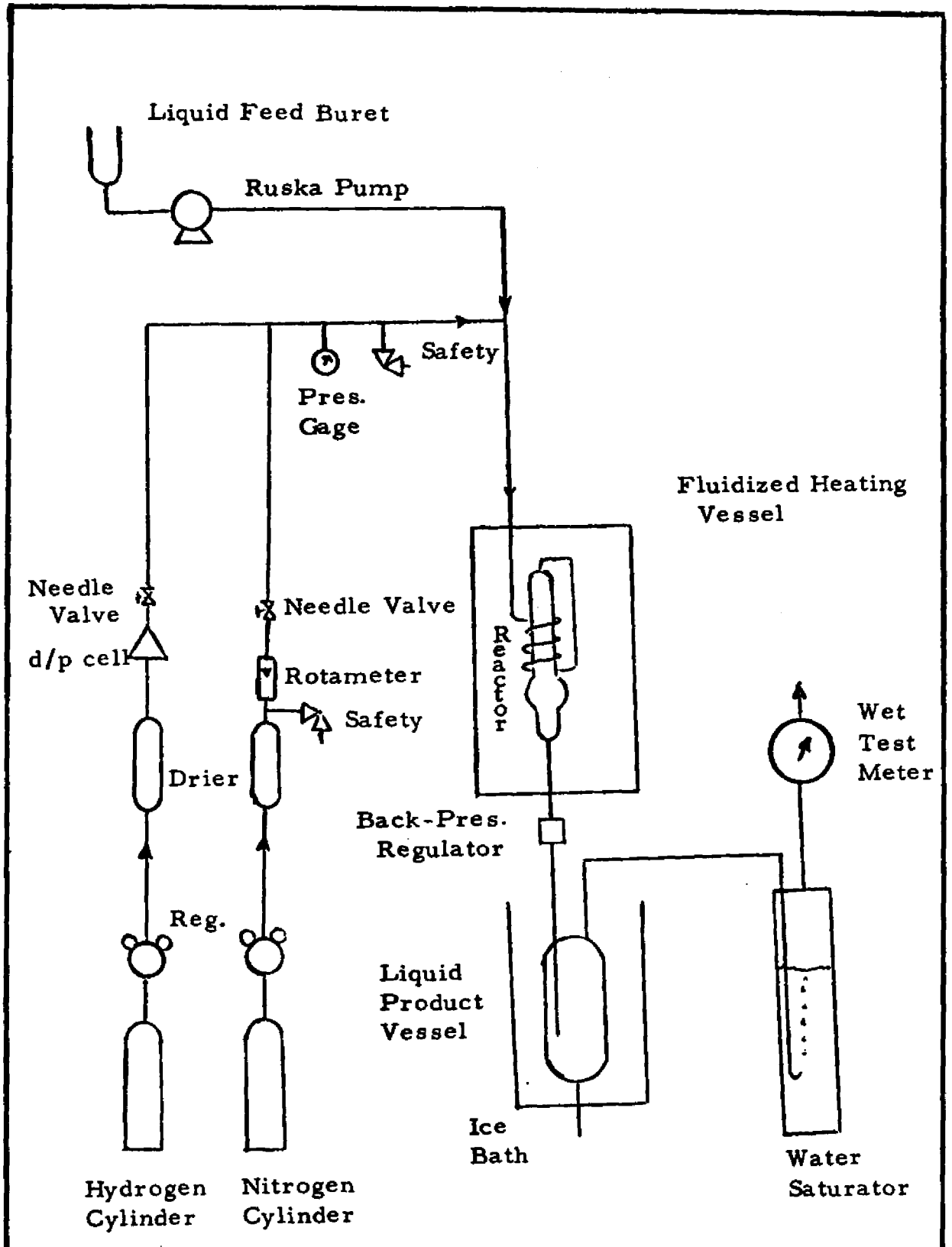

Figure 10. Simplified Flow Plan

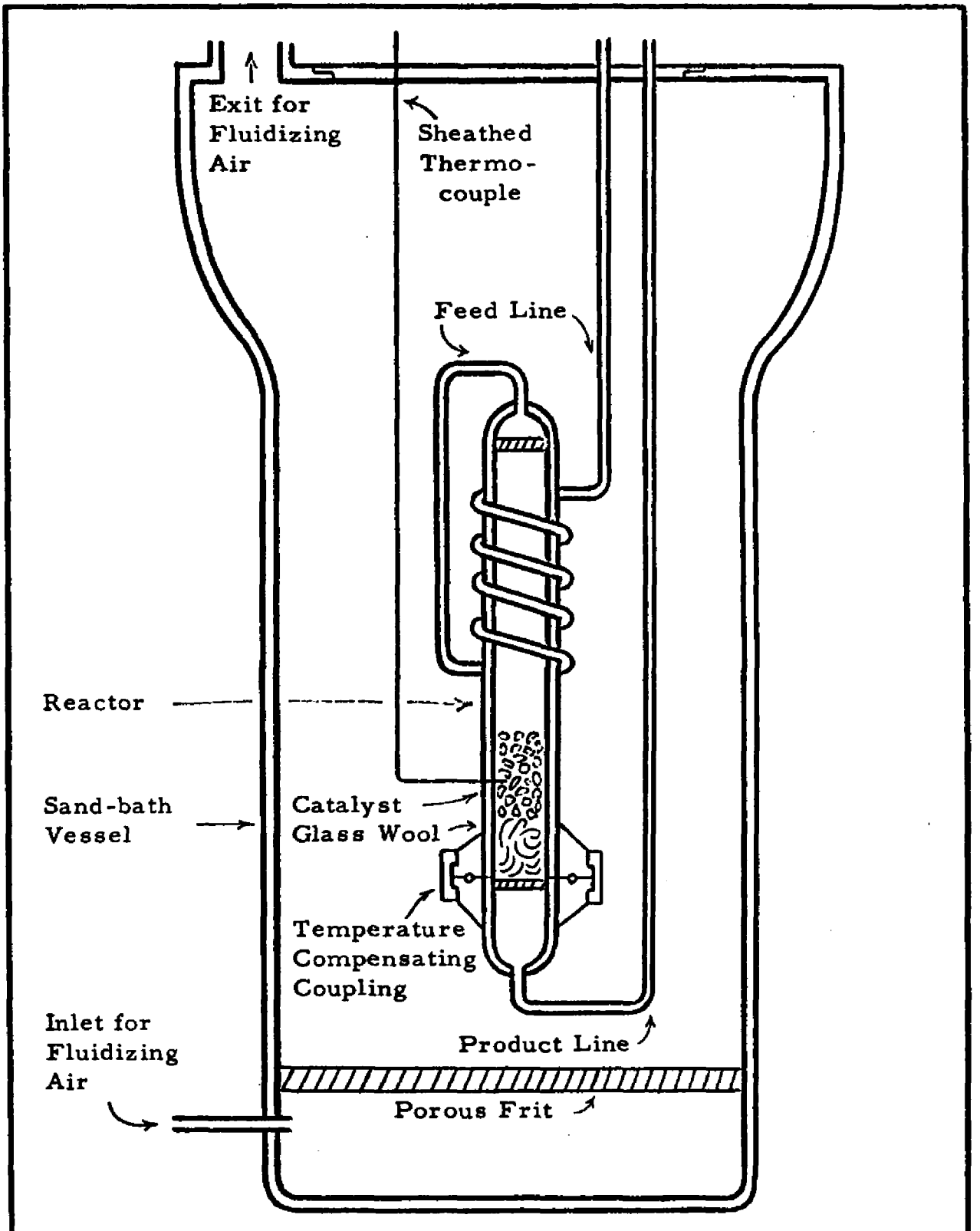

Figure 11. Reactor System in the Sand-bath Vessel.

about 50 cc of catalyst. Porous metal frits were placed above and below the catalyst bed. A means of easily charging and discharging the catalyst was provided by a temperature-compensating coupling. A steel O-ring provided a pressure-tight seal in the coupling.

An iron-constantan thermocouple inside the catalyst bed measured the catalyst temperature. The 1/16" diameter thermocouple passed through the reactor wall through a Conax fitting and 1/4" into the catalyst bed. In order to control the reactor temperature as closely as possible, the reactor was placed in a fluidized bed. This bed consisted of silica-alumina particles fluidized by a continuous stream of air. Electrical strip heaters, five kilowatts on manual control and two kilowatts on automatic control, heated the fluidized bed. The heaters were on the outside walls of the fluidized bed vessel beneath two inches of insulation. The manually controlled heaters were adjusted by a rheostat to provide most of the required heat. The automatically controlled heaters were controlled by a West temperature-indicator-controller. The West instrument used an iron-constantan thermocouple immersed in the fluidized bed. The catalyst bed temperature data were taken by a Leeds and Northrup temperature indicator.

The gas and liquid feeds were mixed in a tee prior to entering the heated zone. The feed line containing the liquid and gas feeds made several turns around the reactor and then entered into the top of the reactor. These turns were made to insure that the total feed would be vaporized and would enter the reactor at the desired temperature.

c. Product Recovery

The reactor products passed through a Grove "Mity-Mite" upstream pressure regulator which maintained the reactor pressure at the desired level. An ice-water bath was available to condense some of the heavier hydrocarbon components when the dew point of the reactor products happened to be above room temperature. This liquid product recovery was not necessary in many of the experimental runs. The gas phase product passed through a water saturator and a wet-test meter.

d. Contacting in Reactor

Bryant[16] made a detailed study of contacting in a reactor similar to the one used in this study. Bryant's results showed that at usual operating conditions the flow was essentially plug flow and that Bischoff's[12] method could predict Peclet numbers for the system. Particle Reynolds numbers for this study ranged from about 2 to 10, and predicted Peclet numbers ranged from about 50 to about 80.

2. Liquid Feed System

The liquid feed system consisted of a 250 cc glass buret and a precision, high pressure Ruska pump. Liquid was forced from the 250 cc pump cylinder by a piston driven by a synchronous motor and an adjustable gear system. Flow rates were adjusted manually by installing the appropriate reduction gears.

3. Gas Feed System

The gas feed system consisted of separate nitrogen and hydrogen feed equipment. Nitrogen and hydrogen cylinders were both located

outside the building. The nitrogen, used for purging the system, went inside the hood to a drier, pressure regulator, rotameter, and then to the reactor inlet. The hydrogen, one of the reactants, went in a separate line to the hood, to a drier, pressure regulator, integral orifice d P cell for measurement, a needle valve for control, past a pressure gage, safety valve, and to the reactor inlet.

4. Layout

The layout of the reactor system and the product recovery equipment is shown in Figure 12 (page 44). As mentioned previously, the reactor and product recovery systems were located in a walk-in hood. Inside the hood the entire system was mounted on a three feet by three feet by six feet high steel frame. A 3000 cfm exhaust fan and sliding safety-glass panels completed the hood assembly.

5. Analytical System

Analyses of the feed and product were made with a F&M Model 810R dual-column gas chromatograph. A ten foot column of 10% silicon rubber, SE-30, on 90% white chromosorb (80-100 mesh) was used for the separation of the hydrocarbon components. The column was maintained at 80°F for n-hexane runs and at 120°F for cyclohexane runs. Additional details appear in Appendix C.

C. Materials

1. Gases

Cylinders of prepurified nitrogen (99.99%) and prepurified hydrogen (99.95%) were used. Both gas streams passed through a

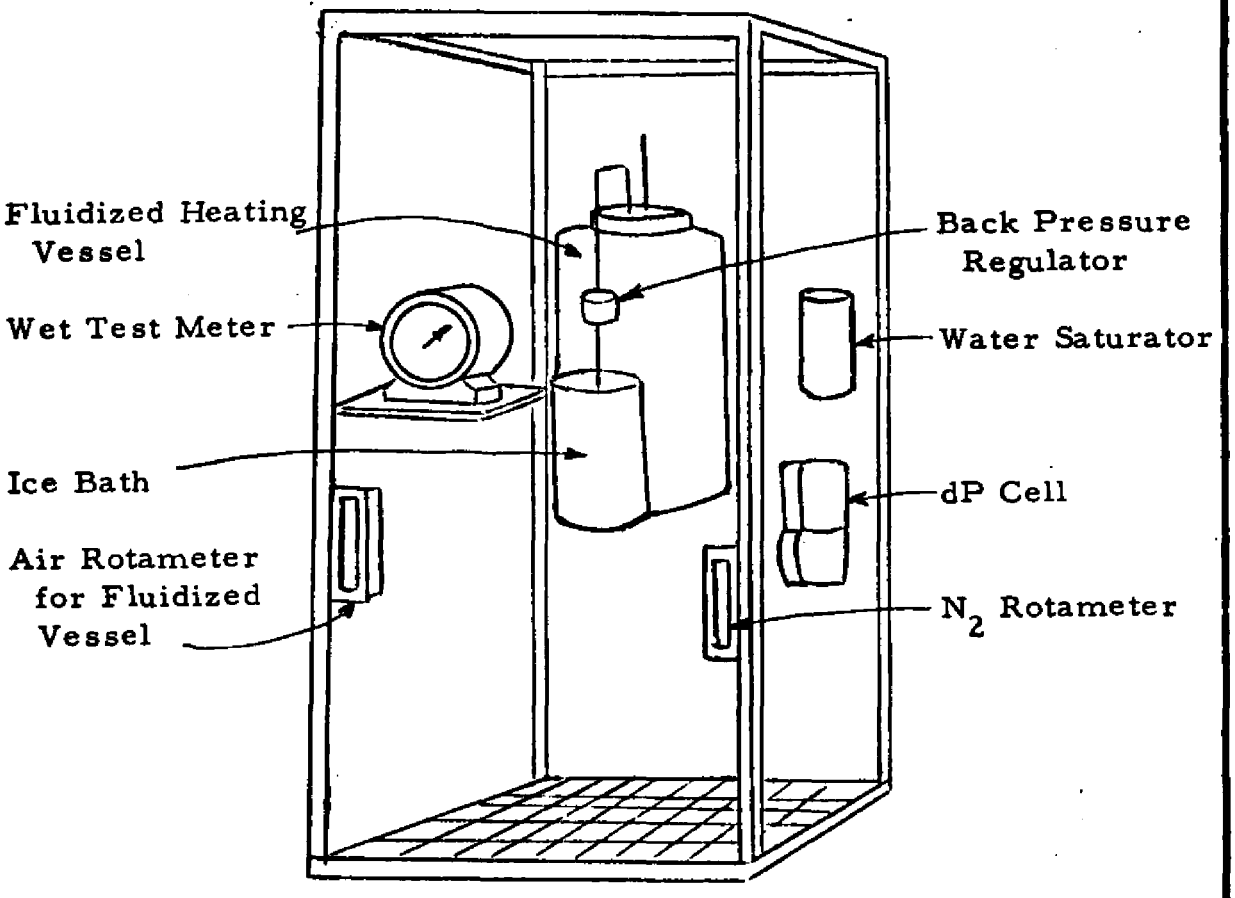

Figure 12. Layout

platinum-on-alumina bed, a 3A molecular sieve bed, and an indicating Drierite bed to insure that the gases were dry.

2. Liquid Feeds

All liquid feeds, n-hexane and cyclohexane, were Phillips pure grade, 99 + mole %. The liquid feeds were stored over 13X molecular sieve.

3. Catalysts

Two catalysts, Pd-H-mordenite and Pd-H-faujasite, were used in this work. The Pd-H-mordenite was prepared at Esso Research Laboratories in Baton Rouge, Louisiana from 1 - 5 micron particles of Na-mordenite obtained from Norton Company. The Na-mordenite was exchanged to NH_4-mordenite, impregnated with 0.5 wt. % palladium, pilled, and then crushed into various size particles. The Pd-NH_4-mordenite then was converted into Pd-H-mordenite as follows:

(1) Shallow glass dish containing the catalyst was placed in an oven.

(2) Dry air was metered at 1000 cc/hr per cc of catalyst across the catalyst.

(3) Temperature was raised from ambient to 350°F at a rate of 100°F/hr.

(4) Temperature was held at 350°F for 16 hours.

(5) Temperature was raised from 350°F to 1000°F at a rate of 100°F/hr.

(6) Temperature was held at 1000°F for 2 hours.

(7) Temperature was cooled to 550°F.

(8) Catalyst was transferred to glass vials with stoppers.

(9) Catalyst was placed in a dessicater at room temperature.

The Pd-H-faujasite, SK100, was obtained from the Linde Company. This catalyst was obtained as pills and subsequently was crushed and separated into various size particles. This catalyst also had 0.5 wt. % palladium. The calcination in dry air treatment described for the mordenite also was used on the faujasite catalyst prior to the experimental studies.

D. Procedure

1. Experimental

The same procedure was followed closely in all experiments. First, a weighed sample of the desired catalyst was charged into the reactor. The standard charge was approximately 15 cc of catalyst, and this volume was used in all experiments except the bulk diffusion studies. The bulk diffusion experiments have the volume of catalyst charged indicated on the data tables in Appendix A.

After the catalyst was placed in the reactor, a piece of glass wool was added to hold the catalyst in place. Then the reactor was sealed with a steel O-ring, and a clamp was tightened around the coupling. The reactor was pressure tested at 800 psig prior to being

placed in the fluidized heating vessel. The heating vessel had been adjusted previously to the desired temperature. After the reactor was placed in the heating vessel, a nitrogen purge was set at 0.5 ft.^{3}/hr. After 30 minutes of purge, the catalyst temperature reached the fluidized bath temperature.

While the reactor was being purged with nitrogen, the feed pump was charged, and the reduction gears were set to give the desired feed rate when started. Hydrogen flow was started through the reactor at 0.5 ft.^{3}/hr. after the 30 minute nitrogen purge. After 30 minutes on hydrogen, the reactor was pressure tested again at 800 psig. Then the system pressure was set at the desired operating level by adjusting the "Mity-Mite" regulator.

Next the hydrogen rate was set by adjusting the needle valve. A stop watch and the wet test meter determined the hydrogen rate. Then the feed pump was started. After 90 minutes of operation, a 20 minute material balance was made.

During the material balance a sample of product gas was taken for analysis by gas chromatograph. Liquid product, collected when the product gas dew point was above ambient temperature, was collected, weighed, and analyzed by gas chromatograph. In most of the experiments no liquid product was collected. The balance temperature, pressure, liquid feed rate, hydrogen feed rate and outlet gas rate were recorded. Then the operating conditions were adjusted for the next material balance. After the final balance period, the liquid and gas

feeds were discontinued, the reactor depressured and removed from the heating vessel.

2. Calculations

Analytical data from the experimental runs were the integrated areas of gas chromatograph peaks related to various hydrocarbon compounds in the product gas and liquid. The composition of the products was calculated from the peak areas as described in Appendix C.

The product composition together with reactor temperature and pressure, inlet and outlet flow rates, time of material balance, weight of catalyst charged, and size of the catalyst particles were used to calculate the results of the experimental run. Calculations made with these data are described in detail in Appendix D.

CHAPTER IV

KINETIC MODEL

A. Initial Simplified Model

1. N-Hexane Hydrocracking

The initial model for hydrocracking n-hexane was based on the following assumptions:

1. The rate-controlling step is the reaction of hydrocarbon and hydrogen to form lower molecular weight paraffins.
2. The hydrocracking reaction can be considered irreversible.
3. The hexane isomers have about the same hydrocracking rate.

The first assumption is based on conclusions from the literature survey. The second assumption appears to be valid from thermodynamic equilibrium considerations. In the temperature range of this study almost complete conversion to hydrocracked products is thermodynamically possible. The third assumption will have to be evaluated by examining experimental results.

The reaction would be

$$[nC_6 \rightleftharpoons iC_6\text{'s}] + H_2 \xrightarrow{k} \text{hydrocracked products.}$$

The rate of hydrocracking hexanes is

$$\text{Rate} = -dC_A/dt = k\,C_A C_B$$

where C_A = concentration of hexanes, moles/unit volume

C_B = concentration of hydrogen, moles/unit volume

t = contact time with the catalyst

k = simplified reaction rate constant.

This form of kinetic expression can be considered pseudo-homogeneous as discussed by Petersen[51] and Levenspiel.[39]

In hydrocracking, the hydrogen concentration is required to be large in comparison with the hydrocarbon concentration in order to prevent catalyst activity loss due to "coking". This means that the hydrocarbon concentration will be rate-controlling, and the rate equation will become

$$\text{Rate} = -dC_A/dt = k\,C_A. \qquad (2)$$

Separating variables and integrating,

$$-\int_{C_{Ao}}^{C_A} dC_A/C_A = k\int_0^{t_H} dt \quad , \qquad (3)$$

and

$$-\ln(C_A/C_{Ao}) = k\,t_H \quad . \qquad (4)$$

where t_H = superficial contact time based on catalyst weight.

Also, since the reaction is equi-molal,

$$C_A = C_{Ao} - C_{Ao}X \quad , \qquad (5)$$

where X = fraction converted.

Substituting in equation (4)

$$- \ln \frac{C_{Ao}(1 - X)}{C_{Ao}} = kt_H, \qquad (6)$$

or $$- \ln (1 - X) = kt_H. \qquad (7)$$

The superficial contact time with the catalyst can be calculated based on catalyst weight by the following equation

$$t_H = 3600\ W \cdot \rho g \cdot M / F(1 + R) \qquad (8)$$

where

t_H = superficial contact time, sec - gm / cc total gas

W = weight of catalyst, gm

ρg = gas density at operating conditions, gm moles/cc

M = molecular weight of hydrocarbon

F = flow rate of hydrocarbon, gm/hr

R = molar ratio of hydrogen to hydrocarbon in feed gas.

Also the contact time could be based on the catalyst volume. The contact time based on volume is related to the time based on weight by

$$t = t_H / \rho c \qquad (9)$$

where

t = contact time based on catalyst volume, sec - cc catalyst/cc gas

t_H = contact time based on catalyst weight, sec - gm/cc gas

ρc = catalyst bulk density, gm/cc.

In this work the contact time based on weight will be used in the calculations because the catalyst weight is measured more precisely than the volume.

2. Cyclohexane Hydrocracking

The simplified model for cyclohexane hydrocracking is based on assumptions similar to the assumptions for n-hexane. The simple ring opening plus hydrogenation reaction is not considered separately. The reaction would be

$$[CH \rightleftharpoons MCP] + nH_2 \xrightarrow{k_1} \text{hydrocracked products}$$

where n = 1 for ring opening, n = 2 for C_1 - C_5 products

CH = cyclohexane

MCP = methylcyclopentane

hydrocracked products = paraffins, methane through hexanes.

This reaction rate is

$$\text{Rate} = -dC_C/dt = k_1 C_C C_B^2 \qquad (10)$$

for the reaction to form methane through pentane,

and

$$\text{Rate} = -dC_C/dt = k_1 C_C C_B \qquad (10a)$$

for the reaction to form hexanes.

where

C_C = concentration of naphthenes (MCP + CH), moles/unit volume

C_B = concentration of hydrogen, moles/unit volume

t = contact time with the catalyst

k_1 = simplified reaction rate constant.

As in hexane hydrocracking, the hydrogen concentration is very large in comparison to the naphthene concentration. Again the hydrocarbon concentration will be rate-controlling. Therefore,

$$\text{Rate} = -dC_C/dt = k_1 C_C. \qquad (11)$$

In the exact manner of equations (2) - (8), equation (11) yields

$$-\ln(1 - X) = k_1 t_H \quad . \qquad (12)$$

B. Langmuir - Hinshelwood Equations

1. N-Hexane Hydrocracking

Assuming the applicability of Langmuir adsorption isotherms [30] for the reaction rate-controlled system, the simplified rate constant will be related to the adsorption terms as follows

$$k = k_o K_A/(1 + K_A p_A + K_B p_B + K_p p_p) \qquad (13)$$

for a "single site" mechanism, and

$$k = k_o K_A/(1 + K_A p_A + K_B p_B + K_p p_p)^2 \qquad (14)$$

for a "dual site" mechanism; where

k = simplified rate constant

k_o = reaction rate constant, depending on the catalyst and the temperature

K_A, K_B, K_p = adsorption equilibrium constants for hexanes, hydrogen, and hydrocracked products, respectively.

p_A, p_B, p_p = partial pressures of hexanes, hydrogen, and hydrocracked products, respectively.

A "single site" mechanism involving two reactants, hydrocracking for example, would be a system wherein one of the reactants is adsorbed on the catalyst surface. Reaction occurs when the other reactant in the gas phase "collides" with the adsorbed reactant. One "dual site" mechanism for hydrocracking would be a system wherein an adsorbed molecule reacts with another molecule on adjacently situated active centers. Another "dual site" mechanism could be a system wherein one of the reactants is adsorbed on one active site. One of the adjacent sites must be unoccupied for the reaction to occur. During the reaction, part of the adsorbed molecule is connected to the original site and part to the site that was originally vacant. At the completion of the reaction, one of the hydrocracked fragments is desorbed from one site and the other fragment from the second site.

Since the data in this study were obtained with an integral reactor, partial pressures of the components were changing along the length of the catalyst bed during every run. However, the hydrogen concentrations were very large and remained almost constant. The hydrocarbon partial pressures varied, but were relatively small.

Several possibilities may simplify equations (13) and (14). For example, if all reactants and products are weakly adsorbed, such that

$$(K_A p_A + K_B p_B + K_p p_p) \ll 1$$

then equations (13) and (14) would reduce to

$$k = k_o K_A \qquad (15)$$

This indicates that the initial simplified model will adequately describe a system with weak adsorption. The simplified model implies that, at a given temperature, the conversion is a function of contact time alone, and is independent of the partial pressures of components in the system.

Another possibility would be that

$$K_B p_B \gg (K_A p_A + K_p p_p)$$

throughout the length of the reactor.

Since high hydrogen partial pressures are required to maintain catalyst activity, this possibility is likely at conventional hydrocracking conditions. This does <u>not</u> mean, of course, that the adsorption constant for hydrogen is much larger than those for hydrocarbons.

In this case equation (13) becomes

$$k = k_o K_A/(1 + K_B p_B) \quad , \qquad (16)$$

and equation (14) becomes

$$k = k_o K_A/(1 + K_B p_B)^2 \quad . \qquad (17)$$

An alternate possibility is

$$K_B p_B \gg (K_A p_A + K_p p_p)$$

and

$$K_B p_B \gg 1.$$

Then equation (13) becomes

$$k = k_o K_A/K_B p_B \quad , \qquad (18)$$

and equation (14) becomes

$$k = k_o K_A/K_B^2 p_B^2 \quad . \qquad (19)$$

2. Cyclohexane Hydrocracking

Again assuming the applicability of Langmuir adsorption isotherms, the simplified rate constant for cyclohexane hydrocracking will be related to the adsorption terms as follows

$$k_1 = k_{1,0}K_C/(1 + K_Cp_C + K_Bp_B + K_pp_p) \qquad (20)$$

for a "single site" system, and

$$k_1 = k_{1,0}K_C/(1 + K_Cp_C + K_Bp_B + K_pp_p)^2 \qquad (21)$$

for a "dual site" system. These equations can be reduced in a similar manner to equations (13) through (19).

The applicability of the kinetic expressions presented in this chapter will be tested for hydrocracking n-hexane and cyclohexane over Pd-H-faujasite and Pd-H-mordenite catalysts. The following chapters present the experimental results from this study.

CHAPTER V

EXPERIMENTAL RESULTS - FAUJASITE CATALYST

A. Introduction

As was discussed earlier, an integral reactor with a fixed bed of catalyst was used to obtain data on hydrocracking n-hexane and cyclohexane over Pd-H-faujasite and Pd-H-mordenite catalysts. The objective of these studies was to determine the activity and selectivity of these catalysts and to develop a mathematical model for the hydrocracking of n-hexane and cyclohexane. The models, presented in the previous chapter, were based on conclusions drawn from the literature. In this chapter and the next the applicability of these models will be examined. This chapter deals with the experimental results on the faujasite catalyst.

B. N-Hexane Hydrocracking

1. Effect of Mass Transfer

In heterogeneous catalysis with porous solid catalysts there are several processes that may cause resistance to the chemical reaction. These processes are normally thought of as

1. Mass transfer from the main body of the fluid to the exterior surface of the catalyst.

2. Diffusion through the catalyst pores to the interior of the catalyst.
3. Adsorption of the reactant on the interior catalyst surface.
4. Chemical reaction on the catalyst surface.
5. Desorption of the products from the catalyst surface.
6. Diffusion of the products out of the catalyst pores.
7. Mass transfer of the products from the exterior of the catalyst into the main gas stream.

The second process, pore diffusion, can be subdivided for certain catalysts. These catalysts are prepared by compacting small particles to form pills or pellets. In the pilled catalysts the reactants diffuse through the "macropores" formed by spaces separating the original small particles and then diffuse through the "micropores" into the interior of the small particles.

One of the early phases of this research was concerned with the first of these processes, mass transfer. An evaluation of the effects of mass transfer was made by making a series of runs with varying gas velocities. Other process conditions were kept relatively constant. These runs are summarized in Table 1 (page 59), and a plot of the simplified reaction rate constant versus the gas velocity is shown in Figure 13 (page 60). As can be seen, the conversions and the observed rate constants were not affected by the gas velocity. If fluid-to-particle

Table 1. Test for Mass Transfer Limitations -- Simplified Reaction Rate Constant vs. Gas Velocity, Faujasite Catalyst

Operating Conditions

Temperature, °F	750
Pressure, psia	765
Feed	n-Hexane
Catalyst	Pd-H-Faujasite

Run Results

Run No.	10	11	12
Gas Velocity, cm/sec	0.71	0.99	0.22
Feed Rate, w/hr-w	2.16	2.25	2.16
H_2 Rate, moles/mole C_6	9.05	8.33	8.20
Hydrocracking, %	46.6	48.2	52.3
Simplified Rate Constant, k, cc/gm-sec	0.0464	0.0467	0.0500

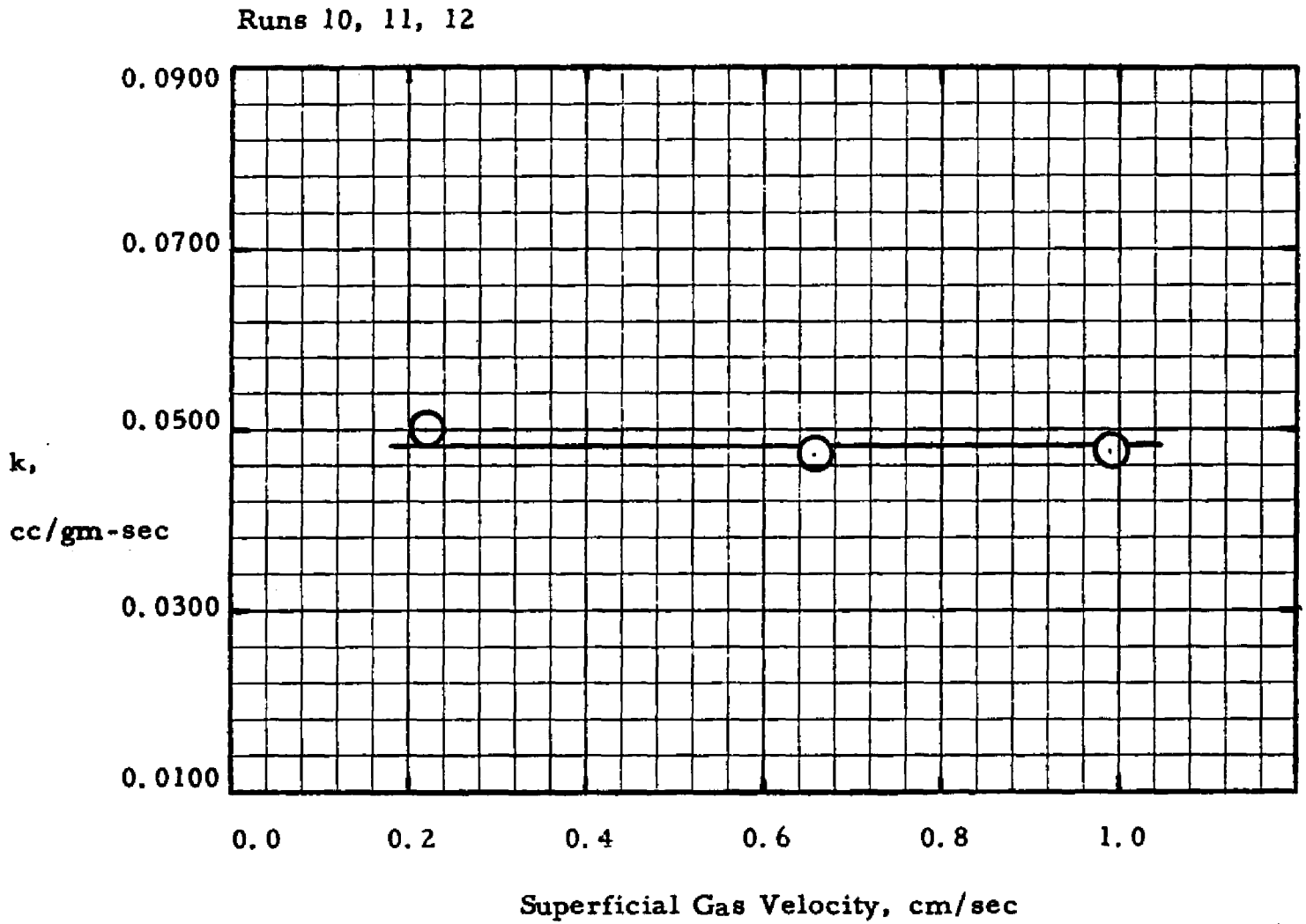

Figure 13. Test for Mass Transfer Limitations, Hexane Hydrocracking Over Pd-H-Faujasite

mass transfer had been a limiting step in the process, the high velocity run would have shown a significantly higher conversion than was observed at the lower gas velocities. These three runs indicate that mass transfer is not limiting within the range of velocities employed in this investigation.

2. Effect of Pore Diffusion

The next step to be investigated was the diffusion resistance. As reported by Bryant[16] and Beecher[9], testing of diffusion in the ultimate zeolite crystallite cannot be determined by the conventional method. Normally, in porous catalysts, the catalyst pellet size is varied to test for pore diffusion. As the pellet size is lowered, the average pore length is shortened. If pore diffusion is a limiting resistance, then the smaller pellet will produce higher conversions as long as the other process conditions remain constant.

Zeolite catalysts, however, are made from particles in the 1-10 micron size range. These particles will be referred to as "microparticles." The microparticles are then pilled. For this study, the faujasite catalyst pills were crushed and sized. Four size ranges were obtained from the crushing and sizing operation. The sizes of these "macroparticles" were 0.043-0.074 mm, 0.074-0.147 mm, 0.147-0.370 mm, and 0.42-0.84 mm. These size ranges of faujasite macroparticles were tested for n-hexane hydrocracking at 750°F, 765 psia, 2 v/hr-v, and 10 moles H_2/mole C_6. The results, shown in Table 2

(page 63) and Figure 14 (page 64) indicate no trend of increased conversion at the smaller sizes.

These results imply that there is no diffusional limitation in the "macropores." These macropores are channels between the microparticles. However, diffusion in the microparticle pores was not tested in these experiments since the microparticles were the same size in all cases. If micropore diffusion is significant, its effect would be included in the overall reaction rate.

3. Pseudo-First Order Reaction

In Chapter IV a simplified reaction model was assumed.

$$[nC_6 \rightleftharpoons iC_6] + H_2 \xrightarrow{k} \text{hydrocracked products}$$

Integration of the rate equation led to

$$-\ln (1-x) = k\, t_H. \qquad (22)$$

Therefore a plot of the function -log (1-x) versus the contact time should yield a linear relationship. A series of runs was made at a constant temperature, constant total pressure, and relatively constant partial pressures. The contact time was varied by varying hydrocarbon and hydrogen feed rates at a relatively constant ratio of these two rates. A plot of these results is shown in Figure 15 (page 65). As can be seen, a linear relationship was obtained. These data represent hydrocracking conversions from 13 to 92%.

4. Effect of Hydrogen Partial Pressure

As mentioned previously, the hydrogen partial pressure must be relatively high in hydrocracking in order to maintain catalyst activity.

Table 2. Effect of Catalyst Particle Size on n-Hexane Hydrocracking over Pd-H-Faujasite

Operating Conditions

Temperature, °F	750
Pressure, psia	765
Feed	n-Hexane
Catalyst	Pd-H-Faujasite
Space velocity, v/hr-v	2
H_2/C_6, mole ratio	9
Run Nos.	1B, 2A, 7, 8, 9

Run Results

Catalyst Size, mm	Hydrocracking, %	Simplified Rate Constant, k, cc/gm sec
0.043-0.074	41.5	0.0457
0.074-0.147	44.5	0.0469
0.147-0.370	47.8	0.0477
0.42-0.84	39.7	0.0470
0.42-0.84	40.8	0.0500

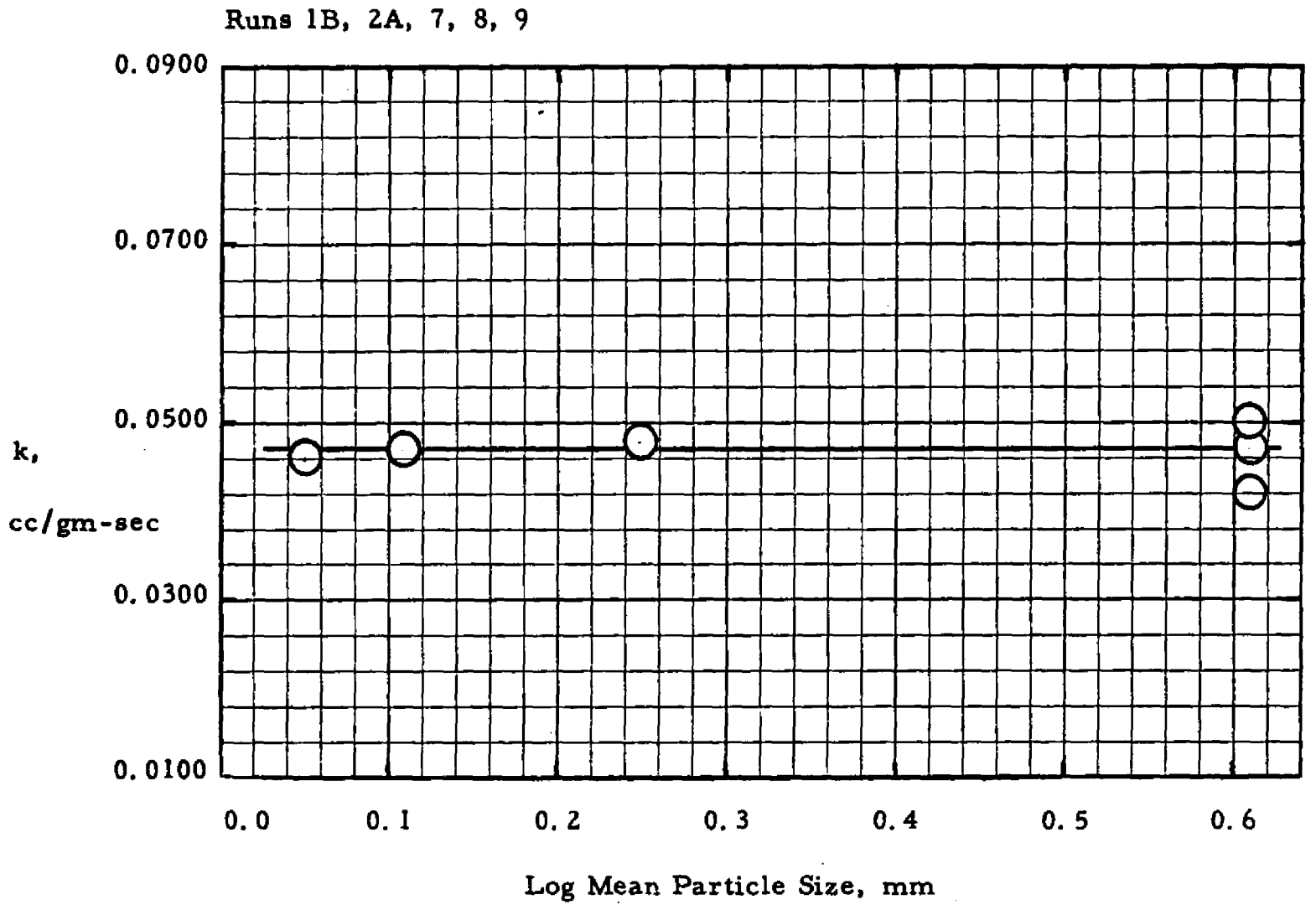

Figure 14. Effect of Catalyst Particle Size on Hexane Hydrocracking Over Pd-H-Faujasite

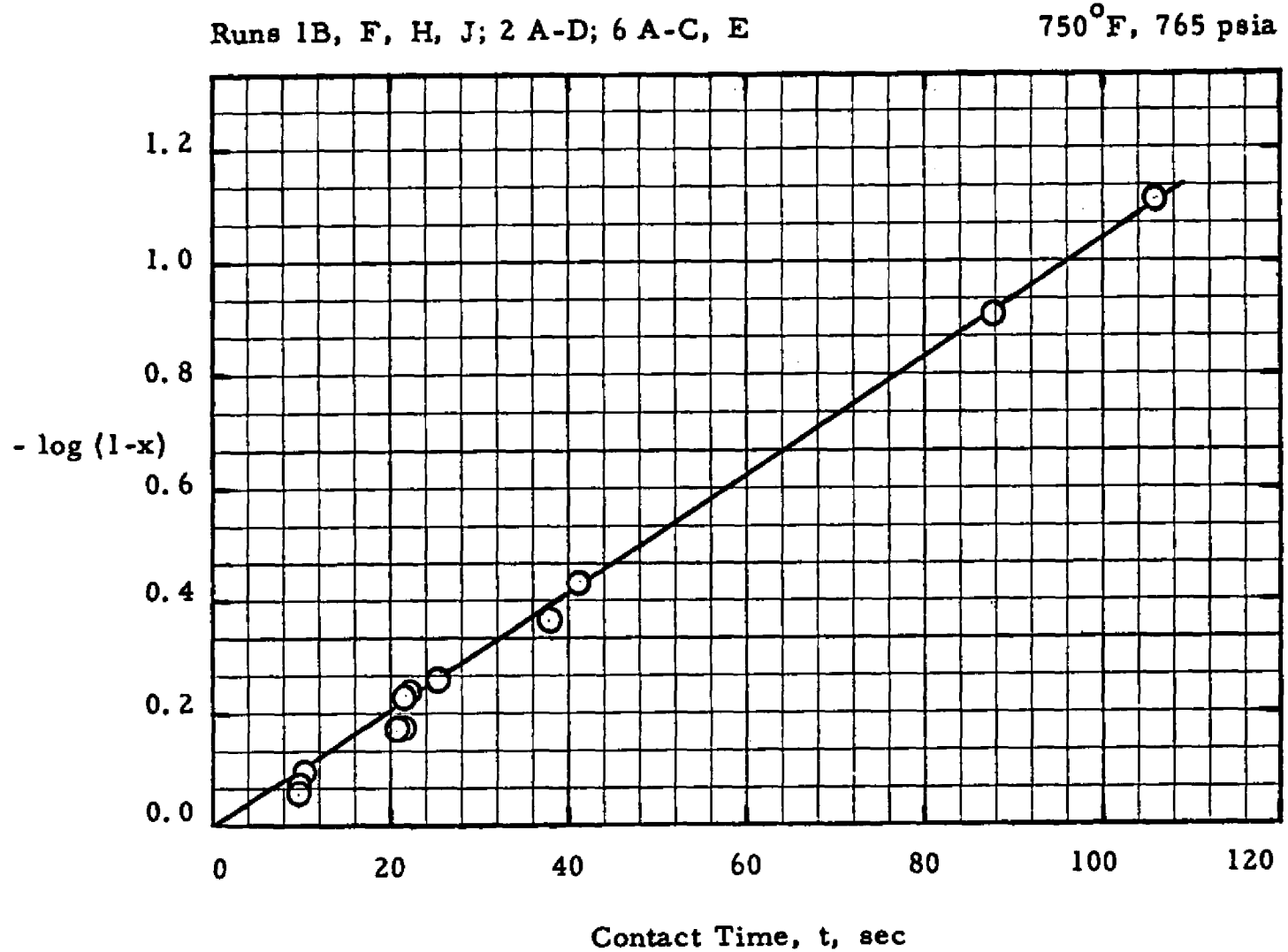

Figure 15. Test of Simplified First Order Model, Hexane Hydrocracking Over Pd-H-Faujasite

Therefore, the hydrogen-to-hexane mole ratio was large in all the experimental runs. A series of runs was made with the hydrogen ratio varying from about 5/1 to about 18/1. In these runs the mole fraction of hydrogen varied from about 0.83 to 0.95. Therefore, at a constant total pressure, the hydrogen partial pressure varied only slightly. Another series of runs was made by varying the total pressure. Again the hydrogen partial pressure was about 90% of the total pressure. Since the hydrogen partial pressure was 80-95% of the total pressure in all cases, and the Langmuir-Hinshelwood model employs an effect of hydrogen partial pressure, the H_2 partial pressure is used in the following correlations. The results of the H_2 ratio and total pressure variable study are shown in Table 3 (page 67). The effect of partial pressure on the simplified rate constant is shown in Figure 16 (page 68).

As presented in Chapter IV, the simplified rate constant, k, is related to the partial pressures by

$$k = k_o K_A/(1 + K_A p_A + K_B p_B + K_p p_p)^n \qquad (23)$$

where n = 1 for a single site mechanism and n = 2 for a dual site mechanism. Since the H_2 partial pressure, p_B, is much larger than the hexane or hydrocracked product partial pressures, it appears logical to assume

$$K_B p_B >> K_A p_A + K_p p_p.$$

Then the rate equation would become

$$\text{Rate} = -dC_A/dt = k_o K_A C_A/(1 + K_B p_B)^n \qquad (24)$$

Table 3. Effect of Hydrogen Partial Pressure on Simplified Rate Constant in n-Hexane Hydrocracking Over Pd-H-Faujasite

Operating Conditions

Temperature, °F	750
Pressure, psia	365-815
Feed	n-Hexane
Catalyst	Pd-H-Faujasite
Space velocity, v/hr-v	2
Run Nos.	2 C-I

Run Results

Run No.	k, cc/gm-sec	Partial Pressures, atm P_B	P_A	P_p
2C	0.0500	38.2	3.7	10.1
2D	0.0416	44.8	3.4	3.8
2E	0.0370	47.3	3.7	4.5
2F	0.0460	39.1	3.1	3.0
2G	0.0767	30.3	2.1	2.6
2H	0.1150	21.3	1.4	2.1
2I	0.0400	45.6	3.4	3.0

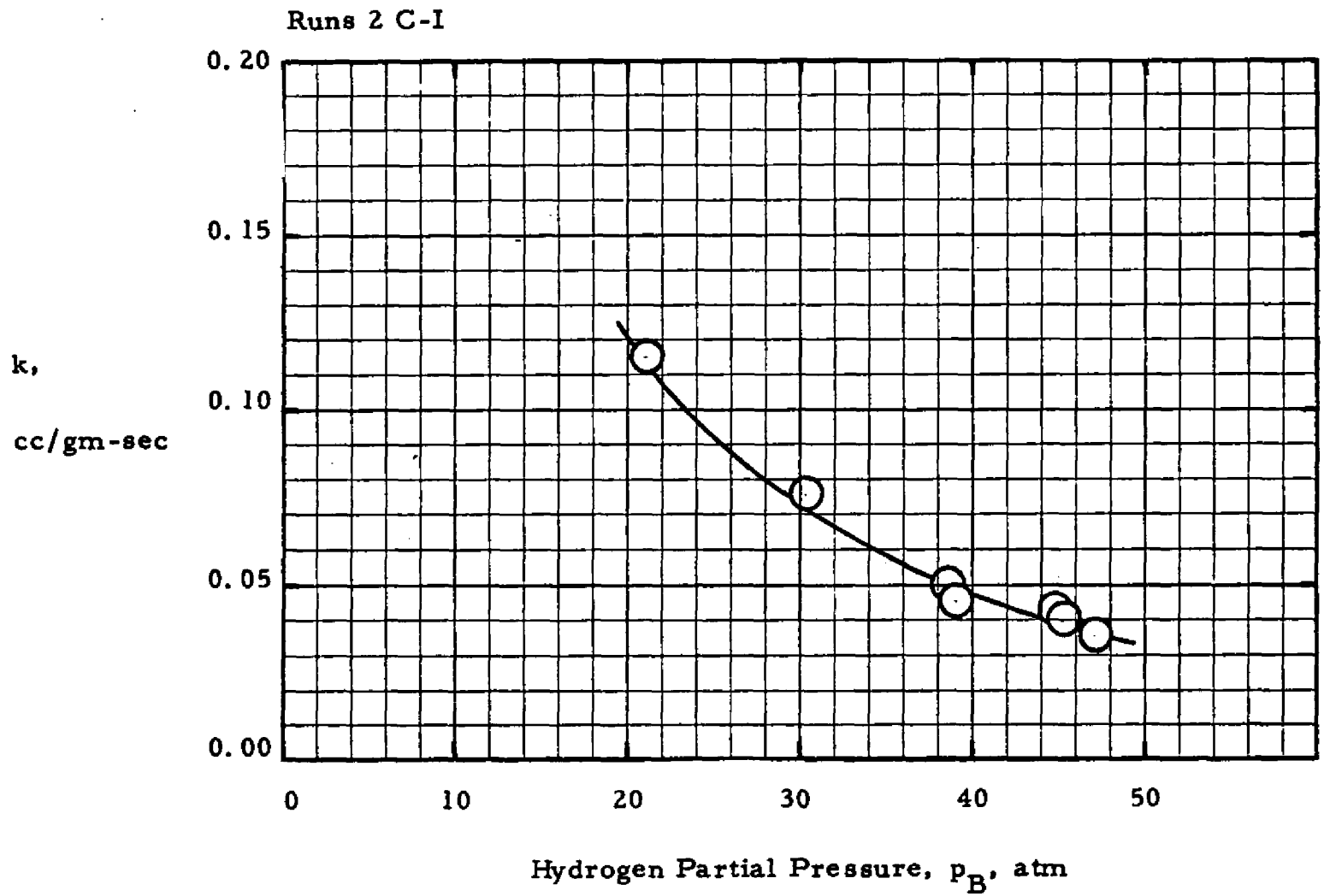

Figure 16. Effect of Hydrogen Partial Pressure on Simplified Rate Constant, Hexane Hydrocracking Over Pd-H-Faujasite

Since the hydrogen mole fractions are very large in all the experimental runs, the change in the hydrogen mole fractions over the length of the catalyst bed is very small. Therefore, the hydrogen partial pressure can be considered independent of the hexane concentration. Then equation (24) can be rearranged and integrated to

$$-\int_{C_{Ao}}^{C_A} dC_A/C_A = k_o K_A/(1 + K_B p_B)^n \int_o^{t_H} dt \quad (25)$$

and

$$- \ln (1-x) = k_o K_A t_H/(1 + K_B p_B)^n. \quad (25a)$$

Dividing equation (25a) by equation (22) and rearranging yields

$$k = k_o K_A/(1 + K_B p_B)^n. \quad (26)$$

Assuming a single site model, n = 1, and rearranging equation (26) yields

$$1/k = 1/k_o K_A + (K_B/k_o K_A) p_B. \quad (27)$$

Equation (27) indicates that the reciprocal of the simplified rate constant, k, should be a linear function of the H_2 partial pressure, p_B. If it is assumed in equation (26) that

$$K_B p_B \gg 1$$

then

$$k = k_o K_A/K_B p_B. \quad (28)$$

Rearranging,

$$1/k = (K_B/k_o K_A) p_B. \quad (29)$$

Equation (29) indicates a linear relationship of 1/k versus p_B passing

through the orgin. Equations (27) and (29) were tested with the data in Table 3 (page 67). The results are illustrated in Figure 17 (page 71). Equation (27) is indicated to have a negative intercept. This is not acceptable since it would mean that $k_o K_A$ would be negative. Equation (29) does not appear to be consistent with the data as indicated by the dashed line in Figure 17.

A dual site mechanism, n = 2, with the same assumptions as in equation (27) yields

$$1/\sqrt{k} = 1/\sqrt{k_o K_A} + (K_B/\sqrt{k_o K_A})\, p_B \qquad (30)$$

and with the same assumptions as in equation (29) yields

$$1/\sqrt{k} = (K_B/\sqrt{k_o K_A})\, p_B. \qquad (31)$$

The data in Table 3 are used to test the dual site mechanism equations in Figure 18 (page 72). Equation (30) appears to be consistent with the data and gives a positive intercept. Equation (31) does not appear to be consistent with the data. Equation (30) then is accepted as the best interpretation of the data.

The fit of equation (30) yields the following numerical results

$$1/\sqrt{k} = 1.1 + 0.086\, p_B \qquad (32)$$

Solving for $k_o K_A$ and K_B yields

$$k_o K_A = 0.826 \qquad (33)$$

$$K_B = 0.0782. \qquad (34)$$

5. Effect of Temperature

The effect of temperature on the simplified rate constant is shown in Figure 19 (page 73). Since the simplified constant is a

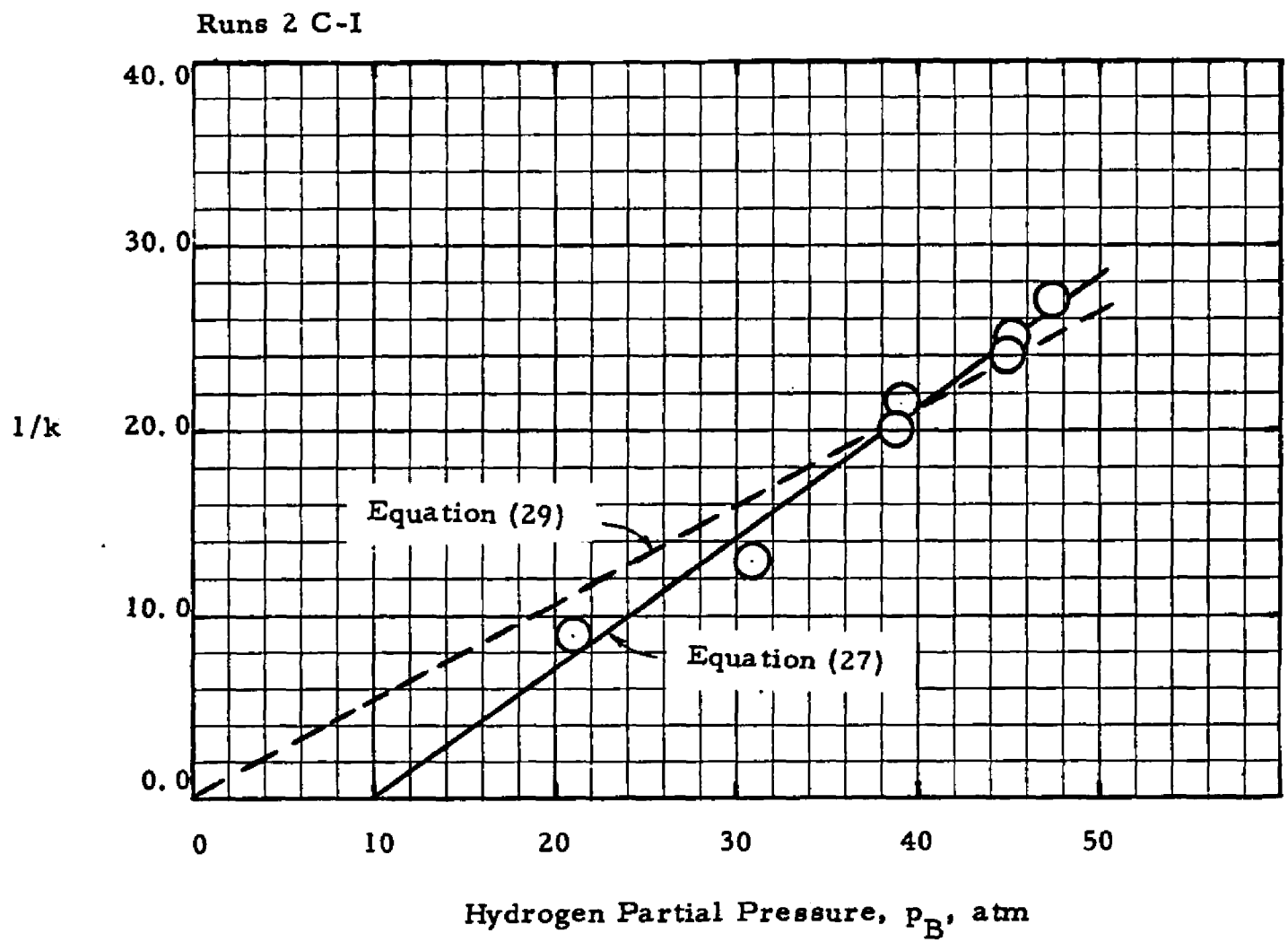

Figure 17. Test for Single Site Mechanism, Hexane Hydrocracking Over Pd-H-Faujasite

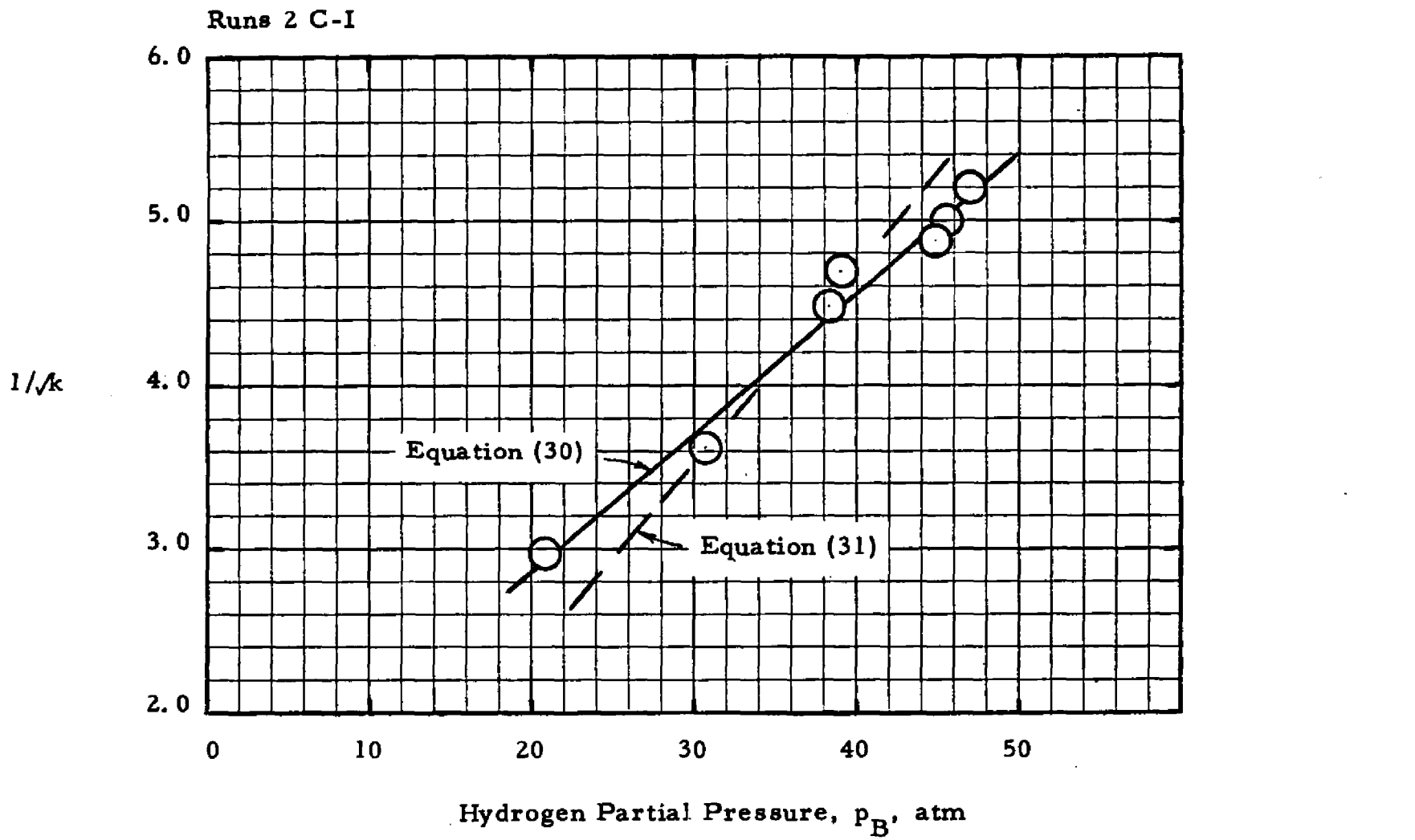

Figure 18. Test for Dual Site Mechanism, Hexane Hydrocracking Over Pd-H-Faujasite

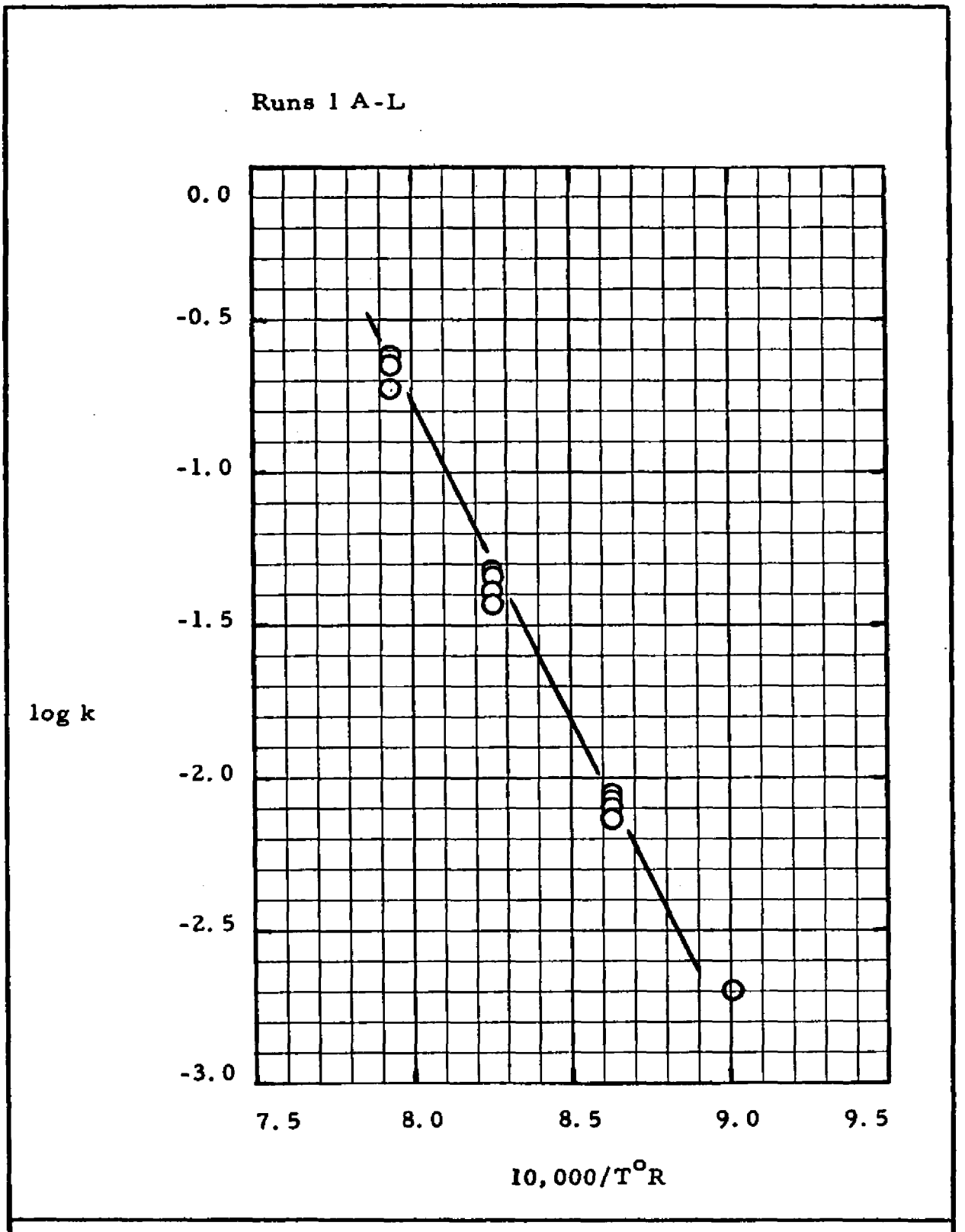

Figure 19. Effect of Temperature on Simplified Rate Constant, Hexane Hydrocracking Over Pd-H-Faujasite

function of H_2 partial pressure as well as temperature, these data are at a relatively constant H_2 partial pressure of 46 atm. The apparent activation energy from the slope of this plot is 54 kcal/gm mole. A value of 60 kcal/gm mole is indicated for a $Pd-Al_2O_3$ catalyst[28] with the data treated in a similar manner.

The effect of temperature on the hydrogen adsorption coefficient was determined by the value of the coefficient calculated from the n-hexane hydrocracking data at 750°F and a value calculated from the cyclohexane hydrocracking data at 700°F. The values of the hydrogen adsorption coefficient at various temperatures are illustrated in Figure 26 (page 89). Using these values of K_B, the values of k_oK_A can be calculated from the equation

$$k_oK_A = k(1 + K_BP_B)^2 \qquad (35)$$

This calculation was made for all n-hexane hydrocracking runs. The following expression was used

$$k'_o = k_oK_A. \qquad (36)$$

An Arrhenius type plot of log k'_o versus reciprocal temperature appears in Figure 20 (page 75). The average of all results at a given temperature is indicated by the data point, and the range of values is indicated by the vertical line. The activation energy calculated from the slope of the plot in Figure 20 was 48 kcal/gm mole. Values of k'_o and K_B for all runs appear in Appendix Table A-1.

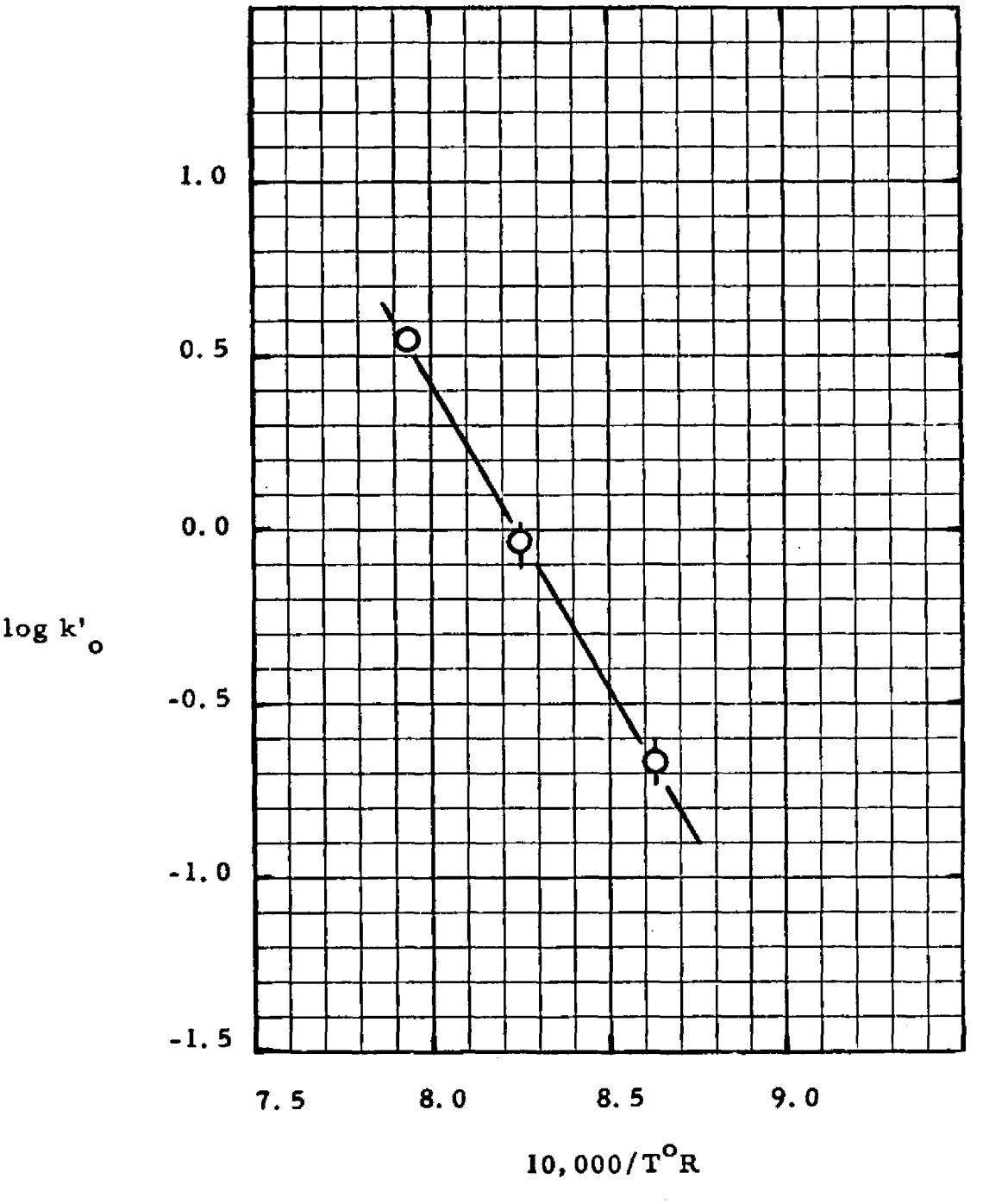

Figure 20. Effect of Temperature on Reaction Rate Constant, Hexane Hydrocracking Over Pd-H-Faujasite

6. Mechanism

The model for hydrocracking n-hexane developed in the preceding sections appears adequate over a wide range of process conditions. The integrated form of this equation was

$$- \ln (1-x) = k'_o t_H / (1 + K_B p_B)^2 \qquad (37)$$

where k'_o and K_B are functions of temperature only. The relationships of k'_o and K_B with temperature can be described as

$$\ln k'_o = 35.4 - (43.0 \times 10^3)/T^oR \qquad (38)$$

and

$$\ln K_B = - 4.63 + (2.54 \times 10^3)/T^oR. \qquad (39)$$

This model was based on the limiting step being the hydrocracking reaction on the catalyst interior surface. Since the experimental data are consistent with a dual site mechanism, this limiting step may be the reaction of an adsorbed hydrogen with the adsorbed hydrocarbon on an adjacent active site.

One of the basic assumptions in this model was that the normal hexane and the iso-hexanes could be treated as a single compound. This assumption is examined in Figure 21 (page 77). This figure shows the hexane isomer concentration in the total hexane paraffin mixture versus the hydrocracking conversion. The data indicate close to a thermodynamic equilibrium mixture of the hexanes from a hydrocracking conversion of about 14% to a conversion of about 94%. The dashed

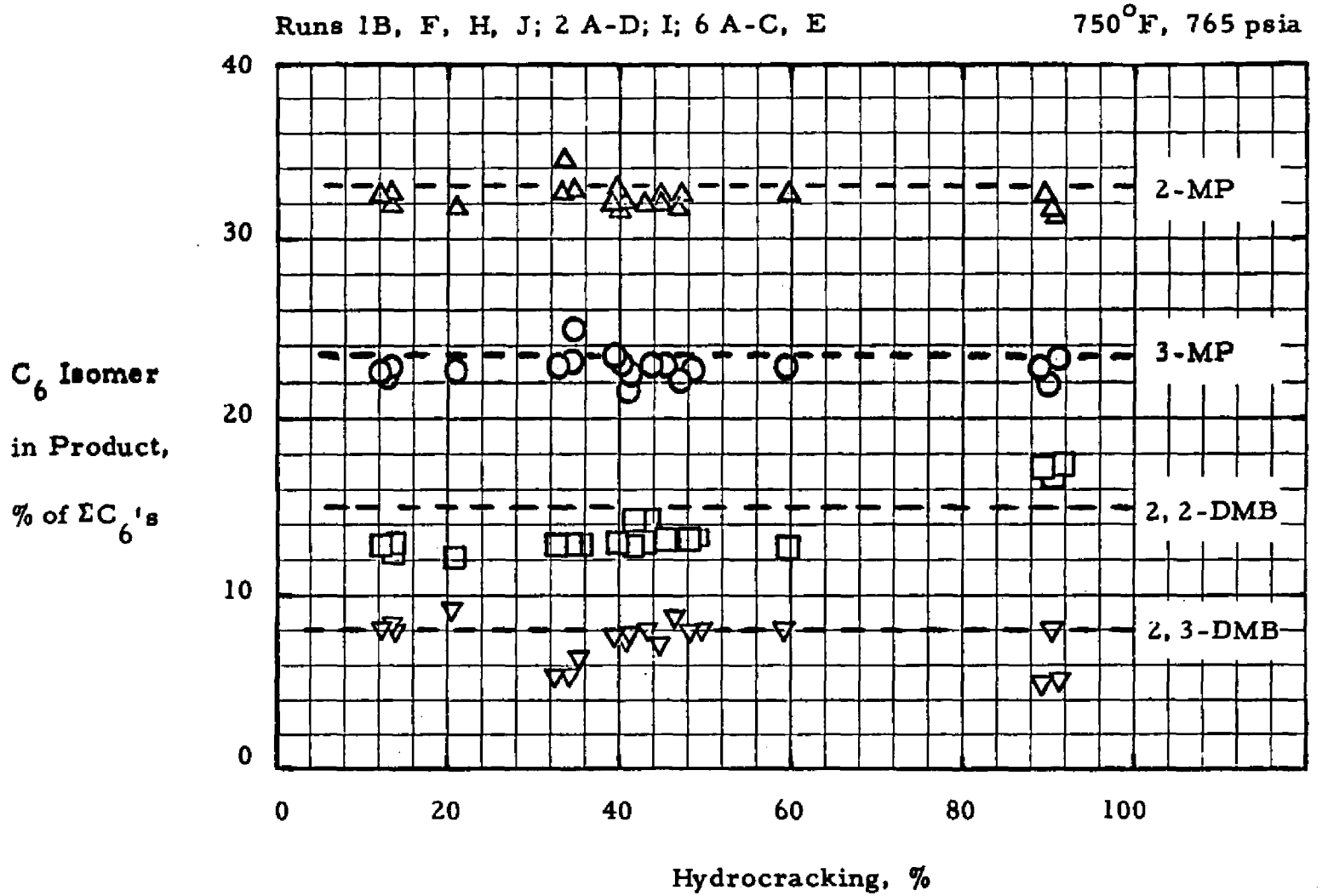

Figure 21. Hexane Isomer Concentration in Product Hexanes, Hexane Hydrocracking Over Pd-H-Faujasite

lines in Figure 21 represent the equilibrium values of the hexane isomers as determined by Ridgway and Schoen.[55] This high isomerization activity is consistent with the studies of Rabo and co-workers[54] on the same type of catalyst. The data in Figure 21 indicate two possibilities: (1) that the hexane isomers all hydrocrack at about the same rate, thus maintaining the same relative concentrations independent of the amount of hydrocracking, or (2) that if one or more of the hexane isomers hydrocrack preferentially, the isomerization rate is rapid enough to prevent that isomer or isomers from being depleted. In any event, the simplifying assumption of handling all the hexane isomers as one compound appears to be justified in that the ratios of hexane isomer concentrations remain constant as the hydrocracking conversion increases.

An examination of the composition of the hydrocracked products can also yield information on the mechanism of hydrocracking. The hexane isomers can hydrocrack to 2 propane molecules, one methane and one pentane molecule, or one ethane and one butane molecule. The butane and pentane molecules can be either straight chain or branched depending on the particular hexane molecule hydrocracked, the particular carbon-to-carbon bond broken, and whether the hydrocracked fragment isomerizes before being desorbed. One of the interesting observations made previously[29, 53] is that the molar ratios of methane to total pentane and of ethane to total butane are less than unity. This is also the case in the present study as shown below

Hydrocracked product	Average of all n-hexane runs over Pd-H-faujasite
C_2/C_4 molar ratio	0.50
C_1/C_5 molar ratio	0.26

The values of these molar ratios from individual runs varied slightly, but no correlations with process variables were found.

Of course, in the case of simple hydrocracking of hexane isomers, these ratios should be unity. Therefore, it has been proposed[29, 53] that a complex of more than six carbon atoms forms and then hydrocracks. For example, a three carbon atom fragment (carbonium ion) may join with an adsorbed six carbon molecule (olefin) and produce a nine carbon atom complex (carbonium ion). The complex could hydrocrack to one butane and one pentane molecule.

The predominant hydrocracked product was propane. The center bond carcking of n-hexane and 2, 3-dimethylbutane produces two propane molecules. Also 2-methylpentane can hydrocrack to two propane molecules. Approximately two-thirds of the hexane isomers converted in a given run were hydrocracked to propane. This selectivity was calculated as follows

$$S = 1/2\ C_3/x \qquad (40)$$

where

S = selectivity to propane, %

C_3 = moles of propane produced per 100 moles of hexane fed

x = fraction of hexanes converted to hydrocracked products.

The selectivity to propane varied from run to run, but did not correlate with temperature or conversion. The range of values and the average values for all n-hexane runs with the faujasite catalyst are shown below.

Selectivity to	Range	Average
propane, S, %	52.9-87.0	65.7

Another interesting feature in hydrocracking is that the isobutane to normal butane ratio and the isopentane to normal pentane ratio can exceed the equilibrium ratios. If the mechanism for isobutane formation was that n-hexane hydrocracked to produce a n-butane molecule which in turn isomerized to isobutane, then the equilibrium ratio of iso-to-normal would be the maximum that could be obtained. A reasonable explanation of the high iso-to-normal ratios is that a branched hydrocarbon intermediate containing nine or more carbon atoms hydrocracks to give isobutane. Then if the hydrocracked products are not re-adsorbed on the catalyst, the isobutane has no opportunity to isomerize to n-butane. A similar explanation holds for isopentane.

There was no apparent correlation of the iso-to-normal ratios with operating variables although the ratios varied from run to run. The range of ratios and the average values are shown below

	N-Hexane Hydrocracking over Pd-H-faujasite	
Molar ratios in product	Range	Average
iC_4/nC_4	0.67-1.97	1.0
iC_5/nC_5	1.07-3.46	1.7

Most of the variation in these ratios can be attributed to experimental error.

7. Catalyst Activity Maintenance

Catalyst activity was relatively constant in the study of n-hexane over Pd-H-faujasite. A few preliminary runs before this research began indicated that high hydrogen-to-hydrocarbon ratios were necessary to maintain catalyst activity. Therefore the range of hydrogen ratios was limited in order to maintain a constant activity. In beginning a run it was noticed that a fresh catalyst would show a high activity for the first few minutes on feed. The activity would decline to a "lined-out" activity after 30-45 minutes on feed. The "lined-out" activity held constant within 5-10% over several hours on feed. Process conditions were repeated from time-to-time during a run to check activity maintenance. No corrections were made to the process data for activity differences since the activity decline was small.

C. Cyclohexane Hydrocracking

1. General

The approach to the study of hydrocracking cyclohexane over Pd-H-faujasite was similar to that of hydrocracking n-hexane. In the hexane study it was concluded that mass transfer and macropore diffusion were not limiting steps. Since the systems and process conditions were similar, it was assumed that mass transfer and macropore diffusion were not

limiting in the cyclohexane study. If a micropore diffusional limitation exists, its effect would be included in the overall reaction rate.

2. Pseudo-First Order Reaction

The simplified model for hydrocracking cyclohexane was

$$[CH \rightleftharpoons MCP] + n\,H_2 \xrightarrow{k_1} \text{hydrocracked products}$$

Integration of the rate equation led to

$$-\ln(1-x) = k_1 t_H \qquad (41)$$

A plot of $-\log(1-x)$ versus the contact time should yield a linear relationship. This test was made at two different temperatures. The results are illustrated in Figures 22 and 23 (pages 83 and 84). The detailed data appear in Appendix Tables A and A-2. As can be seen, a linear relationship was obtained in both studies. These data represent hydrocracking conversions of 17 to 99%.

3. Effect of Hydrogen Partial Pressure

As in n-hexane hydrocracking, the simplified rate constant, k_1, for cyclohexane hydrocracking appeared to be a function of H_2 partial pressure. This effect is illustrated in Table 4 (page 85) and Figure 24 (page 86). As developed in Chapter IV, the simplified rate constant may be related to the partial pressures by

$$k_1 = k_{1,0} K_C/(1 + K_C p_C + K_B p_B + K_p p_p)^n \qquad (42)$$

The dual site mechanism and the simplifying assumption

$$K_B p_B \gg K_C p_C + K_p p_p$$

again gave the best agreement with the data. The test of the equation is

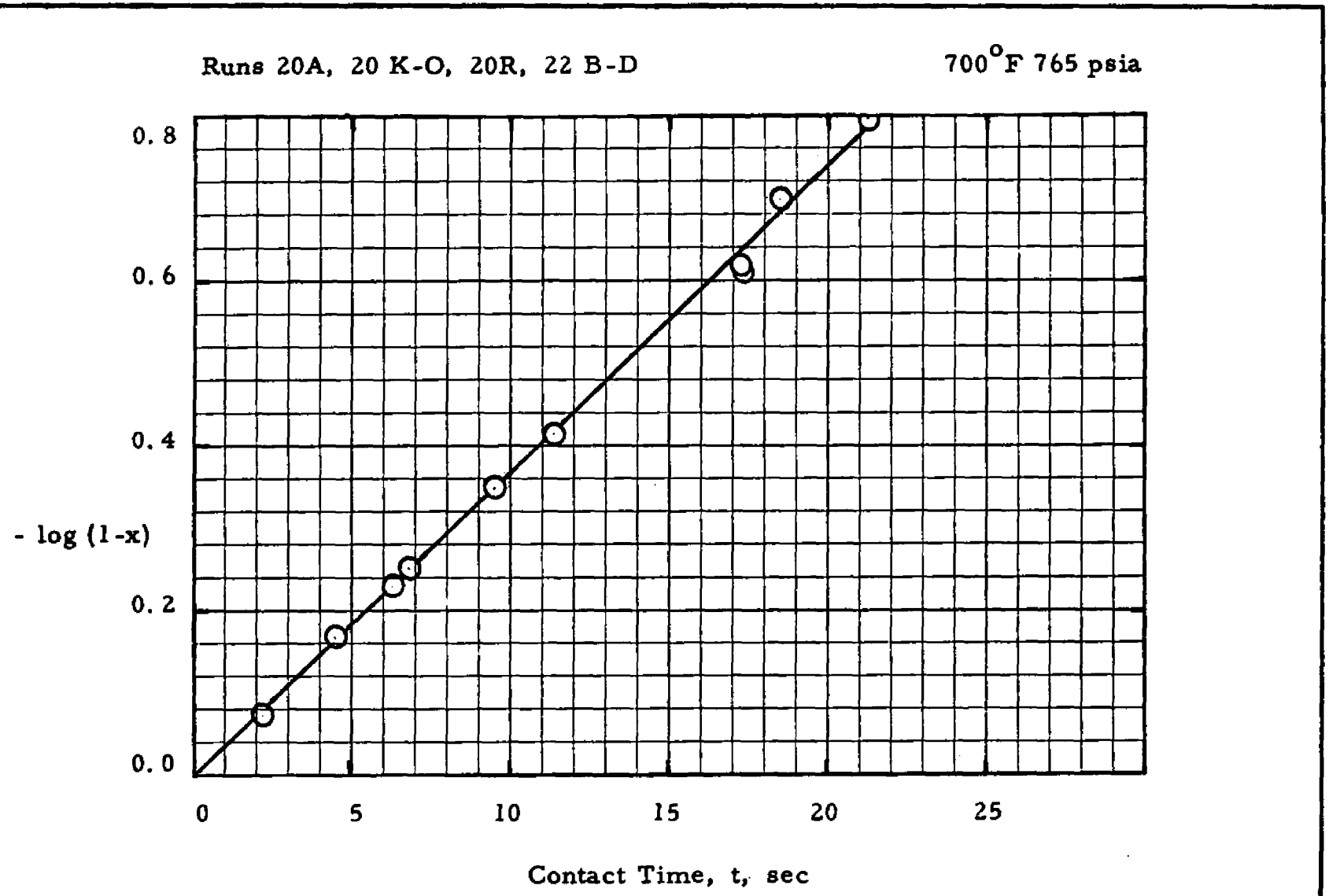

Figure 22. Test for Simplified First Order Model, Cyclohexane Hydrocracking Over Pd-H-Faujasite

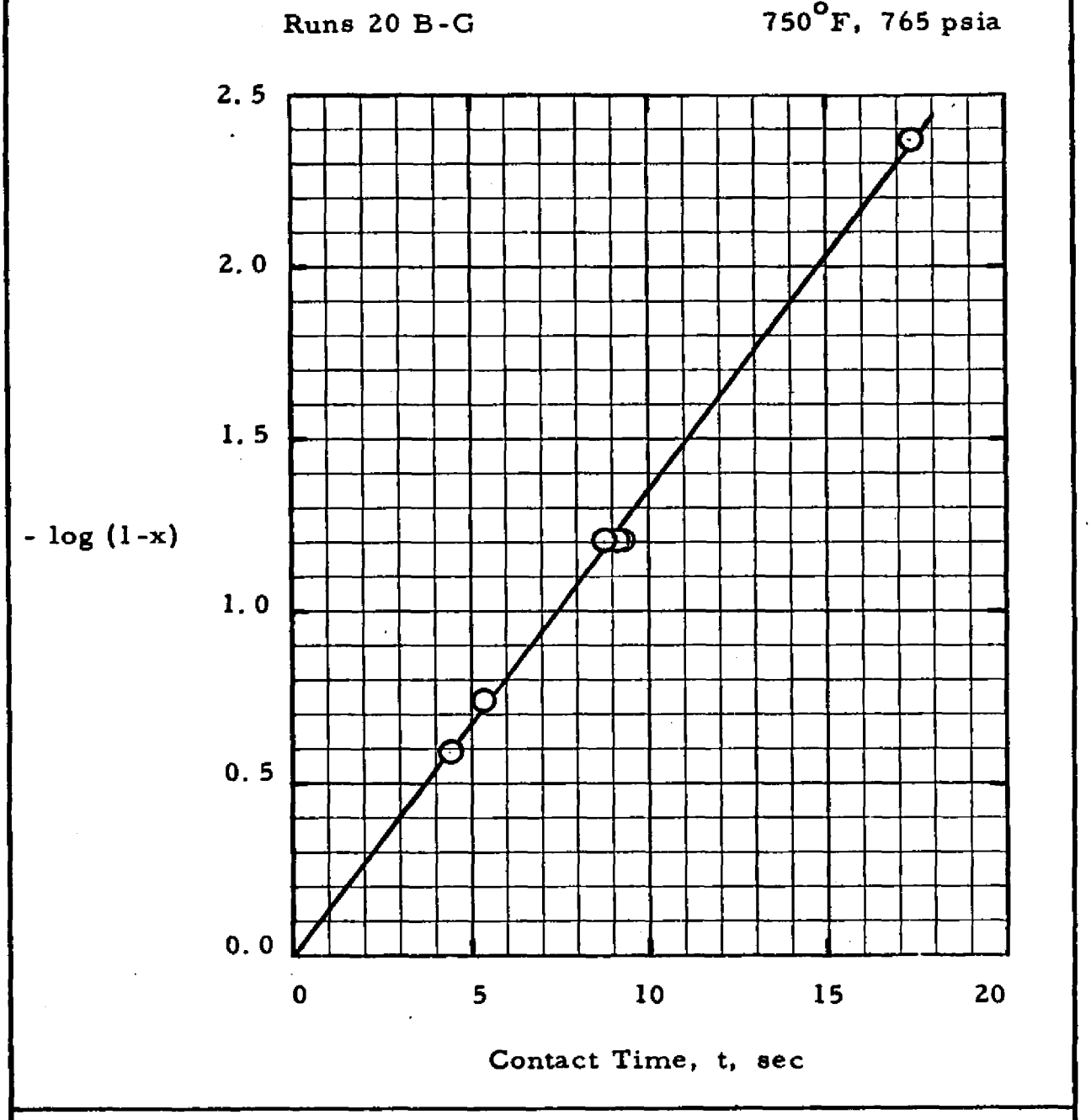

Figure 23. Test for Simplified First Order Model, Cyclohexane Hydrocracking Over Pd-H-Faujasite

Table 4. Effect of Hydrogen Partial Pressure on Simplified Rate Constant in Cyclohexane Hydrocracking Over Pd-H-Faujasite

Operating Conditions

Temperature, °F	700
Pressure, psia	365-765
Feed	Cyclohexane
Catalyst	Pd-H-Faujasite
Run Nos.	20A, 20K-R

Run Results

Run No.	k_1, cc/gm-sec	Partial Pressures, atm			
		P_B	P_C	P_A	P_p
20A	0.180	46.5	3.4	0.7	1.4
20K	0.181	49.5	1.9	0.2	0.4
20L	0.185	45.1	1.1	1.3	4.5
20M	0.180	49.9	1.1	0.5	0.5
20N	0.187	44.0	1.0	1.6	5.4
20O	0.179	46.0	1.2	1.4	3.4
20P	0.249	36.6	0.8	0.8	3.6
20Q	0.520	21.3	0.4	0.2	2.9
20R	0.178	46.0	1.2	1.4	3.4

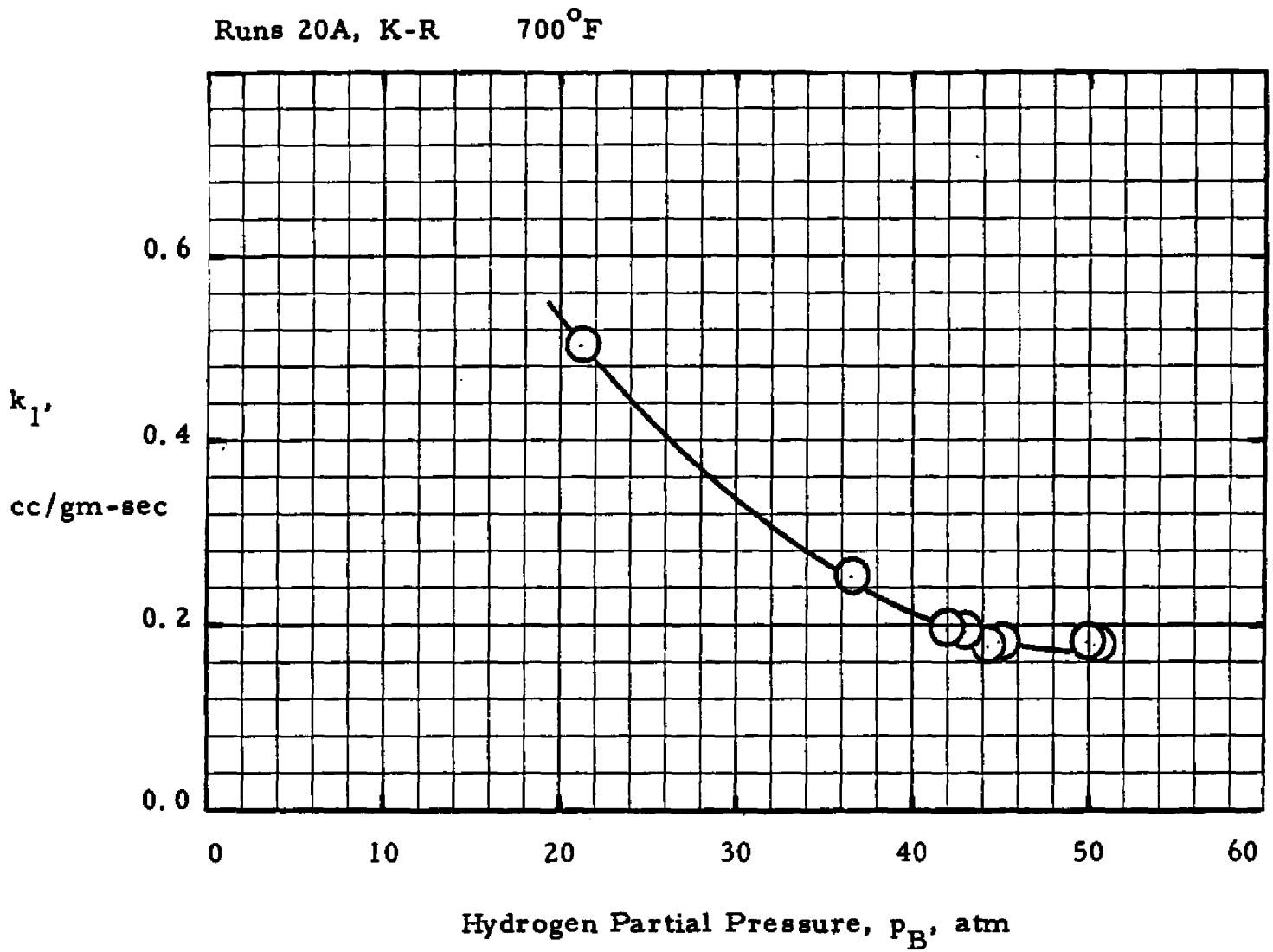

Figure 24. Effect of Hydrogen Partial Pressure on Simplified Rate Constant, Cyclohexane Hydrocracking Over Pd-H-Faujasite

presented in Figure 25 (page 88). The numerical equation obtained from Figure 25 is

$$1/k_1 = 0.44 + 0.0407\, p_B \qquad (43)$$

Solving for K_B and $k_{1,0}\, K_C$ yields

$$K_B = 0.092 \qquad (44)$$

$$k_{1,0}\, K_C = 5.1 \qquad (45)$$

4. Effect of Temperature

The effect of temperature on the H_2 adsorption coefficient, K_B, is shown in Figure 26 (page 89). The values of K_B were used in calculating $k_{1,0}\, K_C$ at various temperatures by the equation

$$k'_{1,0} = k_{1,0}\, K_C = k_1 (1 + K_B p_B)^2 \qquad (46)$$

An Arrhenius type plot of $k'_{1,0}$ for all cyclohexane hydrocracking data appears in Figure 27 (page 90), and the detailed data appear in Appendix Tables A and A-2. The data points in Figure 27 indicate the average values for each temperature level and the vertical lines indicate the range of values. An activation energy of 31 kcal/gm mole was calculated from the slope. A value of 30-35 kcal/gmole was reported for a Pt-Al_2O_3 catalyst based on a first order mechanism.[32]

5. Mechanism

Cyclohexane hydrocracking data are consistent with a model similar to the model for n-hexane hydrocracking. The integrated form of this equation was

$$-\ln(1-x) = k'_{1,0}\, t_H/(1 + K_B p_B)^2 \qquad (47)$$

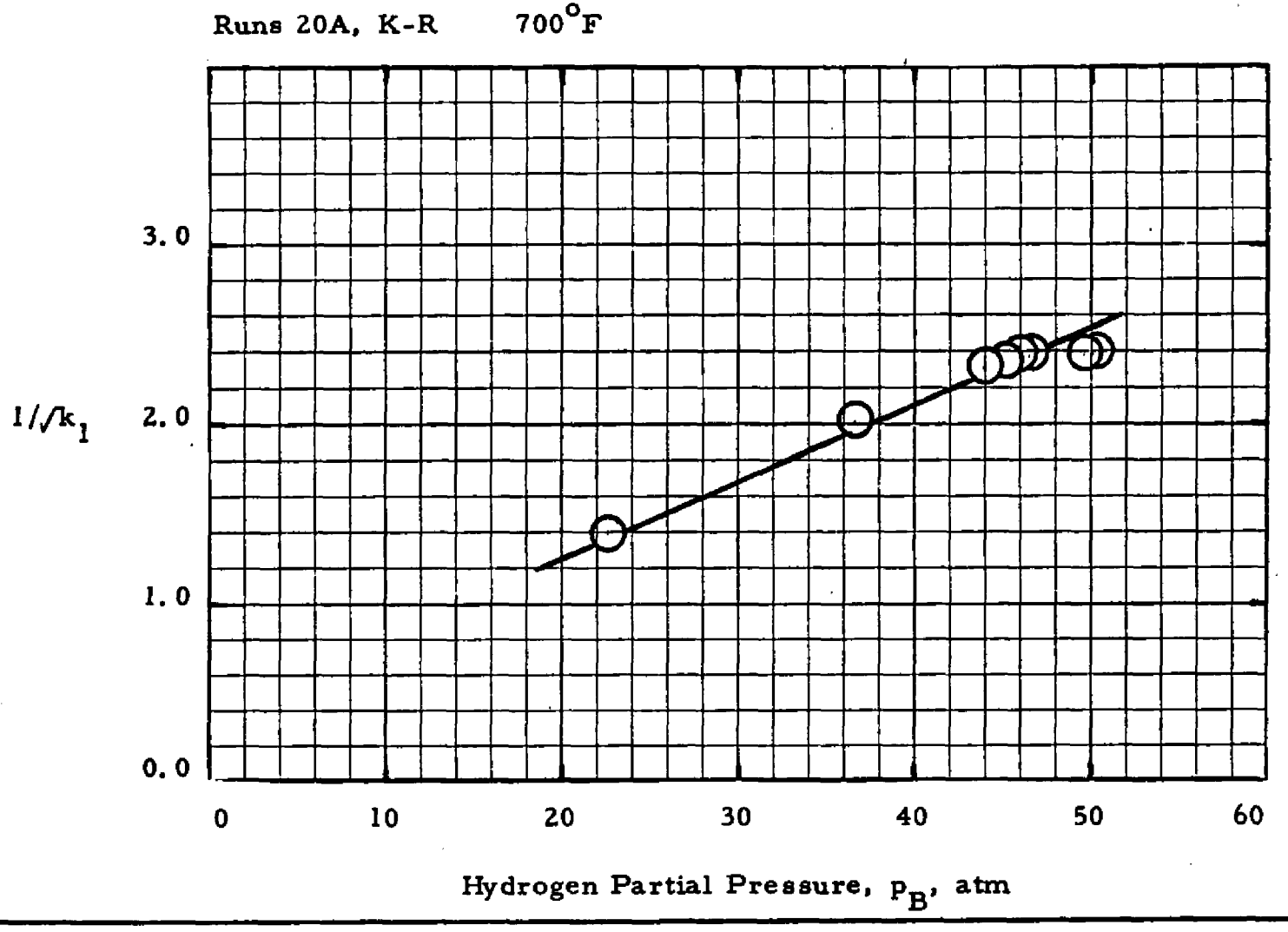

Figure 25. Test for Dual Site Mechanism, Cyclohexane Hydrocracking Over Pd-H-Faujasite

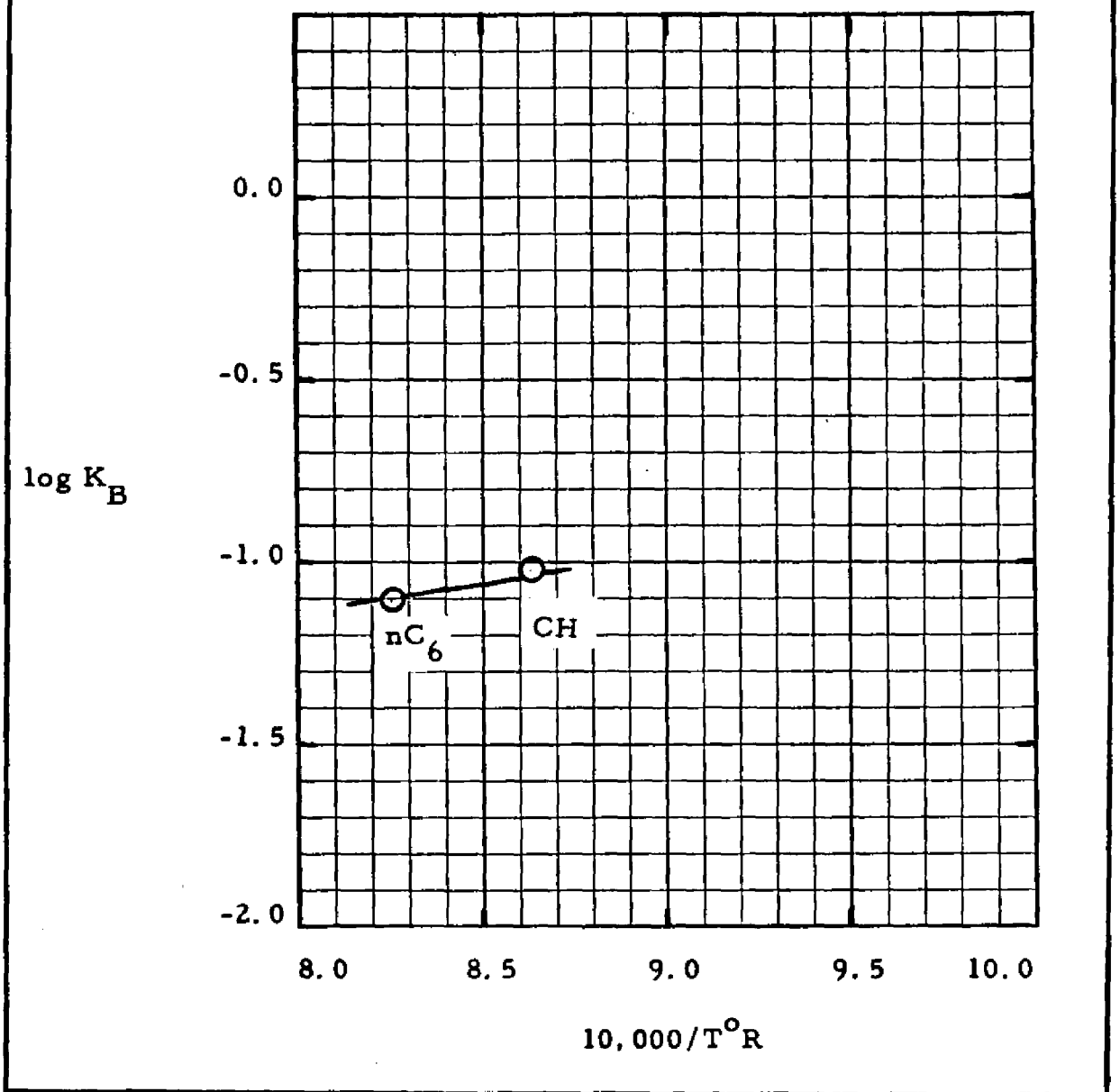

Figure 26. Effect of Temperature on Hydrogen Adsorption Coefficient, Pd-H-Faujasite

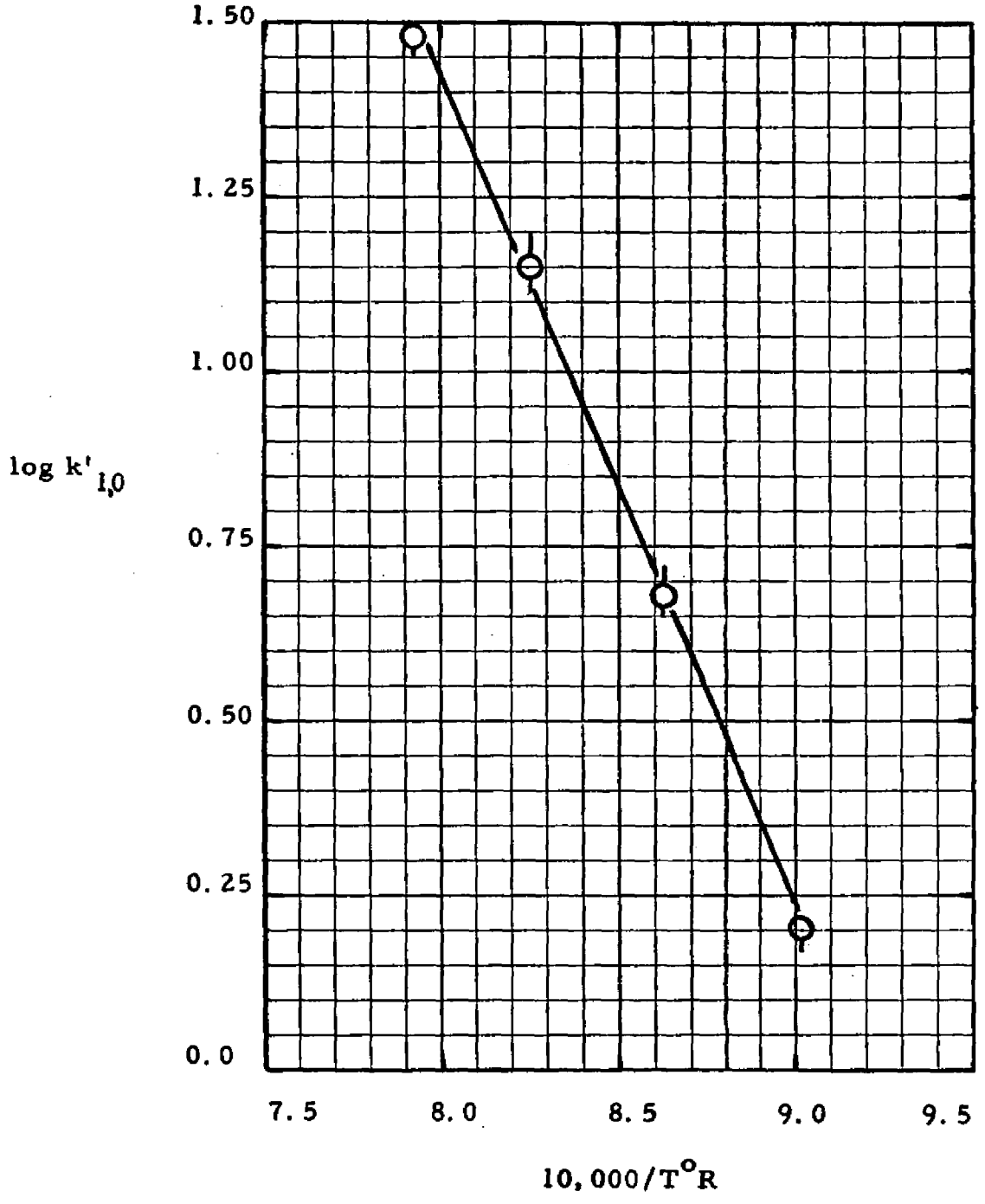

Figure 27. Effect of Temperature on Reaction Rate Constant, Cyclohexane Hydrocracking Over Pd-H-Faujasite

Equation (39) for K_B was reported in the mechanism discussion for n-hexane hydrocracking. The equation for $k'_{1,0}$ is

$$\ln k'_{1,0} = 25.4 - (27,540/T^{\circ}R). \qquad (48)$$

A basic assumption in this model was that the methylcyclopentane and the cyclohexane can be treated as a single compound. The percent of MCP in the MCP + CH product mixture appears to be close to the equilibrium value for hydrocracking conversions of 16 to 85%. The equilibrium level is indicated by the dashed line in Figure 28 (page 92). This equilibrium was calculated from free energy data and may not be as accurate as the experimentally determined hexane isomer equilibrium data. Nevertheless, the data indicate over a 90% approach to the equilibrium as calculated from the free energy data. This high isomerization activity is in agreement with the data from n-hexane hydrocracking. The assumption of treating the MCP and CH sum as one compound appears to be justified since the ratio of their concentrations remains relatively constant over a wide range of conversions.

The hydrocracked product can be of two different types. First, the naphthenes can be opened and hydrogenated to paraffins. This ring-opening reaction is prevalent at low conversions as illustrated in Figure 29 (page 93). The selectivity to C_6 paraffins decreases with increasing conversion and increasing temperature. The second type of hydrocracking would be the formation of two lower molecular weight paraffins.

Table 5 (page 94) summarizes the lower molecular weight hydrocracked products from all the cyclohexane-faujasite runs. As can be

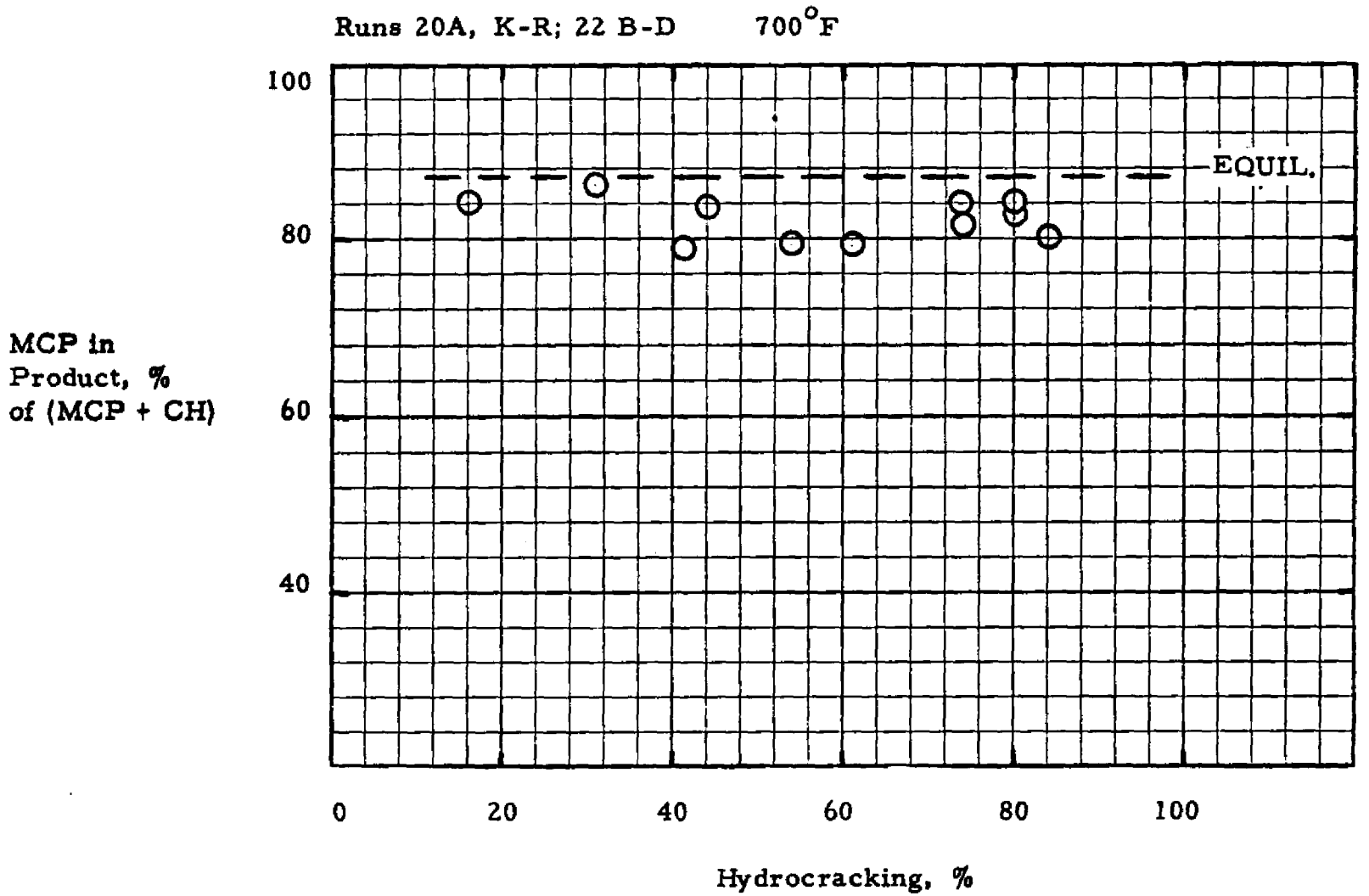

Figure 28. Methylcyclopentane Concentration in Product Naphthenes, Cyclohexane Hydrocracking Over Pd-H-Faujasite

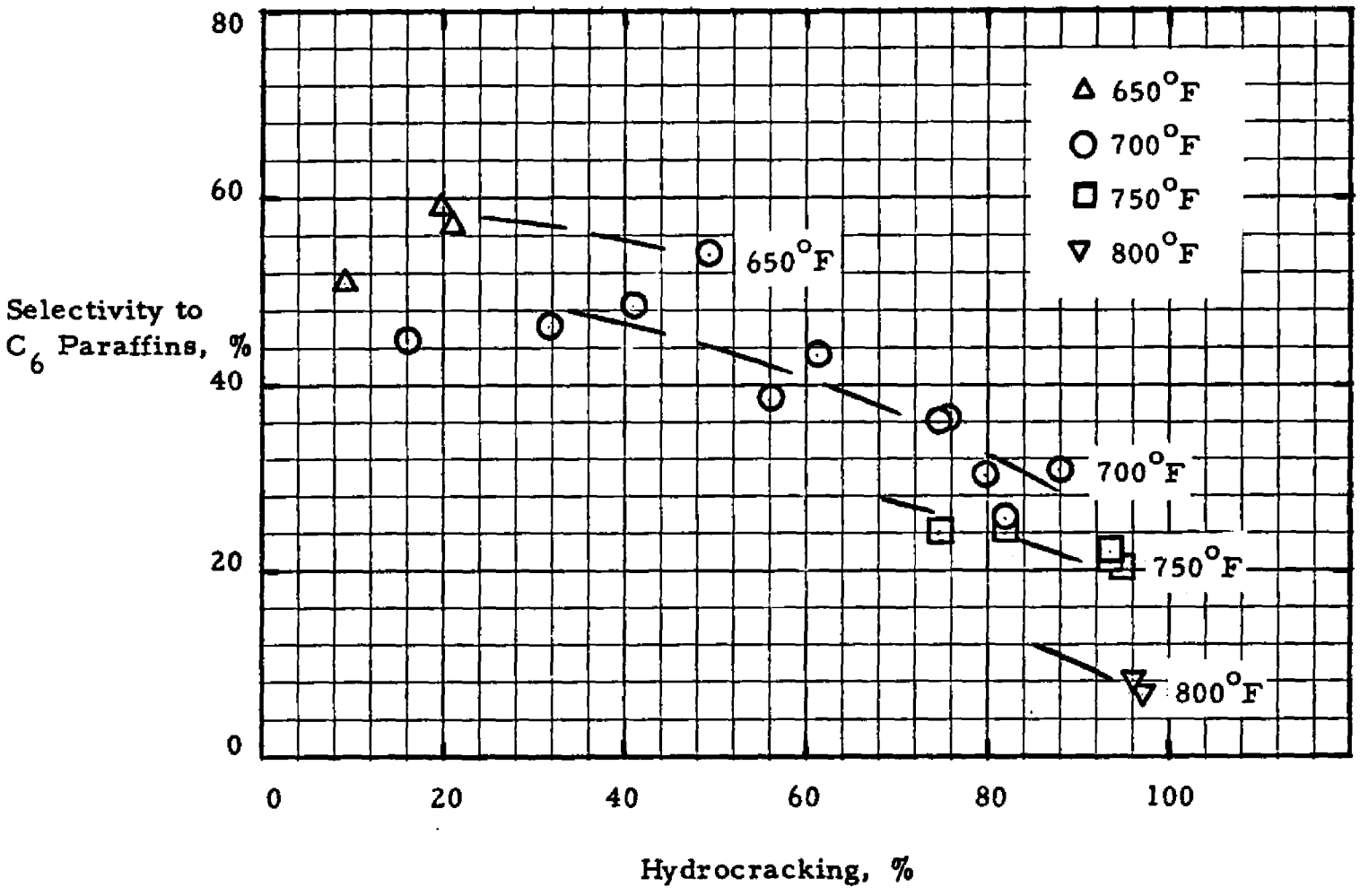

Figure 29. Effect of Conversion and Temperature on Selectivity to C_6 Paraffins, Cyclohexane Hydrocracking Over Pd-H-Faujasite

Table 5. Products from Cyclohexane Hydrocracking Over Pd-H-Faujasite

Operating Conditions

Temperature, °F	650-800
Pressure, psia	365-765
Feed	Cyclohexane
Catalyst	Pd-H-Faujasite
Run Nos.	20A-R, 22A-E

Run Results

Hydrocracked Product	Range	Average
Selectivity to Propane, %	4.9-34.5	14.0
C_2/C_4 molar ratio	0.044-0.151	0.075
C_1/C_5 molar ratio	0.000-0.091	0.037
iC_4/nC_4 molar ratio	1.51-3.99	2.4
iC_5/nC_5 molar ratio	1.57-4.09	2.4
Hydrocracking Conversion, %	8-99	66

seen, the average selectivity to propane is much lower in cyclohexane hydrocracking than in n-hexane hydrocracking (14.0% vs. 65.7%). Also the average C_2/C_4 and C_1/C_5 ratios are much lower in cyclohexane hydrocracking (0.075 vs. 0.50 for C_2/C_4 and 0.037 vs. 0.26 for C_1/C_5). This indicates that the predominant reaction in cyclohexane hydrocracking is the formation of a complex of more than six carbon atoms and the subsequent hydrocracking of this complex. The iC_4/nC_4 and iC_5/nC_5 ratios are much larger than in n-hexane runs. The high concentrations of isobutane and isopentane indicate that the complex is probably a branched chain hydrocarbon.

6. Catalyst Activity Maintenance

Catalyst activity was not a problem in hydrocracking cyclohexane over Pd-H-faujasite. After the "lined-out" activity was reached, the activity declined very slowly with time on feed. In Run 20 the catalyst "saw" feed for over 25 hours, and the activity during the final data period appeared to be about 1% lower than the initial data period.

D. Hydrocracking N-Hexane-Cyclohexane Mixture

A mixture of 56 mole % cyclohexane and 44 mole % n-hexane was hydrocracked over Pd-H-faujasite in order to determine whether or not the previously developed model would apply for mixtures. It is not unusual in heterogeneous catalysis that reaction rate data from pure compound studies do not apply in the case of mixed feeds. One of the major reasons for this is the competitive adsorption of the reactants.

For example, if the less reactive substance is also the more strongly adsorbed, then it can be preferentially converted. Wauquier and Jungers[66] found this to be the case in the hydrogenation of aromatics.

The results of the mixed feed study are summarized in Table 6 (page 97). The predicted conversions compare fairly well to the actual conversions, indicating that the previously developed models also apply to the mixed feed. This implies that the relative adsorption coefficients for n-hexane and cyclohexane are of about the same magnitude. In the analysis of the mixed feed data, since cyclohexane produces some hexane isomers, the amount of hexane in the feed was adjusted to account for this reaction.

Table 6. Hydrocracking of N-Hexane-Cyclohexane Mixture Over Pd-H-Faujasite -- Summary of Results

Operating Conditions						
Catalyst	Pd-H-Faujasite					
Space velocity, v/hr-v	2					
Pressure, psia	765					
Run No.	23A	23B	23C	23D	23E	23F
Temperature, ^{o}F	700	700	725	725	750	750
Conversion of (MCP + CH), %						
Actual	70.2	63.8	80.5	92.3	95.5	96.4
Predicted	69.3	54.0	79.8	91.9	94.3	95.0
Conversion of hexanes, %						
Actual	4.9	4.6	8.9	26.0	22.5	28.3
Predicted	4.8	3.0	8.2	12.1	19.3	20.3

CHAPTER VI

EXPERIMENTAL RESULTS - MORDENITE CATALYST

A. Introduction

This chapter describes the results of hydrocracking n-hexane and cyclohexane over a Pd-H-mordenite catalyst. The approach to the mordenite catalyst study is similar to that discussed in Chapter V for the faujasite catalyst.

B. N-Hexane Hydrocracking

1. Effect of Mass Transfer

Fluid-to-particle mass transfer should not be a limiting step for the mordenite catalyst since mass transfer did not appear limiting for the faujasite catalyst at similar process conditions. Nevertheless, it was decided to make a few runs on the mordenite in order to strengthen this conclusion. These runs were made by varying the gas velocity and holding other conditions relatively constant. The results are summarized in Table 7 (page 99), and a plot of the simplified rate constant versus gas velocity appears in Figure 30 (page 100). If the fluid-to-particle mass transfer were limiting, the higher velocity runs should have indicated higher conversion. Since the rate constant was relatively constant with gas velocity, mass transfer was not limiting.

Table 7. Test for Mass Transfer Limitations -- Simplified Reaction Rate Constant vs. Gas Velocity, Mordenite Catalyst

Operating Conditions

Temperature, ^{o}F	550
Pressure, psia	765
Feed	n-Hexane
Catalyst	Pd-H-Mordenite

Run Results

Run No.	3B	14C	14F	17	18	19
Gas Velocity, cm/sec	0.31	0.32	0.29	0.62	0.95	0.23
Feed Rate, w/hr-w	1.99	2.00	2.00	2.00	2.04	2.02
H_2 Rate, moles/mole C_6	9.66	9.75	9.00	9.54	9.75	10.50
Hydrocracking, %	19.1	18.0	20.5	19.3	19.2	18.3
Simplified Rate Constant, k, cc/gm-sec	0.0132	0.0126	0.0131	0.0129	0.0132	0.0134

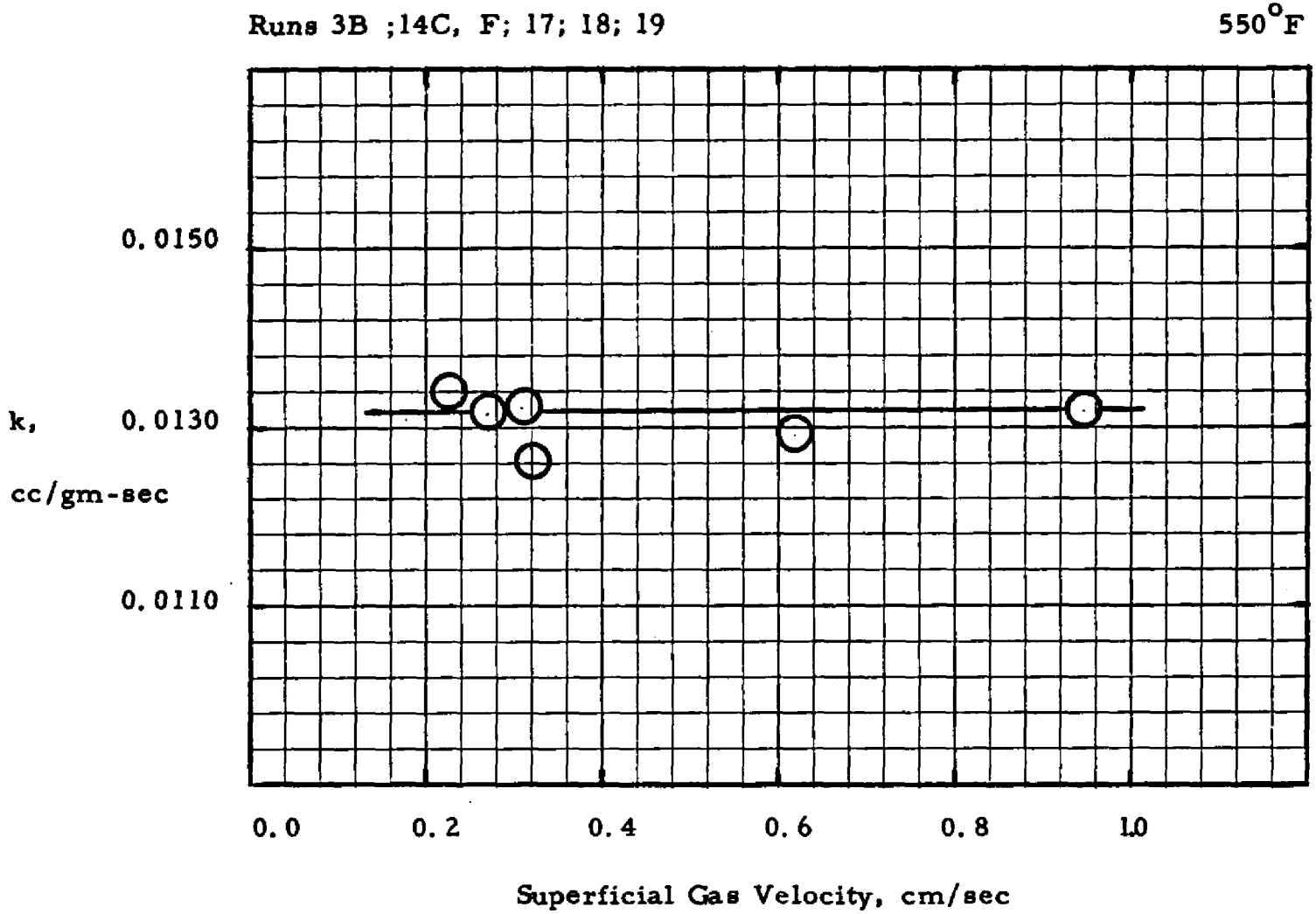

Figure 30. Test for Mass Transfer Limitations, Hexane Hydrocracking Over Pd-H-Mordenite

2. Effect of Pore Diffusion

The mordenite catalyst used in this study was synthesized initially as 1-5 micron crystals. These particles were pilled together, and the pills were subsequently crushed and sized. Three different sized macroparticles were investigated. The size ranges were 0.043-0.074 mm, 0.147-0.210 mm, and 0.210-1.2 mm. These sizes were tested for n-hexane hydrocracking at 550°F, 765 psia, 2 v/hr-v, and 10 moles of H_2/mole C_6. As can be seen in Table 8 (page 102) and Figure 31 (page 103), no trend of increasing activity was noted at the smaller particle sizes. As was the case in the study of the faujasite catalyst, no diffusional limitation exists in the mordenite macropores. No conclusion can be drawn about micropore diffusion since the micro-particle size was the same in all cases.

3. Pseudo-First Order Reaction

Three groups of experiments were made to determine whether the reaction over the mordenite catalyst was first order with respect to the hydrocarbon concentration. Each of the sets of runs were made at a set temperature, total pressure, and relatively constant partial pressures. The contact time was varied by changing n-hexane and hydrogen feed rates. As can be seen in Figures 32 (page 104), 33 (page 105), and 34 (page 106), the function of conversion, $-\log(1-x)$, was linear with contact time. These data strongly reinforce the first order relationship with respect to the hydrocarbon.

Table 8. Effect of Catalyst Particle on n-Hexane Hydrocracking over Pd-H-Mordenite

Operating Conditions

Temperature, °F	550
Pressure, psia	765
Feed	n-Hexane
Catalyst	Pd-H-Mordenite
Run Nos.	3B, 14C, 14F, 15, 16

Run Results

Catalyst Size, mm	Hydrocracking %	Simplified Rate Constant, k, cc/gm-sec
0.043-0.074	19.5	0.0130
0.147-0.210	19.0	0.0128
0.21-1.2	19.1	0.0132
0.21-1.2	18.0	0.0126
0.21-1.2	20.5	0.0131

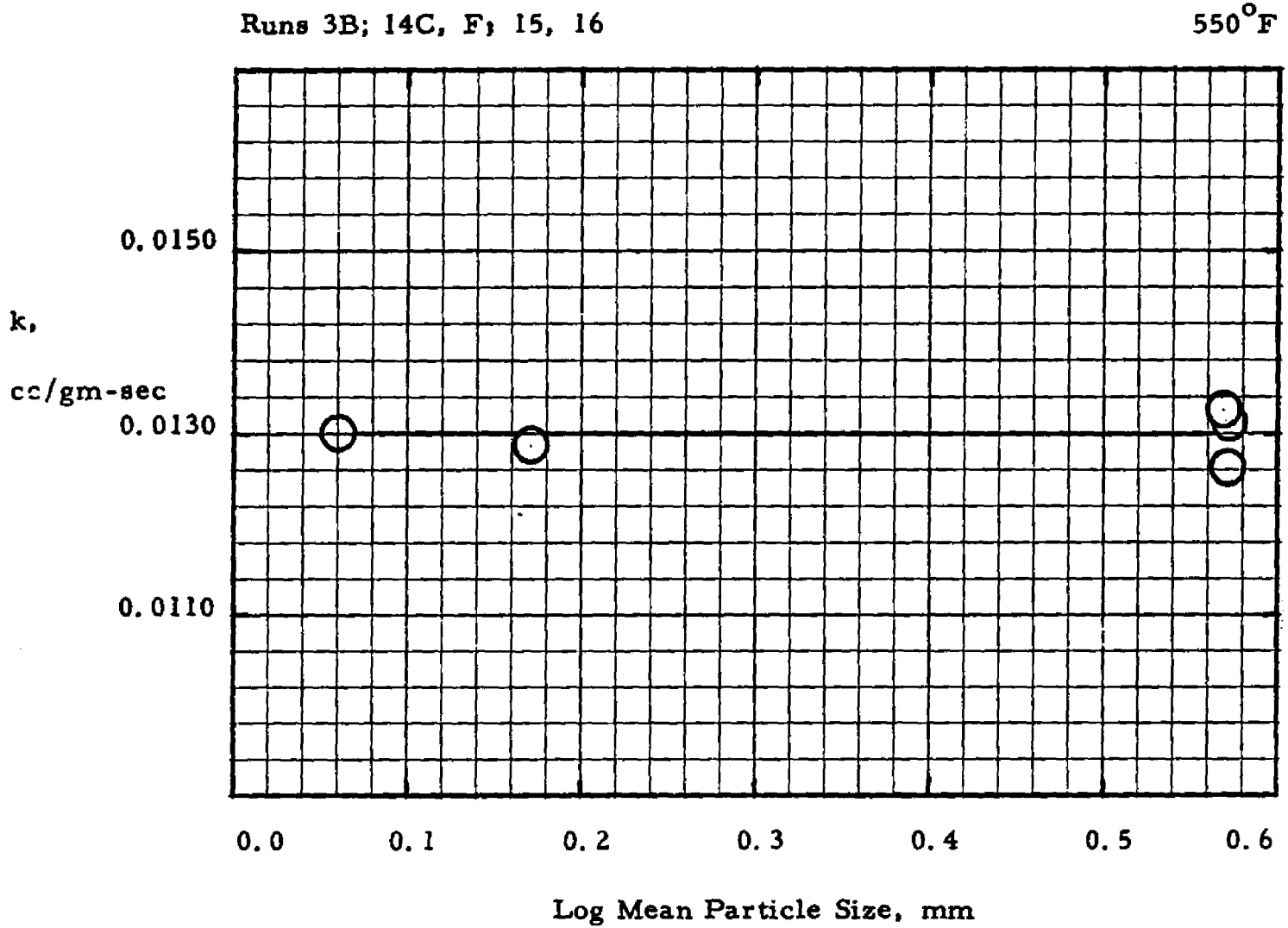

Figure 31. Effect of Catalyst Particle Size on Hexane Hydrocracking Over Pd-H-Mordenite

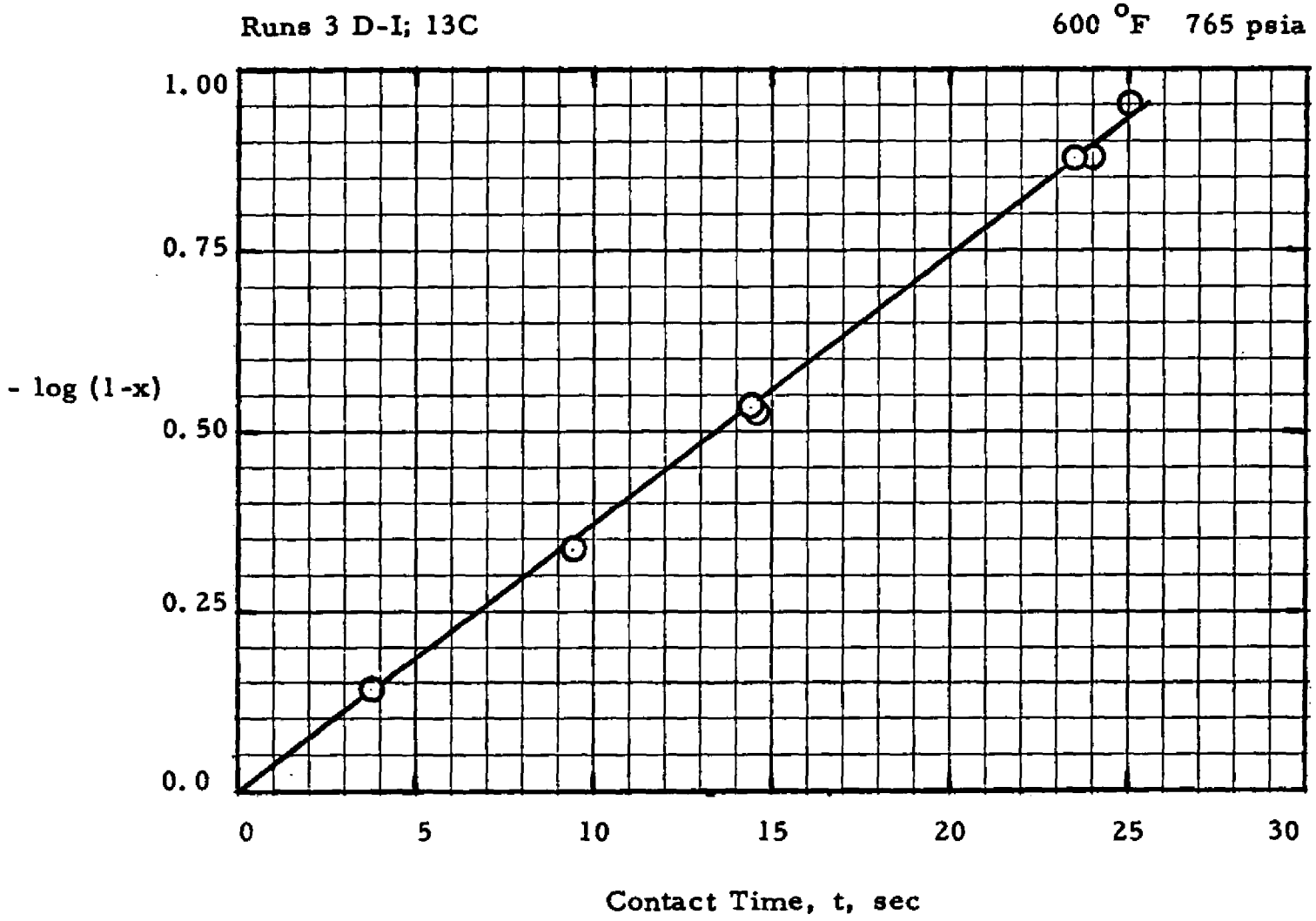

Figure 32. Test for First Order Model, Hexane Hydrocracking Over Pd-H-Mordenite

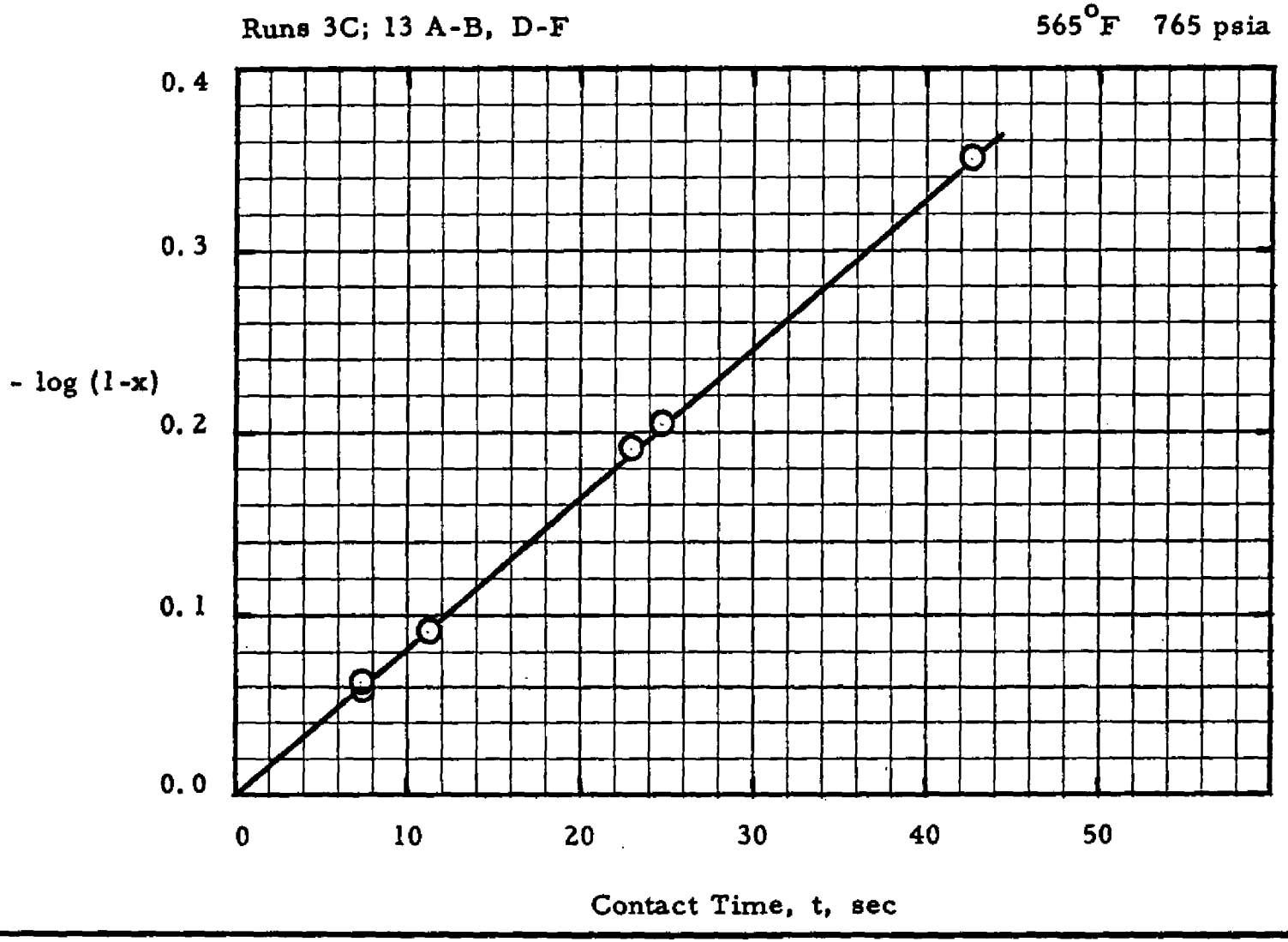

Figure 33. Test for First Order Model, Hexane Hydrocracking Over Pd-H-Mordenite

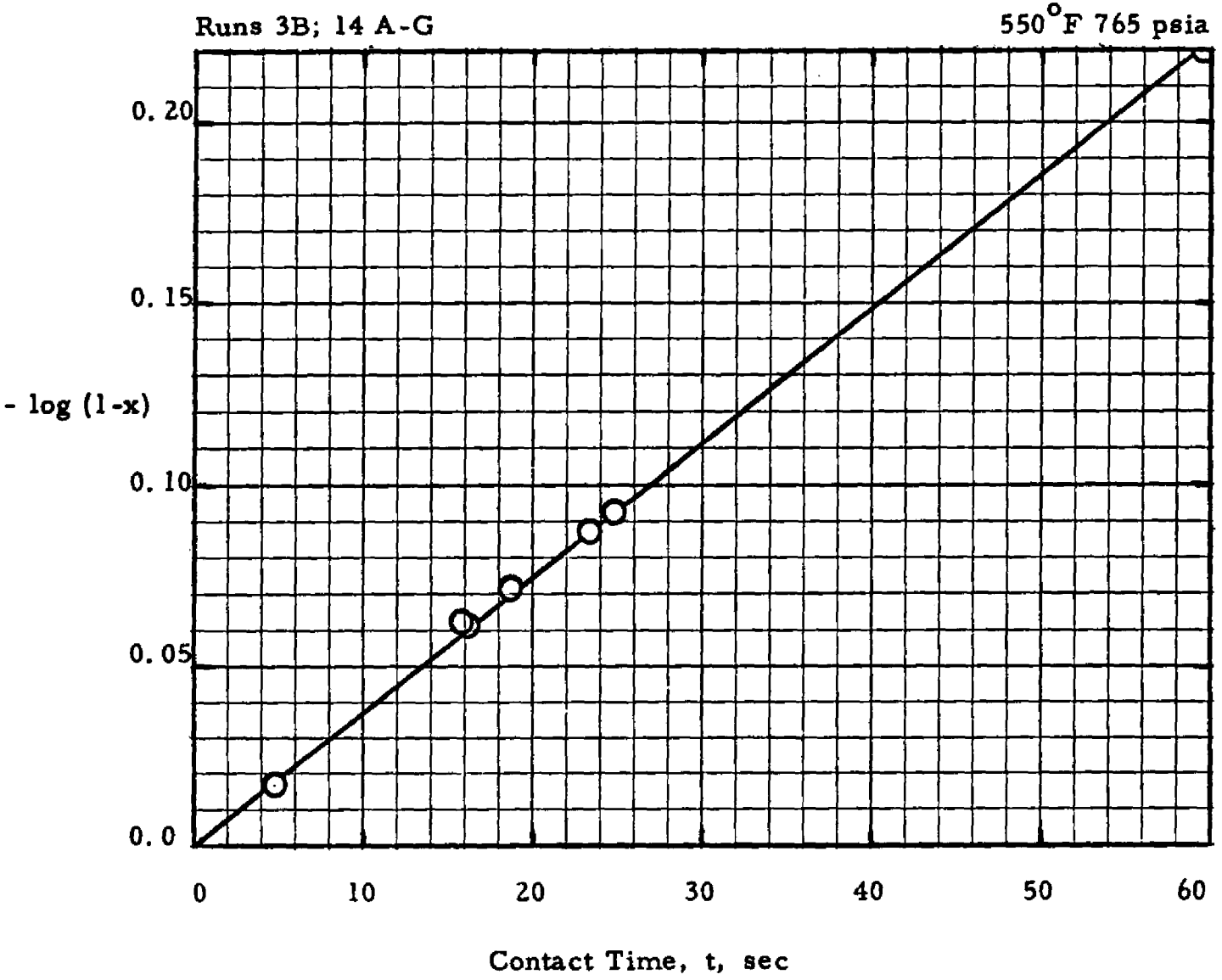

Figure 34. Test for First Order Model, Hexane Hydrocracking Over Pd-H-Mordenite

4. Effect of Hydrogen Partial Pressure

The effect of hydrogen partial pressure on the simplified rate constant for hydrocracking n-hexane over Pd-H-mordenite appears to be similar to the effect described previously for the faujasite catalyst. The data from this study appear in Table 9 (page 108), and a plot of the simplified rate constant versus the H_2 partial pressure appears in Figure 35 (page 109). The single and dual site mechanisms are tested in Figures 36 (page 110) and 37 (page 111). Again the most consistent is the dual site mechanism. Values calculated from the least squares fit of equation (30) are

$$k_o K_A = 1.9 \qquad (49)$$

$$K_B = 0.23. \qquad (50)$$

5. Effect of Temperature

The effect of temperature on the simplified rate constant is shown in Figure 38 (page 112). For comparison, the results with the faujasite are included. As can be seen, the Pd-H-mordenite has about the same activity as Pd-H-faujasite at approximately 180°F lower temperature. About the same difference in activity was found by Miale and co-workers[43, 69] for H-faujasite and H-mordenite in the catalytic cracking of n-hexane. The apparent activation energy calculated from the slope of the plot of log k versus 1/T was 54 kcal/gm mole. This is the same value calculated for hydrocracking n-hexane over Pd-H-faujasite.

Table 9. Effect of Hydrogen Partial Pressure on Simplified Rate Constant in n-Hexane Hydrocracking Over Pd-H-Mordenite

Operating Conditions

Temperature, °F	550
Pressure, psia	215-965
Feed	n-Hexane
Catalyst	Pd-H-Mordenite

Run Results

Run No.	k, cc/gm-sec	Partial Pressures, atm P_B	P_A	P_p
3B	0.0132	48.7	2.1	1.2
3J	0.0100	52.8	2.4	0.2
3K	0.0174	40.6	3.9	0.7
3L	0.0290	31.3	2.4	1.4
3M	0.133	12.8	0.8	1.0
3N	0.00903	62.2	2.9	0.6
14A	0.0128	48.5	3.2	0.3
14B	0.0134	45.3	5.4	1.3
14C	0.0126	46.7	4.0	1.3
14D	0.0133	48.5	2.7	0.8
14E	0.0132	48.0	3.1	0.9
14F	0.0131	46.0	4.2	1.8
14G	0.0130	46.4	2.9	2.7

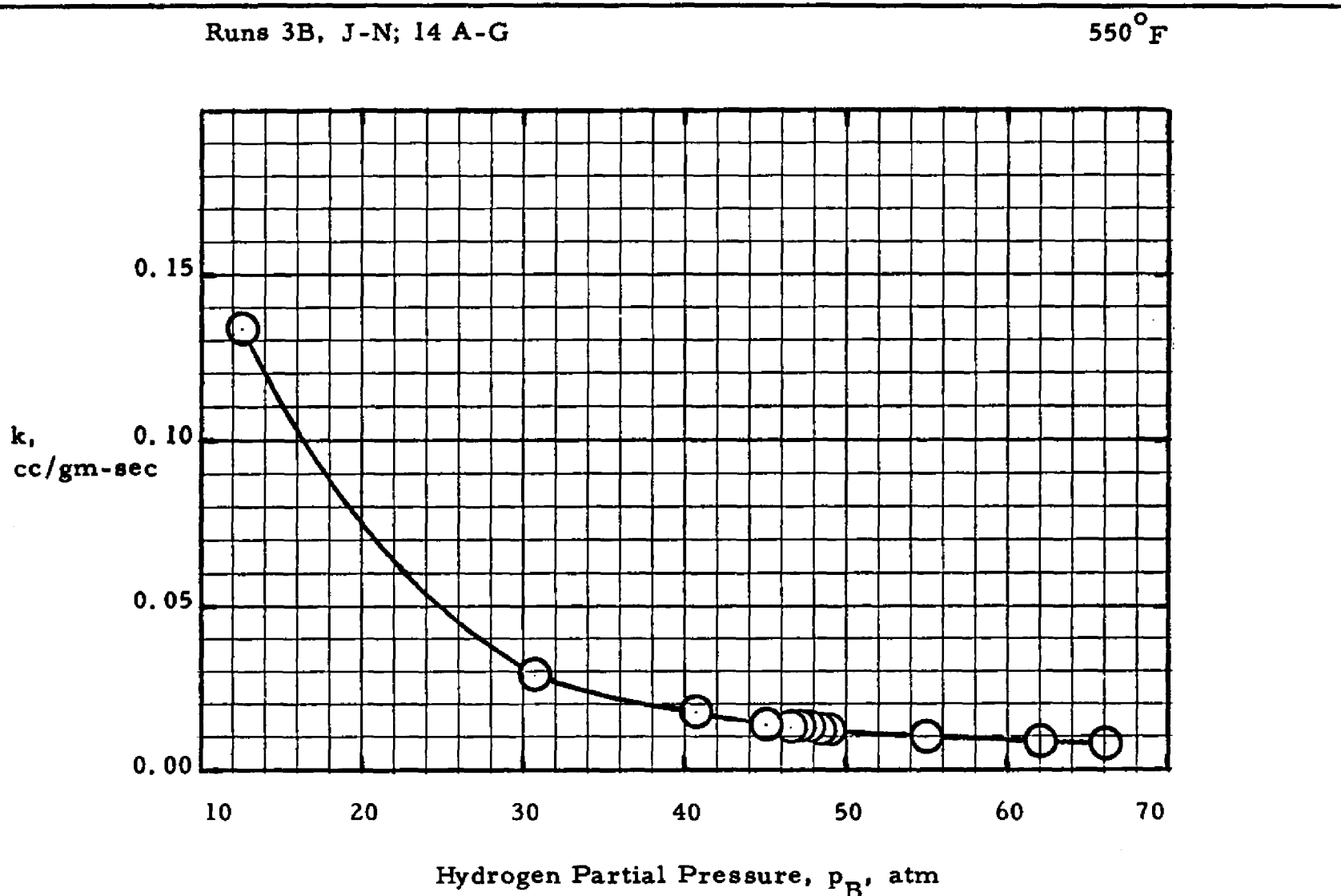

Figure 35. Effect of Hydrogen Partial Pressure on Simplified Rate Constant, Hexane Hydrocracking Over Pd-H-Mordenite

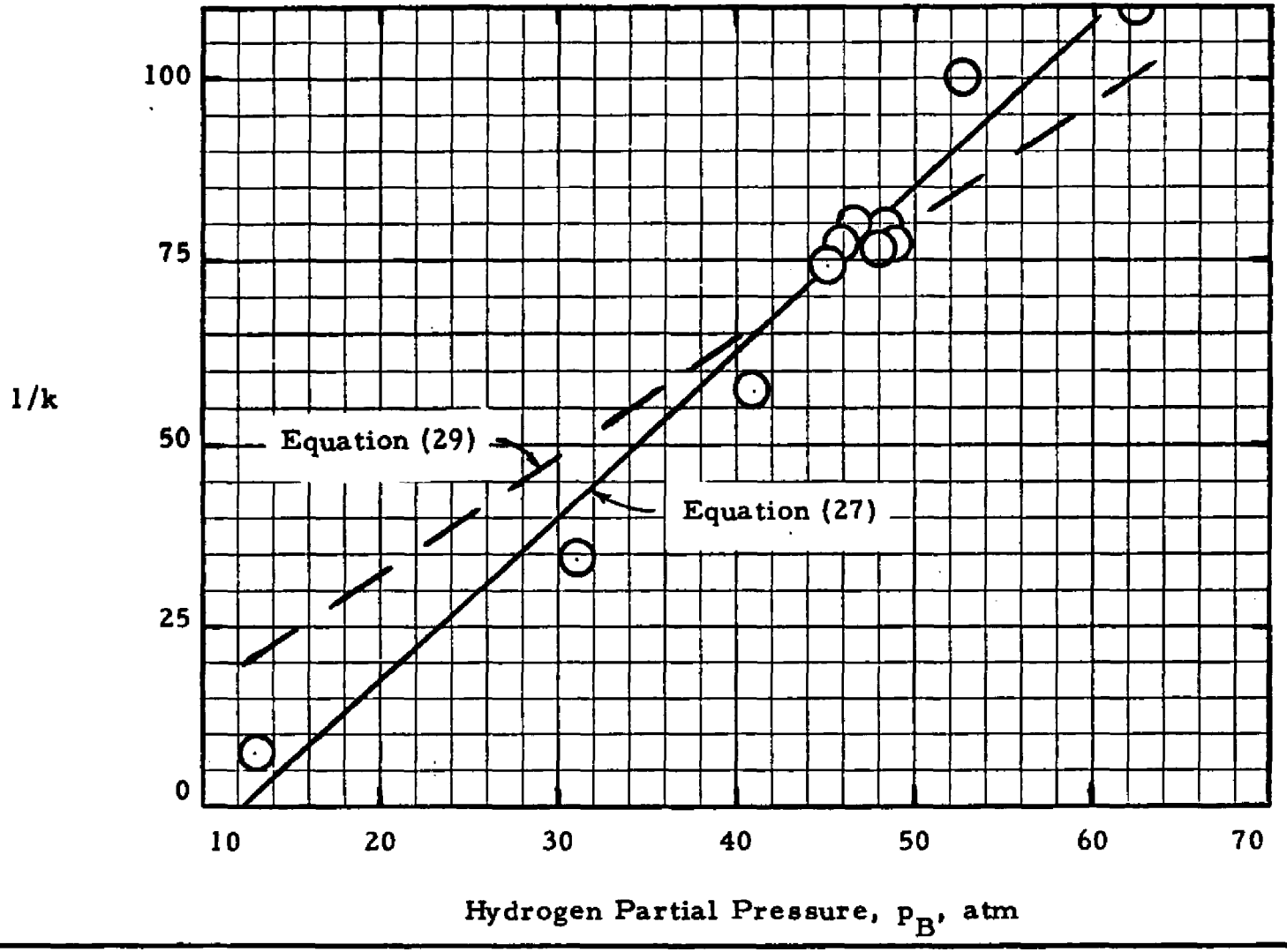

Figure 36. Test for Single Site Mechanism, Hexane Hydrocracking Over Pd-H-Mordenite

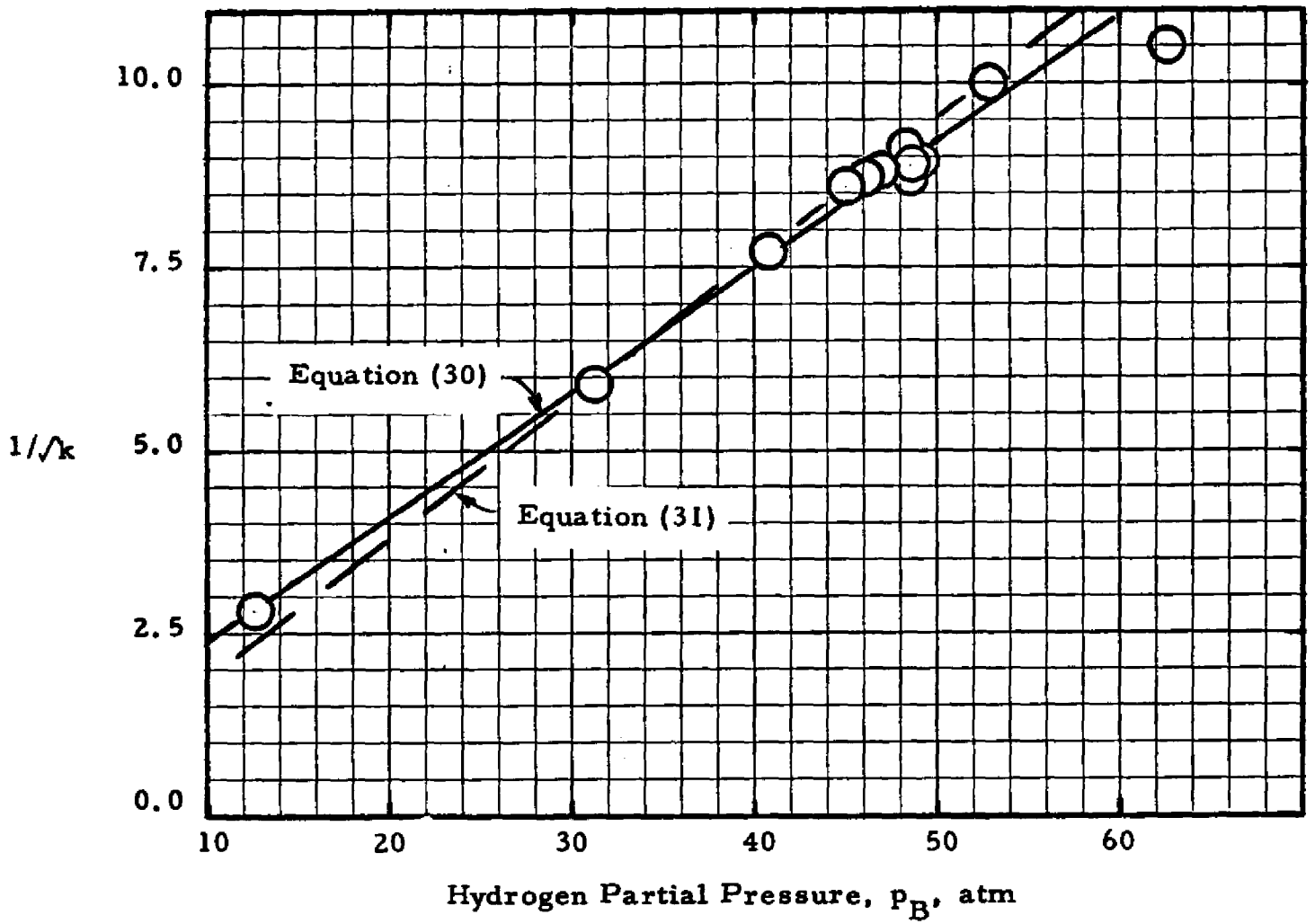

Figure 37. Test for Dual Site Mechanism, Hexane Hydrocracking Over Pd-H-Mordenite

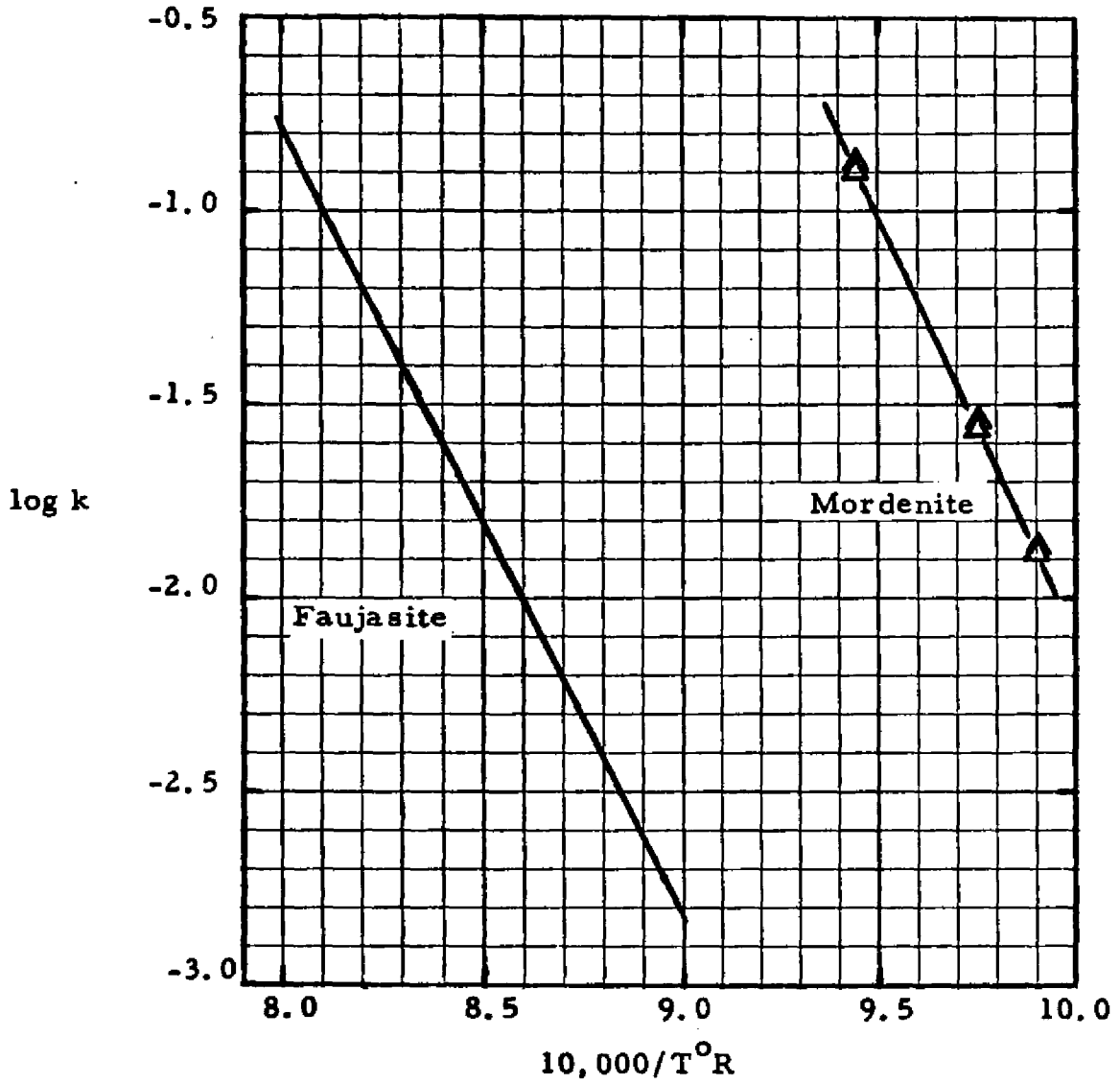

Figure 38. Effect of Temperature on Simplified Rate Constant, Hexane Hydrocracking

Values of $k_o K_A$ were calculated from the relationship

$$k'_o = k_o K_A = k (1 + K_B p_B)^2. \quad (51)$$

Values of K_B were determined from a plot of the value in equation (50) for hydrocracking n-hexane and the value determined for hydrocracking cyclohexane. This plot is shown in Figure 46 (page 127). Using the values of K_B and k, k'_o was calculated for each hydrocracking run. An Arrhenius type plot of log k'_o versus reciprocal temperature appears in Figure 39 (page 114). The data point at each temperature level represents the average value at that particular temperature, and the vertical line represents the range of values. The apparent activation energy calculated from the slope of this plot was 49 kcal/gmole. This compares well with the 48 kcal/gmole activation energy determined for the faujasite catalyst. Detailed data for all hexane runs appear in Appendix Tables A and A-1.

6. Mechanism

The model for n-hexane hydrocracking appears adequate for both the mordenite and faujasite catalysts. The integrated form of this expression was

$$- \ln (1-x) = k'_o t_H / (1 + K_B p_B)^2. \quad (52)$$

For the mordenite catalyst the values of k'_o and K_B can be calculated from

$$\ln k'_o = 44.45 - (44.1 \times 10^3)/T^oR \quad (53)$$

and

$$\ln K_B = - 3.127 + (1.76 \times 10^3)/T^oR. \quad (54)$$

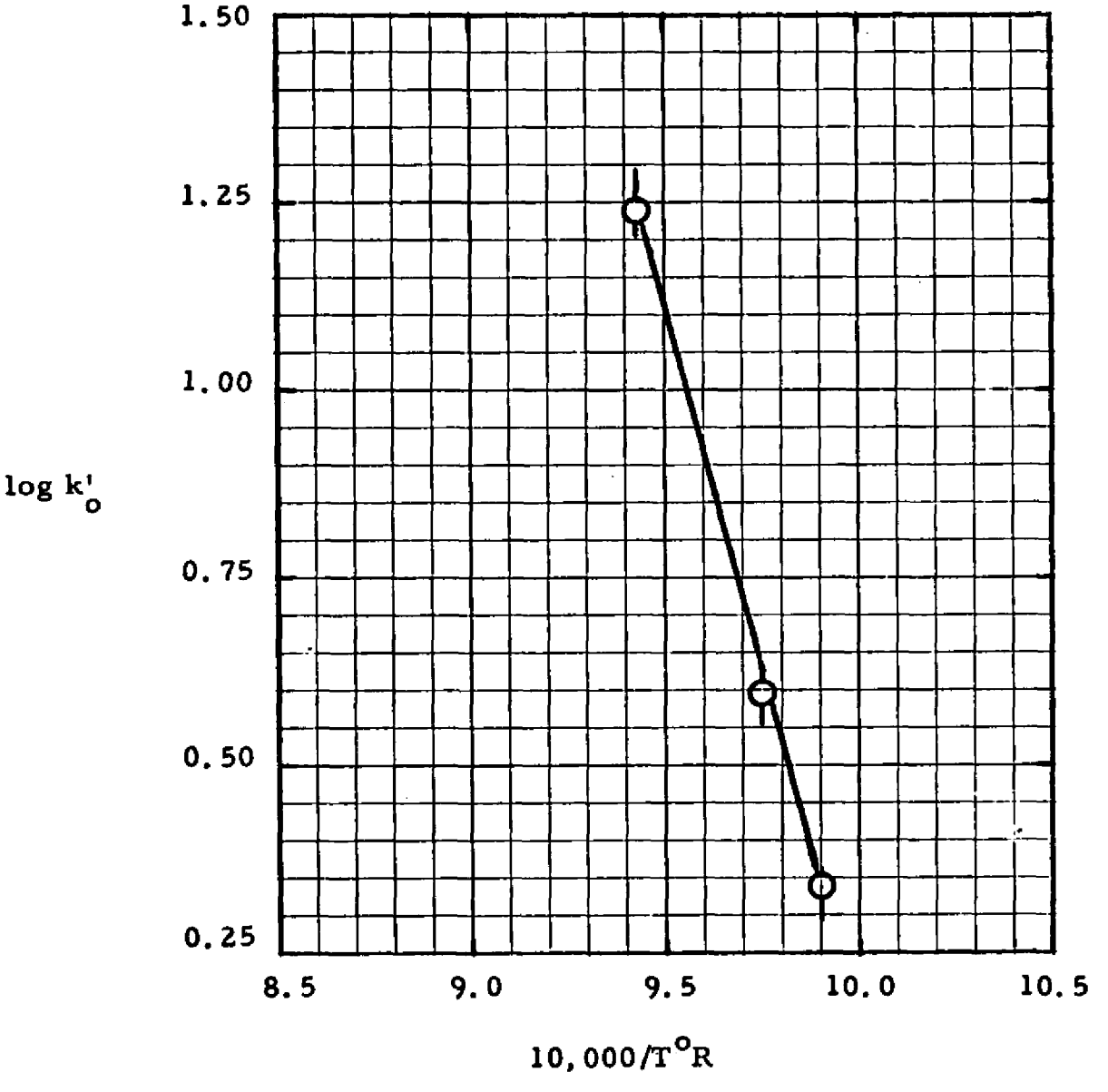

Figure 39. Effect of Temperature on Reaction Rate Constant, Hexane Hydrocracking Over Pd-H-Mordenite

Figure 40 (page 116) presents the hexane isomer concentration in the product hexanes mixture versus hydrocracking conversion. The data indicate a close approach to equilibrium at the higher conversions. The dashed lines indicate the equilibrium values at the temperature of the study, 600°F. The concentrations of the isomers appear to be below the equilibrium values at low hydrocracking conversions, but they still represent 80-90% approach to the equilibrium values. Therefore, the assumption that all hexane isomers can be considered collectively appears to be adequate.

The selectivity of the hydrocracking reaction to form propane was calculated for all hexane over mordenite runs by equation (40). The average selectivity for these runs was 36.1% as compared to 65.7% for the faujasite catalyst. Selectivity values for individual runs varied slightly, but no definite trend with process conditions was indicated. The molar ratios of C_2/C_4 and C_1/C_5 in the product were again much less than unity. The average values for all hexane runs are compared below

	Average for hexane runs over	
Hydrocracked Product	Mordenite	Faujasite
C_2/C_4 molar ratio	0.34	0.50
C_1/C_5 molar ratio	0.11	0.26

Since the C_2/C_4 and C_1/C_5 ratios should be unity for the simple hydrocracking reaction, the data from both catalysts suggest that a more complicated mechanism is taking place. As stated previously, one

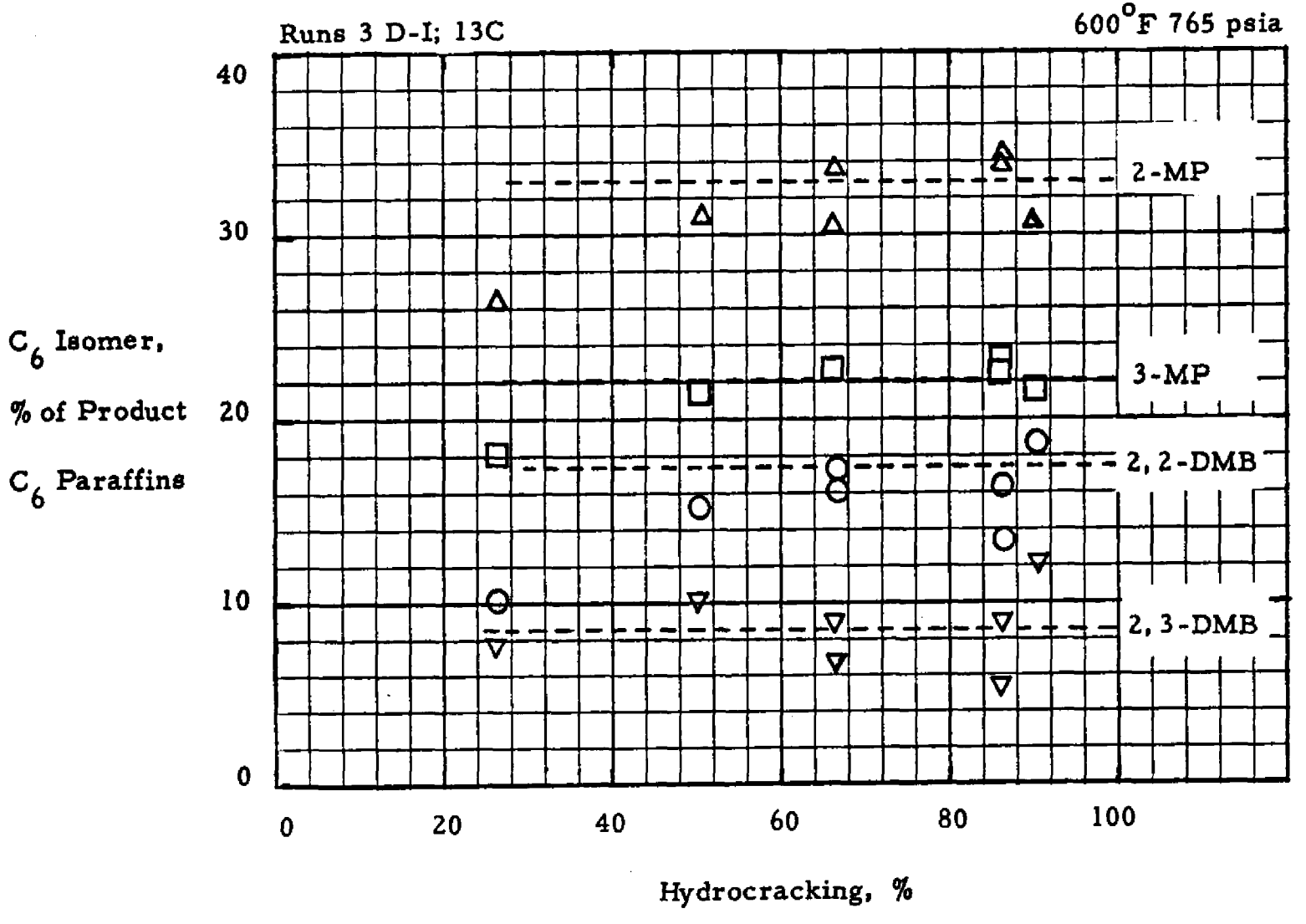

Figure 40. Hexane Isomer Concentration in Product Hexanes, Hexane Hydrocracking Over Pd-H-Mordenite

proposal to explain the data is the formation of a complex containing more than six carbon atoms. This complex would hydrocrack and form butanes and pentanes. The data on the mordenite catalyst indicate that the complex formation reaction is much more prevalent than with the faujasite catalyst. The major hydrocracked product in hexane hydrocracking over Pd-H-mordenite was butanes and pentanes; over Pd-H-faujasite the major product was propane.

The isobutane to n-butane and the isopentane to n-pentane ratios in the product from hydrocracking over the mordenite catalyst are slightly higher than were found for the faujasite catalyst. The average values found for all hexane hydrocracking runs are compared below.

	N-Hexane Hydrocracking over	
Molar ratios in product	Mordenite	Faujasite
iC_4/nC_4	1.2	1.0
iC_5/nC_5	2.3	1.7

7. Catalyst Activity Maintenance

In the study of hydrocracking n-hexane over Pd-H-mordenite, the catalyst activity was relatively constant. No corrections were made for activity differences since the activity decline was negligible.

C. Cyclohexane Hydrocracking

1. General

The approach to this study was similar to that previously discussed for n-hexane hydrocracking over Pd-H-mordenite. Since the mass transfer from fluid to catalyst and the macropore diffusion did not

appear limiting in the study of n-hexane, it was assumed that these steps would not be limiting for the cyclohexane study. The catalyst activity decline in cyclohexane hydrocracking was a problem not encountered in the previous studies. Therefore, catalyst activity will be discussed first.

2. Catalyst Activity Maintenance

Catalyst activity in cyclohexane hydrocracking over Pd-H-mordenite appeared to decline for longer times on feed than was found previously for the faujasite catalyst. In hydrocracking n-hexane over Pd-H-faujasite and Pd-H-mordenite the catalyst activity reached a "lined-out" level after 30-45 minutes on feed. Similar results were found for cyclohexane over faujasite. As shown in Figure 41 (page 119), the activity for cyclohexane hydrocracking over mordenite at 650°F declined until about 250 minutes on feed. After 250 minutes, the simplified rate constant, k_1, appeared to reach a "lined-out" value with time on feed, Θ. Figure 42 (page 120) illustrates similar data at 600°F. In the 600°F study the activity appears fairly constant. It was decided to use a few pentane isomerization runs to investigate the activity of the mordenite.

Bryant[16] reported that Pd-H-mordenite reached a "lined-out" activity after 30-60 minutes on feed, and the decline was very small after the "lined-out" value was reached. After Run 25 at 600°F, a pentane isomerization run was made. This run (26A) was followed by 24 hours of hydrogen stripping at 550°F and 465 psia. Another run

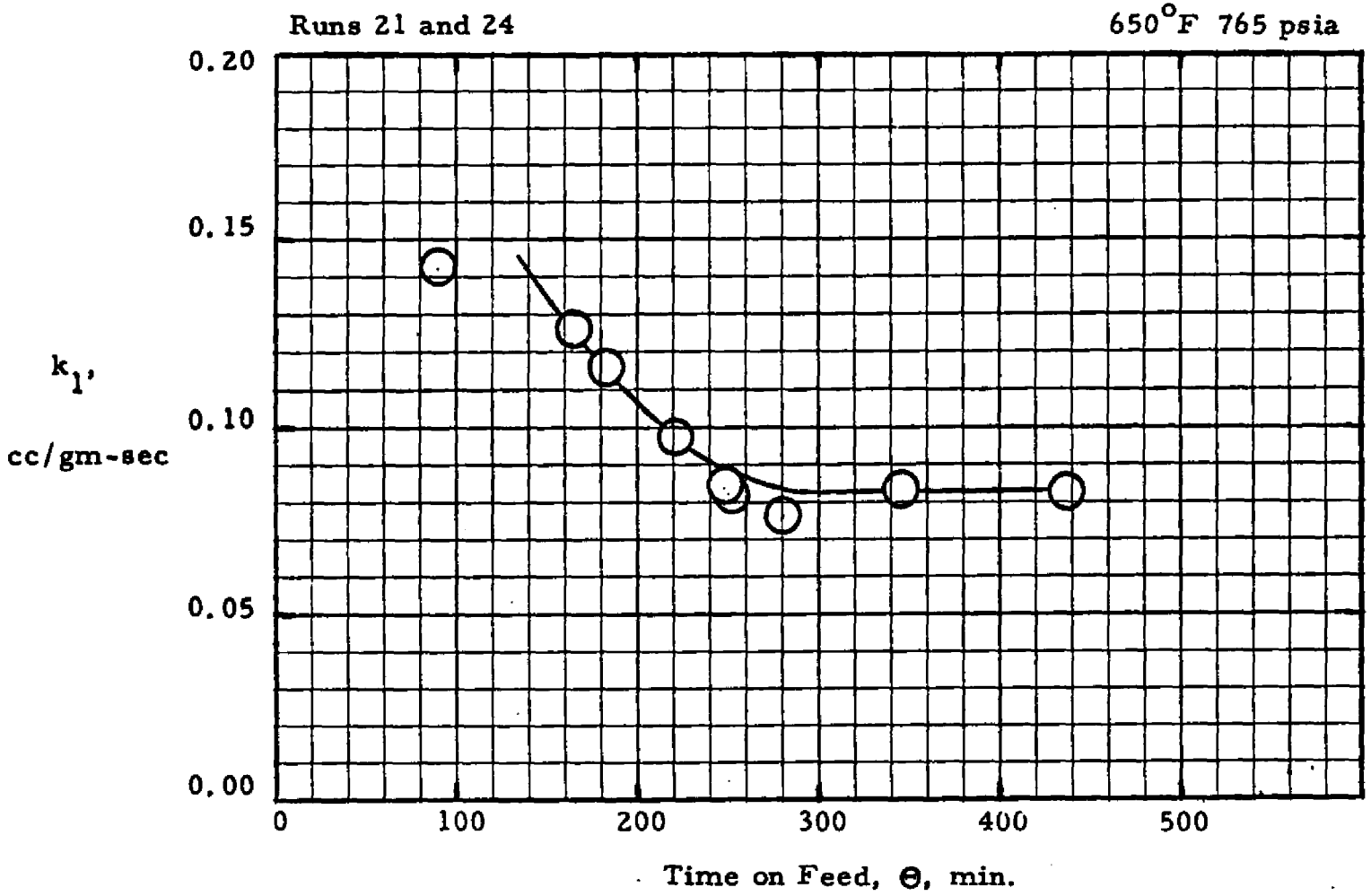

Figure 41. Effect of Catalyst Age on Catalyst Activity, Cyclohexane Hydrocracking Over Pd-H-Mordenite

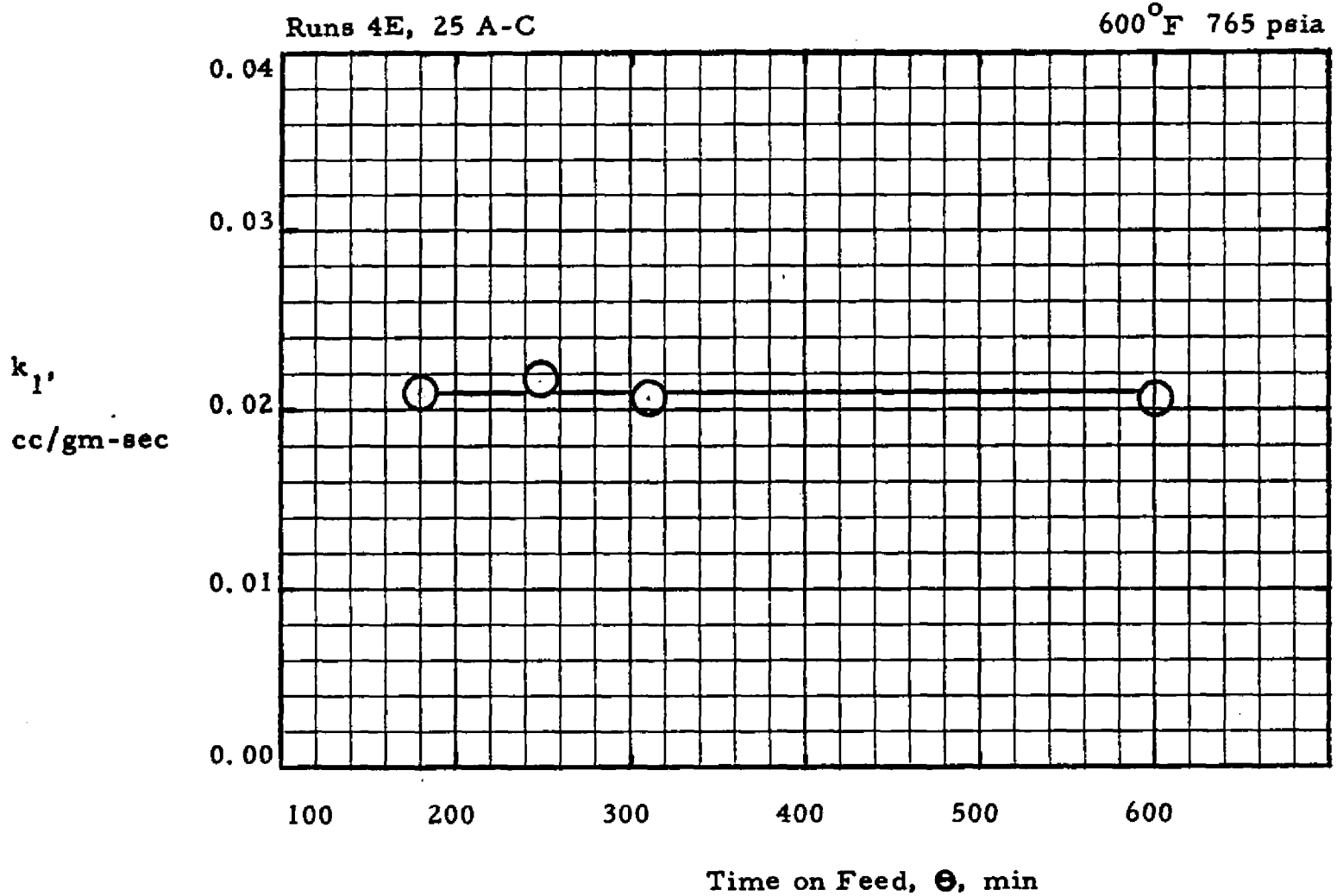

Figure 42. Effect of Catalyst Age on Catalyst Activity, Cyclohexane Hydrocracking Over Pd-H-Mordenite

(26B) was then made on pentane isomerization. Run 27 on pentane isomerization was made with a fresh catalyst charge at its "lined-out" activity. Runs 26A and B and 27 are compared in Table 10 (page 122). These runs were made at Bryant's standard conditions of 550°F, 465 psia, 8 v/hr-v, and 3.4 moles H_2/mole C_5. The simplified rate constants for these runs were calculated by Bryant's method. It appears from these data that cyclohexane operations depressed the isomerization activity. This activity loss was not regained after a 24 hour hydrogen treat. Perhaps the cyclohexane causes coking or some reaction that blocks out some of the active sites. Based on the run made after hydrogen treating, it also appears that this blockage is not removed by hydrogen. No attempt was made to regenerate by air treating.

In correlating the data from cyclohexane hydrocracking it was decided that the "lined-out" activities should be used. Therefore, all data at 650°F and less than 250 minutes on feed were not used in correlations. All data at 600°F appeared to be "lined-out". Therefore, all 600°F data were used.

3. Pseudo-First Order Reaction

In order to test equation (39) for a linear relationship between - log (1-x) and contact time, two sets of runs were made by varying the feed rates. The first test at 650°F appears in Figure 43 (page 123), and the second test at 600°F appears in Figure 44 (page 124). As can be seen, the first order relationship for the hydrocarbon component

Table 10. Summary of Results of Pentane Isomerization Runs Over Pd-H-Mordenite

Operating Conditions

Temperature, ^{o}F	550
Pressure, psia	465
Feed	n-Pentane
Catalyst	Pd-H-Mordenite

Run Results

Run No.	Run Description	Simplified Rate Constant for Pentane Isom.
26A	After Run 25	0.073
26B	24 hours on H_2 after 26A	0.075
27	"Lined-out" activity for pentane isomerization	0.100

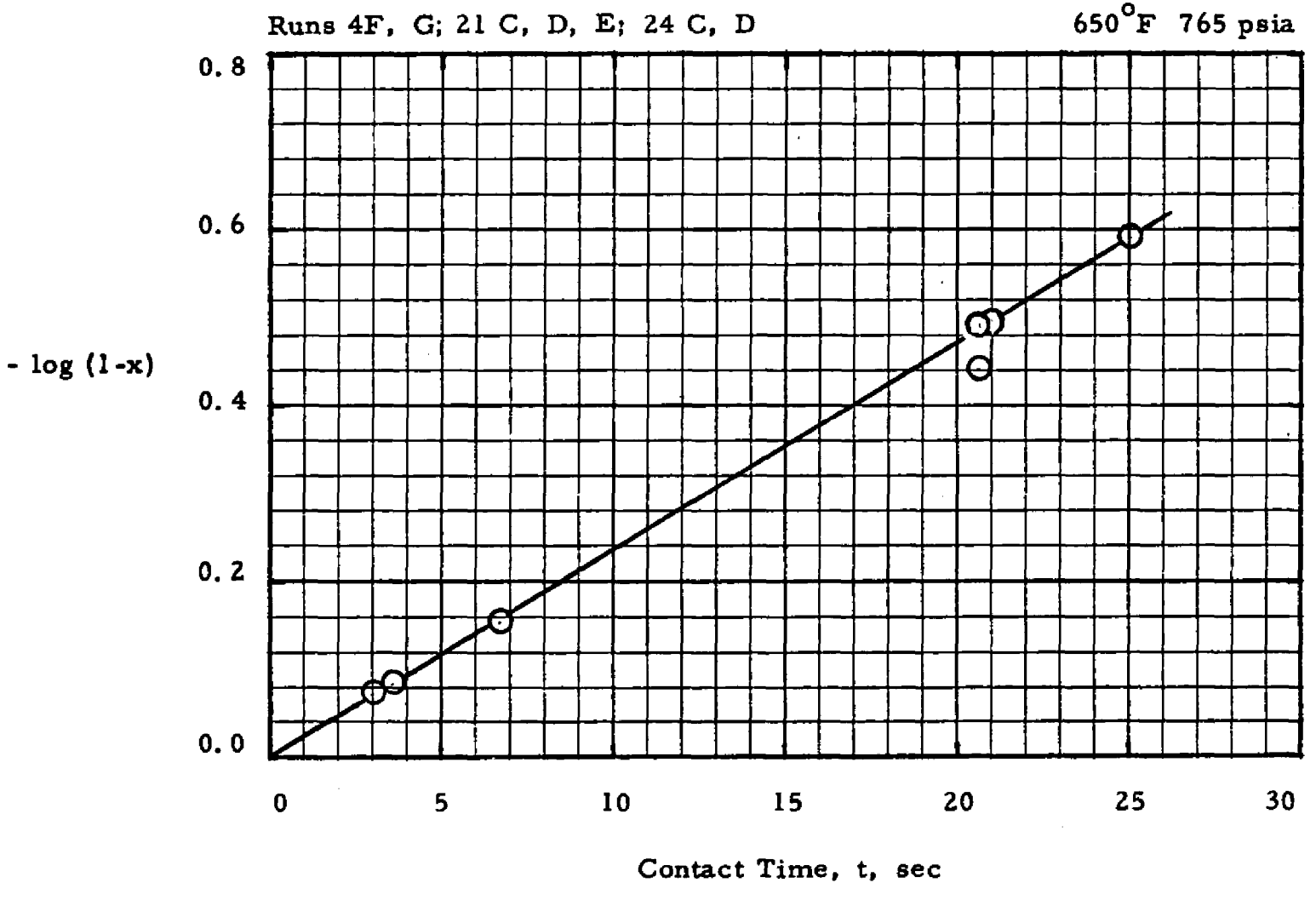

Figure 43. Test for First Order Model, Cyclohexane Hydrocracking Over Pd-H-Mordenite

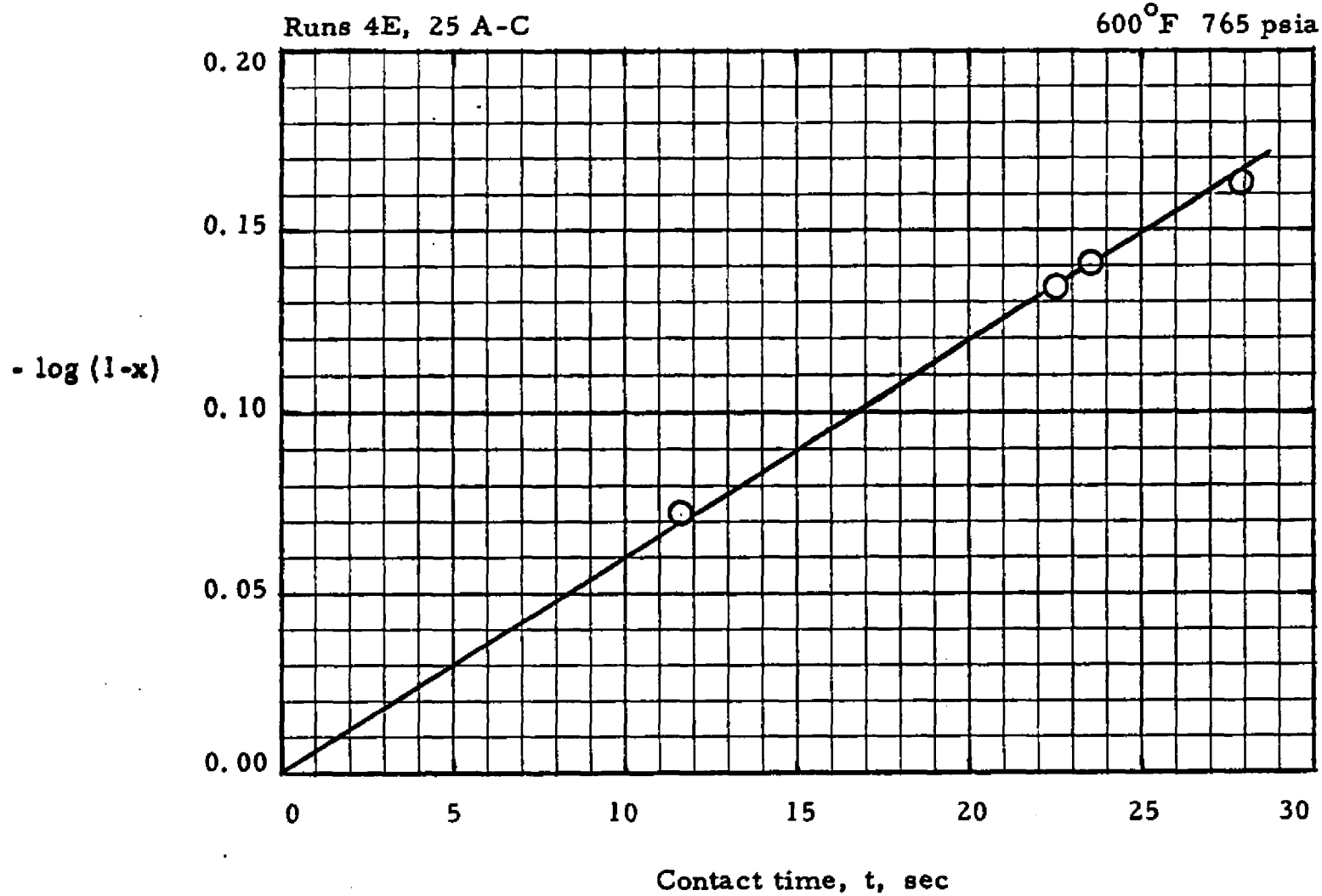

Figure 44. Test for First Order Model, Cyclohexane Hydrocracking Over Pd-H-Mordenite

appears to hold for cyclohexane over mordenite as it has in the previous tests for n-hexane.

4. Effect of Hydrogen Partial Pressure

A test of the relationship of

$$1/\sqrt{k_1} = 1/\sqrt{k_{1,0} K_C} + (K_B/\sqrt{k_{1,0} K_C})\, p_B \qquad (55)$$

was made at 600°F. These data are shown in Figure 45 (page 126). The following values were calculated by equation (53).

$$K_B = 0.24 \qquad (56)$$

$$k'_{1,0} = k_{1,0} K_C = 3.0 \qquad (57)$$

5. Effect of Temperature

The effect of temperature on the hydrogen adsorption coefficient, K_B, is compared with the data from the faujasite catalyst in Figure 46 (page 127). The values for the mordenite catalyst indicate that hydrogen adsorption is higher than for the faujasite catalyst.

Values of K_B and k_1 are used in the following relationship to calculate $k'_{1,0}$.

$$k'_{1,0} = k_1 (1 + K_B p_B)^2 \qquad (58)$$

The calculated values of $k'_{1,0}$ are used in an Arrhenius plot in Figure 47 (page 128). The data point at each temperature indicates the average value, and the vertical line indicates the range of values. The activation energy calculated from the slope of the line between the data points in Figure 47 was 32 kcal/gm mole. This activation energy compares well with the value of 31 kcal/gm mole for cyclohexane over the faujasite catalyst.

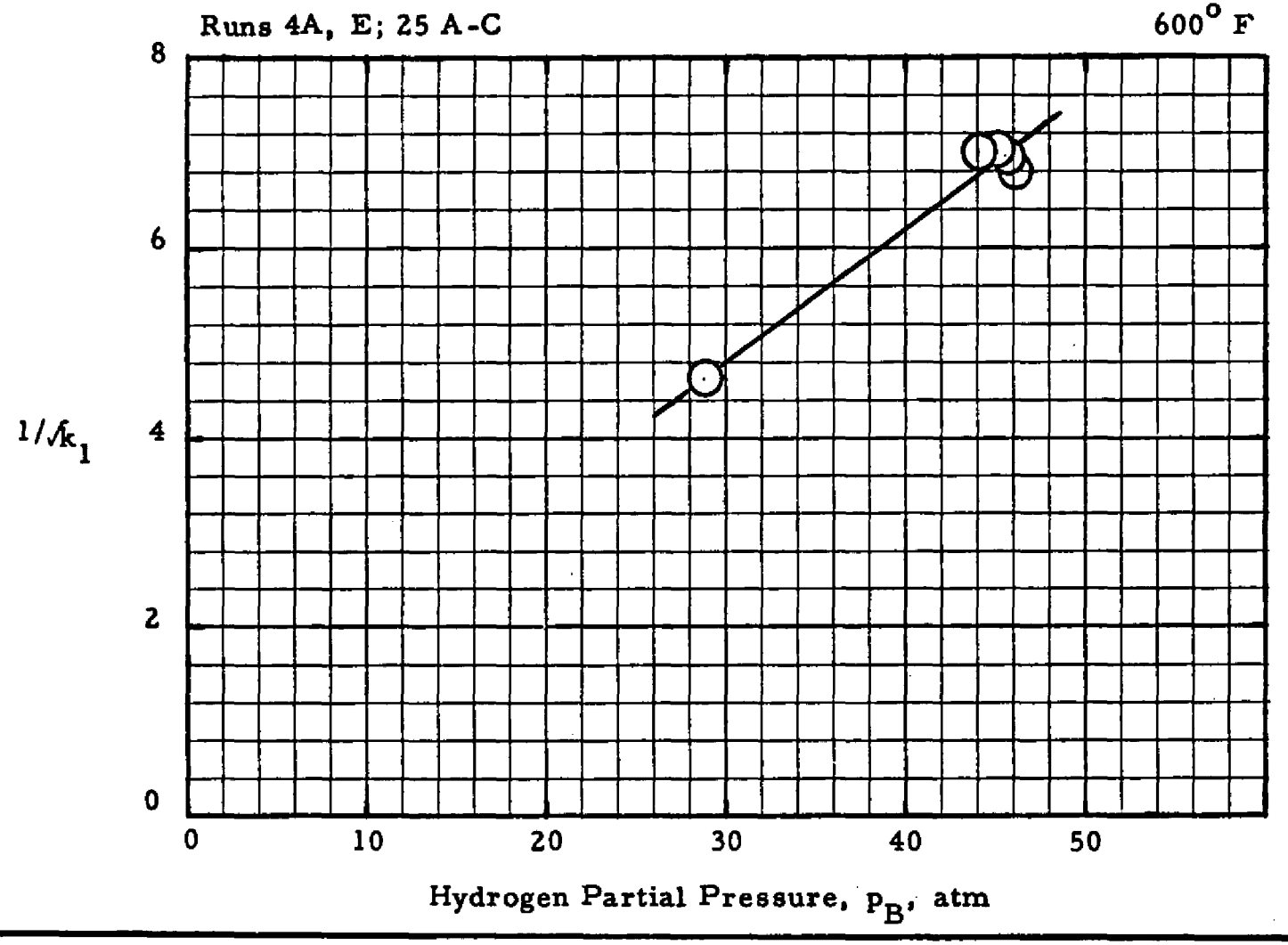

Figure 45. Test for Dual Site Mechanism, Cyclohexane Hydrocracking Over Pd-H-Mordenite

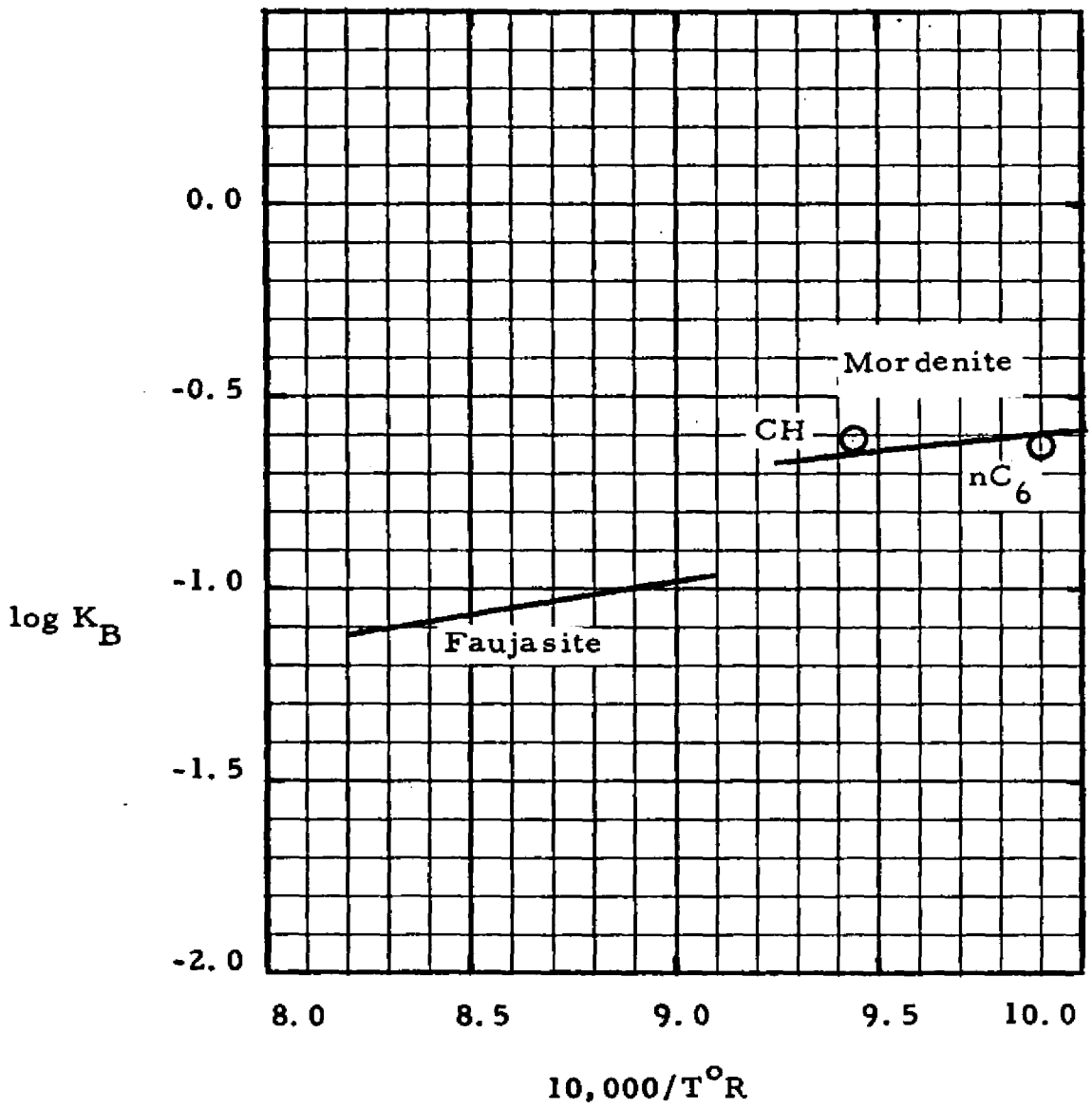

Figure 46. Effect of Temperature on Hydrogen Adsorption Coefficient, Pd-H-Mordenite

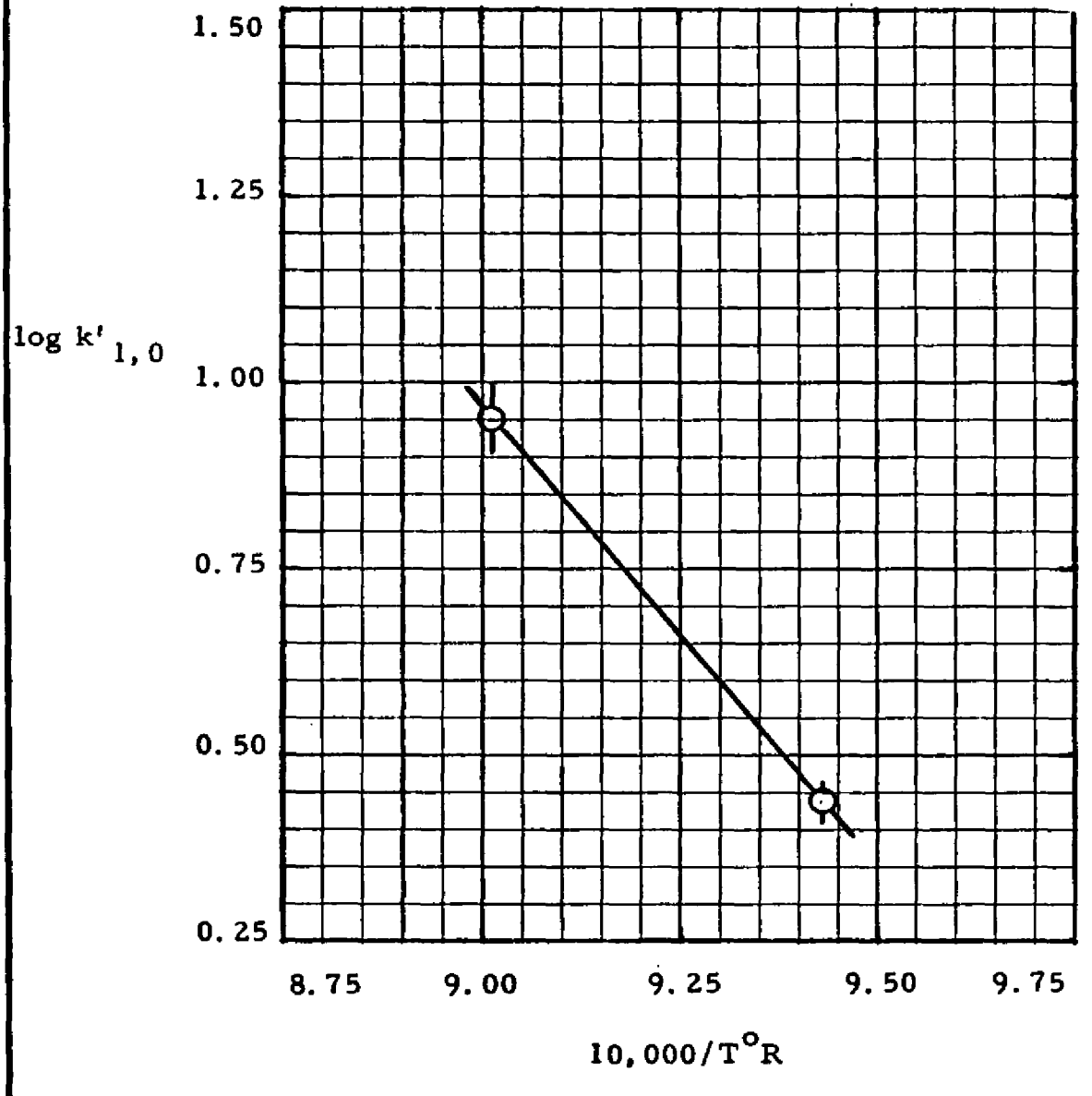

Figure 47. Effect of Temperature on Reaction Rate Constant, Cyclohexane Hydrocracking Over Pd-H-Mordenite

In comparing the reactivity of cyclohexane with n-hexane over mordenite, it is seen that n-hexane is the more reactive. For example, the following values of the rate constants are indicated in Figures 39 and 46 at 600°F.

Reaction rate constant at 600°F Pd-H-Mordenite

n-Hexane	1.22
Cyclohexane	0.43

Adams and co-workers[1] found a similar effect in catalytic cracking n-heptane and methylcyclohexane over H-mordenite. In their study n-heptane, the paraffin, was more reactive than methylcyclohexane, the naphthene. In the present study, the opposite effect was noted in hydrocracking over Pd-H-faujasite. The cyclohexane was more reactive than n-hexane. In comparing the two catalysts used in the present study, both n-hexane and cyclohexane were more reactive over Pd-H-mordenite.

6. Mechanism

The data from cyclohexane hydrocracking over Pd-H-mordenite appear to be consistent with the previously discussed model. The equation for the H_2 adsorption coefficient is the same described in the hexane-over-mordenite study. This was equation (54). The equation for $k'_{1,0}$ is

$$\ln k'_{1,0} = 28.19 - (28,850/T^{\circ}R). \qquad (57)$$

It is now evident that hydrocracking both n-hexane and cyclohexane over both catalysts can be correlated with a single model. This model is

first order with respect to the hydrocarbon concentration, and is based on a dual site mechanism.

Figure 48 (page 131) presents the MCP in the product MCP + CH mixture. At high conversions the MCP concentration appears to be at the equilibrium value indicated by the dashed line. The MCP concentrations are considerably below the equilibrium value at low hydrocracking conversions, but they appear to be rising rapidly. Apparently the intrinsic isomerization activity and hydrocracking activity are fairly close together with the mordenite, whereas the isomerization activity for the faujasite is much higher than the hydrocracking activity.

The ring-opening hydrocracking reaction is much smaller with the mordenite than was found with the faujasite catalyst. The selectivity to hexane isomers formed by hydrocracking the naphthenes is shown in Figure 49 (page 132).

The products from hydrocracking to lower molecular weight paraffins are summarized in Table 11 (page 133). As can be seen, there appears to be an effect of temperature. The selectivity to propanes increases with temperature, and the iso-to-normal butane and pentane ratios increase with temperature. The C_2/C_4 and C_1/C_5 molar ratios are much higher than previously found for any of the other hydrocracking studies. The products from hydrocracking cyclohexane over mordenite indicate more simple carbon-to-carbon bond splitting of the C_6 molecule than was evidenced in previous studies. As noted earlier, the C_2/C_4 and C_1/C_5 molar ratios should be equal to unity for

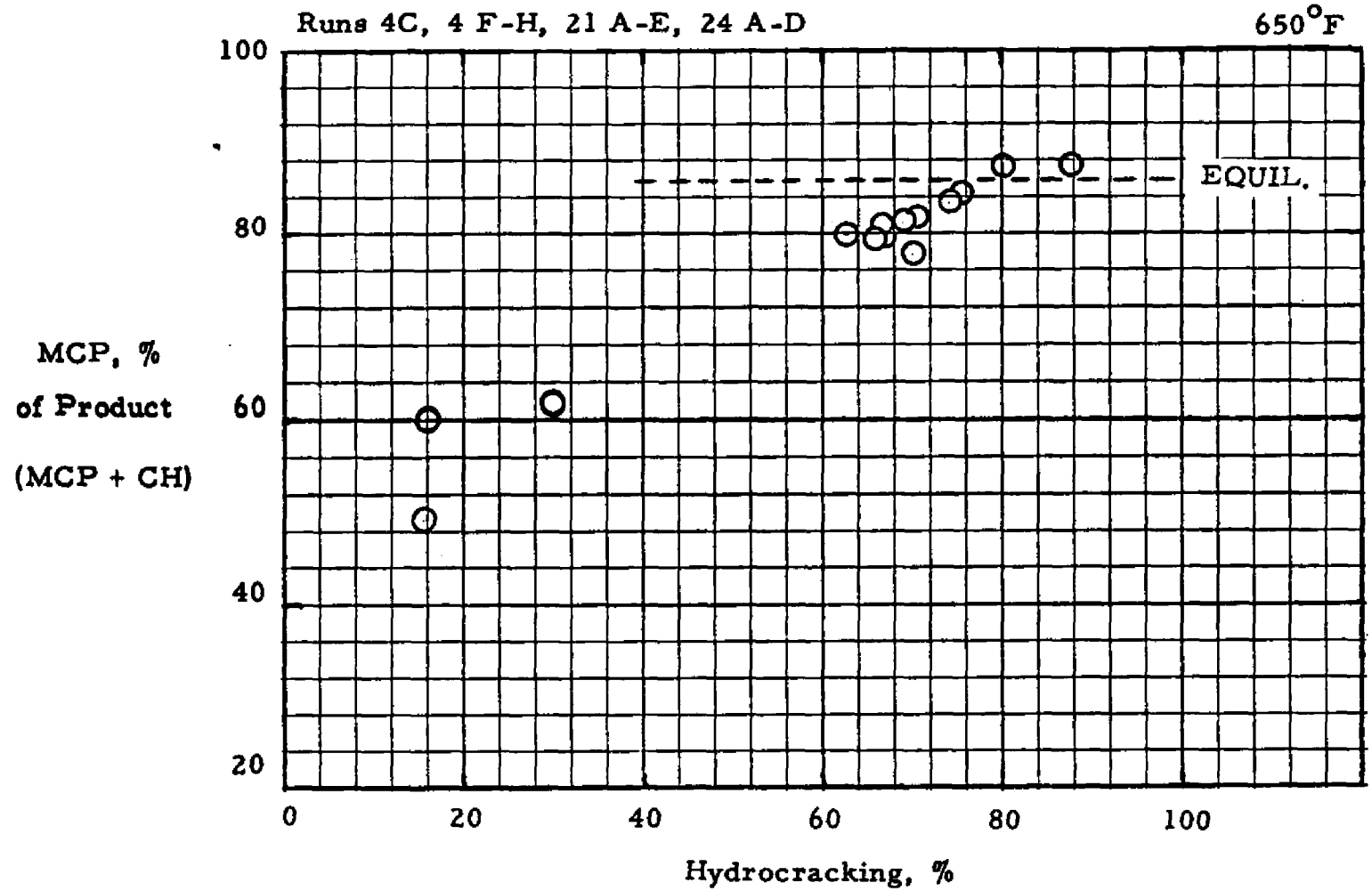

Figure 48. Methylcyclopentane Concentration in Product Naphthenes, Cyclohexane Hydrocracking Over Pd-H-Mordenite

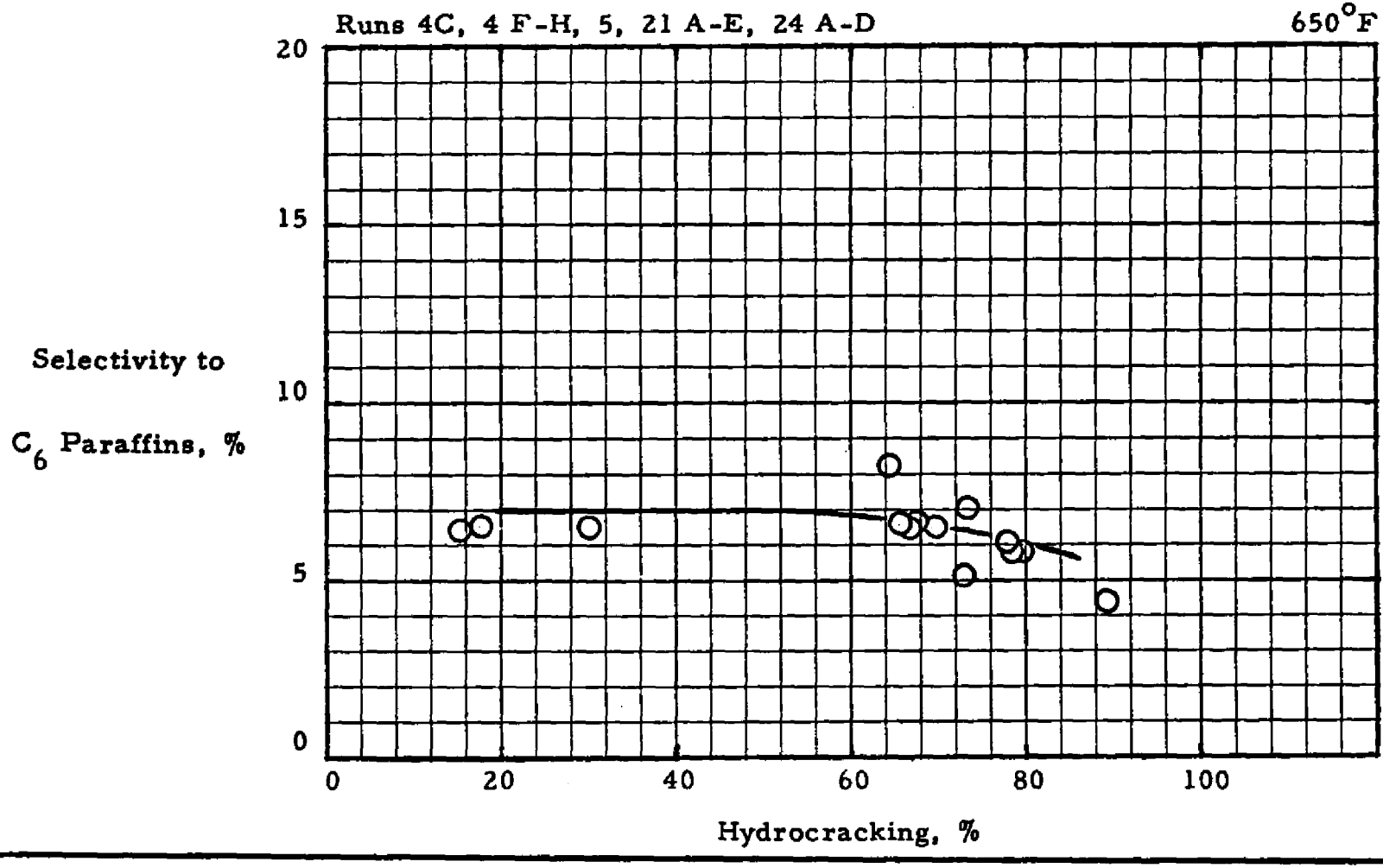

Figure 49. Effect of Conversion on Selectivity to C_6 Paraffins, Cyclohexane Hydrocracking Over Pd-H-Mordenite

Table 11. Products from Hydrocracking Cyclohexane Over Pd-H-Mordenite

Operating Conditions		
Temperature, °F		600-650
Pressure, psia		465-765
Feed		Cyclohexane
Catalyst		Pd-H-Mordenite
Run Nos.		4A, 4E-H, 21C-E, 24C-D, 25A-C
Run Results		
600°F Product	Range	Average
Selectivity to C_3, %	43.3-54.6	47.4
C_2/C_4 molar ratio	0.24-0.29	0.26
C_1/C_5 molar ratio	0.29-0.74	0.41
iC_4/nC_4 molar ratio	0.19-0.25	0.22
iC_5/nC_5 molar ratio	1.00-1.39	1.18
650°F Product		
Selectivity to C_3, %	53.9-61.2	57.1
C_2/C_4 molar ratio	0.42-0.82	0.65
C_1/C_5 molar ratio	0.47-1.00	0.63
iC_4/nC_4 molar ratio	0.58-1.00	0.69
iC_5/nC_5 molar ratio	2.25-3.90	2.75

a straight-forward hydrocracking reaction of a six carbon atom molecule. The C_2/C_4 and C_1/C_5 ratios less than unity were attributed to a higher molecular weight complex which formed by hydrocracked fragments joining to molecules containing six carbon atoms. This complex subsequently must have hydrocracked to butanes and pentanes.

D. Hydrocracking N-Hexane-Cyclohexane Mixture

A few runs were made with a 56 mole % cyclohexane-44 mole % n-hexane mixture feed stock. These data are summarized in Table 12 (page 135). Although pure compound studies indicated than n-hexane was more reactive than cyclohexane, the cyclohexane was preferentially converted in the mixed feed. In Table 12, the actual conversions are compared to the conversions predicted from the models developed for pure feeds. The actual cyclohexane plus methylcyclopentane conversions were consistently higher than the predicted values, and the conversions of the hexanes were consistently lower. These data strongly suggest that cyclohexane and methylcyclopentane are much more highly adsorbed than the hexanes.

In order to adjust for the differences in adsorption, an empirical factor can be added to the conversion equations. For example, the cyclohexane equation becomes

$$-\ln(1-x) = 5.3\, k'_{1,0}\, t_H/(1 + K_B p_B)^2. \qquad (60)$$

The conversions predicted by equation (60) are compared with the actual conversions below.

Table 12. Hydrocracking of N-Hexane-Cyclohexane Mixture Over Pd-H-Mordenite -- Summary of Results

Operating Conditions				
Catalyst	Pd-H-Mordenite			
Space velocity, v/hr-v	2			
Pressure, psia	765			
Run No.	28A	28B	28C	28D
Temperature, °F	600	600	650	650
Conversion of (MCP + CH), %				
Actual	61.3	74.8	99.5	99.6
Predicted	16.2	22.6	63.5	68.1
Conversion of hexanes, %				
Actual	21.3	42.3	93.0	98.0
Predicted	68.3	81.2	~100.0	~100.0

Run No.	MCP + CH Conversion, % Predicted	Actual
28A	60.9	61.3
28B	74.3	74.8
28C	95.1	99.5
28D	97.7	99.6

The adjusted equation for n-hexane hydrocracking becomes

$$- \ln (1-x) = 0.29\, k'_o\, t_H/(1 + K_B p_B)^2. \qquad (61)$$

The conversions predicted by equation (61) are compared with the actual conversions below.

Run No.	Hexanes Conversion, % Predicted	Actual
28A	28.4	21.3
28B	38.3	42.3
28C	98.1	93.0
28D	98.9	98.0

The preferential adsorption of the naphthene on mordenite catalysts also was noted by Beecher and co-workers[10]. In their study of hydrocracking n-decane and decalin over mordenite, decalin was less reactive than n-decane in pure compound studies, but decalin was preferentially converted from a mixture of decalin and n-decane. The present results on cyclohexane and n-hexane are in agreement with this previous work on decalin and n-decane.

CHAPTER VII

CONCLUSIONS AND RECOMMENDATIONS

A. Conclusions

1. Pd-H-mordenite and Pd-H-faujasite are both extremely active catalysts for hydrocracking n-hexane and cyclohexane.
2. Both mordenite and faujasite have commercial possibilities for producing liquefied petroleum gas plus a high octane pentane/hexane fraction by hydrocracking low octane naphtha.
3. In pure compound studies, the results of this investigation are compatible with an irreversible reaction that is first-order with respect to the hydrocarbon and that takes place at a "dual-site."
4. The results of hydrocracking a n-hexane-cyclohexane mixture over Pd-H-faujasite were predicted successfully from the results of pure compound studies. This implies that the adsorption of n-hexane and cyclohexane are about equal on Pd-H-faujasite.
5. The results of hydrocracking a n-hexane-cyclohexane mixture over Pd-H-mordenite indicate that cyclohexane is more adsorbed than n-hexane, and cyclohexane is preferentially converted.

6. Pd-H-mordenite is more active than Pd-H-faujasite for hydrocracking n-hexane, cyclohexane, and mixtures of n-hexane and cyclohexane.

B. Recommendations

1. More is needed to be known about the relative adsorption of various types of hydrocarbons during hydrocracking reactions over mordenite catalysts.
2. Diffusion in the micropores of zeolites should be investigated by using catalysts made from different size crystals.

LIST OF REFERENCES

(1) Adams, C. E., Kimberlin, C. N., Jr., and Shoemaker, D. P., "Structural Influence on Cracking Catalyst Activity and Selectivity," Proceedings of the Third International Congress on Catalysis, II. 8, 1310 (1964).

(2) Archibald, R. C., Greensfelder, B. S., Holzman, G., and Rowe, D. H., "Catalytic Hydrocracking of Aliphatic Hydrocarbons," Industrial and Engineering Chemistry, 52, 745 (1960).

(3) Barrer, R. M., "Synthesis and Reactions of Mordenite," Journal of the Chemical Society, 2158 (1948).

(4) Barrer, R. M., "Transient Flow of Gases in Sorbents Providing Uniform Capillary Networks of Molecular Dimensions," Transactions of the Faraday Society, 45, 358 (1959).

(5) Barrer, R. M., "Molecular Sieves," Endeavor, XXIII (No. 90), 122 (1964).

(6) Barrer, R. M. and Baynham, J. W., "The Hydrothermal Chemistry of the Silicates. Part VII. Synthetic Potassium Aluminosilicates," Journal of the Chemical Society, 2892 (1956).

(7) Barrer, R. M. and Rees, L. V. C., "Sorption of Mixtures. Part 3 - Polar Sorbates as Modifiers of Zeolitic Crystals," Transactions of the Faraday Society, 50, 852 (1954).

(8) Barrer, R. M. and Robins, A. B., "Sorption of Mixtures. Part I - Molecular Sieve Separations of Permanent and Inert Gases," Transactions of the Faraday Society, 49, 807 (1953).

(9) Beecher, R. G., "Hexane Isomerization," Ph. D. dissertation, Department of Chemical Engineering, Louisiana State University, 1967.

(10) Beecher, R. G., Voorhies, A., Jr., and Eberly, P. E., Jr., "Hydrocracking and Diffusion Studies of Pure Compounds on Mordenite Catalysts," American Chemical Society Preprints, Division of Petroleum Chemistry, 12 (No. 4), B-5 (1967).

(11) Beuther, H. and Larson, O. A., "Role of Catalytic Metals in Hydrocracking," Industrial and Engineering Chemistry Process Design and Development, 4 (No. 2), 177 (1965).

(12) Bischoff, K. B., "Patterns of Flow in Chemical Process Vessels," Advances in Chemical Engineering, 4, 95, Academic Press, New York, N. Y., 1963.

(13) Bloch, H. S., Donaldson, G. R., and Haensel, V., "Hydroisomerization of Light Paraffin Hydrocarbons," American Chemical Society Preprints, Division of Petroleum Chemistry, 4 (No. 2), A-13 (1959).

(14) Bolton, A. P., Lanewala, M. A., and Pickert, P. E., "Isomerization of the Diethylbenzenes Using Zeolite Catalysts," American Chemical Society Preprints, Division of Petroleum Chemistry, 11 (No. 4), A-113 (1966).

(15) Breck, D. W., "Crystalline Molecular Sieves," Journal of Chemical Education, 41 (No. 12), 678 (1964).

(16) Bryant, P. A., "Hydroisomerization of Normal Pentane Over a Zeolite Catalyst," Ph. D. dissertation, Department of Chemical Engineering, Louisiana State University, 1966.

(17) Chang, Y. and Kalechits, I. V., "Conversion of Some Six-membered Naphthenes Under Platforming Conditions," K'o Hsueh T'ung Pao, 15, 475 (1958); Chemical Abstracts, 53, 10719i (1960).

(18) Clement, C., Leprince, P., and Montarnal, R., "Caracterisation Cinetique des Catalyseurs d'Hydrocraquage. II-Cinetique des Hydroreactions du Benzene et du Cyclohexane Sur Tamis Moleculaires Impregnes Par un Metal Hydrogenant," Bulletin de la Societie Chimique de France, 3, 1021 (1966).

(19) Coonradt, H. L. and Garwood, W. E., "Mechanism of Hydrocracking-Reactions of Paraffins and Olefins," Industrial and Engineering Chemistry Process Design and Development, 3 (No. 1), 38 (1964).

(20) Eberly, P. E., Jr., "Hydrocarbon Adsorption Studies at Low Pressures on the Sodium and Acid Forms of Synthetic Mordenite," Journal of Physical Chemistry, 67, 2404 (1963).

(21) Egan, C. J., Langlois, G. E., and White, R. J., "Selective Hydrocracking of C_9 to C_{12} - Alkylcyclohexanes on Acidic Catalysts. Evidence for the Paring Reaction," Journal of the American Chemical Society, 84, 1204 (1962).

(22) Evering, B. L. and d'Ouville, E. L., "Experimental Equilibrium Constant for the Isomeric Hexanes," Journal of the American Chemical Society, 71, 440 (1959).

(23) Flinn, R. A., Larson, O. A., and Beuther, H., "The Mechanism of Catalytic Hydrocracking," Industrial and Engineering Chemistry, 52 (No. 2), 153 (1960).

(24) Frilette, V. J. and Rubin, M. K., "Sorption and Catalytic Properties of Natural Mordenite," Journal of Catalysis, 4, 310 (1965).

(25) Frilette, V. J., Weisz, P. B., and Golden, R. L., "Catalysis by Crystalline Aluminosilicates. I. Cracking of Hydrocarbon Types Over Sodium and Calcium X Zeolites," Journal of Catalysis, 1, 301 (1962).

(26) Gould, G. D., Paterson, N. J., Rogers, G. B., and Schultz, T. F., "Hydrocracking From Top to Bottom," Chemical Engineering Progress, 63 (No. 5), 60 (1967).

(27) Guenther, G., "Kinetics of Hydrogenation Reactions: Hydrogenation Cracking of Carbon-Carbon Bonds," Chemische Technik, 13, 718 (1961).

(28) Hartwig, M., "Isomerization and Hydrocracking of n-Paraffins Over Palladium Catalysts," Brennstoff-Chemie, 45 (No. 8), 234 (1964).

(29) Henke, A. M. and Schmid, B. K., "Hydrocracking of Naphtha for LPG Production," Chemical Engineering Progress, 63 (No. 5), 51 (1967).

(30) Hougen, O. A. and Watson, K. M., Chemical Process Principles, Part III, Kinetics and Catalysis, John Wiley and Sons, New York, N. Y., 1947.

(31) Hutchins, J. P., "Reactions of Pentane Over a Platinum Alumina Catalyst," Ph. D. dissertation, Department of Chemical Engineering, University of Wisconsin, 1962.

(32) Iijima, K., Shimizu, S., Furukawa, T., and Yoshida, N., "Hydrodecyclization of Methylcyclopentane and Benzene in the Presence of a Reforming Catalyst," Bulletin of the Japan Petroleum Institute, 5, 1 (1963).

(33) Kaliberdo, L. M. and Kalechits, I. V., "Successive Reactions in Gasoline Production," Trudy Vostochuo-Sibir Filiale, Ser. Khim., 38, 152 (1961); Chemical Abstracts, 56, 11885i (1962).

(34) Keough, A. H., "Catalytic Cracking of Hydrocarbons with Open Synthetic Mordenites," American Chemical Society Preprints, Division of Petroleum Chemistry, 8 (1), 65 (1963).

(35) Keough, A. H. and Sand, L. B., "A New Intracrystalline Catalyst," Journal of the American Chemical Society, 83, 3536 (1961).

(36) Keulemanns, A. I. M. and Voge, H. H., "Reactivities of Naphthenes Over a Platinum Reforming Catalyst by a Gas Chromatographic Technique," Journal of Physical Chemistry, 63, 476 (1959).

(37) Langlois, G. E., Sullivan, R. F., and Egan, C. J., "Hydrocracking of Paraffins With Nickel on Silica-Alumina Catalysts - The Role of Sulfiding," American Chemical Society Preprints, Division of Petroleum Chemistry, 10, B-127 (1965).

(38) Larson, O. A., MacIver, D. S., Tobin, H. H., and Flinn, R. A., "Effects of Platinum Area and Surface Acidity on Hydrocracking Activity," Industrial and Engineering Chemistry Process Design and Development, 1 (No. 4), 300 (1962).

(39) Levenspiel, O., Chemical Reaction Engineering, John Wiley and Sons, New York, 1962.

(40) McBain, J. W., The Sorption of Gases by Solids, Routledge and Kegan Paul, London, 1932.

(41) Mathews, J. W., Robbins, L. V., Jr., and Sosnowski, J., "Hydrocracking With Flexibility," Chemical Engineering Progress, 63 (No. 5), 56 (1967).

(42) Mays, R. L., Pickert, P. E., Bolton, A. P., and Lanewala, M. A., "Molecular Sieve Catalysts Head for Ever-Greater Role," The Oil and Gas Journal, May 17, 1965.

(43) Miale, J. N., Chen, N. Y., and Weisz, P. B., "Catalysis by Crystalline Aluminosilicates. IV. Attainable Catalytic Cracking Rate Constants and Superactivity," Journal of Catalysis, 6, 278 (1966).

(44) Miller, R., "Molecular Sieve Catalysts," Chemical Week, 95, 77 (1964).

(45) Mills, G. A., Heinemann, H., Millikin, T. H., and Oblad, A. G., "Houdriforming Reactions - Catalytic Mechanism," Industrial and Engineering Chemistry, 45, 130 (1953).

(46) Murphree, E. V., Brown, C. L., and Gohr, E. J., "Hydrogenation of Petroleum," Industrial and Engineering Chemistry, 32, 1203 (1940).

(47) Myers, G. C. and Munns, G. W., Jr., "Platinum Hydrocracking of Pentanes, Hexanes and Heptanes," Industrial and Engineering Chemistry, 50 (No. 12), 1727 (1958).

(48) Nikolina, Niemark, and Piontkovskaya, "Molecular Sieves - Preparation, Properties and Applications," Russian Chemical Reviews, 29 (No. 9), 509 (1963).

(49) Norton, C. J., "Olefin Polymerization Over Synthetic Molecular Sieves," Industrial and Engineering Chemistry Process Design and Development, 3 (No. 3), 230 (1964).

(50) Osipov, A. N. and Khavkin, V. A., "Kinetics of Hydrocarbon Transformation During the Second Stage of Hydrocracking of Gas Oil," Kim. Tekhnol. Topl. Masch., 11 (12), 14 (1966); Chemical Abstracts, 66, 67559v (1967).

(51) Petersen, E. E., Chemical Reaction Analysis, Prentice-Hall, Englewood Cliffs, N. J., 1965.

(52) Plank, C. J., Rosinski, E. J., and Hawthorne, W. P., "Acidic Crystalline Aluminosilicates. New Superactive, Superselective Cracking Catalysts," Industrial and Engineering Chemistry Product Research and Development, 3 (No. 3), 165 (1964).

(53) Pollitzer, E. L., Mitsche, R. T., Addison, G. E., and Hamblin, R. J., "Ways to LPG: Reform or Hydrocrack," Hydrocarbon Processing, 46 (No. 5), 175 (1967).

(54) Rabo, J. A., Pickert, P. E., and Mays, R. L., "Pentane and Hexane Isomerization," Industrial and Engineering Chemistry, 53 (No. 9), 733 (1961).

(55) Ridgway, J. A., Jr. and Schoen, W., "Hexane Isomer Equilibrium," American Chemical Society Preprints, Division of Petroleum Chemistry, 4 (No. 2), A-5 (1959).

(56) Rossini, F. D., et al., Selected Values of Physical and Thermodynamic Properties of Hydrocarbons and Related Compounds, Carnegie Press, Pittsburgh, Pa., 1953.

(57) Schriesheim, A. and Khoobiar, S. H., "Hexane Isomer Equilibrium Studies," Journal of the American Chemical Society, 82, 832 (1960).

(58) Scott, J. W. and Paterson, N. J., "Advances in Hydrocracking," Proceedings of the Seventh World Petroleum Congress, (1967).

(59) Scott, J. W., Robbers, S. A., Mason, H. F., Paterson, N. J., and Kozlowski, N. J., "Isomax: A New Hydrocracking Process in Large Scale Commercial Use," Proceedings of the Sixth World Petroleum Congress, (1963).

(60) Sinfelt, J. H. and Rohrer, J. C., "Reactivities of Some C_6-C_8 Paraffins Over Pt-Al_2O_3," Journal of Chemical and Engineering Data, 1 (No. 1), 109 (1963).

(61) Stormont, D. H., "Synthetic Zeolite Offer Unique Properties As Catalytic Supports," The Oil and Gas Journal, November 23, 1964.

(62) Venuto, P. B., Hamilton, L. A., and Landis, P. S., "Alkylation Reactions Catalyzed by Crystalline Aluminosilicates: Mechanistic and Aging Considerations," American Chemical Society Preprints, Division of Petroleum Chemistry, 11 (No. 3), 91 (1966).

(63) Venuto, P. B., Hamilton, L. A., Landis, P. S., and Wise, J. J., "Organic Reactions Catalyzed by Crystalline Aluminosilicates. I. Alkylation Reactions," Journal of Catalysis, 4, 81 (1966).

(64) Venuto, P. B. and Landis, P. S., "Organic Reactions Catalyzed by Crystalline Aluminosilicates. Condensation Reactions of Carbonyl Compounds," American Chemical Society Preprints, Division of Petroleum Chemistry, 11 (No. 4), A-105 (1966).

(65) Voge, H. H., "Catalytic Cracking," Catalysis, Vol. VI, Reinhold, New York, 1958.

(66) Wauquier, J. P. and Jungers, J. C., "Quantitative Kinetics in Heterogeneous Catalysis. The Influence of the Medium on the Activity and Selectivity of the Catalyst," Bulletin of the Society Chimique France, 10, 1280 (1957).

(67) Weisz, P. B., "Polyfunctional Heterogeneous Catalysis," Advances in Catalysis, Vol. 13, Academic Press, New York, 1962.

(68) Weisz, P. B., Frilette, V. J., Maatman, R. W., and Mower, E. B., "Catalysis by Crystalline Aluminosilicates. II. Molecular-Shape Selective Reactions," Journal of Catalysis, 1, 307 (1962).

(69) Weisz, P. B. and Miale, J. N., "Superactive Crystalline Aluminosilicate Hydrocarbon Catalysts," Journal of Catalysis, 4, 527 (1965).

(70) Zhang, F. L. et al., "Influence of Hydrogen Pressure on Isomerization and Hydrocracking Reactions of n-Alkanes," Acta Foculio-Chimica Sinica, 6 (No. 3), 187 (1965); Fuels Abstracts and Current Titles, 7 (No. 7), 64 (1966).

Patents

(71) Belgian 636, 142

(72) Belgian 651, 800

(73) Belgian 660, 897

(74) British 983, 756

(75) British 992, 872

(76) French 1, 285, 510

(77) French 1, 369, 377

(78) French 1, 379, 137

(79) French 1, 386, 551

(80) South African 63/5611

(81) South African 63/5688

(82) U. S. 1, 215, 391

(83) U. S. 2, 971, 904

(84) U. S. 3, 013, 894

(85) U. S. 3, 013, 897

(86) U. S. 3, 013, 990

(87) U. S. 3, 098, 032

(88) U. S. 3, 119, 763

(89) U. S. 3, 121, 754

(90) U. S. 3, 132, 086

(91) U. S. 3, 132, 087

(92) U. S. 3, 132, 088

(93) U. S. 3, 132, 089

(94) U. S. 3,132,090

(95) U. S. 3,132,091

(96) U. S. 3,132,092

(97) U. S. 3,146,279

(98) U. S. 3,190,939

(99) U. S. 3,210,265

(100) U. S. 3,227,660

(101) U. S. 3,239,447

(102) U. S. 3,287,252

(103) U. S. 3,287,256

APPENDIX A

DETAILED HYDROCRACKING DATA

TABLE A-1. Summarized n-Hexane Hydrocracking Data

Run	Catalyst	Temp., °F	t, sec	p_B, atm	Hydrocracking, %	-log (1-x)	k	k'o	K_B
1I	Faujasite	650	44.5	46.6	4.0	0.018	0.002	0.06	0.093
1A	Faujasite	700	23.9	46.0	8.5	0.039	0.008	0.20	0.087
1D	Faujasite	700	23.9	46.0	8.1	0.037	0.008	0.19	0.087
1E	Faujasite	700	7.0	46.9	2.2	0.010	0.007	0.18	0.087
1K	Faujasite	700	42.3	45.9	18.4	0.089	0.010	0.25	0.087
1L	Faujasite	700	21.1	46.7	8.3	0.038	0.009	0.22	0.087
2H	Faujasite	750	10.7	21.3	43.6	0.248	0.115	0.82	0.079
2G	Faujasite	750	14.5	30.3	40.3	0.224	0.077	0.87	0.079
2F	Faujasite	750	19.4	39.1	33.9	0.180	0.046	0.76	0.079
1B	Faujasite	750	23.2	44.3	39.7	0.220	0.047	0.94	0.079
1F	Faujasite	750	9.3	46.5	13.6	0.064	0.034	0.73	0.079
1H	Faujasite	750	9.5	46.5	14.3	0.067	0.035	0.76	0.079
1J	Faujasite	750	41.3	43.8	63.1	0.433	0.052	1.02	0.079
2A	Faujasite	750	22.6	44.9	40.8	0.228	0.050	1.01	0.079
2B	Faujasite	750	11.4	48.7	21.9	0.108	0.047	1.08	0.079
2C	Faujasite	750	38.1	38.2	58.7	0.384	0.050	0.80	0.079
2D	Faujasite	750	21.3	44.8	33.4	0.179	0.037	0.84	0.079
2I	Faujasite	750	21.1	45.6	32.5	0.171	0.040	0.83	0.079
6A	Faujasite	750	25.4	44.2	43.8	0.251	0.049	0.97	0.079
6B	Faujasite	750	87.6	42.5	87.8	0.914	0.052	0.96	0.079
6C	Faujasite	750	106.0	40.1	92.2	1.108	0.052	0.88	0.079

TABLE A-1. Summarized n-Hexane Hydrocracking Data

Run	Catalyst	Temp., °F	t, sec	p_B, atm	Hydrocracking, %	-log (1-x)	k	k'o	K_B
6E	Faujasite	750	22.2	45.3	40.9	0.228	0.051	1.05	0.079
7	Faujasite	750	25.2	45.2	41.5	0.233	0.046	0.95	0.079
8	Faujasite	750	27.0	44.5	44.5	0.256	0.047	0.96	0.079
9	Faujasite	750	29.5	44.5	47.8	0.283	0.048	0.97	0.079
10	Faujasite	750	29.1	44.8	46.6	0.292	0.046	0.96	0.079
11	Faujasite	750	30.3	44.0	48.2	0.286	0.047	0.93	0.079
12	Faujasite	750	31.8	44.0	52.3	0.322	0.050	1.00	0.079
2E	Faujasite	750	28.8	47.3	39.1	0.215	0.037	0.82	0.079
1C	Faujasite	800	22.2	41.3	91.6	1.076	0.240	3.78	0.074
1G	Faujasite	800	9.7	44.4	57.2	0.368	0.188	3.32	0.074
6D	Faujasite	800	24.1	40.6	92.8	1.143	0.235	3.62	0.074
3M	Mordenite	550	6.3	12.8	42.3	0.239	0.133	2.34	0.25
3L	Mordenite	550	16.4	31.3	26.9	0.136	0.029	2.26	0.25
3K	Mordenite	550	8.4	40.6	9.2	0.042	0.017	2.16	0.25
3B	Mordenite	550	24.4	48.7	19.1	0.092	0.013	2.30	0.25
14A	Mordenite	550	4.6	48.5	3.9	0.017	0.013	2.20	0.25
14B	Mordenite	550	15.9	45.3	13.0	0.061	0.013	2.02	0.25
14C	Mordenite	550	23.8	46.7	18.0	0.086	0.013	2.03	0.25
14D	Mordenite	550	16.0	48.5	13.0	0.061	0.013	2.24	0.25
14E	Mordenite	550	18.8	48.0	15.0	0.071	0.013	2.23	0.25
14F	Mordenite	550	26.7	46.0	20.5	0.100	0.013	2.05	0.25
14G	Mordenite	550	59.7	46.4	40.2	0.223	0.013	2.06	0.25

TABLE A-1. Summarized n-Hexane Hydrocracking Data

Run	Catalyst	Temp., °F	t, sec	p_B, atm	Hydrocracking, %	-log (1-x)	k	k'o	K_B
15	Mordenite	550	25.5	46.3	19.5	0.095	0.013	2.06	0.25
16	Mordenite	550	25.0	46.2	19.0	0.092	0.013	2.02	0.25
17	Mordenite	550	25.5	46.5	19.3	0.094	0.013	2.06	0.25
18	Mordenite	550	24.6	46.8	19.2	0.093	0.013	2.13	0.25
19	Mordenite	550	22.9	46.9	18.3	0.088	0.013	2.17	0.25
3J	Mordenite	550	10.5	52.8	6.5	0.030	0.010	2.02	0.25
3N	Mordenite	550	15.9	62.2	9.0	0.041	0.009	2.48	0.25
3C	Mordenite	565	24.7	45.8	37.1	0.202	0.029	4.12	0.24
13A	Mordenite	565	7.4	46.2	12.1	0.056	0.027	3.89	0.24
13B	Mordenite	565	23.0	41.4	35.5	0.190	0.029	3.46	0.24
13D	Mordenite	565	10.9	45.3	18.9	0.091	0.029	4.12	0.24
13E	Mordenite	565	42.6	37.1	55.6	0.352	0.029	2.82	0.24
13F	Mordenite	565	7.8	45.8	13.9	0.065	0.029	4.18	0.24
3D	Mordenite	600	24.0	43.8	86.5	0.870	0.127	15.7	0.23
3E	Mordenite	600	9.3	46.6	53.7	0.335	0.125	17.1	0.23
3F	Mordenite	600	3.8	48.3	27.2	0.138	0.126	18.4	0.23
3G	Mordenite	600	14.5	49.5	70.5	0.531	0.128	19.7	0.23
3H	Mordenite	600	23.4	43.8	86.7	0.876	0.131	16.1	0.23
3I	Mordenite	600	25.0	43.4	88.8	0.951	0.133	16.1	0.23
13C	Mordenite	600	14.5	47.9	70.6	0.532	0.128	18.4	0.23
3A	Mordenite	650	22.9	42.3	99.4	2.215	0.337	33.3	0.21

TABLE A-2. Summarized Cyclohexane Hydrocracking Data

Run	Catalyst	Temp., °F	t, sec	p_B, atm	Hydrocracking, %	-log (1-x)	k_1	$k'_{1,0}$	K_B
20J	Faujasite	650	3.57	48.0	8.1	0.037	0.051	1.64	0.093
22A	Faujasite	650	10.7	49.2	22.1	0.108	0.050	1.66	0.093
22E	Faujasite	650	10.8	46.3	21.4	0.106	0.049	1.47	0.093
20Q	Faujasite	700	7.98	21.3	85.5	0.838	0.520	4.38	0.087
20P	Faujasite	700	14.1	36.6	80.4	0.708	0.249	4.50	0.087
20A	Faujasite	700	4.54	46.5	31.5	0.165	0.180	4.73	0.087
20K	Faujasite	700	2.15	49.5	16.7	0.079	0.181	5.29	0.087
20L	Faujasite	700	18.5	45.1	79.6	0.690	0.185	4.64	0.087
20M	Faujasite	700	6.85	49.9	43.8	0.250	0.180	5.33	0.087
20N	Faujasite	700	21.2	44.0	84.3	0.802	0.187	4.53	0.087
20O	Faujasite	700	17.1	46.0	75.9	0.618	0.179	4.66	0.087
20R	Faujasite	700	17.1	46.0	75.9	0.616	0.178	4.63	0.087
22B	Faujasite	700	11.3	48.4	61.5	0.414	0.181	5.10	0.087
22C	Faujasite	700	6.32	50.2	41.0	0.230	0.180	5.39	0.087
22D	Faujasite	700	9.62	46.8	55.3	0.350	0.180	4.65	0.087
20B	Faujasite	750	4.35	44.9	74.8	0.598	0.680	14.3	0.079
20C	Faujasite	750	17.5	42.5	99.6	2.369	0.672	13.1	0.079
20D	Faujasite	750	8.72	48.3	93.6	1.197	0.680	16.1	0.079
20E	Faujasite	750	9.18	44.4	93.5	1.188	0.640	13.3	0.079
20F	Faujasite	750	9.27	44.4	93.6	1.190	0.635	13.2	0.079
20G	Faujasite	750	5.32	44.0	81.6	0.736	0.684	14.0	0.079
20H	Faujasite	800	4.86	42.5	97.5	1.594	1.62	28.5	0.074
20I	Faujasite	800	4.34	43.4	96.9	1.506	1.71	31.0	0.074

TABLE A-2. Summarized Cyclohexane Hydrocracking Data

Run	Catalyst	Temp., °F	t, sec	p_B, atm	Hydrocracking, %	-log (1-x)	k_1	$k'_{1,0}$	K_B
4A	Mordenite	600	9.14	28.9	24.8	0.124	0.047	2.77	0.23
4E	Mordenite	600	22.6	45.1	24.8	0.133	0.021	2.66	0.23
25A	Mordenite	600	23.6	45.2	27.5	0.140	0.021	2.69	0.23
25B	Mordenite	600	11.6	46.0	15.2	0.072	0.022	2.90	0.23
25C	Mordenite	600	27.9	43.8	31.4	0.164	0.021	2.53	0.23
4H	Mordenite	650	10.1	27.3	66.7	0.477	0.165	7.60	0.21
4F	Mordenite	650	21.1	42.8	68.0	0.494	0.082	8.33	0.21
4G	Mordenite	650	6.76	47.5	30.6	0.158	0.082	10.0	0.21
21C	Mordenite	650	25.0	41.2	74.2	0.589	0.082	7.8	0.21
21D	Mordenite	650	2.97	48.7	14.9	0.070	0.082	10.5	0.21
21E	Mordenite	650	3.58	47.9	17.5	0.084	0.082	10.3	0.21
24C	Mordenite	650	20.7	44.0	67.6	0.489	0.082	8.8	0.21
24D	Mordenite	650	20.7	44.3	63.5	0.438	0.074	8.0	0.21

TABLE A

RUN DATA

Run Number	1A
Feed Stock	n-Hexane
Catalyst Type	Pd-H-faujasite
Size, mm	0.84-0.42
Temperature, °F	700
Pressure, psia	765
Feed, v/hr-v	2.04
w/hr-w	2.92
Hydrogen, moles/mole C_6	8.33
Minutes on Feed	90
Product, moles per 100 moles feed	
Hydrogen	824.0
Methane	1.07
Ethane	1.24
Propane	11.17
I-Butane	3.04
N-Butane	1.54
I-Pentane	1.54
N-Pentane	0.64
2,2-DMB	12.60
2,3-DMB	6.60
2-MP	30.40
3-MP	21.20
N-Hexane	20.70
MCP	0.00
Cyclohexane	0.00
Hydrocracking, %	8.5
Isomerization, %	70.8
Hydrogen Balance, %	101.0
Rate constant, cc/gm-sec	0.0081

TABLE A

RUN DATA

Run Number	1B
Feed Stock	n-Hexane
Catalyst Type	Pd-H-faujasite
Size, mm	0.84-0.42
Temperature, °F	750
Pressure, psia	765
Feed, v/hr-v	2.04
w/hr-w	2.92
Hydrogen, moles/mole C_6	8.33
Minutes on Feed	210
Product, moles per 100 moles feed	
Hydrogen	793.0
Methane	4.62
Ethane	4.79
Propane	50.90
I-Butane	5.26
N-Butane	5.34
I-Pentane	3.76
N-Pentane	2.26
2,2-DMB	7.90
2,3-DMB	5.10
2-MP	19.30
3-MP	13.77
N-Hexane	14.22
MCP	0.00
Cyclohexane	0.00
Hydrocracking, %	39.7
Isomerization, %	46.1
Hydrogen Balance, %	101.0
Rate constant, cc/gm-sec	0.0470

TABLE A

RUN DATA

Run Number	1C
Feed Stock	n-Hexane
Catalyst Type	Pd-H-faujasite
Size, mm	0.84-0.42
Temperature, °F	800
Pressure, psia	765
Feed, v/hr-v	2.04
w/hr-w	2.92
Hydrogen, moles/mole C_6	8.33
Minutes on Feed	280
Product, moles per 100 moles feed	
Hydrogen	742.0
Methane	3.93
Ethane	10.34
Propane	133.00
I-Butane	7.05
N-Butane	9.31
I-Pentane	7.48
N-Pentane	4.79
2,2-DMB	1.03
2,3-DMB	0.40
2-MP	2.76
3-MP	2.01
N-Hexane	2.22
MCP	0.00
Cyclohexane	0.00
Hydrocracking, %	91.6
Isomerization, %	6.2
Hydrogen Balance, %	101.9
Rate constant, cc/gm-sec	0.240

TABLE A

RUN DATA

Run Number	1D
Feed Stock	n-Hexane
Catalyst Type	Pd-H-faujasite
Size, mm	0.84-0.42
Temperature, °F	700
Pressure, psia	765
Feed, v/hr-v	2.04
w/hr-w	2.92
Hydrogen, moles/mole C_6	8.33
Minutes on Feed	420
Product, moles per 100 moles feed	
Hydrogen	825.0
Methane	0.73
Ethane	1.07
Propane	9.88
I-Butane	1.37
N-Butane	1.37
I-Pentane	1.07
N-Pentane	0.30
2,2-DMB	12.90
2,3-DMB	7.90
2-MP	29.80
3-MP	20.80
N-Hexane	20.50
MCP	0.00
Cyclohexane	0.00
Hydrocracking, %	8.1
Isomerization, %	71.4
Hydrogen Balance, %	100.4
Rate constant, cc/gm-sec	0.0077

TABLE A

RUN DATA

Run Number	1E
Feed Stock	n-Hexane
Catalyst Type	Pd-H-faujasite
Size, mm	0.84-0.42
Temperature, °F	700
Pressure, psia	765
Feed, v/hr-v	4.08
w/hr-w	5.84
Hydrogen, moles/mole C_6	9.68
Minutes on Feed	480
Product, moles per 100 moles feed	
Hydrogen	966.0
Methane	0.09
Ethane	0.45
Propane	3.83
I-Butane	0.32
N-Butane	0.41
I-Pentane	0.00
N-Pentane	0.00
2,2-DMB	13.20
2,3-DMB	7.00
2-MP	32.10
3-MP	22.40
N-Hexane	23.10
MCP	0.00
Cyclohexane	0.00
Hydrocracking, %	2.2
Isomerization, %	74.7
Hydrogen Balance, %	100.8
Rate constant, cc/gm-sec	0.0071

TABLE A

RUN DATA

Run Number	1F
Feed Stock	n-Hexane
Catalyst Type	Pd-H-faujasite
Size, mm	0.84-0.42
Temperature, °F	750
Pressure, psia	765
Feed, v/hr-v	4.08
w/hr-w	5.84
Hydrogen, moles/mole C_6	9.68
Minutes on Feed	545
Product, moles per 100 moles feed	
Hydrogen	954.0
Methane	0.53
Ethane	1.35
Propane	19.50
I-Butane	1.73
N-Butane	1.73
I-Pentane	1.35
N-Pentane	0.39
2,2-DMB	11.30
2,3-DMB	7.60
2-MP	27.20
3-MP	19.90
N-Hexane	20.40
MCP	0.00
Cyclohexane	0.00
Hydrocracking, %	13.6
Isomerization, %	66.0
Hydrogen Balance, %	101.9
Rate constant, cc/gm-sec	0.0340

TABLE A

RUN DATA

Run Number	1G
Feed Stock	n-Hexane
Catalyst Type	Pd-H-faujasite
Size, mm	0.84-0.42
Temperature, °F	800
Pressure, psia	765
Feed, v/hr-v	4.08
w/hr-w	5.84
Hydrogen, moles/mole C_6	9.68
Minutes on Feed	620
Product, moles per 100 moles feed	
Hydrogen	911.0
Methane	1.77
Ethane	5.88
Propane	79.80
I-Butane	5.52
N-Butane	8.22
I-Pentane	4.62
N-Pentane	2.93
2,2-DMB	5.32
2,3-DMB	3.00
2-MP	13.70
3-MP	9.93
N-Hexane	10.80
MCP	0.00
Cyclohexane	0.00
Hydrocracking, %	57.2
Isomerization, %	32.0
Hydrogen Balance, %	102.2
Rate constant, cc/gm-sec	0.188

TABLE A

RUN DATA

Run Number	1H
Feed Stock	n-Hexane
Catalyst Type	Pd-H-faujasite
Size, mm	0.84-0.42
Temperature, °F	750
Pressure, psia	765
Feed, v/hr-v	4.08
w/hr-w	5.84
Hydrogen, moles/mole C_6	9.68
Minutes on Feed	660
Product, moles per 100 moles feed	
Hydrogen	954.0
Methane	0.70
Ethane	1.60
Propane	19.30
I-Butane	1.73
N-Butane	1.93
I-Pentane	1.65
N-Pentane	0.79
2,2-DMB	11.35
2,3-DMB	6.80
2-MP	27.60
3-MP	19.70
N-Hexane	20.20
MCP	0.00
Cyclohexane	0.00
Hydrocracking, %	14.3
Isomerization, %	65.5
Hydrogen Balance, %	101.9
Rate constant, cc/gm-sec	0.0350

TABLE A

RUN DATA

Run Number	II
Feed Stock	n-Hexane
Catalyst Type	Pd-H-faujasite
Size, mm	0.84-0.42
Temperature, °F	650
Pressure, psia	765
Feed, v/hr-v	1.09
w/hr-w	1.55
Hydrogen, moles/mole C_6	8.94
Minutes on Feed	850
Product, moles per 100 moles feed	
Hydrogen	890.0
Methane	Tr
Ethane	0.64
Propane	3.60
I-Butane	0.64
N-Butane	0.80
I-Pentane	0.40
N-Pentane	0.40
2,2-DMB	14.00
2,3-DMB	7.60
2-MP	31.60
3-MP	21.60
N-Hexane	21.20
MCP	0.00
Cyclohexane	0.00
Hydrocracking, %	4.0
Isomerization, %	74.8
Hydrogen Balance, %	100.0
Rate constant, cc/gm-sec	0.0020

TABLE A

RUN DATA

Run Number	1J
Feed Stock	n-Hexane
Catalyst Type	Pd-H-faujasite
Size, mm	0.84-0.42
Temperature, °F	750
Pressure, psia	765
Feed, v/hr-v	1.09
w/hr-w	1.55
Hydrogen, moles/mole C_6	8.94
Minutes on Feed	940
Product, moles per 100 moles feed	
Hydrogen	831.0
Methane	2.64
Ethane	7.68
Propane	86.00
I-Butane	6.48
N-Butane	9.36
I-Pentane	4.80
N-Pentane	2.80
2,2-DMB	5.04
2,3-DMB	2.15
2-MP	12.40
3-MP	8.48
N-Hexane	8.80
MCP	0.00
Cyclohexane	0.00
Hydrocracking, %	63.1
Isomerization, %	28.1
Hydrogen Balance, %	99.1
Rate constant, cc/gm-sec	0.0520

TABLE A

RUN DATA

Run Number	1K
Feed Stock	n-Hexane
Catalyst Type	Pd-H-faujasite
Size, mm	0.84-0.42
Temperature, °F	700
Pressure, psia	765
Feed, v/hr-v	1.09
w/hr-w	1.55
Hydrogen, moles/mole C_6	8.94
Minutes on Feed	1020
Product, moles per 100 moles feed	
Hydrogen	876.0
Methane	0.56
Ethane	2.00
Propane	23.20
I-Butane	1.84
N-Butane	2.48
I-Pentane	2.16
N-Pentane	1.44
2,2-DMB	11.03
2,3-DMB	7.00
2-MP	26.70
3-MP	18.60
N-Hexane	18.25
MCP	0.00
Cyclohexane	0.00
Hydrocracking, %	18.4
Isomerization, %	63.3
Hydrogen Balance, %	98.9
Rate constant, cc/gm-sec	0.0104

TABLE A

RUN DATA

Run Number	1L
Feed Stock	n-Hexane
Catalyst Type	Pd-H-faujasite
Size, mm	0.84-0.42
Temperature, °F	700
Pressure, psia	765
Feed, v/hr-v	2.04
w/hr-w	2.92
Hydrogen, moles/mole C_6	9.61
Minutes on Feed	1145
Product, moles per 100 moles feed	
Hydrogen	953.0
Methane	0.34
Ethane	1.80
Propane	10.20
I-Butane	0.73
N-Butane	0.90
I-Pentane	1.20
N-Pentane	0.78
2,2-DMB	13.30
2,3-DMB	7.00
2-MP	29.80
3-MP	20.80
N-Hexane	20.80
MCP	0.00
Cyclohexane	0.00
Hydrocracking, %	8.3
Isomerization, %	70.9
Hydrogen Balance, %	99.7
Rate constant, cc/gm-sec	0.0089

TABLE A

RUN DATA

Run Number	2A
Feed Stock	n-Hexane
Catalyst Type	Pd-H-faujasite
Size, mm	0.84-0.42
Temperature, °F	750
Pressure, psia	765
Feed, v/hr-v	2.04
w/hr-w	2.87
Hydrogen, moles/mole C_6	8.81
Minutes on Feed	130
Product, moles per 100 moles feed	
Hydrogen	840.0
Methane	1.41
Ethane	3.38
Propane	50.40
I-Butane	5.64
N-Butane	5.72
I-Pentane	5.22
N-Pentane	3.21
2,2-DMB	7.88
2,3-DMB	5.60
2-MP	18.40
3-MP	13.12
N-Hexane	14.15
MCP	0.00
Cyclohexane	0.00
Hydrocracking, %	40.8
Isomerization, %	45.0
Hydrogen Balance, %	101.4
Rate constant, cc/gm-sec	0.050

TABLE A

RUN DATA

Run Number	2B
Feed Stock	n-Hexane
Catalyst Type	Pd-H-faujasite
Size, mm	0.84-0.42
Temperature, °F	750
Pressure, psia	765
Feed, v/hr-v	2.04
w/hr-w	2.87
Hydrogen, moles/mole C_6	18.4
Minutes on Feed	250
Product, moles per 100 moles feed	
Hydrogen	1818.0
Methane	0.81
Ethane	2.86
Propane	35.10
I-Butane	1.34
N-Butane	1.97
I-Pentane	1.28
N-Pentane	0.56
2,2-DMB	9.23
2,3-DMB	7.40
2-MP	25.00
3-MP	17.80
N-Hexane	18.70
MCP	0.00
Cyclohexane	0.00
Hydrocracking, %	21.9
Isomerization, %	59.4
Hydrogen Balance, %	101.2
Rate constant, cc/gm-sec	0.0470

TABLE A

RUN DATA

Run Number	2C
Feed Stock	n-Hexane
Catalyst Type	Pd-H-faujasite
Size, mm	0.84-0.42
Temperature, °F	750
Pressure, psia	765
Feed, v/hr-v	2.04
w/hr-w	2.87
Hydrogen, moles/mole C_6	4.90
Minutes on Feed	330
Product, moles per 100 moles feed	
Hydrogen	431.0
Methane	1.78
Ethane	6.77
Propane	81.70
I-Butane	9.45
N-Butane	10.78
I-Pentane	2.63
N-Pentane	1.21
2,2-DMB	5.12
2,3-DMB	3.45
2-MP	13.60
3-MP	9.68
N-Hexane	9.50
MCP	0.00
Cyclohexane	0.00
Hydrocracking, %	58.7
Isomerization, %	31.8
Hydrogen Balance, %	103.0
Rate constant, cc/gm-sec	0.0500

TABLE A

RUN DATA

Run Number	2D
Feed Stock	n-Hexane
Catalyst Type	Pd-H-faujasite
Size, mm	0.84-0.42
Temperature, °F	750
Pressure, psia	765
Feed, v/hr-v	2.04
w/hr-w	2.87
Hydrogen, moles/mole C_6	9.08
Minutes on Feed	400
Product, moles per 100 moles feed	
Hydrogen	875.0
Methane	1.41
Ethane	3.91
Propane	44.80
I-Butane	4.48
N-Butane	4.39
I-Pentane	2.86
N-Pentane	1.71
2,2-DMB	8.78
2,3-DMB	3.50
2-MP	23.40
3-MP	16.70
N-Hexane	14.25
MCP	0.00
Cyclohexane	0.00
Hydrocracking, %	33.4
Isomerization, %	52.4
Hydrogen Balance, %	98.8
Rate constant, cc/gm-sec	0.0416

TABLE A

RUN DATA

Run Number	2E
Feed Stock	n-Hexane
Catalyst Type	Pd-H-faujasite
Size, mm	0.84-0.42
Temperature, °F	750
Pressure, psia	815
Feed, v/hr-v	2.04
w/hr-w	2.87
Hydrogen, moles/mole C_6	8.10
Minutes on Feed	460
Product, moles per 100 moles feed	
Hydrogen	771.0
Methane	1.43
Ethane	6.05
Propane	49.60
I-Butane	4.80
N-Butane	5.44
I-Pentane	4.20
N-Pentane	2.42
2,2-DMB	8.20
2,3-DMB	4.50
2-MP	19.60
2-MP	14.00
N-Hexane	14.60
MCP	0.00
Cyclohexane	0.00
Hydrocracking, %	39.1
Isomerization, %	46.3
Hydrogen Balance, %	99.4
Rate constant, cc/gm-sec	0.0370

TABLE A

RUN DATA

Run Number	2F
Feed Stock	n-Hexane
Catalyst Type	Pd-H-faujasite
Size, mm	0.84-0.42
Temperature, °F	750
Pressure, psia	665
Feed, v/hr-v	2.04
w/hr-w	2.87
Hydrogen, moles/mole C_6	8.81
Minutes on Feed	520
Product, moles per 100 moles feed	
Hydrogen	847.0
Methane	0.71
Ethane	4.63
Propane	48.30
I-Butane	3.92
N-Butane	3.38
I-Pentane	2.85
N-Pentane	1.50
2,2-DMB	8.67
2,3-DMB	3.70
2-MP	22.20
3-MP	15.80
N-Hexane	15.70
MCP	0.00
Cyclohexane	0.00
Hydrocracking, %	33.9
Isomerization, %	50.4
Hydrogen Balance, %	99.8
Rate constant, cc/gm-sec	0.0460

TABLE A

RUN DATA

Run Number	2G
Feed Stock	n-Hexane
Catalyst Type	Pd-H-faujasite
Size, mm	0.84-0.42
Temperature, ^{o}F	750
Pressure, psia	515
Feed, v/hr-v	2.04
w/hr-w	2.87
Hydrogen, moles/mole C_6	9.18
Minutes on Feed	590
Product, moles per 100 moles feed	
Hydrogen	878.0
Methane	1.06
Ethane	4.63
Propane	52.50
I-Butane	5.80
N-Butane	3.56
I-Pentane	4.28
N-Pentane	3.20
2,2-DMB	8.03
2,3-DMB	5.30
2-MP	18.80
3-MP	13.40
N-Hexane	14.20
MCP	0.00
Cyclohexane	0.00
Hydrocracking, %	40.3
Isomerization, %	45.5
Hydrogen Balance, %	97.3
Rate constant, cc/gm-sec	0.0767

TABLE A

RUN DATA

Run Number	2H
Feed Stock	n-Hexane
Catalyst Type	Pd-H-faujasite
Size, mm	0.84-0.42
Temperature, °F	750
Pressure, psia	365
Feed, v/hr-v	2.04
w/hr-w	2.87
Hydrogen, moles/mole C_6	8.83
Minutes on Feed	650
Product, moles per 100 moles feed	
Hydrogen	839.0
Methane	0.71
Ethane	4.82
Propane	54.30
I-Butane	7.31
N-Butane	7.85
I-Pentane	3.70
N-Pentane	2.20
2, 2-DMB	7.50
2, 3-DMB	4.40
2-MP	18.20
3-MP	13.00
N-Hexane	13.30
MCP	0.00
Cyclohexane	0.00
Hydrocracking, %	43.6
Isomerization, %	43.1
Hydrogen Balance, %	100.4
Rate constant, cc/gm-sec	0.1150

TABLE A

RUN DATA

Run Number	2I
Feed Stock	n-Hexane
Catalyst Type	Pd-H-faujasite
Size, mm	0.84-0.42
Temperature, °F	750
Pressure, psia	765
Feed, v/hr-v	2.04
w/hr-w	2.87
Hydrogen	9.30
Minutes on Feed	710
Product, moles per 100 moles feed	
Hydrogen	897.0
Methane	1.06
Ethane	4.10
Propane	42.20
I-Butane	4.63
N-Butane	4.63
I-Pentane	3.06
N-Pentane	1.64
2,2-DMB	9.09
2,3-DMB	4.80
2-MP	22.10
3-MP	15.75
N-Hexane	15.75
MCP	0.00
Cyclohexane	0.00
Hydrocracking, %	32.5
Isomerization, %	51.7
Hydrogen Balance, %	99.5
Rate constant, cc/gm-sec	0.0400

TABLE A

RUN DATA

Run Number	3A
Feed Stock	n-Hexane
Catalyst Type	Pd-H-mordenite
Size, mm	1.2-0.21
Temperature, °F	650
Pressure, psia	765
Feed, v/hr-v	2.04
w/hr-w	1.97
Hydrogen, moles/mole C_6	9.66
Minutes on Feed	120
Product, moles per 100 moles feed	
Hydrogen	866.0
Methane	5.68
Ethane	20.30
Propane	114.80
I-Butane	19.68
N-Butane	24.15
I-Pentane	4.13
N-Pentane	2.35
2,2-DMB	0.48
2,3-DMB	0.02
2-MP	0.04
3-MP	0.03
N-Hexane	0.04
MCP	0.00
Cyclohexane	0.00
Hydrocracking, %	99.4
Isomerization, %	0.5
Hydrogen Balance, %	103.0
Rate constant, cc/gm-sec	0.337

TABLE A

RUN DATA

Run Number	3B
Feed Stock	n-Hexane
Catalyst Type	Pd-H-mordenite
Size, mm	1.2-0.21
Temperature, °F	550
Pressure, psia	765
Feed, v/hr-v	2.04
w/hr-w	1.99
Hydrogen, moles/mole C_6	9.66
Minutes on Feed	180
Product, moles per 100 moles feed	
Hydrogen	947.0
Methane	0.73
Ethane	2.86
Propane	8.55
I-Butane	5.08
N-Butane	2.95
I-Pentane	8.20
N-Pentane	2.26
2,2-DMB	7.57
2,3-DMB	5.30
2-MP	27.20
3-MP	17.30
N-Hexane	23.50
MCP	0.00
Cyclohexane	0.00
Hydrocracking, %	19.1
Isomerization, %	57.4
Hydrogen Balance, %	100.8
Rate constant, cc/gm-sec	0.0132

TABLE A

RUN DATA

Run Number	3C
Feed Stock	n-Hexane
Catalyst Type	Pd-H-mordenite
Size, mm	1.2-0.21
Temperature, °F	565
Pressure, psia	765
Feed, v/hr-v	2.04
w/hr-w	1.99
Hydrogen, moles/mole C_6	9.66
Minutes on Feed	290
Product, moles per 100 moles feed	
Hydrogen	929.0
Methane	1.41
Ethane	5.51
Propane	23.10
I-Butane	9.23
N-Butane	6.67
I-Pentane	11.60
N-Pentane	4.28
2,2-DMB	8.55
2,3-DMB	3.50
2-MP	22.60
3-MP	14.40
N-Hexane	13.80
MCP	0.00
Cyclohexane	0.00
Hydrocracking, %	37.1
Isomerization, %	49.1
Hydrogen Balance, %	101.2
Rate constant, cc/gm-sec	0.0286

TABLE A.

RUN DATA

Run Number	3D
Feed Stock	n-Hexane
Catalyst Type	Pd-H-mordenite
Size, mm	1.2-0.21
Temperature, °F	600
Pressure, psia	765
Feed, v/hr-v	2.04
w/hr-w	1.99
Hydrogen, moles/mole C_6	9.66
Minutes on Feed	350
Product, moles per 100 moles feed	
Hydrogen	880.0
Methane	2.14
Ethane	12.80
Propane	74.80
I-Butane	24.40
N-Butane	18.35
I-Pentane	13.20
N-Pentane	6.32
2,2-DMB	1.80
2,3-DMB	1.15
2-MP	4.62
3-MP	3.08
N-Hexane	2.87
MCP	0.00
Cyclohexane	0.00
Hydrocracking, %	86.5
Isomerization, %	10.6
Hydrogen Balance, %	101.8
Rate constant, cc/gm-sec	0.127

TABLE A

RUN DATA

Run Number	3E
Feed Stock	n-Hexane
Catalyst Type	Pd-H-mordenite
Size, mm	1.2-0.21
Temperature, ^{o}F	600
Pressure, psia	765
Feed, v/hr-v	4.08
w/hr-w	3.98
Hydrogen, moles/mole C_6	12.6
Minutes on Feed	400
Product, moles per 100 moles feed	
Hydrogen	1206.0
Methane	0.89
Ethane	5.35
Propane	41.10
I-Butane	18.50
N-Butane	11.60
I-Pentane	9.40
N-Pentane	4.16
2,2-DMB	7.20
2,3-DMB	4.57
2-MP	14.38
3-MP	9.58
N-Hexane	10.60
MCP	0.00
Cyclohexane	0.00
Hydrocracking, %	53.7
Isomerization, %	35.7
Hydrogen Balance, %	99.2
Rate constant, cc/gm-sec	0.125

TABLE A

RUN DATA

Run Number	3F
Feed Stock	n-Hexane
Catalyst Type	Pd-H-mordenite
Size, mm	1.2-0.21
Temperature, °F	600
Pressure, psia	765
Feed, v/hr-v	8.17
w/hr-w	7.96
Hydrogen, moles/mole C_6	15.7
Minutes on Feed	450
Product, moles per 100 moles feed	
Hydrogen	1543.0
Methane	0.62
Ethane	2.72
Propane	19.55
I-Butane	8.35
N-Butane	6.17
I-Pentane	5.58
N-Pentane	2.53
2,2-DMB	6.97
2,3-DMB	5.30
2-MP	19.35
3-MP	12.90
N-Hexane	28.30
MCP	0.00
Cyclohexane	0.00
Hydrocracking, %	27.2
Isomerization, %	44.5
Hydrogen Balance, %	100.4
Rate constant, cc/gm-sec	0.126

TABLE A

RUN DATA

Run Number	3G
Feed Stock	n-Hexane
Catalyst Type	Pd-H-mordenite
Size, mm	1.2-0.21
Temperature, °F	600
Pressure, psia	765
Feed, v/hr-v	1.07
w/hr-w	1.06
Hydrogen, moles/mole C_6	32.1
Minutes on Feed	510
Product, moles per 100 moles feed	
Hydrogen	3140.0
Methane	2.67
Ethane	8.33
Propane	62.70
I-Butane	19.20
N-Butane	15.30
I-Pentane	10.53
N-Pentane	5.07
2,2-DMB	4.89
2,3-DMB	2.62
2-MP	8.85
3-MP	5.90
N-Hexane	7.25
MCP	0.00
Cyclohexane	0.00
Hydrocracking, %	70.5
Isomerization, %	22.2
Hydrogen Balance, %	99.6
Rate constant, cc/gm-sec	0.128

TABLE A

RUN DATA

Run Number	3H
Feed Stock	n-Hexane
Catalyst Type	Pd-H-mordenite
Size, mm	1.2-0.21
Temperature, °F	600
Pressure, psia	765
Feed, v/hr-v	2.04
w/hr-w	1.99
Hydrogen, moles/mole C_6	9.83
Minutes on Feed	570
Product, moles per 100 moles feed	
Hydrogen	896.0
Methane	3.55
Ethane	15.30
Propane	81.70
I-Butane	20.10
N-Butane	15.20
I-Pentane	13.05
N-Pentane	7.27
2,2-DMB	2.09
2,3-DMB	0.57
2-MP	4.56
3-MP	3.04
N-Hexane	2.99
MCP	0.00
Cyclohexane	0.00
Hydrocracking, %	86.7
Isomerization, %	10.3
Hydrogen Balance, %	101.1
Rate constant, cc/gm-sec	0.131

TABLE A

RUN DATA

Run Number	3I
Feed Stock	n-Hexane
Catalyst Type	Pd-H-mordenite
Size, mm	1.2-0.21
Temperature, °F	600
Pressure, psia	765
Feed, v/hr-v	2.04
w/hr-w	1.99
Hydrogen, moles/mole C_6	9.22
Minutes on Feed	750
Product, moles per 100 moles feed	
Hydrogen	833.0
Methane	2.14
Ethane	8.72
Propane	78.80
I-Butane	24.20
N-Butane	22.20
I-Pentane	12.60
N-Pentane	5.90
2,2-DMB	2.14
2,3-DMB	1.44
2-MP	3.39
3-MP	2.26
N-Hexane	1.96
MCP	0.00
Cyclohexane	0.00
Hydrocracking, %	88.8
Isomerization, %	9.2
Hydrogen Balance, %	97.0
Rate constant, cc/gm-sec	0.133

TABLE A

RUN DATA

Run Number	3J
Feed Stock	n-Hexane
Catalyst Type	Pd-H-mordenite
Size, mm	1.2-0.21
Temperature, °F	550
Pressure, psia	815
Feed, v/hr-v	2.04
w/hr-w	1.99
Hydrogen, moles/mole C_6	20.8
Minutes on Feed	960
Product, moles per 100 moles feed	
Hydrogen	2074.0
Methane	0.23
Ethane	0.89
Propane	4.87
I-Butane	1.25
N-Butane	1.51
I-Pentane	1.92
N-Pentane	0.78
2,2-DMB	9.87
2,3-DMB	6.70
2-MP	27.80
3-MP	17.70
N-Hexane	31.40
MCP	0.00
Cyclohexane	0.00
Hydrocracking, %	6.5
Isomerization, %	62.1
Hydrogen Balance, %	101.5
Rate constant, cc/gm-sec	0.0100

TABLE A

RUN DATA

Run Number	3K
Feed Stock	n-Hexane
Catalyst Type	Pd-H-mordenite
Size, mm	1.2-0.21
Temperature, °F	550
Pressure, psia	665
Feed, v/hr-v	2.04
w/hr-w	1.99
Hydrogen, moles/mole C_6	9.57
Minutes on Feed	1000
Product, moles per 100 moles feed	
Hydrogen	948.0
Methane	0.36
Ethane	1.96
Propane	7.00
I-Butane	1.96
N-Butane	1.78
I-Pentane	2.64
N-Pentane	0.71
2,2-DMB	11.05
2,3-DMB	7.50
2-MP	29.20
3-MP	18.55
N-Hexane	24.50
MCP	0.00
Cyclohexane	0.00
Hydrocracking, %	9.2
Isomerization, %	66.3
Hydrogen Balance, %	100.2
Rate constant, cc/gm-sec	0.0174

TABLE A

RUN DATA

Run Number	3L
Feed Stock	n-Hexane
Catalyst Type	Pd-H-mordenite
Size, mm	1.2-0.21
Temperature, °F	550
Pressure, psia	515
Feed, v/hr-v	2.04
w/hr-w	1.99
Hydrogen, moles/mole C_6	9.92
Minutes on Feed	1040
Product, moles per 100 moles feed	
Hydrogen	965.0
Methane	0.36
Ethane	2.14
Propane	19.10
I-Butane	9.73
N-Butane	5.62
I-Pentane	5.98
N-Pentane	1.99
2,2-DMB	12.10
2,3-DMB	4.40
2-MP	23.20
3-MP	14.75
N-Hexane	18.65
MCP	0.00
Cyclohexane	0.00
Hydrocracking, %	26.9
Isomerization, %	54.4
Hydrogen Balance, %	101.2
Rate constant, cc/gm-sec	0.0290

TABLE A

RUN DATA

Run Number	3M
Feed Stock	n-Hexane
Catalyst Type	Pd-H-mordenite
Size, mm	1.2-0.21
Temperature, ^{o}F	550
Pressure, psia	215
Feed, v/hr-v	2.04
w/hr-w	1.99
Hydrogen, moles/mole C_6	9.30
Minutes on Feed	1080
Product, moles per 100 moles feed	
Hydrogen	888.0
Methane	0.36
Ethane	1.60
Propane	33.90
I-Butane	13.20
N-Butane	11.05
I-Pentane	7.41
N-Pentane	3.49
2,2-DMB	3.50
2,3-DMB	5.65
2-MP	12.25
3-MP	7.80
N-Hexane	28.50
MCP	0.00
Cyclohexane	0.00
Hydrocracking, %	42.3
Isomerization, %	29.2
Hydrogen Balance, %	100.3
Rate constant, cc/gm-sec	0.133

TABLE A

RUN DATA

Run Number	3N
Feed Stock	n-Hexane
Catalyst Type	Pd-H-mordenite
Size, mm	1.2-0.21
Temperature, °F	550
Pressure, psia	965
Feed, v/hr-v	2.04
w/hr-w	1.99
Hydrogen, moles/mole C_6	19.69
Minutes on Feed	1120
Product, moles per 100 moles feed	
Hydrogen	1960.0
Methane	0.36
Ethane	1.61
Propane	5.94
I-Butane	1.78
N-Butane	1.96
I-Pentane	2.78
N-Pentane	1.07
2,2-DMB	10.18
2,3-DMB	6.20
2-MP	28.20
3-MP	17.95
N-Hexane	28.50
MCP	0.00
Cyclohexane	0.00
Hydrocracking, %	9.0
Isomerization, %	62.5
Hydrogen Balance, %	100.9
Rate constant, cc/gm-sec	0.00903

TABLE A

RUN DATA

Run Number	4A
Feed Stock	Cyclohexane
Catalyst Type	Pd-H-mordenite
Size, mm	1.2-0.21
Temperature, °F	600
Pressure, psia	465
Feed, v/hr-v	2.04
w/hr-w	2.32
Hydrogen, moles/mole C_6	13.2
Minutes on Feed	120
Product, moles per 100 moles feed	
Hydrogen	1274.0
Methane	1.20
Ethane	3.25
Propane	27.10
I-Butane	1.77
N-Butane	9.26
I-Pentane	0.81
N-Pentane	0.81
2,2-DMB	0.35
2,3-DMB	0.30
2-MP	0.43
3-MP	0.30
N-Hexane	0.28
MCP	41.00
Cyclohexane	34.20
Hydrocracking, %	24.8
Isomerization, %	41.0
Hydrogen Balance, %	99.6
Rate constant, cc/gm-sec	0.0473

TABLE A

RUN DATA

Run Number	4B
Feed Stock	Cyclohexane
Catalyst Type	Pd-H-mordenite
Size, mm	1.2-0.21
Temperature, °F	640
Pressure, psia	465
Feed, v/hr-v	2.04
w/hr-w	2.32
Hydrogen, moles/mole C_6	15.1
Minutes on Feed	240
Product, moles per 100 moles feed	
Hydrogen	1415.0
Methane	4.70
Ethane	12.80
Propane	51.90
I-Butane	6.40
N-Butane	12.60
I-Pentane	1.94
N-Pentane	1.06
2,2-DMB	0.50
2,3-DMB	0.50
2-MP	0.86
3-MP	0.60
N-Hexane	0.60
MCP	36.10
Cyclohexane	14.60
Hydrocracking, %	49.3
Isomerization, %	36.1
Hydrogen Balance, %	99.0
Rate constant, cc/gm-sec	0.133

TABLE A

RUN DATA

Run Number	4C
Feed Stock	Cyclohexane
Catalyst Type	Pd-H-mordenite
Size, mm	1.2-0.21
Temperature, °F	650
Pressure, psia	465
Feed, v/hr-v	2.04
w/hr-w	2.32
Hydrogen, moles/mole C_6	10.4
Minutes on Feed	360
Product, moles per 100 moles feed	
Hydrogen	904.0
Methane	3.91
Ethane	15.25
Propane	80.20
I-Butane	10.52
N-Butane	16.05
I-Pentane	4.21
N-Pentane	1.92
2,2-DMB	0.18
2,3-DMB	0.71
2-MP	1.29
3-MP	0.90
N-Hexane	1.50
MCP	23.00
Cyclohexane	6.60
Hydrocracking, %	70.4
Isomerization, %	23.0
Hydrogen Balance, %	101.0
Rate constant, cc/gm-sec	0.170

TABLE A

RUN DATA

Run Number	4D
Feed Stock	Cyclohexane
Catalyst Type	Pd-H-mordenite
Size, mm	1.2-0.21
Temperature, °F	550
Pressure, psia	465
Feed, v/hr-v	2.04
w/hr-w	2.32
Hydrogen, moles/mole C_6	9.62
Minutes on Feed	480
Product, moles per 100 moles feed	
Hydrogen	943.0
Methane	0.88
Ethane	3.10
Propane	12.00
I-Butane	0.96
N-Butane	2.43
I-Pentane	0.47
N-Pentane	0.35
2,2-DMB	0.20
2,3-DMB	0.18
2-MP	0.36
3-MP	0.25
N-Hexane	0.20
MCP	41.20
Cyclohexane	47.70
Hydrocracking, %	11.1
Isomerization, %	41.2
Hydrogen Balance, %	99.1
Rate constant, cc/gm-sec	0.0125

TABLE A

RUN DATA

Run Number	4E
Feed Stock	Cyclohexane
Catalyst Type	Pd-H-mordenite
Size, mm	1.2-0.21
Temperature, °F	600
Pressure, psia	765
Feed, v/hr-v	2.04
w/hr-w	2.32
Hydrogen, moles mole C_6	8.45
Minutes on Feed	600
Product, moles per 100 moles feed	
Hydrogen	797.0
Methane	0.88
Ethane	3.39
Propane	24.90
I-Butane	2.60
N-Butane	10.50
I-Pentane	1.40
N-Pentane	1.39
2,2-DMB	0.10
2,3-DMB	0.21
2-MP	0.43
3-MP	0.30
N-Hexane	0.30
MCP	58.00
Cyclohexane	17.20
Hydrocracking, %	24.8
Isomerization, %	58.0
Hydrogen Balance, %	100.9
Rate constant, cc/gm-sec	0.0205

TABLE A

RUN DATA

Run Number	4F
Feed Stock	Cyclohexane
Catalyst Type	Pd-H-mordenite
Size, mm	1.2-0.21
Temperature, °F	650
Pressure, psia	765
Feed, v/hr-v	2.04
w/hr-w	2.32
Hydrogen, moles/mole C_6	8.70
Minutes on Feed	720
Product, moles per 100 moles feed	
Hydrogen	738.0
Methane	2.66
Ethane	13.00
Propane	78.50
I-Butane	9.50
N-Butane	14.10
I-Pentane	3.94
N-Pentane	1.75
2,2-DMB	0.30
2,3-DMB	0.88
2-MP	1.22
3-MP	0.85
N-Hexane	1.02
MCP	25.80
Cyclohexane	6.20
Hydrocracking, %	68.0
Isomerization, %	25.8
Hydrogen Balance, %	100.5
Rate constant, cc/gm-sec	0.0820

TABLE A

RUN DATA

Run Number	4G
Feed Stock	Cyclohexane
Catalyst Type	Pd-H-mordenite
Size, mm	1.2-0.21
Temperature, °F	650
Pressure, psia	765
Feed, v/hr-v	4.08
w/hr-w	4.64
Hydrogen, moles/mole C_6	14.1
Minutes on Feed	840
Product, moles per 100 moles feed	
Hydrogen	1351.0
Methane	1.66
Ethane	6.71
Propane	36.50
I-Butane	2.90
N-Butane	5.00
I-Pentane	2.05
N-Pentane	0.75
2, 2-DMB	0.10
2, 3-DMB	0.11
2-MP	0.69
3-MP	0.48
N-Hexane	0.50
MCP	42.50
Cyclohexane	26.90
Hydrocracking, %	30.6
Isomerization, %	42.5
Hydrogen Balance, %	99.5
Rate constant, cc/gm-sec	0.0815

TABLE A

RUN DATA

Run Number	4H
Feed Stock	Cyclohexane
Catalyst Type	Pd-H-mordenite
Size, mm	1.2-0.21
Temperature, °F	650
Pressure, psia	465
Feed, v/hr-v	2.04
w/hr-w	2.32
Hydrogen, moles/mole C_6	11.2
Minutes on Feed	920
Product, moles per 100 moles feed	
Hydrogen	990.0
Methane	3.30
Ethane	14.80
Propane	74.90
I-Butane	9.15
N-Butane	15.00
I-Pentane	3.72
N-Pentane	1.48
2,2-DMB	0.40
2,3-DMB	0.70
2-MP	1.22
3-MP	0.85
N-Hexane	1.15
MCP	25.90
Cyclohexane	7.40
Hydrocracking, %	66.7
Isomerization, %	25.9
Hydrogen Balance, %	98.5
Rate constant, cc/gm-sec	0.165

TABLE A

RUN DATA

Run Number	5
Feed Stock	Cyclohexane
Catalyst Type	Pd-H-mordenite
Size, mm	1.2-0.21
Temperature, °F	650
Pressure, psia	465
Feed, v/hr-v	2.04
w/hr-w	2.17
Hydrogen, moles/mole C_6	12.7
Minutes on Feed	120
Product, moles per 100 moles feed	
Hydrogen	1141.0
Methane	3.83
Ethane	14.90
Propane	72.70
I-Butane	9.35
N-Butane	14.95
I-Pentane	3.89
N-Pentane	1.59
2,2-DMB	0.42
2,3-DMB	0.73
2-MP	1.17
3-MP	0.82
N-Hexane	1.13
MCP	26.00
Cyclohexane	7.35
Hydrocracking, %	66.6
Isomerization, %	26.0
Hydrogen Balance, %	99.3
Rate constant, cc/gm-sec	0.173

TABLE A

RUN DATA

Run Number	6A
Feed Stock	n-Hexane
Catalyst Type	Pd-H-faujasite
Size, mm	0.84-0.42
Temperature, ^{o}F	750
Pressure, psia	765
Feed, v/hr-v	2.04
w/hr-w	2.73
Hydrogen, moles/mole C_6	8.16
Minutes on Feed	90
Product, moles per 100 moles feed	
Hydrogen	772.0
Methane	3.20
Ethane	7.12
Propane	46.20
I-Butane	7.75
N-Butane	6.88
I-Pentane	6.13
N-Pentane	3.99
2,2-DMB	7.25
2,3-DMB	4.40
2-MP	18.00
3-MP	12.80
N-Hexane	13.72
MCP	0.00
Cyclohexane	0.00
Hydrocracking, %	43.8
Isomerization, %	42.5
Hydrogen Balance, %	99.5
Rate constant, cc/gm-sec	0.0491

TABLE A

RUN DATA

Run Number	6B
Feed Stock	n-Hexane
Catalyst Type	Pd-H-faujasite
Size, mm	0.84-0.42
Temperature, °F	750
Pressure, psia	765
Feed, v/hr-v	0.530
w/hr-w	0.727
Hydrogen, moles/mole C_6	8.90
Minutes on Feed	270
Product, moles per 100 moles feed	
Hydrogen	802.0
Methane	2.67
Ethane	9.01
Propane	118.20
I-Butane	10.59
N-Butane	14.10
I-Pentane	6.40
N-Pentane	4.50
2,2-DMB	2.14
2,3-DMB	0.48
2-MP	3.95
3-MP	2.81
N-Hexane	2.76
MCP	0.00
Cyclohexane	0.00
Hydrocracking, %	87.8
Isomerizaion, %	9.4
Hydrogen Balance, %	100.5
Rate constant, cc/gm-sec	0.0517

TABLE A

RUN DATA

Run Number	6C
Feed Stock	n-Hexane
Catalyst Type	Pd-H-faujasite
Size, mm	0.84-0.42
Temperature, °F	750
Pressure, psia	765
Feed, v/hr-v	0.530
w/hr-w	0.727
Hydrogen, moles/mole C_6	7.15
Minutes on Feed	420
Product, moles per 100 moles feed	
Hydrogen	623.0
Methane	1.33
Ethane	8.81
Propane	144.80
I-Butane	5.41
N-Butane	5.92
I-Pentane	6.80
N-Pentane	4.42
2,2-DMB	1.27
2,3-DMB	0.59
2-MP	2.44
3-MP	1.74
N-Hexane	1.80
MCP	0.00
Cyclohexane	0.00
Hydrocracking, %	92.2
Isomerization, %	6.0
Hydrogen Balance, %	99.0
Rate constant, cc/gm-sec	0.0515

TABLE A

RUN DATA

Run Number	6D
Feed Stock	n-Hexane
Catalyst Type	Pd-H-faujasite
Size, mm	0.84-0.42
Temperature, °F	800
Pressure, psia	765
Feed, v/hr-v	2.04
w/hr-w	2.73
Hydrogen, moles/mole C_6	8.17
Minutes on Feed	530
Product, moles per 100 moles feed	
Hydrogen	724.0
Methane	3.60
Ethane	9.05
Propane	135.30
I-Butane	13.62
N-Butane	10.15
I-Pentane	3.99
N-Pentane	2.99
2, 2-DMB	1.25
2, 3-DMB	0.32
2-MP	2.36
3-MP	1.72
N-Hexane	1.55
MCP	0.00
Cyclohexane	0.00
Hydrocracking, %	92.8
Isomerization, %	5.6
Hydrogen Balance, %	99.5
Rate constant, cc/gm-sec	0.235

TABLE A

RUN DATA

Run Number	6E
Feed Stock	n-Hexane
Catalyst Type	Pd-H-faujasite
Size, mm	0.84-0.42
Temperature, ^{o}F	750
Pressure, psia	765
Feed, v/hr-v	2.04
w/hr-w	2.73
Hydrogen, moles/mole C_6	9.48
Minutes on Feed	680
Product, moles per 100 moles feed	
Hydrogen	907.0
Methane	1.06
Ethane	5.70
Propane	47.90
I-Butane	4.53
N-Butane	5.08
I-Pentane	6.19
N-Pentane	4.27
2, 2-DMB	8.25
2, 3-DMB	4.30
2-MP	19.10
3-MP	13.60
N-Hexane	13.85
MCP	0.00
Cyclohexane	0.00
Hydrocracking, %	40.9
Isomerization, %	45.2
Hydrogen Balance, %	99.3
Rate constant, cc/gm-sec	0.0510

TABLE A

RUN DATA

Run Number	7
Feed Stock	n-Hexane
Catalyst Type	Pd-H-faujasite
Size, mm	0.074-0.043
Temperature, °F	750
Pressure, psia	765
Feed, v/hr-v	2.04
w/hr-w	2.44
Hydrogen, moles/mole C_6	9.23
Minutes on Feed	90
Product, moles per 100 moles feed	
Hydrogen	881.0
Methane	1.07
Ethane	4.79
Propane	50.90
I-Butane	5.00
N-Butane	6.59
I-Pentane	4.41
N-Pentane	4.13
2, 2-DMB	8.37
2, 3-DMB	3.90
2-MP	18.80
3-MP	13.40
N-Hexane	14.00
MCP	0.00
Cyclohexane	0.00
Hydrocracking, %	41.5
Isomerization, %	44.5
Hydrogen Balance, %	99.5
Rate constant, cc/gm-sec	0.0457

TABLE A

RUN DATA

Run Number	8
Feed Stock	n-Hexane
Catalyst Type	Pd-H-faujasite
Size, mm	0.147-0.074
Temperature, °F	750
Pressure, psia	765
Feed, v/hr-v	2.04
w/hr-w	2.40
Hydrogen, moles/mole C_6	8.72
Minutes on Feed	90
Product, moles per 100 moles feed	
Hydrogen	827.0
Methane	1.07
Ethane	6.23
Propane	56.00
I-Butane	6.78
N-Butane	6.69
I-Pentane	3.85
N-Pentane	2.78
2,2-DMB	7.30
2,3-DMB	3.73
2-MP	18.42
3-MP	13.12
N-Hexane	12.90
MCP	0.00
Cyclohexane	0.00
Hydrocracking, %	44.5
Isomerization, %	42.6
Hydrogen Balance, %	99.2
Rate constant, cc/gm-sec	0.0469

TABLE A

RUN DATA

Run Number	9
Feed Stock	n-Hexane
Catalyst Type	Pd-H-faujasite
Size, mm	0.370-0.147
Temperature, ^{o}F	750
Pressure, psia	765
Feed, v/hr-v	2.04
w/hr-w	2.27
Hydrogen, moles/mole C_6	8.49
Minutes on Feed	90
Product, moles per 100 moles feed	
Hydrogen	801.0
Methane	1.42
Ethane	6.23
Propane	55.50
I-Butane	5.55
N-Butane	5.55
I-Pentane	6.20
N-Pentane	4.83
2,2-DMB	6.83
2,3-DMB	4.60
2-MP	16.40
3-MP	11.70
N-Hexane	12.60
MCP	0.00
Cyclohexane	0.00
Hydrocracking, %	47.8
Isomerization, %	39.6
Hydrogen Balance, %	100.5
Rate constant, cc/gm-sec	0.0477

TABLE A

RUN DATA

Run Number	10
Feed Stock	n-Hexane
Catalyst Type	Pd-H-faujasite
Size, mm	0.84-0.42
	30cc catalyst charge
Temperature, ^{o}F	750
Pressure, psia	765
Feed, v/hr-v	2.04
w/hr-w	2.16
Hydrogen, moles/mole C_6	9.05
Minutes on Feed	90
Product, moles per 100 moles feed	
Hydrogen	858.0
Methane	1.42
Ethane	4.98
Propane	56.70
I-Butane	6.50
N-Butane	6.50
I-Pentane	5.27
N-Pentane	4.33
2,2-DMB	7.87
2,3-DMB	3.02
2-MP	17.28
3-MP	12.30
N-Hexane	12.90
MCP	0.00
Cyclohexane	0.00
Hydrocracking, %	46.6
Isomerization, %	40.5
Hydrogen Balance, %	99.1
Rate constant, cc/gm-sec	0.0464

TABLE A

RUN DATA

Run Number	11
Feed Stock	n-Hexane
Catalyst Type	Pd-H-faujasite
Size, mm	0.84-0.42
	45cc catalyst charge
Temperature, °F	750
Pressure, psia	765
Feed, v/hr-v	2.04
w/hr-w	2.23
Hydrogen, moles/mole C_6	8.33
Minutes on Feed	90
Product, moles per 100 moles feed	
Hydrogen	784.0
Methane	1.42
Ethane	7.48
Propane	62.00
I-Butane	6.41
N-Butane	6.50
I-Pentane	4.43
N-Pentane	2.93
2,2-DMB	6.60
2,3-DMB	4.50
2-MP	16.70
3-MP	11.90
N-Hexane	12.10
MCP	0.00
Cyclohexane	0.00
Hydrocracking, %	48.2
Isomerization, %	39.7
Hydrogen Balance, %	99.8
Rate constant, cc/gm-sec	0.0467

TABLE A

RUN DATA

Run Number	12
Feed Stock	n-Hexane
Catalyst Type	Pd-H-faujasite
Size, mm	0.84-0.42
	10 catalyst charge
Temperature, °F	750
Pressure, psia	765
Feed, v/hr-v	2.04
w/hr-w	2.16
Hydrogen, moles/mole C_6	8.20
Minutes on Feed	90
Product, moles per 100 moles feed	
Hydrogen	768.0
Methane	1.06
Ethane	4.44
Propane	64.10
I-Butane	5.98
N-Butane	5.88
I-Pentane	7.55
N-Pentane	5.12
2,2-DMB	6.30
2,3-DMB	3.65
2-MP	15.35
3-MP	10.95
N-Hexane	11.50
MCP	0.00
Cyclohexane	0.00
Hydrocracking, %	52.3
Isomerization, %	36.2
Hydrogen Balance, %	101.1
Rate constant, cc/gm-sec	0.0500

TABLE A

RUN DATA

Run Number	13A
Feed Stock	n-Hexane
Catalyst Type	Pd-H-mordenite
Size, mm	1.2-0.21
Temperature, °F	565
Pressure, psia	765
Feed, v/hr-v	8.17
w/hr-w	7.27
Hydrogen, moles/mole C_6	8.84
Minutes on Feed	90
Product, moles per 100 moles feed	
Hydrogen	872.0
Methane	0.45
Ethane	2.59
Propane	9.48
I-Butane	2.47
N-Butane	2.70
I-Pentane	2.52
N-Pentane	1.29
2,2-DMB	7.01
2,3-DMB	5.80
2-MP	22.40
3-MP	14.95
N-Hexane	37.70
MCP	0.00
Cyclohexane	0.00
Hydrocracking, %	12.1
Isomerization, %	50.2
Hydrogen Balance, %	98.5
Rate constant, cc/gm-sec	0.0266

TABLE A

RUN DATA

Run Number	13B
Feed Stock	n-Hexane
Catalyst Type	Pd-H-mordenite
Size, mm	1.2-0.21
Temperature, °F	565
Pressure, psia	765
Feed, v/hr-v	4.09
w/hr-w	3.64
Hydrogen, moles/mole C_6	5.25
Minutes on Feed	180
Product, moles per 100 moles feed	
Hydrogen	490.0
Methane	1.07
Ethane	5.17
Propane	26.40
I-Butane	8.43
N-Butane	8.15
I-Pentane	7.76
N-Pentane	3.95
2,2-DMB	6.84
2,3-DMB	5.10
2-MP	21.10
3-MP	14.05
N-Hexane	17.40
MCP	0.00
Cyclohexane	0.00
Hydrocracking, %	35.5
Isomerization, %	47.1
Hydrogen Balance, %	99.2
Rate constant, cc/gm-sec	0.0288

TABLE A

RUN DATA

Run Number	13C
Feed Stock	n-Hexane
Catalyst Type	Pd-H-mordenite
Size, mm	1.2-0.21
Temperature, °F	600
Pressure, psia	765
Feed, v/hr-v	2.04
w/hr-w	1.82
Hydrogen, moles/mole C_6	18.3
Minutes on Feed	270
Product, moles per 100 moles feed	
Hydrogen	1759.0
Methane	2.50
Ethane	12.10
Propane	65.75
I-Butane	14.80
N-Butane	11.80
I-Pentane	12.50
N-Pentane	6.55
2,2-DMB	4.70
2,3-DMB	1.60
2-MP	10.00
3-MP	6.66
N-Hexane	6.48
MCP	0.00
Cyclohexane	0.00
Hydrocracking, %	70.6
Isomerization, %	22.9
Hydrogen Balance, %	99.8
Rate constant, cc/gm-sec	0.128

TABLE A

RUN DATA

Run Number	13D
Feed Stock	n-Hexane
Catalyst Type	Pd-H-mordenite
Size, mm	1.2-0.21
Temperature, °F	565
Pressure, psia	765
Feed, v/hr-v	5.45
w/hr-w	4.84
Hydrogen, moles/mole C_6	8.92
Minutes on Feed	330
Product, moles per 100 moles feed	
Hydrogen	873.0
Methane	0.80
Ethane	3.74
Propane	21.60
I-Butane	7.42
N-Butane	5.20
I-Pentane	6.83
N-Pentane	3.85
2,2-DMB	8.58
2,3-DMB	13.20
2-MP	22.20
3-MP	14.80
N-Hexane	22.30
MCP	0.00
Cyclohexane	0.00
Hydrocracking, %	18.9
Isomerization, %	58.8
Hydrogen Balance, %	99.1
Rate constant, cc/gm-sec	0.0291

TABLE A

RUN DATA

Run Number	13E
Feed Stock	n-Hexane
Catalyst Type	Pd-H-mordenite
Size, mm	1.2-0.21
Temperature, °F	565
Pressure, psia	765
Feed, v/hr-v	2.72
w/hr-w	2.42
Hydrogen, moles/mole C_6	4.05
Minutes on Feed	420
Product, moles per 100 moles feed	
Hydrogen	349.0
Methane	1.85
Ethane	6.67
Propane	47.80
I-Butane	14.25
N-Butane	7.89
I-Pentane	11.83
N-Pentane	5.77
2,2-DMB	7.49
2,3-DMB	3.30
2-MP	14.40
3-MP	9.62
N-Hexane	9.60
MCP	0.00
Cyclohexane	0.00
Hydrocracking, %	55.6
Isomerization, %	34.8
Hydrogen Balance, %	99.0
Rate constant, cc/gm-sec	0.0288

TABLE A

RUN DATA

Run Number	13F
Feed Stock	n-Hexane
Catalyst Type	Pd-H-mordenite
Size, mm	1.2-0.21
Temperature, °F	565
Pressure, psia	765
Feed, v/hr-v	8.17
w/hr-w	7.27
Hydrogen, moles/mole C_6	8.20
Minutes on Feed	510
Product, moles per 100 moles feed	
Hydrogen	806.0
Methane	0.45
Ethane	2.00
Propane	9.58
I-Butane	3.68
N-Butane	2.74
I-Pentane	3.35
N-Pentane	2.03
2,2-DMB	6.68
2,3-DMB	5.30
2-MP	19.70
3-MP	13.15
N-Hexane	41.25
MCP	0.00
Cyclohexane	0.00
Hydrocracking, %	13.9
Isomerization, %	44.8
Hydrogen Balance, %	99.7
Rate constant, cc/gm-sec	0.0290

TABLE A

RUN DATA

Run Number	14A
Feed Stock	n-Hexane
Catalyst Type	Pd-H-mordenite
Size, mm	1.2-0.21
Temperature, °F	550
Pressure, psia	765
Feed, v/vr-v	8.17
w/hr-w	8.00
Hydrogen, moles/mole C_6	14.72
Minutes on Feed	590
Product, moles per 100 moles feed	
Hydrogen	1468.0
Methane	0.00
Ethane	0.57
Propane	3.80
I-Butane	1.60
N-Butane	1.60
I-Pentane	0.00
N-Pentane	0.00
2,2-DMB	1.98
2,3-DMB	4.20
2-MP	8.85
3-MP	5.62
N-Hexane	75.50
MCP	0.00
Cyclohexane	0.00
Hydrocracking, %	3.9
Isomerization, %	20.6
Hydrogen Balance, %	99.3
Rate constant, cc/gm-sec	0.0128

TABLE A

RUN DATA

Run Number	14B
Feed Stock	n-Hexane
Catalyst Type	Pd-H-mordenite
Size, mm	1.2-0.21
Temperature, °F	550
Pressure, psia	765
Feed, v/hr-v	4.08
w/hr-w	4.00
Hydrogen, moles/mole C_6	7.40
Minutes on Feed	680
Product, moles per 100 moles feed	
Hydrogen	727.0
Methane	0.36
Ethane	1.69
Propane	8.91
I-Butane	2.05
N-Butane	2.63
I-Pentane	3.52
N-Pentane	2.57
2,2-DMB	5.47
2,3-DMB	4.90
2-MP	19.60
3-MP	12.50
N-Hexane	44.50
MCP	0.00
Cyclohexane	0.00
Hydrocracking, %	13.0
Isomerization, %	42.5
Hydrogen Balance, %	100.4
Rate constant, cc/gm-sec	0.0134

TABLE A

RUN DATA

Run Number	14C
Feed Stock	n-Hexane
Catalyst Type	Pd-H-mordenite
Size, mm	1.2-0.21
Temperature, °F	550
Pressure, psia	765
Feed, v/hr-v	2.04
w/hr-w	2.00
Hydrogen, moles/mole C_6	9.75
Minutes on Feed	770
Product, moles per 100 moles feed	
Hydrogen	957.0
Methane	0.53
Ethane	2.67
Propane	10.80
I-Butane	3.39
N-Butane	3.65
I-Pentane	4.76
N-Pentane	1.96
2,2-DMB	9.42
2,3-DMB	4.00
2-MP	27.50
3-MP	17.50
N-Hexane	23.60
MCP	0.00
Cyclohexane	0.00
Hydrocracking, %	18.0
Isomerization, %	58.4
Hydrogen Balance, %	101.0
Rate constant, cc/gm-sec	0.0126

TABLE A

RUN DATA

Run Number	14D
Feed Stock	n-Hexane
Catalyst Type	Pd-H-mordenite
Size, mm	1.2-0.21
Temperature, °F	550
Pressure, psia	765
Feed, v/hr-v	2.04
w/hr-w	2.00
Hydrogen, moles/mole C_6	15.60
Minutes on Feed	860
Product, moles per 100 moles feed	
Hydrogen	1547.0
Methane	0.35
Ethane	2.49
Propane	8.55
I-Butane	2.23
N-Butane	2.58
I-Pentane	3.70
N-Pentane	2.06
2,2-DMB	7.25
2,3-DMB	6.20
2-MP	21.70
3-MP	13.80
N-Hexane	38.10
MCP	0.00
Cyclohexane	0.00
Hydrocracking, %	13.0
Isomerization, %	48.9
Hydrogen Balance, %	100.0
Rate constant, cc/gm-sec	0.0133

TABLE A

RUN DATA

Run Number	14E
Feed Stock	n-Hexane
Catalyst Type	Pd-H-mordenite
Size, mm	1.2-0.21
Temperature, °F	550
Pressure, psia	765
Feed, v/hr-v	2.04
w/hr-w	2.00
Hydrogen, moles/mole C_6	13.12
Minutes on Feed	950
Product, moles per 100 moles feed	
Hydrogen	1297.0
Methane	0.36
Ethane	2.14
Propane	8.32
I-Butane	2.85
N-Butane	2.76
I-Pentane	5.27
N-Pentane	2.49
2,2-DMB	8.90
2,3-DMB	5.40
2-MP	23.90
3-MP	15.20
N-Hexane	31.60
MCP	0.00
Cyclohexane	0.00
Hydrocracking, %	15.0
Isomerization, %	53.4
Hydrogen Balance, %	99.2
Rate constant, cc/gm-sec	0.0132

TABLE A

RUN DATA

Run Number	14F
Feed Stock	n-Hexane
Catalyst Type	Pd-H-mordenite
Size, mm	1.2-0.21
Temperature, ^{o}F	550
Pressure, psia	765
Feed, v/hr-v	2.04
w/hr-w	2.00
Hydrogen, moles/mole C_6	9.00
Minutes on Feed	1040
Product, moles per 100 moles feed	
Hydrogen	880.0
Methane	0.57
Ethane	4.83
Propane	11.90
I-Butane	5.17
N-Butane	4.27
I-Pentane	5.62
N-Pentane	2.42
2,2-DMB	10.50
2,3-DMB	5.50
2-MP	26.00
3-MP	16.60
N-Hexane	20.90
MCP	0.00
Cyclohexane	0.00
Hydrocracking, %	20.5
Isomerization, %	58.6
Hydrogen Balance, %	99.3
Rate constant, cc/gm-sec	0.0131

TABLE A

RUN DATA

Run Number	14G
Feed Stock	n-Hexane
Catalyst Type	Pd-H-mordenite
Size, mm	1.2-0.21
Temperature, °F	550
Pressure, psia	765
Feed, v/hr-v	0.740
w/hr-w	0.725
Hydrogen, moles/mole C_6	11.20
Minutes on Feed	1130
Product, moles per 100 moles feed	
Hydrogen	1080.0
Methane	1.43
Ethane	8.04
Propane	28.30
I-Butane	15.00
N-Butane	8.95
I-Pentane	6.25
N-Pentane	2.50
2,2-DMB	10.60
2,3-DMB	4.60
2-MP	20.00
3-MP	12.70
N-Hexane	11.90
MCP	0.00
Cyclohexane	0.00
Hydrocracking, %	40.2
Isomerization, %	47.9
Hydrogen Balance, %	98.2
Rate constant, cc/gm-sec	0.0130

TABLE A

RUN DATA

Run Number	15
Feed Stock	n-Hexane
Catalyst Type	Pd-H-mordenite
Size, mm	0.074-0.043
Temperature, ^{o}F	550
Pressure, psia	765
Feed, v/hr-v	2.04
w/hr-w	2.05
Hydrogen, moles/mole C_6	9.25
Minutes on Feed	90
Product, moles per 100 moles feed	
Hydrogen	905.0
Methane	0.80
Ethane	2.70
Propane	9.02
I-Butane	4.88
N-Butane	2.82
I-Pentane	8.50
N-Pentane	2.21
2,2-DMB	7.60
2,3-DMB	5.90
2-MP	26.90
3-MP	17.10
N-Hexane	23.00
MCP	0.00
Cyclohexane	0.00
Hydrocracking, %	19.5
Isomerization, %	57.5
Hydrogen Balance, %	99.5
Rate constant, cc/gm-sec	0.0130

TABLE A

RUN DATA

Run Number	16
Feed Stock	n-Hexane
Catalyst Type	Pd-H-mordenite
Size, mm	0.21-0.147
Temperature, °F	550
Pressure, psia	765
Feed, v/hr-v	2.04
w/hr-w	2.12
Hydrogen, moles/mole C_6	9.12
Minutes on Feed	90
Product, moles per 100 moles feed	
Hydrogen	893.0
Methane	0.50
Ethane	3.10
Propane	8.02
I-Butane	4.12
N-Butane	4.02
I-Pentane	7.86
N-Pentane	3.57
2,2-DMB	8.05
2,3-DMB	5.25
2-MP	26.70
3-MP	17.00
N-Hexane	24.00
MCP	0.00
Cyclohexane	0.00
Hydrocracking, %	19.0
Isomerization, %	57.0
Hydrogen Balance, %	101.0
Rate constant, cc/gm-sec	0.0128

TABLE A

RUN DATA

Run Number	17
Feed Stock	n-Hexane
Catalyst Type	Pd-H-mordenite
Size, mm	1.2-0.21
	30cc catalyst charge
Temperature, °F	550
Pressure, psia	765
Feed, v/hr-v	2.04
w/hr-w	2.00
Hydrogen, moles/mole C_6	9.54
Minutes on Feed	90
Product, moles per 100 moles feed	
Hydrogen	935.0
Methane	0.61
Ethane	2.90
Propane	8.05
I-Butane	3.95
N-Butane	4.07
I-Pentane	6.20
N-Pentane	3.15
2,2-DMB	7.60
2,3-DMB	6.20
2-MP	26.70
3-MP	17.00
N-Hexane	23.20
MCP	0.00
Cyclohexane	0.00
Hydrocracking, %	19.3
Isomerization, %	57.5
Hydrogen Balance, %	100.0
Rate constant, cc/gm-sec	0.0129

TABLE A

RUN DATA

Run Number	18
Feed Stock	n-Hexane
Catalyst Type	Pd-H-mordenite
Size, mm	1.2-0.21
	45cc catalyst charge
Temperature, °F	550
Pressure, psia	765
Feed, v/hr-v	2.04
w/hr-w	2.04
Hydrogen, moles/mole C_6	9.75
Minutes on Feed	90
Product, moles per 100 moles feed	
Hydrogen	956.0
Methane	0.41
Ethane	2.50
Propane	8.62
I-Butane	2.42
N-Butane	2.50
I-Pentane	5.90
N-Pentane	2.95
2,2-DMB	7.70
2,3-DMB	5.50
2-MP	27.00
3-MP	17.20
N-Hexane	23.40
MCP	0.00
Cyclohexane	0.00
Hydrocracking, %	19.2
Isomerization, %	57.4
Hydrogen Balance, %	99.0
Rate constant, cc/gm-sec	0.0132

TABLE A

RUN DATA

Run Number	19
Feed Stock	n-Hexane
Catalyst Type	Pd-H-mordenite
Size, mm	1.2-0.21
	10cc catalyst charge
Temperature, °F	550
Pressure, psia	765
Feed, v/hr-v	2.04
w/hr-w	2.02
Hydrogen, moles/mole C_6	10.50
Minutes on Feed	90
Product, moles per 100 moles feed	
Hydrogen	1032.0
Methane	0.51
Ethane	2.49
Propane	8.62
I-Butane	4.01
N-Butane	4.10
I-Pentane	6.92
N-Pentane	3.45
2,2-DMB	7.80
2,3-DMB	5.90
2-MP	27.00
3-MP	17.20
N-Hexane	23.80
MCP	0.00
Cyclohexane	0.00
Hydrocracking, %	18.3
Isomerization, %	57.9
Hydrogen Balance, %	101.2
Rate constant, cc/gm-sec	0.0134

TABLE A

RUN DATA

Run Number	20A
Feed Stock	Cyclohexane
Catalyst Type	Pd-H-faujasite
Size, mm	0.84-0.42
Temperature, °F	700
Pressure, psia	765
Feed, v/hr-v	8.17
w/hr-w	12.9
Hydrogen, moles/mole C_6	9.95
Minutes on Feed	90
Product, moles per 100 moles feed	
Hydrogen	946.0
Methane	0.12
Ethane	0.72
Propane	3.79
I-Butane	9.97
N-Butane	3.02
I-Pentane	8.92
N-Pentane	2.51
2,2-DMB	0.54
2,3-DMB	1.90
2-MP	5.08
3-MP	3.54
N-Hexane	3.50
MCP	58.50
Cyclohexane	10.00
Hydrocracking, %	31.5
Isomerization, %	58.5
Hydrogen Balance, %	99.7
Rate constant, cc/gm-sec	0.180

TABLE A

RUN DATA

Run Number	20B
Feed Stock	Cyclohexane
Catalyst Type	Pd-H-faujasite
Size, mm	0.84-0.42
Temperature, °F	750
Pressure, psia	765
Feed, v/hr-v	8.17
w/hr-w	12.9
Hydrogen, moles/mole C_6	9.95
Minutes on Feed	180
Product, moles per 100 moles feed	
Hydrogen	863.0
Methane	0.52
Ethane	3.02
Propane	25.91
I-Butane	30.10
N-Butane	12.77
I-Pentane	15.95
N-Pentane	5.98
2,2-DMB	0.40
2,3-DMB	1.48
2-MP	6.17
3-MP	4.30
N-Hexane	5.99
MCP	20.30
Cyclohexane	4.90
Hydrocracking, %	74.8
Isomerization, %	20.3
Hydrogen Balance, %	100.5
Rate constant, cc/gm-sec	0.680

TABLE A

RUN DATA

Run Number	20C
Feed Stock	Cyclohexane
Catalyst Type	Pd-H-faujasite
Size, mm	0.84-0.42
Temperature, °F	750
Pressure, psia	765
Feed, v/hr-v	2.04
w/hr-w	3.22
Hydrogen, moles/mole C_6	9.95
Minutes on Feed	300
Product, moles per 100 moles feed	
Hydrogen	795.0
Methane	2.02
Ethane	4.62
Propane	68.30
I-Butane	59.00
N-Butane	31.70
I-Pentane	8.46
N-Pentane	4.24
2,2-DMB	0.07
2,3-DMB	0.10
2-MP	0.47
3-MP	0.33
N-Hexane	0.45
MCP	0.43
Cyclohexane	0.00
Hydrocracking, %	99.6
Isomerization, %	0.4
Hydrogen Balance, %	98.2
Rate constant, cc/gm-sec	0.672

TABLE A

RUN DATA

Run Number	20D
Feed Stock	Cyclohexane
Catalyst Type	Pd-H-faujasite
Size, mm	0.84-0.42
Temperature, °F	750
Pressure, psia	765
Feed, v/hr-v	2.04
w/hr-w	3.22
Hydrogen, moles/mole C_6	20.9
Minutes on Feed	390
Product, moles per 100 moles feed	
Hydrogen	1923.0
Methane	0.84
Ethane	3.84
Propane	39.10
I-Butane	35.00
N-Butane	16.20
I-Pentane	16.10
N-Pentane	10.25
2,2-DMB	2.04
2,3-DMB	1.44
2-MP	6.46
3-MP	4.51
N-Hexane	5.92
MCP	5.45
Cyclohexane	0.90
Hydrocracking, %	93.6
Isomerization, %	5.5
Hydrogen Balance, %	99.3
Rate constant, cc/gm-sec	0.680

TABLE A

RUN DATA

Run Number	20E
Feed Stock	Cyclohexane
Catalyst Type	Pd-H-faujasite
Size, mm	0.84-0.42
Temperature, °F	750
Pressure, psia	765
Feed, v/hr-v	4.08
w/hr-w	6.43
Hydrogen, moles/mole C_6	9.27
Minutes on Feed	480
Product, moles per 100 moles feed	
Hydrogen	833.0
Methane	0.92
Ethane	3.89
Propane	37.90
I-Butane	34.10
N-Butane	16.05
I-Pentane	15.50
N-Pentane	8.85
2,2-DMB	2.10
2,3-DMB	1.58
2-MP	6.17
3-MP	4.30
N-Hexane	5.91
MCP	5.30
Cyclohexane	1.20
Hydrocracking, %	93.5
Isomerization, %	5.3
Hydrogen Balance, %	100.8
Rate constant, cc/gm-sec	0.640

TABLE A

RUN DATA

Run Number	20F
Feed Stock	Cyclohexane
Catalyst Type	Pd-H-faujasite
Size, mm	0.84-0.42
Temperature, ^{o}F	750
Pressure, psia	765
Feed, v/hr-v	4.08
w/hr-w	6.43
Hydrogen, moles/mole C_6	9.26
Minutes on Feed	550
Product, moles per 100 moles feed	
Hydrogen	832.0
Methane	1.03
Ethane	3.98
Propane	38.40
I-Butane	33.90
N-Butane	15.55
I-Pentane	15.65
N-Pentane	8.63
2,2-DMB	2.14
2,3-DMB	1.58
2-MP	6.09
3-MP	4.24
N-Hexane	5.83
MCP	5.25
Cyclohexane	1.20
Hydrocracking, %	93.5
Isomerization, %	5.3
Hydrogen Balance, %	100.6
Rate constant, cc/gm-sec	0.635

TABLE A

RUN DATA

Run Number	20G
Feed Stock	Cyclohexane
Catalyst Type	Pd-H-faujasite
Size, mm	0.84-0.42
Temperature, ^{o}F	750
Pressure, psia	765
Feed, v/hr-v	8.17
w/hr-w	12.9
Hydrogen, moles/mole C_6	8.18
Minutes on Feed	630
Product, moles per 100 moles feed	
Hydrogen	736.0
Methane	0.44
Ethane	3.12
Propane	26.65
I-Butane	31.20
N-Butane	13.65
I-Pentane	15.40
N-Pentane	6.22
2,2-DMB	0.42
2,3-DMB	1.29
2-MP	6.48
3-MP	4.53
N-Hexane	6.63
MCP	14.20
Cyclohexane	4.21
Hydrocracking, %	81.6
Isomerization, %	14.2
Hydrogen Balance, %	101.9
Rate constant, cc/gm-sec	0.684

TABLE A

RUN DATA

Run Number	20H
Feed Stock	Cyclohexane
Catalyst Type	Pd-H-faujasite
Size, mm	0.84-0.42
Temperature, °F	800
Pressure, psia	765
Feed, v/hr-v	8.17
w/hr-w	12.9
Hydrogen, moles/mole C_6	8.00
Minutes on Feed	690
Product, moles per 100 moles feed	
Hydrogen	703.0
Methane	2.02
Ethane	8.45
Propane	60.10
I-Butane	34.05
N-Butane	21.95
I-Pentane	14.60
N-Pentane	7.52
2,2-DMB	0.15
2,3-DMB	0.51
2-MP	2.29
3-MP	1.60
N-Hexane	3.40
MCP	2.20
Cyclohexane	0.35
Hydrocracking, %	97.4
Isomerization, %	2.2
Hydrogen Balance, %	99.2
Rate constant, cc/gm-sec	1.620

TABLE A

RUN DATA

Run Number	201
Feed Stock	Cyclohexane
Catalyst Type	Pd-H-faujasite
Size, mm	0.84-0.42
Temperature, °F	800
Pressure, psia	765
Feed, v/hr-v	8.17
w/hr-w	12.9
Hydrogen, moles/mole C_6	9.02
Minutes on Feed	750
Product, moles per 100 moles feed	
Hydrogen	805.0
Methane	1.92
Ethane	8.32
Propane	59.60
I-Butane	33.80
N-Butane	22.40
I-Pentane	14.50
N-Pentane	7.42
2,2-DMB	0.17
2,3-DMB	0.44
2-MP	2.35
3-MP	1.64
N-Hexane	3.45
MCP	2.74
Cyclohexane	0.38
Hydrocracking, %	96.9
Isomerization, %	2.7
Hydrogen Balance, %	99.8
Rate constant, cc/gm-sec	1.71

TABLE A

RUN DATA

Run Number	20J
Feed Stock	Cyclohexane
Catalyst Type	Pd-H-faujasite
Size, mm	0.84-0.42
Temperature, ^{o}F	650
Pressure, psia	765
Feed, v/hr-v	8.17
w/hr-w	12.9
Hydrogen, moles/mole C_6	12.5
Minutes on Feed	830
Product, moles per 100 moles feed	
Hydrogen	1242.0
Methane	0.00
Ethane	0.15
Propane	0.66
I-Butane	2.26
N-Butane	0.74
I-Pentane	1.58
N-Pentane	0.41
2,2-DMB	0.30
2,3-DMB	0.10
2-MP	1.56
3-MP	1.09
N-Hexane	1.13
MCP	65.40
Cyclohexane	26.50
Hydrocracking, %	8.1
Isomerization, %	65.4
Hydrogen Balance, %	99.8
Rate constant, cc/gm-sec	0.0513

TABLE A

RUN DATA

Run Number	20K
Feed Stock	Cyclohexane
Catalyst Type	Pd-H-faujasite
Size, mm	0.84-0.42
Temperature, °F	700
Pressure, psia	765
Feed, v/hr-v	8.17
w/hr-w	12.9
Hydrogen, moles/mole C_6	22.0
Minutes on Feed	920
Product, moles per 100 moles feed	
Hydrogen	2183.0
Methane	0.00
Ethane	0.29
Propane	1.92
I-Butane	5.30
N-Butane	1.33
I-Pentane	3.68
N-Pentane	0.90
2,2-DMB	0.25
2,3-DMB	0.97
2-MP	2.47
3-MP	1.73
N-Hexane	1.92
MCP	69.00
Cyclohexane	14.30
Hydrocracking, %	16.7
Isomerization, %	69.0
Hydrogen Balance, %	100.3
Rate constant, cc/gm-sec	0.181

TABLE A

RUN DATA

Run Number	20L
Feed Stock	Cyclohexane
Catalyst Type	Pd-H-faujasite
Size, mm	0.84-0.42
Temperature, °F	700
Pressure, psia	765
Feed, v/hr-v	2.04
w/hr-w	3.22
Hydrogen, moles/mole C_6	9.32
Minutes on Feed	1010
Product, moles per 100 moles feed	
Hydrogen	852.0
Methane	0.88
Ethane	2.35
Propane	20.50
I-Butane	29.60
N-Butane	10.40
I-Pentane	14.07
N-Pentane	6.84
2,2-DMB	1.72
2,3-DMB	2.30
2-MP	8.15
3-MP	5.70
N-Hexane	6.50
MCP	17.00
Cyclohexane	3.39
Hydrocracking, %	79.6
Isomerization, %	17.0
Hydrogen Balance, %	102.0
Rate constant, cc/gm-sec	0.185

TABLE A

RUN DATA

Run Number	20M
Feed Stock	Cyclohexane
Catalyst Type	Pd-H-faujasite
Size, mm	0.84-0.42
Temperature, °F	700
Pressure, psia	765
Feed, v/hr-v	2.04
w/hr-w	3.22
Hydrogen, moles/mole C_6	25.9
Minutes on Feed	1100
Product, moles per 100 moles feed	
Hydrogen	2546.0
Methane	0.29
Ethane	1.03
Propane	7.08
I-Butane	10.40
N-Butane	5.15
I-Pentane	5.17
N-Pentane	2.00
2,2-DMB	1.18
2,3-DMB	1.82
2-MP	8.28
3-MP	5.79
N-Hexane	6.48
MCP	46.60
Cyclohexane	9.65
Hydrocracking, %	43.7
Isomerization, %	46.6
Hydrogen Balance, %	99.8
Rate constant, cc/gm-sec	0.180

TABLE A

RUN DATA

Run Number	20N
Feed Stock	Cyclohexane
Catalyst Type	Pd-H-faujasite
Size, mm	0.84-0.42
Temperature, °F	700
Pressure, psia	765
Feed, v/hr-v	2.04
w/hr-w	3.22
Hydrogen, moles/mole C_6	8.00
Minutes on Feed	1190
Product, moles per 100 moles feed	
Hydrogen	716.0
Methane	0.29
Ethane	1.62
Propane	22.80
I-Butane	31.40
N-Butane	11.50
I-Pentane	14.15
N-Pentane	7.65
2,2-DMB	1.80
2,3-DMB	2.51
2-MP	8.44
3-MP	5.90
N-Hexane	7.61
MCP	12.45
Cyclohexane	3.29
Hydrocracking, %	84.2
Isomerization, %	12.5
Hydrogen Balance, %	99.3
Rate constant, cc/gm-sec	0.187

TABLE A

RUN DATA

Run Number	200
Feed Stock	Cyclohexane
Catalyst Type	Pd-H-faujasite
Size, mm	0.84-0.42
Temperature, °F	700
Pressure, psia	765
Feed, v/hr-v	2.04
w/hr-w	3.22
Hydrogen, moles/mole C_6	10.20
Minutes on Feed	1280
Product, moles per 100 moles feed	
Hydrogen	944.0
Methane	0.29
Ethane	1.91
Propane	16.40
I-Butane	24.40
N-Butane	9.22
I-Pentane	12.95
N-Pentane	6.84
2,2-DMB	1.23
2,3-DMB	2.47
2-MP	9.48
3-MP	6.63
N-Hexane	8.44
MCP	19.45
Cyclohexane	4.62
Hydrocracking, %	75.9
Isomerization, %	19.5
Hydrogen Balance, %	101.0
Rate constant, cc/gm-sec	0.179

TABLE A

RUN DATA

Run Number	20P
Feed Stock	Cyclohexane
Catalyst Type	Pd-H-faujasite
Size, mm	0.84-0.42
Temperature, °F	700
Pressure, psia	615
Feed, v/hr-v	2.04
w/hr-w	3.22
Hydrogen, moles/mole C_6	9.88
Minutes on Feed	1370
Product, moles per 100 moles feed	
Hydrogen	908.0
Methane	0.59
Ethane	2.79
Propane	19.45
I-Butane	31.50
N-Butane	14.85
I-Pentane	14.55
N-Pentane	7.60
2, 2-DMB	1.18
2, 3-DMB	2.04
2-MP	6.76
3-MP	4.73
N-Hexane	5.70
MCP	16.10
Cyclohexane	3.48
Hydrocracking, %	80.4
Isomerization, %	16.1
Hydrogen Balance, %	99.3
Rate constant, cc/gm-sec	0.249

TABLE A

RUN DATA

Run Number	20Q
Feed Stock	Cyclohexane
Catalyst Type	Pd-H-faujasite
Size, mm	0.84-0.42
Temperature, °F	700
Pressure, psia	365
Feed, v/hr-v	2.04
w/hr-w	3.22
Hydrogen, moles/mole C_6	9.39
Minutes on Feed	1460
Product, moles per 100 moles feed	
Hydrogen	854.0
Methane	1.77
Ethane	7.20
Propane	24.00
I-Butane	40.60
N-Butane	17.30
I-Pentane	21.70
N-Pentane	6.95
2,2-DMB	0.44
2,3-DMB	0.89
2-MP	2.60
3-MP	1.82
N-Hexane	2.60
MCP	10.95
Cyclohexane	3.58
Hydrocracking, %	85.4
Isomerization, %	11.0
Hydrogen Balance, %	100.1
Rate constant, cc/gm-sec	0.520

TABLE A

RUN DATA

Run Number	20R
Feed Stock	Cyclohexane
Catalyst Type	Pd-H-faujasite
Size, mm	0.84-0.42
Temperature, °F	700
Pressure, psia	765
Feed, v/hr-v	2.04
w/hr-w	3.22
Hydrogen, moles/mole C_6	10.2
Minutes on Feed	1550
Product, moles per 100 moles feed	
Hydrogen	944.0
Methane	0.29
Ethane	2.01
Propane	16.32
I-Butane	24.20
N-Butane	9.50
I-Pentane	13.00
N-Pentane	6.60
2,2-DMB	1.23
2,3-DMB	3.18
2-MP	8.82
3-MP	6.59
N-Hexane	8.42
MCP	20.00
Cyclohexane	4.10
Hydrocracking, %	75.9
Isomerization, %	20.0
Hydrogen Balance, %	100.8
Rate constant, cc/gm-sec	0.178

TABLE A

RUN DATA

Run Number	21A
Feed Stock	Cyclohexane
Catalyst Type	Pd-H-mordenite
Size, mm	1.2-0.21
Temperature, °F	650
Pressure, psia	765
Feed, v/hr-v	2.04
w/hr-w	2.20
Hydrogen, moles/mole C_6	7.92
Minutes on Feed	90
Product, moles per 100 moles feed	
Hydrogen	616.0
Methane	2.65
Ethane	11.90
Propane	96.80
I-Butane	16.22
N-Butane	21.00
I-Pentane	6.95
N-Pentane	3.30
2,2-DMB	0.39
2,3-DMB	0.44
2-MP	1.13
3-MP	0.79
N-Hexane	0.93
MCP	9.18
Cyclohexane	1.42
Hydrocracking, %	89.4
Isomerization, %	9.2
Hydrogen Balance, %	100.5
Rate constant, cc/gm-sec	0.141

TABLE A

RUN DATA

Run Number	21B
Feed Stock	Cyclohexane
Catalyst Type	Pd-H-mordenite
Size, mm	1.2-0.21
Temperature, °F	650
Pressure, psia	765
Feed, v/hr-v	2.04
w/hr-w	2.20
Hydrogen, moles/mole C_6	12.25
Minutes on Feed	165
Product, moles per 100 moles feed	
Hydrogen	1074.0
Methane	3.53
Ethane	12.95
Propane	83.10
I-Butane	13.30
N-Butane	17.50
I-Pentane	5.12
N-Pentane	2.41
2,2-DMB	0.44
2,3-DMB	0.41
2-MP	1.25
3-MP	0.88
N-Hexane	1.67
MCP	19.20
Cyclohexane	2.90
Hydrocracking, %	77.9
Isomerization, %	19.2
Hydrogen Balance, %	98.8
Rate constant, cc/gm-sec	0.125

TABLE A

RUN DATA

Run Number	21C
Feed Stock	Cyclohexane
Catalyst Type	Pd-H-mordenite
Size, mm	1.2-0.21
Temperature, °F	650
Pressure, psia	765
Feed, v/hr-v	2.04
w/hr-w	2.20
Hydrogen, moles/mole C_6	7.60
Minutes on Feed	255
Product, moles per 100 moles feed	
Hydrogen	616.0
Methane	3.24
Ethane	13.25
Propane	80.00
I-Butane	13.65
N-Butane	18.00
I-Pentane	4.00
N-Pentane	1.47
2,2-DMB	0.30
2,3-DMB	0.66
2-MP	1.06
3-MP	0.74
N-Hexane	0.98
MCP	21.40
Cyclohexane	4.40
Hydrocracking, %	74.2
Isomerization, %	21.4
Hydrogen Balance, %	100.4
Rate constant, cc/gm-sec	0.0820

TABLE A

RUN DATA

Run Number	21D
Feed Stock	Cyclohexane
Catalyst Type	Pd-H-mordenite
Size, mm	1.2-0.21
Temperature, °F	650
Pressure, psia	765
Feed, v/hr-v	8.17
w/hr-w	8.80
Hydrogen, moles/mole C_6	17.1
Minutes on Feed	345
Product, moles per 100 moles feed	
Hydrogen	1681.0
Methane	0.73
Ethane	3.31
Propane	18.20
I-Butane	1.47
N-Butane	2.57
I-Pentane	0.88
N-Pentane	0.29
2,2-DMB	0.04
2,3-DMB	0.01
2-MP	0.36
3-MP	0.25
N-Hexane	0.25
MCP	41.40
Cyclohexane	43.70
Hydrocracking, %	14.9
Isomerization, %	41.4
Hydrogen Balance, %	99.6
Rate constant, cc/gm-sec	0.0822

TABLE A

RUN DATA

Run Number	21E
Feed Stock	Cyclohexane
Catalyst Type	Pd-H-mordenite
Size, mm	1.2-0.21
Temperature, °F	650
Pressure, psia	765
Feed, v/hr-v	8.17
w/hr-w	8.80
Hydrogen, moles/mole C_6	14.1
Minutes on Feed	435
Product, moles per 100 moles feed	
Hydrogen	1377.0
Methane	1.47
Ethane	4.42
Propane	19.65
I-Butane	3.00
N-Butane	3.00
I-Pentane	1.17
N-Pentane	0.30
2,2-DMB	0.06
2,3-DMB	0.14
2-MP	0.36
3-MP	0.25
N-Hexane	0.25
MCP	49.10
Cyclohexane	33.40
Hydrocracking, %	17.5
Isomerization, %	49.1
Hydrogen Balance, %	99.6
Rate constant, cc/gm-sec	0.0819

TABLE A

RUN DATA

Run Number	22A
Feed Stock	Cyclohexane
Catalyst Type	Pd-H-faujasite
Size, mm	0.84-0.42
Temperature, °F	650
Pressure, psia	765
Feed, v/hr-v	2.04
w/hr-w	3.17
Hydrogen, moles/mole C_6	18.8
Minutes on Feed	120
Product, moles per 100 moles feed	
Hydrogen	1832.0
Methane	0.15
Ethane	0.44
Propane	2.26
I-Butane	5.23
N-Butane	1.91
I-Pentane	3.24
N-Pentane	1.00
2,2-DMB	0.79
2,3-DMB	1.05
2-MP	4.02
3-MP	2.80
N-Hexane	3.94
MCP	64.80
Cyclohexane	13.10
Hydrocracking, %	22.1
Isomerization, %	64.8
Hydrogen Balance, %	99.3
Rate constant, cc/gm-sec	0.0500

TABLE A

RUN DATA

Run Number	22B
Feed Stock	Cyclohexane
Catalyst Type	Pd-H-faujasite
Size, mm	0.84-0.42
Temperature, °F	700
Pressure, psia	765
Feed, v/hr-v	2.04
w/hr-w	3.17
Hydrogen, moles/mole C_6	16.8
Minutes on Feed	270
Product, moles per 100 moles feed	
Hydrogen	1583.0
Methane	0.29
Ethane	1.77
Propane	9.92
I-Butane	16.90
N-Butane	9.13
I-Pentane	9.92
N-Pentane	4.70
2,2-DMB	1.38
2,3-DMB	1.45
2-MP	9.45
3-MP	6.58
N-Hexane	7.51
MCP	30.10
Cyclohexane	8.43
Hydrocracking, %	61.5
Isomerization, %	30.1
Hydrogen Balance, %	100.3
Rate constant, cc/gm-sec	0.181

TABLE A

RUN DATA

Run Number	22C
Feed Stock	Cyclohexane
Catalyst Type	Pd-H-faujasite
Size, mm	0.84-0.42
Temperature, ^{o}F	700
Pressure, psia	765
Feed, v/hr-v	2.04
w/hr-w	3.17
Hydrogen, moles/mole C_6	31.0
Minutes on Feed	360
Product, moles per 100 moles feed	
Hydrogen	3038.0
Methane	0.29
Ethane	1.33
Propane	6.29
I-Butane	10.70
N-Butane	4.49
I-Pentane	5.65
N-Pentane	3.40
2,2-DMB	1.08
2,3-DMB	1.28
2-MP	6.77
3-MP	4.72
N-Hexane	5.85
MCP	45.60
Cyclohexane	13.40
Hydrocracking, %	41.0
Isomerization, %	45.6
Hydrogen Balance, %	99.0
Rate constant, cc/gm-sec	0.180

TABLE A

RUN DATA

Run Number	22D
Feed Stock	Cyclohexane
Catalyst Type	Pd-H-faujasite
Size, mm	0.84-0.42
Temperature, °F	700
Pressure, psia	765
Feed, v/hr-v	4.08
w/hr-w	6.34
Hydrogen, moles/mole C_6	9.50
Minutes on Feed	480
Product, moles per 100 moles feed	
Hydrogen	861.0
Methane	0.74
Ethane	2.50
Propane	8.54
I-Butane	17.50
N-Butane	6.70
I-Pentane	11.50
N-Pentane	4.47
2,2-DMB	1.35
2,3-DMB	1.32
2-MP	6.91
3-MP	4.82
N-Hexane	6.43
MCP	34.50
Cyclohexane	10.20
Hydrocracking, %	55.3
Isomerization, %	34.5
Hydrogen Balance, %	100.2
Rate constant, cc/gm-sec	0.180

TABLE A

RUN DATA

Run Number	22E
Feed Stock	Cyclohexane
Catalyst Type	Pd-H-faujasite
Size, mm	0.84-0.42
Temperature, °F	650
Pressure, psia	765
Feed, v/hr-v	4.08
w/hr-w	6.34
Hydrogen, moles/mole C_6	8.85
Minutes on Feed	570
Product, moles per 100 moles feed	
Hydrogen	855.0
Methane	0.16
Ethane	0.50
Propane	2.10
I-Butane	5.02
N-Butane	1.80
I-Pentane	3.15
N-Pentane	0.92
2,2-DMB	0.84
2,3-DMB	1.16
2-MP	4.00
3-MP	2.79
N-Hexane	3.95
MCP	65.20
Cyclohexane	13.40
Hydrocracking, %	21.4
Isomerization, %	65.2
Hydrogen Balance, %	98.5
Rate constant, cc/gm-sec	0.0487

TABLE A

RUN DATA

Run Number	23A
Feed Stock	56 mole % Cyclohexane, 44 mole % n-Hexane
Catalyst Type	Pd-H-faujasite
Size, mm	0.84-0.42
Temperature, ^{o}R	700
Pressure, psia	765
Feed, v/hr-v	2.04
w/hr-w	2.91
Hydrogen, moles/mole C_6	15.02
Minutes on Feed	120
Product, moles per 100 moles feed	
Hydrogen	1460.0
Methane	0.32
Ethane	1.45
Propane	16.00
I-Butane	13.10
N-Butane	5.71
I-Pentane	7.28
N-Pentane	4.18
2,2-DMB	6.98
2,3-DMB	3.55
2-MP	17.35
3-MP	12.10
N-Hexane	12.90
MCP	13.34
Cyclohexane	3.33
Hydrocracking, %	--
Isomerization, %	--
Hydrogen Balance, %	100.4
Rate constant, cc/gm-sec	--

TABLE A

RUN DATA

Run Number	23B
Feed Stock	56 mole % Cyclohexane, 44 mole % n-Hexane
Catalyst Type	Pd-H-faujasite
Size, mm	0.84-0.42
Temperature, ^{o}F	700
Pressure, psia	765
Feed, v/hr-v	2.04
w/hr-w	2.91
Hydrogen, moles/mole C_6	23.4
Minutes on Feed	210
Product, moles per 100 moles feed	
Hydrogen	2240.0
Methane	0.58
Ethane	1.45
Propane	10.20
I-Butane	10.53
N-Butane	5.23
I-Pentane	6.56
N-Pentane	3.28
2, 2-DMB	6.87
2, 3-DMB	2.20
2-MP	19.20
3-MP	13.40
N-Hexane	13.90
MCP	16.90
Cyclohexane	3.33
Hydrocracking, %	--
Isomerization, %	--
Hydrogen Balance, %	98.0
Rate constant, cc/gm-sec	--

TABLE A

RUN DATA

Run Number	23C
Feed Stock	56 mole % Cyclohexane, 44 mole % n-Hexane
Catalyst Type	Pd-H-faujasite
Size, mm	0.84-0.42
Temperature, ^{o}F	725
Pressure, psia	765
Feed, v/hr-v	2.04
w/hr-w	2.91
Hydrogen, moles/mole C_6	23.1
Minutes on Feed	300
Product, moles per 100 moles feed	
Hydrogen	2220.0
Methane	0.64
Ethane	2.74
Propane	20.90
I-Butane	15.95
N-Butane	7.23
I-Pentane	8.81
N-Pentane	4.70
2,2-DMB	7.08
2,3-DMB	3.75
2-MP	16.20
3-MP	11.30
N-Hexane	12.70
MCP	8.68
Cyclohexane	2.20
Hydrocracking, %	--
Isomerization, %	--
Hydrogen Balance, %	99.2
Rate constant, cc/gm-sec	--

TABLE A

RUN DATA

Run Number	23D
Feed Stock	56 mole % Cyclohexane, 44 mole % n-Hexane
Catalyst Type	Pd-H-faujasite
Size, mm	0.84-0.42
Temperature, °F	725
Pressure, psia	765
Feed, v/hr-v	2.04
w/hr-w	2.91
Hydrogen, moles/mole C_6	14.4
Minutes on Feed	390
Product, moles per 100 moles feed	
Hydrogen	1320.0
Methane	2.25
Ethane	4.34
Propane	40.25
I-Butane	18.27
N-Butane	9.00
I-Pentane	13.00
N-Pentane	6.18
2,2-DMB	3.01
2,3-DMB	2.50
2-MP	13.95
3-MP	9.72
N-Hexane	9.97
MCP	3.80
Cyclohexane	0.54
Hydrocracking, %	--
Isomerization, %	--
Hydrogen Balance, %	98.5
Rate constant, cc/gm-sec	--

TABLE A

RUN DATA

Run Number	23E
Feed Stock	56 mole % Cyclohexane, 44 mole % n-Hexane
Catalyst Type	Pd-H-faujasite
Size, mm	0.84-0.42
Temperature, °F	750
Pressure, psia	765
Feed, v/hr-v	2.04
w/hr-w	2.91
Hydrogen, moles/mole C_6	21.0
Minutes on Feed	480
Product, moles per 100 moles feed	
Hydrogen	2020.0
Methane	1.61
Ethane	5.94
Propane	47.30
I-Butane	20.10
N-Butane	12.63
I-Pentane	11.84
N-Pentane	55.92
2,2-DMB	3.33
2,3-DMB	3.77
2-MP	11.15
3-MP	7.78
N-Hexane	9.08
MCP	2.20
Cyclohexane	0.27
Hydrocracking, %	--
Isomerization, %	--
Hydrogen Balance, %	101.5
Rate constant, cc/gm-sec	--

TABLE A

RUN DATA

Run Number	23F
Feed Stock	56 mole % Cyclohexane, 44 mole % n-Hexane
Catalyst Type	Pd-H-faujasite
Size, mm	0.84-0.42
Temperature, °F	750
Pressure, psia	765
Feed, v/hr-v	2.04
w/hr-w	2.91
Hydrogen, moles/mole C_6	20.1
Minutes on Feed	570
Product, moles per 100 moles feed	
Hydrogen	1880.0
Methane	0.64
Ethane	4.02
Propane	36.20
I-Butane	27.00
N-Butane	15.70
I-Pentane	13.25
N-Pentane	7.32
2,2-DMB	4.62
2,3-DMB	2.75
2-MP	10.15
3-MP	7.08
N-Hexane	8.39
MCP	1.82
Cyclohexane	0.22
Hydrocracking, %	--
Isomerization, %	--
Hydrogen Balance, %	98.3
Rate constant, cc/gm-sec	--

TABLE A

RUN DATA

Run Number	24A
Feed Stock	Cyclohexane
Catalyst Type	Pd-H-mordenite
Size, mm	1.2-0.21
Temperature, °F	650
Pressure, psia	765
Feed, v/hr-v	2.04
w/hr-w	2.09
Hydrogen, moles/mole C_6	9.92
Minutes on Feed	180
Product, moles per 100 moles feed	
Hydrogen	837.0
Methane	4.13
Ethane	15.40
Propane	82.50
I-Butane	9.35
N-Butane	17.40
I-Pentane	8.65
N-Pentane	4.12
2,2-DMB	0.39
2,3-DMB	0.79
2-MP	1.13
3-MP	0.79
N-Hexane	1.08
MCP	17.20
Cyclohexane	3.29
Hydrocracking, %	79.5
Isomerization, %	17.2
Hydrogen Balance, %	100.0
Rate constant, cc/gm-sec	0.116

TABLE A

RUN DATA

Run Number	24B
Feed Stock	Cyclohexane
Catalyst Type	Pd-H-mordenite
Size, mm	1.2-0.21
Temperature, °F	650
Pressure, psia	765
Feed, v/hr-v	2.04
w/hr-w	2.09
Hydrogen, moles/mole C_6	9.92
Minutes on Feed	220
Product, moles per 100 moles feed	
Hydrogen	848.0
Methane	4.13
Ethane	15.90
Propane	88.00
I-Butane	9.65
N-Butane	14.31
I-Pentane	4.00
N-Pentane	1.12
2,2-DMB	0.54
2,3-DMB	0.83
2-MP	1.33
3-MP	0.93
N-Hexane	1.03
MCP	21.50
Cyclohexane	3.97
Hydrocracking, %	74.5
Isomerization, %	21.5
Hydrogen Balance, %	99.3
Rate constant, cc/gm-sec	0.0985

TABLE A

RUN DATA

Run Number	24C
Feed Stock	Cyclohexane
Catalyst Type	Pd-H-mordenite
Size, mm	1.2-0.21
Temperature, ^{o}F	650
Pressure, psia	765
Feed, v/hr-v	2.04
w/hr-w	2.09
Hydrogen, moles/mole C_6	9.92
Minutes on Feed	250
Product, moles per 100 moles feed	
Hydrogen	862.0
Methane	2.94
Ethane	13.55
Propane	77.20
I-Butane	9.27
N-Butane	13.70
I-Pentane	3.82
N-Pentane	1.65
2,2-DMB	0.34
2,3-DMB	0.81
2-MP	1.21
3-MP	0.84
N-Hexane	1.08
MCP	26.00
Cyclohexane	6.38
Hydrocracking, %	67.6
Isomerization, %	26.0
Hydrogen Balance, %	99.9
Rate constant, cc/gm-sec	0.0824

TABLE A

RUN DATA

Run Number	24D
Feed Stock	Cyclohexane
Catalyst Type	Pd-H-mordenite
Size, mm	1.2-0.21
Temperature, °F	650
Pressure, psia	765
Feed, v/hr-v	2.04
w/hr-w	2.09
Hydrogen, moles/mole C_6	9.92
Minutes on Feed	280
Product, moles per 100 moles feed	
Hydrogen	871.0
Methane	2.94
Ethane	12.65
Propane	69.90
I-Butane	8.70
N-Butane	12.90
I-Pentane	3.60
N-Pentane	1.41
2,2-DMB	0.64
2,3-DMB	0.92
2-MP	1.48
3-MP	1.03
N-Hexane	1.33
MCP	29.10
Cyclohexane	7.35
Hydrocracking, %	63.5
Isomerization, %	29.1
Hydrogen Balance, %	99.7
Rate constant, cc/gm-sec	0.0739

TABLE A

RUN DATA

Run Number	25A
Feed Stock	Cyclohexane
Catalyst Type	Pd-H-mordenite
Size, mm	1.2-0.21
Temperature, °F	600
Pressure, psia	765
Feed, v/hr-v	2.04
w/hr-w	2.21
Hydrogen, moles/mole C_6	8.53
Minutes on Feed	180
Product, moles per 100 moles feed	
Hydrogen	800.0
Methane	0.88
Ethane	3.39
Propane	24.10
I-Butane	2.80
N-Butane	11.12
I-Pentane	1.65
N-Pentane	1.35
2, 2-DMB	0.20
2, 3-DMB	0.36
2-MP	0.92
3-MP	0.64
N-Hexane	0.54
MCP	56.00
Cyclohexane	16.50
Hydrocracking, %	27.5
Isomerization, %	56.0
Hydrogen Balance, %	100.2
Rate constant, cc/gm-sec	0.0207

TABLE A

RUN DATA

Run Number	25B
Feed Stock	Cyclohexane
Catalyst Type	Pd-H-mordenite
Size, mm	1.2-0.21
Temperature, °F	600
Pressure, psia	765
Feed, v/hr-v	4.08
w/hr-w	4.42
Hydrogen, moles/mole C_6	8.68
Minutes on Feed	250
Product, moles per 100 moles feed	
Hydrogen	840.0
Methane	0.47
Ethane	2.06
Propane	13.17
I-Butane	1.40
N-Butane	6.12
I-Pentane	0.82
N-Pentane	0.59
2,2-DMB	0.20
2,3-DMB	0.11
2-MP	0.63
3-MP	0.44
N-Hexane	0.49
MCP	48.70
Cyclohexane	36.10
Hydrocracking, %	15.2
Isomerization, %	48.7
Hydrogen Balance, %	99.1
Rate constant, cc/gm-sec	0.0216

TABLE A

RUN DATA

Run Number	25C
Feed Stock	Cyclohexane
Catalyst Type	Pd-H-mordenite
Size, mm	1.2-0.21
Temperature, °F	600
Pressure, psia	765
Feed, v/hr-v	2.04
w/hr-w	2.21
Hydrogen, moles/mole C_6	7.20
Minutes on Feed	310
Product, moles per 100 moles feed	
Hydrogen	660.0
Methane	1.18
Ethane	3.97
Propane	28.30
I-Butane	2.94
N-Butane	12.24
I-Pentane	1.71
N-Pentane	1.35
2,2-DMB	0.29
2,3-DMB	0.74
2-MP	0.78
3-MP	0.54
N-Hexane	0.59
MCP	52.30
Cyclohexane	16.30
Hydrocracking, %	31.4
Isomerization, %	52.3
Hydrogen Balance, %	102.0
Rate constant, cc/gm-sec	0.0205

TABLE A

RUN DATA

Run Number	26A
Feed Stock	n-Pentane
Catalyst Type	Pd-H-mordenite
Size, mm	1.2-0.21
Temperature, °F	550
Pressure, psia	465
Feed, v/hr-v	8.17
w/hr-w	7.19
Hydrogen, moles/mole C_6	3.35
Minutes on Feed	390
Product, moles per 100 moles feed	
Hydrogen	335.0
Methane	0.00
Ethane	0.19
Propane	0.34
I-Butane	0.12
N-Butane	0.27
I-Pentane	31.10
N-Pentane	68.70
2,2-DMB	0.00
2,3-DMB	0.00
2-MP	0.00
3-MP	0.00
N-Hexane	0.00
MCP	0.00
Cyclohexane	0.00
Hydrocracking, %	0.2
Isomerization, %	31.1
Hydrogen Balance, %	99.0
Rate constant, cc/gm-sec	0.073

TABLE A

RUN DATA

Run Number	26B
Feed Stock	n-Pentane
Catalyst Type	Pd-H-mordenite
Size, mm	1.2-0.21
Temperature, °F	550
Pressure, psia	465
Feed, v/hr-v	8.17
w/hr-w	7.19
Hydrogen, moles/mole C_6	3.29
Minutes on Feed	470
Product, moles per 100 moles feed	
Hydrogen	329.0
Methane	0.00
Ethane	0.29
Propane	0.39
I-Butane	0.21
N-Butane	0.25
I-Pentane	32.00
N-Pentane	67.50
2,2-DMB	0.00
2,3-DMB	0.00
2-MP	0.00
3-MP	0.00
N-Hexane	0.00
MCP	0.00
Cyclohexane	0.00
Hydrocracking, %	0.5
Isomerization, %	32.0
Hydrogen Balance, %	99.7
Rate constant, cc/gm-sec	0.075

TABLE A

RUN DATA

Run Number	27
Feed Stock	n-Pentane
Catalyst Type	Pd-H-mordenite
Size, mm	1.2-0.21
Temperature, °F	550
Pressure, psia	465
Feed, v/hr-v	8.17
w/hr-w	7.95
Hydrogen, moles/mole C_6	3.37
Minutes on Feed	120
Product, moles per 100 moles feed	
Hydrogen	335.0
Methane	0.00
Ethane	0.23
Propane	0.41
I-Butane	0.75
N-Butane	0.51
I-Pentane	35.60
N-Pentane	62.50
2,2-DMB	0.00
2,3-DMB	0.00
2-MP	0.00
3-MP	0.00
N-Hexane	0.60
MCP	0.00
Cyclohexane	0.00
Hydrocracking, %	1.9
Isomerization, %	35.6
Hydrogen Balance, %	99.8
Rate constant, cc/gm-sec	0.100

TABLE A

RUN DATA

Run Number	28A
Feed Stock	56 mol % Cyclohexane, 44 mol % n-Hexane
Catalyst Type	Pd-H-mordenite
Size, mm	1.2-0.21
Temperature, °F	600
Pressure, psia	765
Feed, v/hr-v	2.04
w/hr-w	1.97
Hydrogen, moles/mole C_6	18.0
Minutes on Feed	150
Product, moles per 100 moles feed	
Hydrogen	1720.0
Methane	1.29
Ethane	3.87
Propane	30.90
I-Butane	10.22
N-Butane	16.42
I-Pentane	5.35
N-Pentane	3.67
2, 2-DMB	2.68
2, 3-DMB	4.23
2-MP	5.00
3-MP	3.49
N-Hexane	20.80
MCP	17.70
Cyclohexane	4.02
Hydrocracking, %	--
Isomerization, %	--
Hydrogen Balance, %	99.4
Rate constant, cc/gm-sec	--

TABLE A

RUN DATA

Run Number	28B
Feed Stock	56 mol % Cyclohexane, 44 mol % n-Hexane
Catalyst Type	Pd-H-mordenite
Size, mm	1.2-0.21
Temperature, °F	600
Pressure, psia	765
Feed, v/hr-v	2.04
w/hr-w	1.97
Hydrogen, moles/mole C_6	12.1
Minutes on Feed	260
Product, moles per 100 moles feed	
Hydrogen	1050.0
Methane	1.61
Ethane	6.59
Propane	50.30
I-Butane	16.90
N-Butane	19.00
I-Pentane	6.03
N-Pentane	3.34
2,2-DMB	2.04
2,3-DMB	2.35
2-MP	5.00
3-MP	3.49
N-Hexane	13.80
MCP	11.40
Cyclohexane	2.68
Hydrocracking, %	--
Isomerization, %	--
Hydrogen Balance, %	99.8
Rate constant, cc/gm-sec	--

TABLE A

RUN DATA

Run Number	28C
Feed Stock	56 mole % Cyclohexane, 44 mol % n-Hexane
Catalyst Type	Pd-H-mordenite
Size, mm	1.2-0.21
Temperature, °F	650
Pressure, psia	765
Feed, v/hr-v	2.04
w/hr-w	1.97
Hydrogen, moles/mole C_6	12.1
Minutes on Feed	370
Product, moles per 100 moles feed	
Hydrogen	1050.0
Methane	3.86
Ethane	16.40
Propane	118.00
I-Butane	17.95
N-Butane	24.30
I-Pentane	2.57
N-Pentane	1.22
2,2-DMB	0.38
2,3-DMB	0.25
2-MP	1.09
3-MP	0.76
N-Hexane	0.76
MCP	0.21
Cyclohexane	0.05
Hydrocracking, %	--
Isomerization, %	--
Hydrogen Balance, %	99.0
Rate constant, cc/gm-sec	--

TABLE A

RUN DATA

Run Number	28D
Feed Stock	56 mol % Cyclohexane, 44 mol % n-Hexane
Catalyst Type	Pd-H-mordenite
Size, mm	1.2-0.21
Temperature, ^{o}F	650
Pressure, psia	765
Feed, v/hr-v	2.04
w/hr-w	1.97
Hydrogen, moles/mole C_6	10.5
Minutes on Feed	480
Product, moles per 100 moles feed	
Hydrogen	920.0
Methane	5.16
Ethane	20.40
Propane	128.20
I-Butane	13.82
N-Butane	20.70
I-Pentane	3.21
N-Pentane	1.93
2,2-DMB	0.32
2,3-DMB	0.22
2-MP	0.16
3-MP	0.11
N-Hexane	0.16
MCP	0.21
Cyclohexane	0.03
Hydrocracking, %	--
Isomerization, %	--
Hydrogen Balance, %	101.2
Rate constant, cc/gm-sec	--

APPENDIX B

NOMENCLATURE

APPENDIX B

NOMENCLATURE

C	-	Concentration
C_A	-	Concentration of hexanes
C_B	-	Concentration of hydrogen
C_C	-	Concentration of naphthenes (MCP + CH)
C_p	-	Concentration of hydrocracked products
F	-	Hydrocarbon flow rate
k	-	Simplified reaction rate constant for hydrocracking hexanes
k_1	-	Simplified reaction rate constant for hydrocracking naphthenes (MCP + CH)
k_o	-	Reaction rate constant for hydrocracking hexanes
$k_{1,0}$	-	Reaction rate constant for hydrocracking naphthenes (MCP + CH)
k'_o	-	Product of reaction rate constant times adsorption coefficient for hexanes, $k_o K_A$
$k'_{1,0}$	-	Product of reaction rate constant times adsorption coefficient for naphthenes, $k_{1,0} K_C$
K_A	-	Dynamic adsorption coefficient for hexanes

K_B	-	Dynamic adsorption coefficient for hydrogen
K_C	-	Dynamic adsorption coefficient for naphthenes
K_p	-	Dynamic adsorption coefficient for hydrocracked products
M	-	Molecular weight
p_A	-	Partial pressure of hexanes
p_B	-	Partial pressure of hydrogen
p_C	-	Partial pressure of naphthenes (MCP + CH)
p_p	-	Partial pressure of hydrocracked products
R	-	Molar ratio of hydrogen to hydrocarbon in feed gas
S	-	Selectivity to propane, mole %
t	-	Superficial contact time based on catalyst volume
t_H	-	Superficial contact time based on catalyst weight
T	-	Temperature, degrees Rankine, unless otherwise specified
W	-	Catalyst weight in reactor

x	-	Fraction converted by hydrocracking
ρc	-	Catalyst bulk density, gm/cc
ρg	-	Gas density at operating conditions, gm moles/cc
θ	-	Time on feed

APPENDIX C

ANALYTICAL SYSTEM

APPENDIX C

ANALYTICAL SYSTEM

A. Introduction

A F&M Model 810R dual-column gas chromatograph with a ten foot column of 10% silicone rubber, SE-30, on 90% white chromosorb (80-100 mesh) was used to obtain the product analysis from the experimental runs. Generally the product consisted of about 90% hydrogen and 10% hydrocarbons. Typical chromatograph charts are shown in Figures C-1 and C-2 (pages 281 and 282).

B. Method of Analysis

A packed column and a thermal conductivity detector were the basic elements of the gas chromatograph. Each hydrocarbon component had a different retention time due to varying adsorptivity constants for the packing in the column. Helium was used as a carrier gas, and a uniform flow of the carrier gas was maintained through the packed column and past the thermal conductivity detector. The gas sample was injected as a pulse into the carrier stream. The carrier gas swept the sample through the packed column and detector. The gas stream passing the detector at any given time consisted of a mixture of helium and a single hydrocarbon component due to the varying retention times of the hydrocarbons in the packed column.

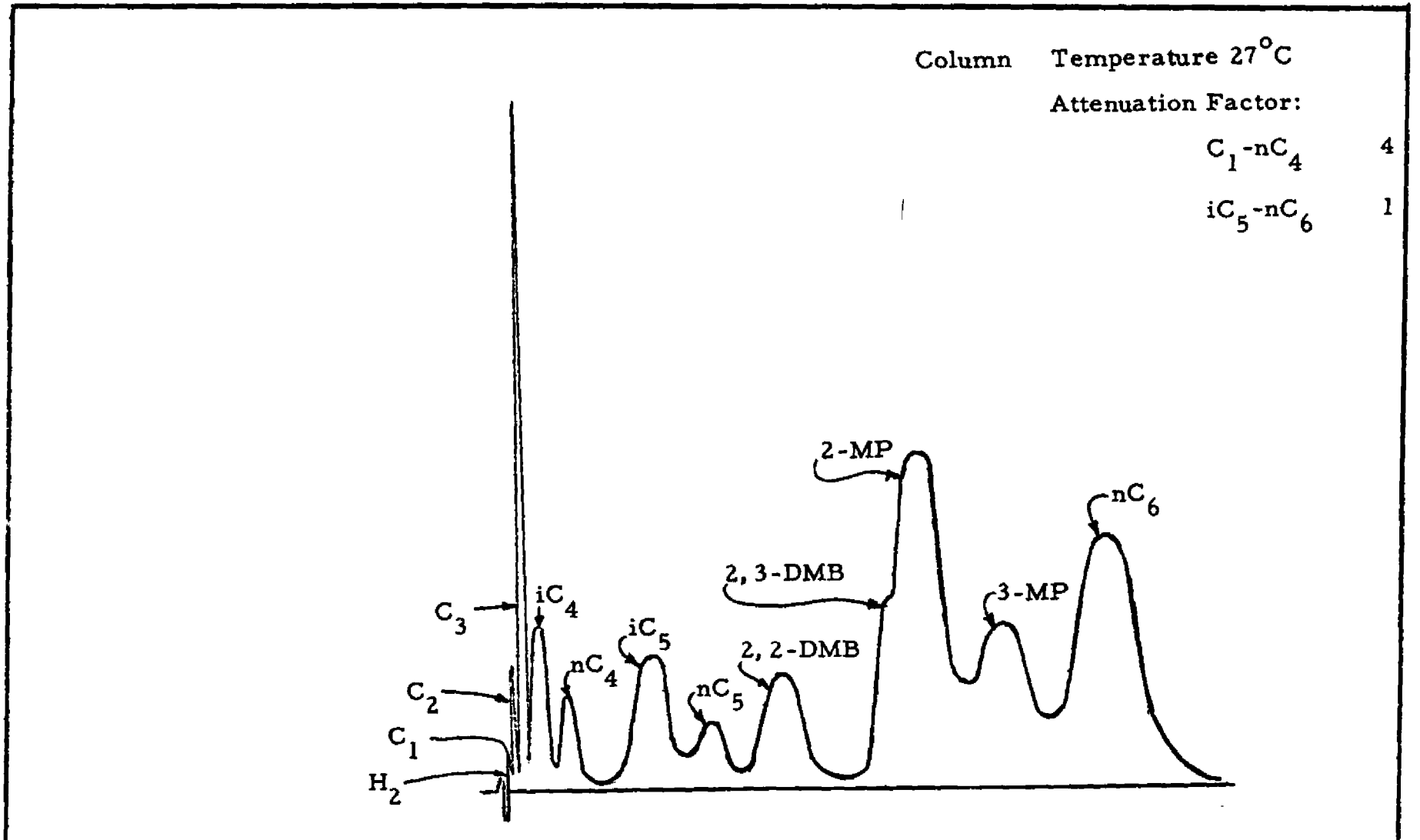

Figure C-1. Gas Chromatograph Output, Hexane Hydrocracking

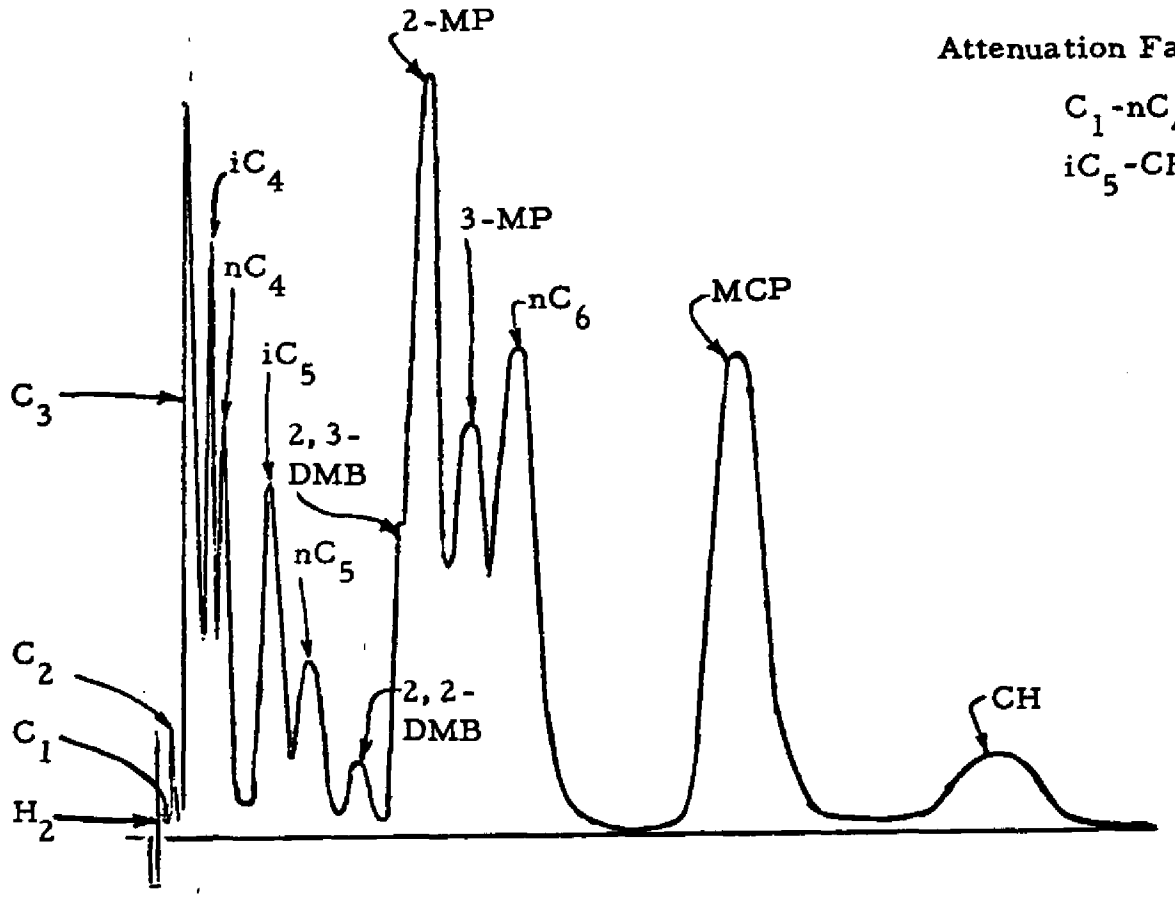

Figure C-2. Gas Chromatograph Output, Cyclohexane Hydrocracking

The response from the thermal conductivity detector was a linear function of the instantaneous hydrocarbon concentration in the carrier gas stream. Then the instantaneous concentration of a component "j" was

$$yj = C^{1}_{j}\, Dj$$

where yj = mole fraction of "j" in the carrier gas

C^{1} = constant

D = detector output

To obtain the overall concentration of "j", the detector output was integrated with respect to time. This integration was done automatically by a ball-and-disc integrator in the gas chromatograph recorder system. Then a "peak area" was recorded by the integrator, corresponding to each hydrocarbon "peak". This "peak area" was related to the hydrogen-free concentration in the gas sample by

$$Yj = Cj\, Aj / \sum_{k=1}^{n} C_k A_k$$

where Y = hydrogen-free mole fraction

C = experimentally determined calibration constant

A = peak area

n = total number of components in hydrogen-free sample

An electronic "attenuator" was used to extend the range and accuracy of the gas chromatograph. The "attenuator" scaled down the response of large peaks by selected factors. The "attenuation" factors, F, are then used in the final equation

$$Yj = Fj\ Cj\ Aj / \sum_{k=1}^{n} F_k\ C_k\ A_k.$$

C. Determination of Calibration Constants

Precise volumes of each hydrocarbon compound were injected separately into the gas chromatograph in order to determine the calibration constants. The integrated response (including the attenuation factor) was used to calculate the gram moles of hydrocarbon compound per unit integrator reading: These calibration constants are given in Table C-1.

Table C-1. Calibration Constants for Gas Chromatograph.

Component	C, gram-moles per unit area x 10^3
Methane	3.765
Ethane	2.496
Propane	2.006
i-Butane	1.707
n-Butane	1.685
i-Pentane	1.580
n-Pentane	1.495
2,2-DMB	1.352
2,3-DMB	1.352
2-MP	1.308
3-MP	1.318
n-Hexane	1.278
Cyclohexane	1.471
Methylcyclopentane	1.411

APPENDIX D

SAMPLE CALCULATIONS

APPENDIX D

SAMPLE CALCULATIONS

A. Typical Process Data

Run number	6A
Feed stock	n-Hexane
Catalyst type	Pd-H-faujasite
Catalyst volume	15.0 cc
Catalyst weight	7.405 gm
Catalyst size	0.84-0.42 mm
Temperature	750°F
Pressure	765 psia
Time at start of balance period	80 min
Length of balance period	20 min
Volume of hydrogen in	0.583 ft^3
Temperature of hydrogen in	85°F
Volume of Liquid hydrocarbon in	10.2 cc
Total gas out volume	0.650 ft^3
Temperature of gas out	85°F

B. Typical Analytical Data

Component	Peak Area	Attenuation Factor
C_1	0.17	4
C_2	0.60	4
C_3	4.85	4
iC_4	0.95	4
nC_4	0.85	4
iC_5	3.25	1
nC_5	2.25	1
2,2-DMB	4.50	1
2,3-DMB	2.76	1
2-MP	11.70	1
3-MP	8.15	1
nC_6	9.00	1

C. Material Balance Calculations

Basis: 20 minute balance period

Weight of nC_6 fed = (10.2 cc)(0.659 gm/cc) = 6.72 grams

Gram moles of nC_6 fed = 6.72/86.2 = 0.0780

Grams of carbon in nC_6 fed = 72.1 (0.078) = 5.62

Grams of hydrogen in nC_6 fed = 14.1 (0.078) = 1.10

Liquid hourly space velocity = (10.2 cc/20 min.)(60 min./hr.)/(15.0 cc) = 2.04 cc/hr.-cc

Weight hourly space velocity = (6.72 gm/20 min.)(60 min./hr.)/(7.41 gm) = 2.73 gm/hr.-gm

Volume of H_2 gas in at STP = (0.583 ft.^{3})(492/545)(29.92 - 1.17)/(29.92) = 0.505 ft.^{3}

Gram moles of H_2 gas in = (0.505 ft.^{3})(1.26 gm moles/ft.^{3}) = 0.637 gm moles

Volume of gas out at STP = (0.650 ft.^{3})(492/545)(29.92 - 1.17/29.92) = 0.565 ft.^{3}

Assumed grams of carbon in gas out = 5.62 gm

Hydrogen-to-nC_6 mole ratio = 0.637/0.078 = 8.16

Molar Weighting Factors for Hydrocarbons in Gas Out

C_1	(0.17)(4.00)(3.765)	=	2.57
C_2	(0.60)(4.00)(2.496)	=	6.00
C_3	(4.85)(4.00)(2.006)	=	38.80
iC_4	(0.95)(4.00)(1.707)	=	6.48
nC_4	(0.85)(4.00)(1.685)	=	5.73
iC_5	(3.25)(1.00)(1.580)	=	5.13
nC_5	(2.25)(1.00)(1.495)	=	3.36
2,2-DMB	(4.50)(1.00)(1.352)	=	6.09
2,3-DMB	(2.76)(1.00)(1.352)	=	3.73
2-MP	(11.70)(1.00)(1.308)	=	15.30
3-MP	(8.15)(1.00)(1.318)	=	10.70
nC_6	(9.00)(1.00)(1.278)	=	11.50
MCP	(0.00)(1.00)(1.411)	=	0.00
CH	(0.00)(1.00)(1.471)	=	0.00
			115.39

H_2 Free Mole Fractions of Hydrocarbons in Gas Out

C_1	2.57/115.39	=	0.0223
C_2	6.00/115.39	=	0.0520
C_3	38.80/115.39	=	0.3360
iC_4	6.48/115.39	=	0.0561
nC_4	5.73/115.39	=	0.0496
iC_5	5.13/115.39	=	0.0444
nC_5	3.36/115.39	=	0.0291
2,2-DMB	6.09/115.39	=	0.0528
2,3-DMB	3.73/115.39	=	0.0323
2-MP	15.30/115.39	=	0.1328
3-MP	10.70/115.39	=	0.0928
nC_6	11.50/115.39	=	0.0996
			1.0000

Grams of Carbon Per Gram Mole of Hydrocarbon Gas Out

C_1	(12.01)(0.0223)	=	0.27
C_2	(24.02)(0.0520)	=	1.25
C_3	(36.03)(0.3360)	=	12.10
iC_4	(48.04)(0.0561)	=	2.69
nC_4	(48.04)(0.0496)	=	2.38
iC_5	(60.05)(0.0444)	=	2.66
nC_5	(60.05)(0.0291)	=	1.75
2,2-DMB	(72.06)(0.0528)	=	3.80
2,3-DMB	(72.06)(0.0323)	=	2.32
2-MP	(72.06)(0.1328)	=	9.56
3-MP	(72.06)(0.0928)	=	6.68
nC_6	(72.06)(0.0996)	=	7.18
			52.64

Actual gram moles of hydrocarbon out = actual grams of carbon out/grams of carbon per gm mole of hydrocarbon gas out = 5.62/52.64 = 0.10716

Gram Moles of Hydrocarbon Components in Gas Out

C_1	(0.10716)(0.0223)	=	0.00250
C_2	(0.10716)(0.0520)	=	0.00555
C_3	(0.10716)(0.3360)	=	0.03600
iC_4	(0.10716)(0.0561)	=	0.00605
nC_4	(0.10716)(0.0496)	=	0.00536
iC_5	(0.10716)(0.0444)	=	0.00477
nC_5	(0.10716)(0.0291)	=	0.00311
2,2-DMB	(0.10716)(0.0528)	=	0.00565
2,3-DMB	(0.10716)(0.0323)	=	0.00345
2-MP	(0.10716)(0.1328)	=	0.01405
3-MP	(0.10716)(0.0928)	=	0.00997
nC_6	(0.10716)(0.0996)	=	0.01070
			0.10716

Grams of H_2 in Hydrocarbon Gas Out

C_1	(4.0)(0.00250)	=	0.010
C_2	(6.0)(0.00555)	=	0.033
C_3	(8.0)(0.03600)	=	0.288
iC_4	(10.1)(0.00605)	=	0.061
nC_4	(10.1)(0.00536)	=	0.054
iC_5	(12.1)(0.00477)	=	0.058
nC_5	(12.1)(0.00311)	=	0.038
2,2-DMB	(14.1)(0.00565)	=	0.080
2,3-DMB	(14.1)(0.00345)	=	0.049
2-MP	(14.1)(0.01405)	=	0.198
3-MP	(14.1)(0.00997)	=	0.141
nC_6	(14.1)(0.01070)	=	0.151
			1.161

Gram Moles of Hydrocarbon Components in Gas Out Per 100 Moles of nC_6 Fed

C_1	(100)(0.00250)/0.0780	=	3.20
C_2	(100)(0.00555)/0.0780	=	7.12
C_3	(100)(0.03600)/0.0780	=	46.20
iC_4	(100)(0.00605)/0.0780	=	7.75
nC_4	(100)(0.00536)/0.0780	=	6.88
iC_5	(100)(0.00477)/0.0780	=	6.13
nC_5	(100)(0.00311)/0.0780	=	3.99
2,2-DMB	(100)(0.00565)/0.0780	=	7.25
2,3-DMB	(100)(0.00345)/0.0780	=	4.40
2-MP	(100)(0.01405)/0.0780	=	18.00
3-MP	(100)(0.00997)/0.0780	=	12.80
nC_6	(100)(0.01070)/0.0780	=	13.72

Gram moles of gas out = (0.565 ft.^{3})(1.26 gm moles/ft.^{3}) =

0.712

Actual grams of H_2 gas in gas out = 2.016 (0.712 - 0.1072) =

1.21 gm

H_2 Balance = (100) H_2 out/H_2 in = (100)(H_2 in hydrocarbon out

+ H_2 as H_2 gas out) ÷ (H_2 in hydrocarbon in + H_2 as

H_2 gas in) = 100 (1.16 + 1.21)/(1.10 + 1.28) = 99.5%

Gram moles H_2 out per 100 moles nC_6 fed = (100)(1.21/2.016)/

0.0780 = 772.0

Isomerization = 7.25 + 4.40 + 18.00 + 12.80 = 42.45%

Hydrocracking = 100 - 13.72 - 42.45 = 43.8%

Simplified reaction rate constant = k = [(H_2-to-hydrocarbon

mole ratio) + 1] x (weight hourly space velocity)(hr. /

3600 sec.) x [ln (100/(100 - % hydrocracking))]/(mol.

wt. of C_6)(gm moles of gas/cc) = [8.16 + 1][2.73]

[1/3600][ln (100/(100 - 43.8))] ÷ (86.2)(1/22, 410)

(765/14.7)(492/1210) = 0.0491 cc/gm - sec.

AUTOBIOGRAPHY

William Julian Hatcher, Jr. was born on July 21, 1935, in Augusta, Georgia. In 1953, he was graduated from Decatur High School in Decatur, Georgia. He received a Bachelor of Chemical Engineering Degree from Georgia Institute of Technology in 1957. After serving three years in the United States Marine Corps, he was employed by Esso Research Laboratories in Baton Rouge, Louisiana.

In 1960, while employed at Esso Research Laboratories, he began graduate work by enrolling in evening classes at Louisiana State University. He received a Master of Science Degree in chemical engineering in 1964. In 1966, he came to Louisiana State University to complete his work toward a Ph. D degree in chemical engineering. After receiving his doctorate, he returned to Esso Research Laboratories in Baton Rouge.

In 1958 he married the former Sharon Lynn Hancock, and is now the father of three children.

EXAMINATION AND THESIS REPORT

Candidate: William Julian Hatcher, Jr.

Major Field: Chemical Engineering

Title of Thesis: Hydrocracking of Normal Hexane and Cyclohexane Over Zeolite Catalysts

Approved:

Alexis Voorhies, Jr.
Major Professor and Chairman

Max Goodrich
Dean of the Graduate School

EXAMINING COMMITTEE:

Ralph W. Pike

E E Ames

Arthur Mole

Frank R. Groves Jr.

Date of Examination:

Jan. 3, 1968